Fluvial and tectonic geomorphology of orogenic plateaux – Christopher Saville

Abstract

Geomorphology is an expression of processes acting upon an area. The links between driving processes and the resulting geomorphology are far from being fully understood. This thesis investigates controls on the dynamics and behaviour of fluvial systems from the interior of orogenic plateaux to the tectonically active plateaux margins. Orogenic plateaux provide a good study area by juxtaposing different tectonic and climatic settings that are served by the same sediment transport systems, allowing for observation of different variables on the same or similar fluvial systems. This is the first time that rivers draining orogenic plateaux have been extensively investigated.

The Turkish-Iranian and Tibetan plateaux are the study areas. Forms of rivers draining from plateaux interiors, through the plateaux margins are analysed, along with alluvial fans within both the plateaux interior and plateaux margins. Plateau draining rivers act as the major route for material leaving the plateau region and a first-order control on erosive processes retarding plateau growth. Alluvial fans redistribute material within the plateau interior, enhancing the low relief topography diagnostic of a plateau.

It is found that rivers draining plateaux show a sigmoidal form associated with the edge of the plateaux. High gradients and curvatures occur within the mountain ranges at the plateaux margins, while low values are present within the plateau interiors. Modelling work demonstrates that such forms to be likely responses for all plateau-draining rivers, but are most sensitive to the effects of precipitation upon a river's ability to incise in-to the underlying sedimentary cover and bedrock lithologies.

Alluvial fans in orogenic plateau regions are larger and with a lower surface gradient within the plateau interior than those nearer the active tectonic margins. It is theorised that this is due to the lack of lateral control on the accommodation space of alluvial fans within the plateau interior.

Department of Earth Sciences, University of Durham

Fluvial and tectonic geomorphology of orogenic plateaux

A thesis submitted to Durham University
for the degree of Doctor of Philosophy
in the Faculty of Science

Christopher Saville MSci (cantab), MA (Ed)

2012

Contents

List of Figures

Acknowledgements

Despite the next page declaring that the thesis is entirely the work of the author a lot of the essential processes (inspiration, support, psyche-welding etc.) that form part of this PhD have been outsourced to other people. They deserve lots of credit. I probably won't give it to them because I'm far too reserved to give them the effusive praise they deserve. Instead I want to mention some of the people I have been thankful to have in my life while doing this work.

First up are my supervisors Stuart Jones and Mark Allen. Their double act as a rotating Janus-figure has been the key part of making this feel like a genuine science apprenticeship. They've given me room to think of my own ideas and been good enough to not point out why they're stupid straight off. Figuring out for myself why my ideas are stupid has been a key part of my growth as a scientist. They have provided emotional support, a valuable sounding board, a metaphorical kicking, perspective, a framework for me to insert my skills, exceptional opportunity. I'll leave them to figure out which comments apply to which supervisor but I'm very thankful to have had the pair of them watching my back.

I have to thank James McLaughlin for helping me understand vector calculus; Jean-Paul Muscat for help applying simple harmonic oscillators to things that are physically possible of existing; Jen Waters for helping me understand alluvial fans; Alec Finlay for helping me understand other things look like bendy rivers; Catherine Nelson for helping me push ArcGIS; The people who deserve more credit but haven't been listed because of space and forgetfulness.

My family have meant that I'm writing this at my desk and not sobbing under it (at other moments in time it has been the other way around though). The importance of them accomplishing this can't be overestimated. I'd like to thank my parents for successfully deluding me about what I can do. Andrew has to take credit for forcibly balancing my priorities in the same way a candle burning at both ends can be described as 'balanced'. Matthew's consistently awful timing has been the egg breaking step of making a truly delicious omelette. And Tara has been truly exceptional at making negotiations with my funding board enjoyable even if I've never felt like I've ever walked away a winner from one of those conversations. She's been far too good to me and I look forward to paying her back during the rest of my life.

Declaration

No part of this thesis has previously been submitted for a degree at this or any other university. The work described in this thesis is entirely that of the author, except where reference is made to previously published or unpublished work.

Christopher Saville
Department of Earth Sciences
Durham University
December 2012

1. Introduction

The geomorphology of an area is an expression of the sum of tectonic, climatic and autocyclic processes acting upon the area over time (Ahnert, 1998). The links between these driving forces and the resulting topography are complicated by delays between a forcing factor changing and the topographic expression of that change, leading to a system response time characteristic of the forcing factor and the properties of the system it is acting upon (Whipple, 2001; Whipple and Tucker, 1999; Wu et al., 2012). The response times depend on the combination of the forcing factor and the area's conditions, meaning that a region's topography will respond to different factors at different timescales (Allen and Allen, 2005; Molnar, 2003; Whittaker, 2012). This concept of response times precludes making a direct, simple, correlation between observed geomorphology and present forcing conditions. Furthermore, tectonic and climatic forcing factors are influenced by the topography of the area they act upon, resulting in feedbacks where changing topography changes the forces further shaping the geomorphology. Both tectonics and climate being affected by topography also provides a mechanism for these two forcing factors to be linked, instead of being completely independent.

This means that understanding the linkages between tectonics, climate and topography is non-trivial. This thesis aims to further understand and describe these linkages in the context of the tectonic and climatic settings of orogenic plateaux. As such, it contains studies looking at specific relationships between aspects of the geomorphology of orogenic plateaux and their surrounding mountain ranges and the factors shaping that geomorphology. The specific plateaux used in the studies are the Turkish-Iranian and Tibetan plateaux (see figure 1.1). These are the only active large scale plateaux caused by continental collisions. Similar zones have presumably existed throughout Earth's geological past (although their identification is problematic, as the geomorphic signatures have long since disappeared) , making an investigation into the controls on their formation

relevant to fully understanding the geological record, where they act as an analogue for ancient events (Gilotti and McClelland, 2007; Jackson et al., 2004; Karlstrom et al., 2012). The Andean Altiplano is a comparable sized plateau, but is the result of a continental-oceanic convergence, instead of continental-continental convergence. Studying both the Tibetan and Turkish-Iranian plateaux allows for the comparison of observations of their geomorphology to ascertain which features are diagnostic of orogenic plateaux and which are particular to an individual setting.

A)

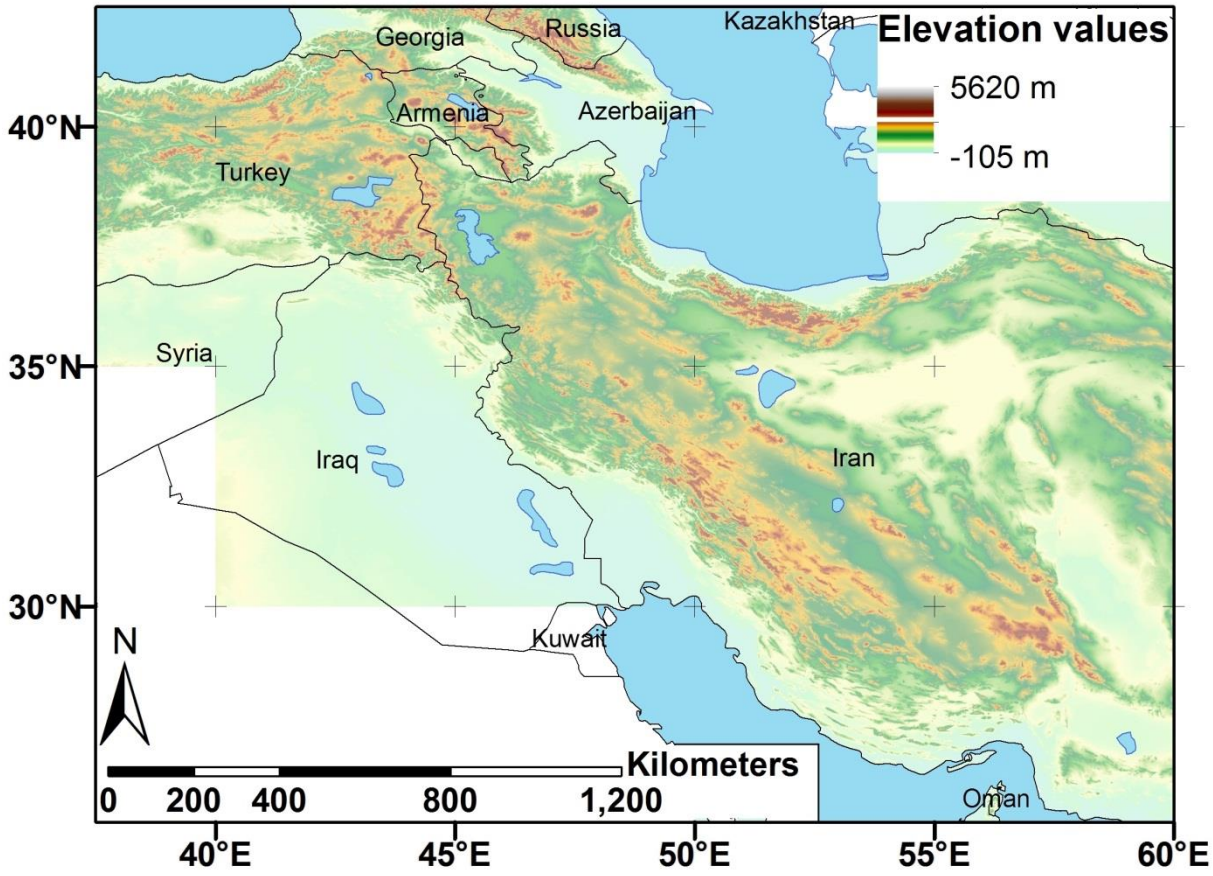

B)

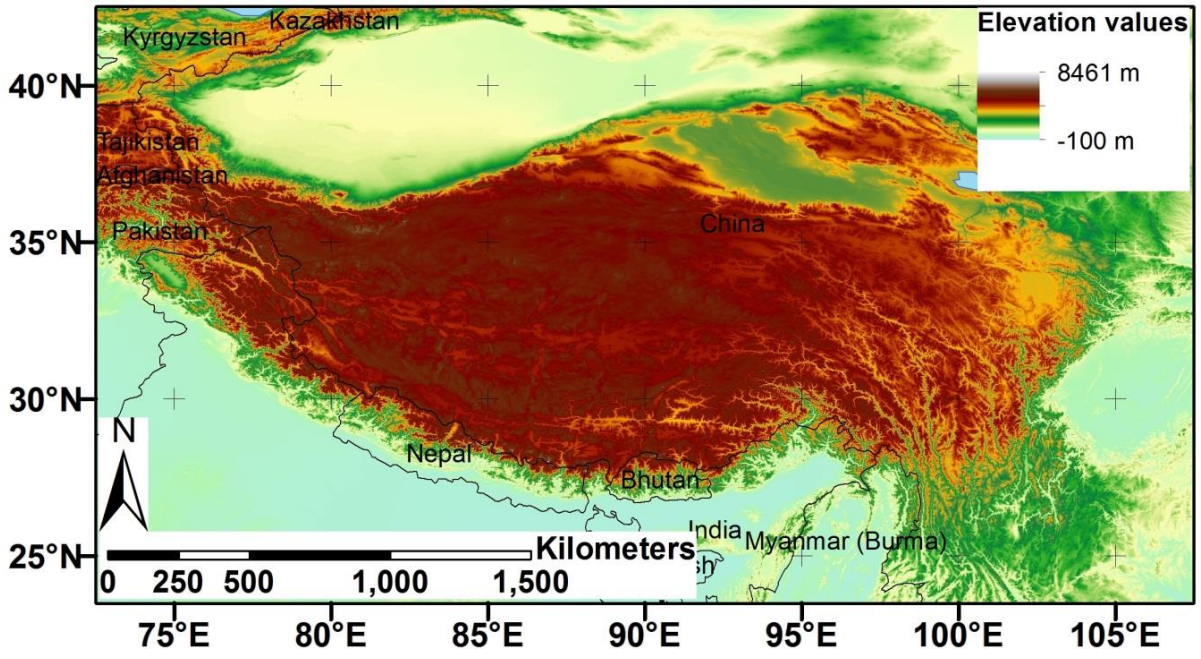

1.1 – Maps of thesis study areas. *Topographic maps of thesis study areas. A) Turkish-Iranian plateau. B) Tibetan plateau. Data used is SRTM v4 from CGIAR (Jarvis et al., 2008). Elevation scales are linear. Both show flat high elevation regions in the plateau interior.*

1.1 Aims

As described above, studying fluvial and tectonic geomorphology allows for the deduction of the tectonic and climatic setting of a region through time. This is of particular interest in plateaux settings where the dynamics and kinematics of these regions growth is unknown.

However, geomorphology's response to tectonics and climate is not yet completely defined, so examining the geomorphology of a region cannot yet be used as a deterministic tool to describe the current setting and geological past of an area. This thesis aims to further define the behaviour of this tool in the setting of an orogenic plateau. The specific questions that this thesis will investigate are:

1) What form do rivers draining from the interior of an orogenic plateau to its margins take? (Chapter 2)

2) How do the properties of an orogenic plateau cause the sigmoidal/non-concave up form of a river longitudinal profile observed in plateau-draining rivers? (Chapter 3)

3) What are the forms of alluvial fans within an orogenic plateau and how do they vary across the differing settings of an orogenic plateau? (Chapter 4)

The answers to these questions form part of the description of the linkage between geomorphology and the controlling tectonics and climate. In all of these cases it is important to realise that these linkages are not simple one-to-one relationships. These questions are complicated by controls on a region's geomorphology often being spatially removed from their expression in the landscape (Allen, 2008; Allen and Allen, 2005; Molnar, 2003; Wohl, 2000). This means that the scale over which geomorphology and tectonic/climatic setting variables are measured has to be carefully considered, to ensure

that the geomorphology recorded is actually being controlled by the local conditions, or if the landscape is being shaped by conditions which are far removed. This is particularly important for fluvial systems where the material that makes up the local landscape can be sourced a significant distance upstream and then transported to a region experiencing completely different conditions to the source catchment Furthermore the material being deposited may have been extensively reworked and then further cannibalised, making the distinction between source and depositional catchments blurred.

When describing geomorphology, quantitative measures should be used as much as possible, to keep comparisons of geomorphology in different areas as objective as can be. This can't make the assessment of the geomorphology completely objective, as deciding what numerical measures to use is still a subjective process.

If the relationships between tectonics, climate and topography are described for one region, the relationships need to be tested on a separate region, to see if they hold (as they would obviously work for the region they are derived from). This need for regions to derive relationships and test relationships being separate areas requires an awareness of the scale that relationships between tectonics, climate and topography are observed over. These relationships are scale dependent. For example it is inappropriate to look at the effect of plateau scale uplift on plateau-draining rivers and then compare to smaller scale features in rivers that look similar as they could be controlled by individual faults, rather than being representations of the plateau uplift. When a relationship is described for one area it should be compared to as similar an area as possible.

If possible, the questions are to be subdivided to describe the effect of tectonics on geomorphology and the separate effects of climate on geomorphology. However, as outlined above, these two forcing factors are closely linked (often through the topography they are driving, setting up feedback loops in the process), meaning pulling apart their distinct effects on observable geomorphology may be impossible. If this is the case, then a

more holistic description of linked tectonics, climate and geomorphology can still be useful in constructing conceptual models of how the landscape evolves.

1.2 Geomorphology as a record of tectonic and climatic processes

Geomorphology is modified by tectonic and climatic processes. Examples of this include, movement on faults, topographic expression of tectonically-driven folds, incision of rivers into the landscape, initiation of landslides due to seismic shaking or storm events, soil creep and isostatic compensation for the erosional removal of material, among others (Allen, 2008; Dadson et al., 2004; Dadson et al., 2003; Hovius et al., 1997; Owens and Slaymaker, 2004; Quigley et al., 2007; Ramsey et al., 2008; Sobel et al., 2003). Climatic and tectonic processes therefore leave a record in the landscape. At its simplest this allows for the geomorphology of an area to be quantified and the tectonic and climatic setting of the area to be inferred by comparison of the geomorphology to areas where the setting is already well quantified. Unfortunately, the correlation between geomorphological parameters and regional tectonic and climatic values is complicated by a number of factors detailed below:

1) Geomorphology is a record of the history of tectonic and climatic processes acting on an area. Therefore, the observed landscape shape is a representation of the different tectonic and climatic conditions the region has experienced, if they have changed significantly, the observed geomorphology may be representative of tectonics and climate that are not observable at the present time.

    1a) With geomorphology being a record of tectonic and climatic history, different responses to changing conditions can be superimposed, giving observed geomorphology that represents neither the current conditions, nor a condition that has existed in the past.

1b) There is a lag between tectonic and climatic conditions being imposed upon an area and the geomorphological response. This response time means even if the response to the latest tectonic and climatic conditions would completely overprint previous geomorphology, the conditions may have changed by the time they are expressed in the landscapes.

2) The response of landscape to tectonic and climatic processes can be spatially removed from those processes. This can be due to far field tectonics driven by processes far removed from the region of interest, movement of sediment from one setting to another and gravity-driven spreading in an orogen, due to excess topography in a different location (England and Molnar, 1991; Hatzfeld and Molnar, 2010; Jade et al., 2004; Zhang et al., 2004).

3) The geomorphological responses to tectonic and climatic forcing are not independent. A particular geomorphological feature could be due to either tectonic or climatic causes (for example, progradation of an alluvial fan could be due to increased sediment supply, due to either increased rainfall transporting more sediment from the source catchment to the fan, or because reduced subsidence in the depositional area reduces the available vertical accommodation space), but be unable to be designated as being caused by one or the other. The inability to distinguish between tectonic or climatic causes for a landform is particularly pronounced when using only remotely sensed data and there is no possibility of observing the sedimentology of the material that makes up the geomorphology.

4) Some tectonic and climatic processes acting on the Earth's surface erode the landscape, instead of building up a landform. While this is still a record of the

processes acting on an area, by being subtractive, it removes previous traces of processes.

The responses of geomorphology to forcing factors are physically limited. This is either done by physical cut-offs or due to the presence of negative feedbacks in the earth surface system (Clarke et al., 2010; Humphrey and Heller, 1995; Masek et al., 1994; Molnar and England, 1990; Wobus et al., 2006). Examples of geomorphological responses limited by physical cut-offs are the inability of rivers to incise below its base-level, the elevation of topography being limited by lithospheric strength and playa lakes putting a limit on the progradation length of alluvial fans. Negative feedbacks can be seen in rivers adjusting to changing conditions over time. For example, movement on a fault that crosses a river can cause a local increase in gradient along the river; this will increase the ability of the river to incise along that reach, thereby reducing the gradient (Humphrey and Heller, 1995; Peakall et al., 2000; Whittaker et al., 2007). Examples of similar negative feedbacks are seen in the adjustment of over-steepened hill slopes by undergoing soil creep and landslides, reducing their gradients and high elevations being reduced by gravitationally driven spreading, driven by the excess elevation (England and McKenzie, 1982, 1983; Molnar et al., 2006; Rey et al., 2001).

Negative feedbacks and limits on geomorphological responses make a direct correlation between the magnitude of a geomorphological response and the forcing factor unreliable. For example, increasing rainfall in a plateau interior would increase the amount of incision in catchments feeding alluvial fans across the plateau. This is controlled by the stream power incision law (Howard and Kerby, 1983; Kirby and Whipple, 2001; Whipple and Tucker, 1999):

$$E = kQ^{m}S^{n}$$

Where: E is the local incision rate

Q is the local stream discharge

S is the local stream slope

And k, m and n are empirically determined constants that vary depending on channel incision processes, rock resistance, channel armouring by sediment, and the availability of erosional tools in the water

Increasing the incision of a river in a catchment will also increase erosion across the catchment as the rivers act as a local base level for the adjacent landscape and increased incision undermines the adjacent interfluves. This relationship shows that the increase of incision with rainfall (which controls stream discharge) is not a linear relationship, so an observed doubling of incision cannot be inferred to be caused by a doubling of rainfall. Increasing incision will also increase the amount of sediment available to be transported to terminal depositional environments such as alluvial fans. That doesn't mean that an increase in rainfall can be simply correlated to an increase in the observed geomorphological characteristics of fan area or progradation length. Besides the non-linear linkages in the systems connecting rainfall levels to sediment supply, many fans in an orogenic plateau setting are close by, or constrained by playa lakes (relatively low lying, low relief topography being suitable for both lake formation and terminal sediment deposition systems). In this case a change to regional rainfall would also increase lake levels, reducing the lateral accommodation space available for alluvial fans, working against the simple increased rainfall producing larger fan area inference that might otherwise be expected (Allen and Hovius, 1998; Dade and Verdeyen, 2007; Hartley et al., 2005; Patranabis-Deb and Chaudhuri, 2007).

Fluvial geomorphology is particularly sensitive to changes in the setting conditions. As gravity driven water flow will always follow the steepest local gradient

changes in this can be seen by looking at river patterns (Allen and Davies, 2007; Jones, 2004; Pratt-Sitaula et al., 2004; Ramsey et al., 2008; Schumm et al., 2000). This opens up the possibility of using drainage patterns to investigate sub-seismic tectonics (Allen and Davies, 2007). This is partially offset by rivers also acting as an erosional agent. Down cutting along a river course will work to entrench its position and ensure that the local gradient is steepest along its course overwhelming any regional gradient changes that may affect river positioning. If rivers are being used to detect subtle shifts in the landscape, alluvial, rather than bedrock rivers would be more suitable because of this.

1.3 Controlling factors on fluvial systems

Fluvial systems are a subset of gravity-driven erosional, sediment transport and deposition systems. Compared to most sub-aerial gravity-driven transport systems (landslides, soil creep, they can move sediment a large distance with the source and sink of sediment being 100s or even 1000s of kilometres removed from each other. This property means that the systems can experience a variation in their tectonic and climatic setting along their length, with the conditions being far removed from those at the sediment sink. In some cases it is the differences between those conditions that can make an area a sediment source or a sediment sink. Transporting sediment over large distances also introduces a time lag between a tectonic or climatic signal in the source area and its expression in the depositional area (Whipple, 2001). The size of this time lag is not fixed as it depends on the conditions within the sediment transport system, which are subject to change. The time lag can also be dependent on the size of erosional and depositional responses. For example, a large influx of sediment to a fluvial system (e.g. a large landslide) can temporarily dam a river, increasing the lag time for that sediment input signal. This time lag and the possible disconnection between the driving conditions and the conditions at deposition prevent fluvial systems being used as direct record of tectonics and climate.

Tectonic signals effecting gross geomorphology of orogens tend to be constructive, increasing the elevation of a region, while climatic signals are often destructive, with increased rainfall driving erosion and temperature changes controlling weathering rates, but unable to actually reverse the process (Allen, 2008; Allen and Allen, 2005; Codilean et al., 2006; Owens and Slaymaker, 2004; Whittaker, 2012; Willett, 1999). In contrast, tectonic controls on fluvial geomorphology can both increase the elevation along river profiles and increase the gradient of rivers' longitudinal profiles, increasing incision. Similarly, increased discharge in a river, due to increased regional rainfall can enhance incision along the river's profile and also increase the river's transport capacity allowing it to deposit more sediment into its lower reaches. The expression of tectonic and climatic

signals in the longitudinal profiles of rivers is primarily a change of the rivers' gradient. This may be a long term adjustment to a change in conditions, in which case it is often expressed by a change to the rivers' plan-form shape (e.g. increased meandering to reduce the gradient along a river), or a transient change to the river gradient.

Identifying changes in river gradient is a valid method of finding regions that have been affected by tectonic and climatic signals that are different from the background conditions, or reaches where the underlying lithology has changed (due to river incision) or is different from that further upstream or downstream. Merely looking for changes in gradient is not sufficient as the idealised form for river's longitudinal profile is a smooth, concave-up shape, whose gradient changes all the way along its length. Instead the topographic signals take the form of discontinuous changes in gradient. Looking for changes in gradient that are not part of a well-adjusted river profile make methods such as plotting the ln of downstream distance (D) against the ln of river slope (S) a useful way of identifying discontinuities in river gradient (Goldrick and Bishop, 2007). Using LnS vs. lnD graphs in this manner is effective at seeing tectonic and climatically-driven changes that are superimposed on a river's longitudinal profile.

A)

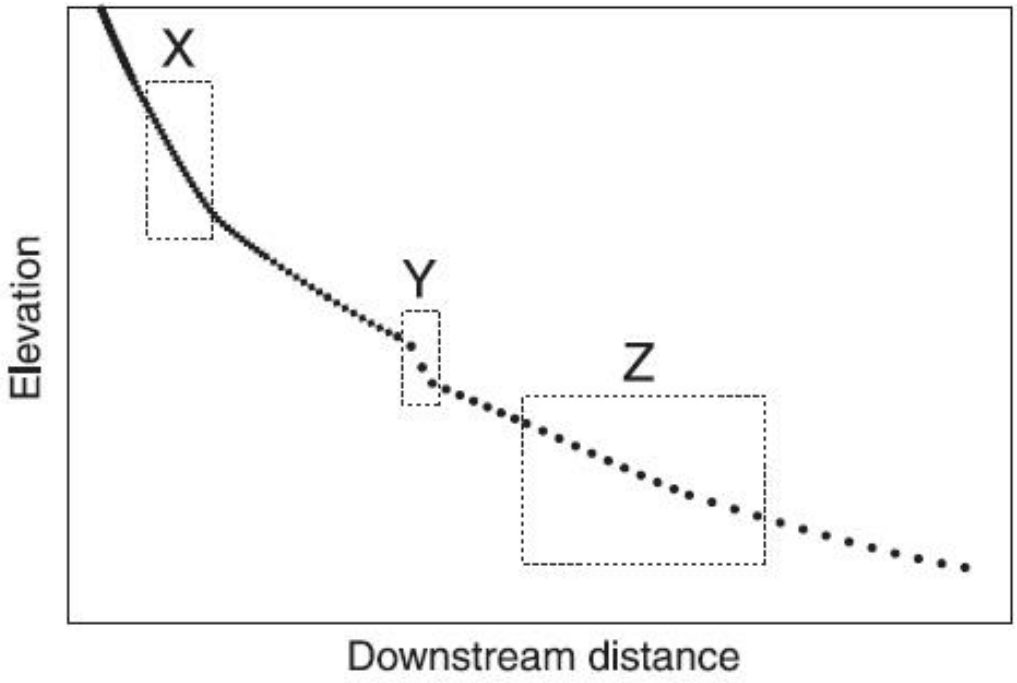

B)

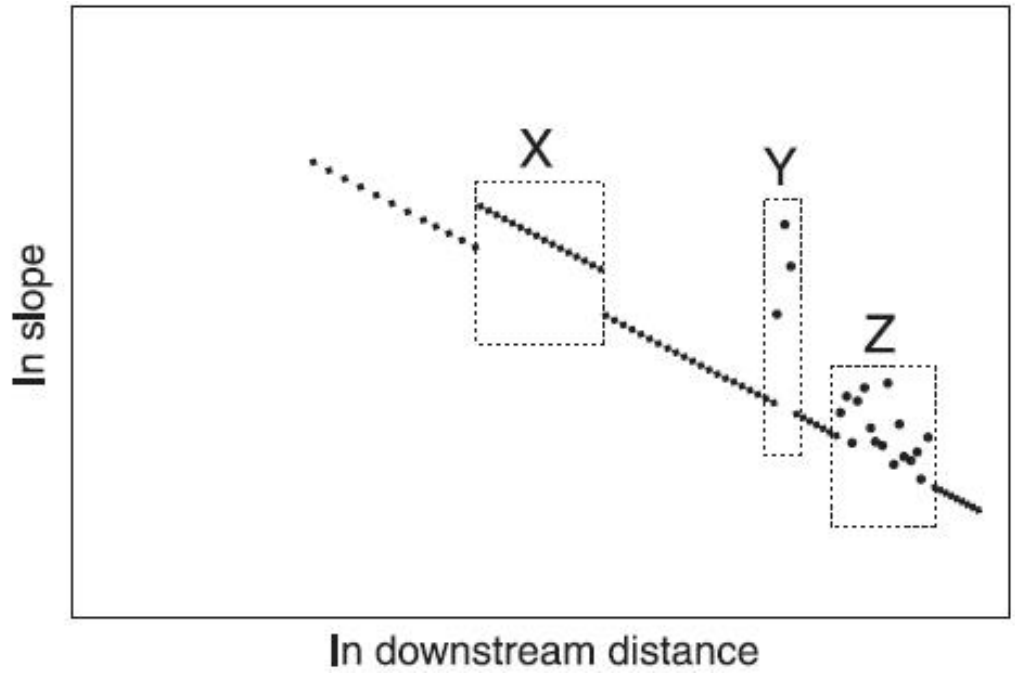

1.2 – Uses of lnS vs. lnD graphs for locating river reaches out of topographic equilibrium *A comparison of an idealised longitudinal river profile (A) and its representation on a lnS vs. lnD graph (B). The lnS vs. lnD graph shows more sensitivity to changes along the river. A change in lithological erodability is shown at X, the spike associated with a knickpoint is shown at Y, while a disordered response to general river disequilibrium is shown at Z. Modified from (Goldrick and Bishop, 2007)*

The main controls on fluvial systems are their tectonic setting, their climatic setting and the underlying lithology. These controls are considered in the context of fluvial systems as a whole and their effect on river longitudinal profiles in particular.

Tectonics is the primary control on the location of fluvial systems. It achieves this by changing the topography that surface water flows over. Tectonic activity is the main way of generating the elevation, and therefore the gradient needed to drive moving water. Magmatism and base level fall can also be responsible for creating the relief necessary for a fluvial system, but are not regionally important processes for controlling relief in a plateau setting. In addition, topography generated by tectonic activity constrains the locations the water flows through. This is seen in alluvial fans where the head of the fan is located in gaps between fault segments (Jones, 2004). As well as controlling the location of fluvial systems, tectonic activity affects the form of those systems. Movement on faults that cross river paths can reroute rivers path with strike-slip motions and change the gradient of rivers' longitudinal profile with normal and reverse motion. If a fault changing a river's gradient has a repeat period that is a lot longer than river response time, the river will be able to adjust back to its previous form, through either enhanced incision or deposition, between fault movements. Should the fault repeat period be relatively short compared to river response time, then the river will adjust its profile to this new setting, assuming a new equilibrium form. Particularly large movements on faults can increase the elevation at a point in a river, dissecting the river. The controlling parameters for river dissection are the relative rates of fault movement (rather than the absolute size of specific fault movements) and the rate of incision along the river. If the incision rate is unable to keep up with the tectonically driven elevation increase then river dissection occurs (Sobel et al., 2003). Situations where uplift is more pronounced off a river path and in the adjacent interfluves (either due to uplift being located away from a river path or regional uplift being counteracted by along the river by incision) can increase the sediment flux along a river. In this situation the steepness of the interfluves increases, enhancing

processes that deliver sediment in to the river system (soil creep, landslides) (Bishop, 2007; Codilean et al., 2006; Hovius et al., 1997).

Climate can affect fluvial systems through two mechanisms, varying rainfall and varying temperature. Temperature is a primary control on many weathering processes and therefore sediment supply, this is of most importance to sediment limited systems (Hobley et al., 2011; Velbel, 1993; Wright et al., 2010). The primary climatic control on fluvial systems though, is rainfall. This is not just the case for transport limited systems, where water discharge controls how much sediment can be mobilised (Schumm et al., 2000; Wohl, 1993), but more generally as the discharge along rivers is also a primary control on how much incision a river undertakes along its course. Increasing rainfall channelled into a river does not affect the fluvial system in an obvious linear fashion as it can increase both incision and transport capacities, therefore it is capable of increasing the destructive (incision) and constructive (transport leading to deposition) properties of a river. When considering the effect of fluvial systems in an orogenic setting, rainfall's effect on incision is often more important as sediment transport will remove material from the orogen to be deposited in the surrounding lowlands. The effect of rainfall on river incision is parameterised in the stream power incision law (Howard and Kerby, 1983; Kirby and Whipple, 2001; Roe et al., 2002; Whipple and Tucker, 1999). Water discharge along a river depends on the upstream drainage area, the amount of groundwater infiltration happening in a river's catchment, the amount of water storage in the catchment and rainfall across the catchment, which is climate's input to river incision (Bouwer, 1978; Higgins, 1984; Roe et al., 2002, 2003; Rorabaugh, 1964; Tucker and Bras, 1998). The stream power incision model depends on water discharge along a river, but incision along a river is not directly related to the amount of water that flows along a river. The temporal pattern of rainfall is also important, as the erosivity of a mass of water depends on how long it is applied over. Seasonal, concentrated rainfall over a short time will have a more pronounced effect on incision than the same amount of rain spread evenly over time

(Dadson et al., 2003; Palmer and Ralsanen, 2002). The stream power incision law only parameterises a snapshot in time, so the value of water discharge used in it has to be carefully considered to ensure that it is representative of incision processes happening over the timescale being investigated.

The third major control on fluvial systems is the lithology underlying them. Lithology is seen as being a control on the rate of river adjustment, as can be seen in the stream power incision law, where lithological hardness is a big control on the value of k. It is also a control on the final shape of an adjusted river as given in the often used formulation for the slope of a river in equilibrium:

$$S=k_2A^{-\theta}$$

Where : S is the slope of the river

k_2 is an empirically derived constant that is effected by rock properties and rock uplift processes

A is the upstream drainage area from a point where the slope is measured

θ is the concavity index of the river

In this, lithology is a control on k_2. Furthermore, lithology can be the cause of knickpoints in an equilibrium river where two different lithologies are next to each other along the course of a river. Different rate of adjusting and different final equilibrium forms for varying lithologies next to each other set up relatively sharp changes in slope as a river passes from one underlying lithology to another. These changes from one lithology to another can also be achieved by incision along a river unroofing a different lithology with a variation in erodability. Like many controls on river form, lithology is subject to negative feedbacks that make it self-correcting. Reduced rock resistance along a river

allows for an increase in gradient as the river flows into the low resistance zone and cuts further into that material. This increase in gradient will then lead to increased incision, which will act to reduce the gradient (Humphrey and Heller, 1995; Wohl, 2000).

Fluvial systems are self-adjusting, particularly with regards to gradient. Just considering the longitudinal profiles of rivers, when a part of a river's profile has its gradient increased this enhances a river's ability to incise, acting to reduce the gradient at that point. Conversely, when a river's gradient is lowered, the rate of incision is reduced, and in some case deposition occurs, when the lower gradient means the river loses the kinetic energy necessary to carry the sediment load at that point. Both these factors act to allow the gradient to increase in response. Changes in a river's ability to incise act against fluvial geomorphological changes, returning the river gradient to an equilibrium form that is set by lithology and the longer term uplift and water discharge trends along the river. This adjustment is not instantaneous, so while a river will return to a form that represents the longer term tectonic and climatic conditions it experiences, if it has experienced an event (storm, fault movement, etc.) that diverges from this longer term trend there is a response time before the river adjusts. Response time lengths are in the order of 0.25 – 2.5myr, increasing with larger fluvial systems (Hobley et al., 2010; Whipple, 2001). The ability of rivers to adjust to compensate for tectonic and climatic forcing events can cause cyclic patterns in their geomorphic and sedimentary expressions. When a river's gradient adjusts by changing the rate of incision or moving to a depositional mode it is possible for it to move past the equilibrium point, requiring an adjustment that works in the opposite direction, this in turn can move past the equilibrium form, setting off a series of oscillations, that are only the topographic/sedimentary expression of one event. This tintinnabulation of the system can produce cyclic responses that are similar to what would be expected of a cyclic forcing factor, such as climate oscillations or repeat movement on a fault (Begin et al., 1981; Clarke et al., 2010; Humphrey and Heller, 1995).

Rivers' forms ability to self-adjust is a subset of the larger concept of landscape equilibrium. In a similar manner to river form, surface processes that mobilise material at the surface are dependent on local topographic curvature for their rate. This is often summed up in the following diffusion law when modelling mass-wasting processes that are not happening in a river channel (Carson and Kirby, 1972; Codilean et al., 2006):

$$\frac{dz}{dt} = k\nabla^2 z$$

Where: z is elevation

t is time

and k is a constant that allows the mass wasting processes to be scaled depending on the local conditions

This approach to modelling erosion across a landscape simulates multiple processes including soil creep, rain splash and when considered over a large enough time that the effect of single events is averaged out, land sliding. Removing material from across the landscape reduces the relief of the landscape and the rate at which further surface mobilisation takes place, returning the landscape to an equilibrium state. In addition, rivers also act as a major control on the evolution of the landscape they are located in. Rivers act as the sink for material removed from the adjacent land surfaces, so act as a base level for the relief driven erosive processes that take place there (Allen and Allen, 2005; Allen and Hovius, 1998; Burbank et al., 1996; Ramsey et al., 2008).

1.3.1 Graded rivers

A graded river is one that is relative topographic equilibrium along its length, meaning that its form does not change over time relative to any point along its length. This often

the same thing as absolute topographic equilibrium relative to the earth's surface, as most rivers drain into the sea. In these cases the river base level is fixed independently of the processes acting in the river itself, so to maintain a fixed relative shape along its length this shape must also be fixed relative to sea level. It is possible to imagine a situation where a river maintains relative topographic equilibrium, but is moving relative to the earth's surface. Such a case may be an internally draining river where an entire region is being subjected to uplift such that it is uniform along a river's length. In such a case the relative from would remain constant, but just be raised or lowered relative to the earth surface.

There are two main categories of graded river, rivers with a comparatively low ability to incise into the underlying rock, but are also subjected to little or no tectonic movement, and those where the incision of the river into the underlying rock is similar in magnitude to the rock uplift along the river length. The first type has limited incision either because of sediment armouring protecting the underlying bedrock or because there is no excess stream power along the river length. In this case, the river has adjusted to transport its sediment load along its length, but with no energy left for incision. In the second case, a balance between rock uplift and bedrock incision implies a river that has been present long enough to adjust to the tectonic and climatic setting it is set in. It is possible for a river to vary from the first (alluvial) type to the second (bedrock) river type along its length as the conditions change along its length. A graded river is a dynamic equilibrium system, where internal negative feedbacks adjust the river's form to compensate for changes caused by variations in rock uplift, sediment supply or water discharge along the river length. As a result a river's long profile is never completely static over time. When designating a river as graded, the timescale and length scale that a regularity of form is assumed for should be born in mind. At short length scales, sediment movement as part of river's normal transport processes will cause small scale fluctuations in the form of river's longitudinal profile. The landscape a river is located in will never be

completely static over a long enough time, meaning that a graded form has to be considered a transitory state, which will never remain completely static if considered over a long enough timescale. The particular gradient the equilibrium settles upon depends on the setting conditions for the river, with higher rock uplift and water discharge producing higher gradients.

The standard form for the longitudinal profile of a graded river is that of a smooth concave up curve. The concavity of a river in equilibrium is often observed to be around 0.45 (Harkins et al., 2007; Kirby and Whipple, 2001; Moglen and Bras, 1995; Roe et al., 2003; Snyder et al., 2000; Tarboton et al., 2006). Many rivers, which are presumed to be well adjusted, demonstrate a concave-up shape (Knighton, 1998), however it is entirely possible for an adjusted river to not have a smooth, concave-up shape if the controlling factors (rock uplift, water discharge, rock hardness etc.) are not also smoothly distributed along the length of the river. The concave-up shape is a consequence of water discharge increasing downstream and discharge and slope being the controlling variables. In a situation where balancing rock uplift (the condition for a graded river) requires incision to be either constant along river length or increasing upstream, local slope must reduce downstream as water discharge increases. This highlights two assumptions that underpin the smooth concave-up paradigm for a river in topographic equilibrium. Firstly, that rock uplift along a river length can be approximated as either a uniform constant along river length, or a quantity that increases towards the river head (Ahnert, 1998; Knighton, 1998; Masek et al., 1994; Roe et al., 2003). These are suitable for modelling a river in a growing orogenic setting where uplift is concentrated at an orogen's collision and dies off with distance. A river's head would be expected to be found close to the locus of collision, as that is where elevations would be highest. The second assumption is that water discharge increases with distance downstream. This is a natural effect of a river's catchment area increasing with downstream distance. Exactly how a river's drainage area increases

depends on the geometry of the drainage area. This is parameterised by the following power law relationship (Ijjasz-Vasquez and Bras, 1995; Rodriguez-Iturbe et al., 1992):

$$L=xA^{y}$$

Where: L is the downstream distance

A is the drainage area upstream from the measurement point

x and y are empirically determined constants that can vary between different rivers.

For many rivers, x is approximately 1.4 and y is close to 0.6 and generally agreed to be over 0.5 (Knighton, 1998; Maritan et al., 1996). y being larger than 0.5 suggests that as a drainage basin increases in size with downstream distance the geometry changes to a more elongate form. This makes sense for rivers draining orogens where the lateral extent of a river's catchment would be limited by the catchment of orogen draining rivers running parallel to it. A smooth change in gradient along a river minimises the dispersion of stream power along the river length, part of the condition necessary for a river in equilibrium, as all systems move towards the lowest flow resistance configuration (Chang, 1979).

There is little agreement on the correct way to mathematically represent the long profile of a graded river. Possible functions that produce a smooth, concave-up shape are power functions, negative exponentials and decaying logarithmic functions (Knighton, 1998; Lague et al., 2005; Larue, 2011; Snow and Slingerland, 1987). A cycloid is also a smooth, concave-up shape and is the solution to the brachistochrone problem (what is the fastest path for an object to follow to get from a high point to a laterally removed lower point, driven only by gravity?). In this way a cycloid represents the most efficient conversion of gravitational potential energy into kinetic energy for a falling object, whose

finishing point is not directly under its starting point. The brachistochrone curve is also a tautochrone curve (where objects falling along the curve all reach the bottom in the same time, irrespective of where they start on the curve). While such a cycloid allows for a minimal dispersal of stream power along the curve, it does not allow for a continuum of water discharge as discharge would increase downstream, more than as controlled by the increase of catchment area downstream. This rules out a cycloid as a suitable shape for a graded river (Nandi, 2000). Of the other possible candidates for mathematically representing a graded river, they can all be shown to be the best fit for particular graded rivers. (Hack, 1973; Hack and Young, 1961) initially suggested that river longitudinal profiles were either power forms or negative logarithms, depending on the distribution of grain size downstream. Further studies showed the shape of river profiles to not be dependent on grain size distribution in such a prescriptive way (Knighton, 1998; Snow and Slingerland, 1987). Exponential functions have been reasoned to be the form of a graded river by derivations based on a random walk and models of river form where river slope scales in proportion to elevation (Leopold and Langbein, 1962; Morris and Williams, 1997), but that does not lead to better fits for exponential functions than power and logarithmic functions. One of the problems with determining what form of function to use to represent a graded river's profile is the difficulty in assessing whether a river is actually in a graded state, while a particular function may fit a river's longitudinal profile well, evidence that a river is graded may not be available. Ascertaining the levels of rock uplift and incision along a river is very difficult, particularly without a protracted longitudinal study. Observing longitudinal profiles through time to look whether the profile is changing is obviously impossible. The best guide to the previous positions of river profiles are river terraces (Burbank et al., 1996; Jones et al., 1999; Maddy et al., 2005), but by their very nature they indicate a non-graded river, whose position must have changed since when the terrace was formed. Mathematical forms of river profiles have been shown to fit well the shapes of rivers known not to be in equilibrium, showing that

good fits to river profiles is not necessarily a sign that a particular function is a good representation of graded rivers. Ultimately, as there is no function known to be a best fit for graded rivers, an empirical approach is usually taken, where the function that best fits the rivers being studied is used.

1.4 Orogenic plateaux as study areas

Orogenic plateaux are good study areas to look at when investigating fluvial systems. The two main benefits of orogenic plateaux are that they have a variation in tectonic and climatic settings from the plateau interior to the fringing mountain ranges and that they are active settings.

The general pattern of the tectonic and climatic settings for orogenic plateaux is that uplift and rainfall are both low in plateaux interiors, while both quantities increase in the fringing mountain ranges, where the plateaux are expanding into. Rock uplift is limited in the plateaux interior as the high elevation of the interiors makes it energetically unfavourable for thickening (and so uplift) to continue and therefore deformation moves out to the lower elevations in the surrounding mountain ranges stepping out over geological time (Bollinger et al., 2006; Dewey et al., 1988; England and Molnar, 1991; McClay, 1992; Szulc et al., 2006). There are several possible models for uplift in an orogen that lead to a plateau configuration. These include crustal thickening that moves outwards towards thinner crust as thicker crust becomes energetically unfavourable to thicken any further (England and Housemann, 1988), shortening and crustal thickening that is evenly distributed throughout the orogen (Tapponnier and Armijo, 1986) and uplift of the region that is not accompanied by further crustal shortening (Molnar, 1993). In the first case a zone of seismic thrusting would move outwards as the plateau evolves, shortening and thickening the crust until it reaches the thickness of the plateau, at which point the zone would move outwards. Elevations higher than those associated with current day seismicity are present in the studied plateau regions, so there must be some other

factor that is further thickening the crust beyond the thickness associated with the observed seismicity. As this is happening outside the zone of observed seismic thrusting this must be associated with more ductile shortening, so is likely to be happening at a lower depth than the observed brittle thrust ringing the studied plateaux. Seismic thrust events being associated with lower elevations within the Tibetan plateau have been observed in the work of Molnar (1993) (see figure 1.3) where most thrusts were seen to be present in regions whose elevation were less than 3.5 km and only one was present above 4.5 km.

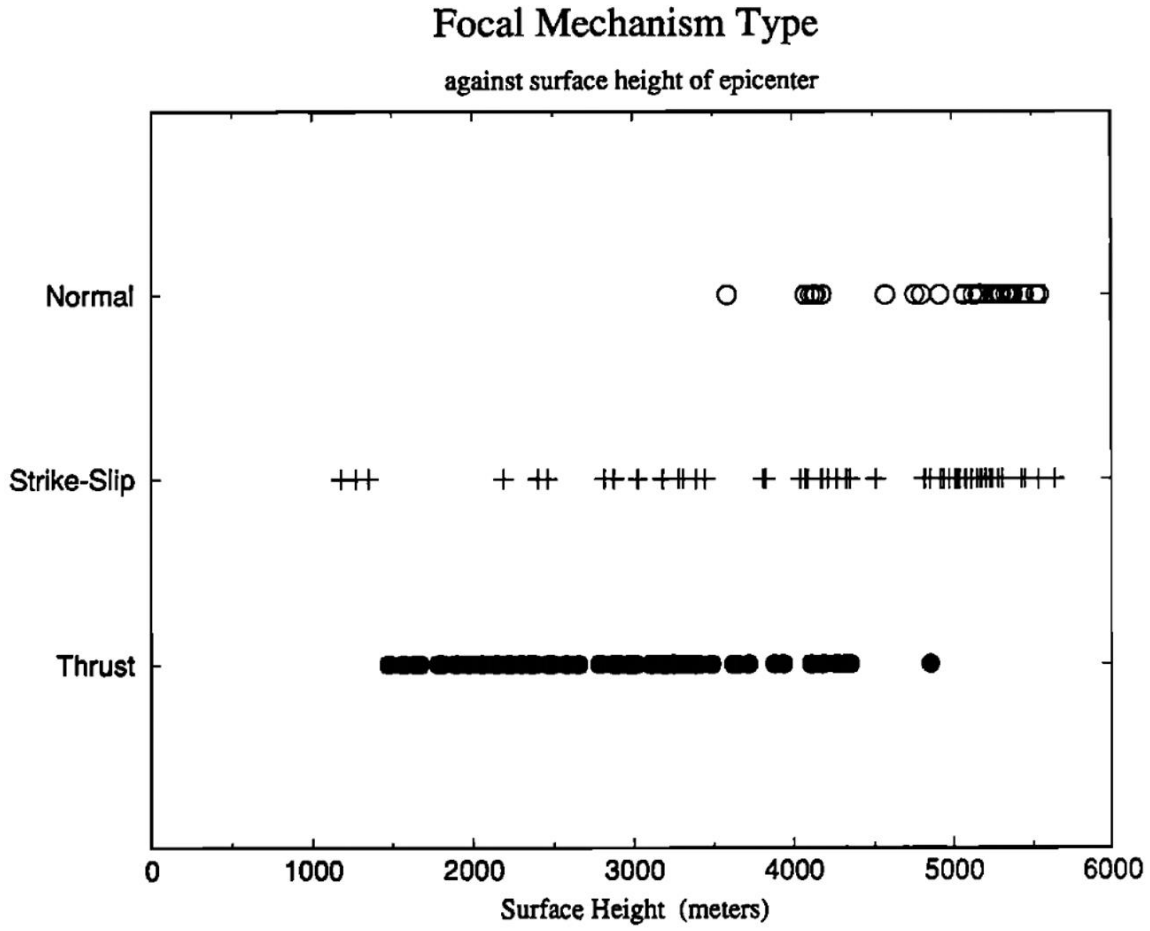

1.3 – Distribution of earthquake types with respect to elevation in the Tibetan plateau *Thrust events are seen to be concentrated at lower elevations, while movement on normal faults is at the higher elevations. These may represent gravitationally driven spreading of regions with thickened crust. From (Molnar, 1993).*

Irrespective of what mechanism is being used to thicken the crust in this stepping-out model the pattern of rock uplift experienced at the surface is of low to no uplift in the

plateau interior, increasing out in the plateau margins, until it reduces down to zero again in the surrounding lowlands. The other two models for generating plateau uplift both produce rock uplift at the surface that is near uniform across the plateau region. In the second case uniform shortening could be envisaged to occur due to a process such as lower crustal flow across the plateau region (Cook and Royden, 2008), while the third model could be explained by delamination of a lithosphere previously thickened by other crustal shortening processes, allowing for buoyant asthenosphere to replace the lost lithosphere and raising the area's elevation (Molanr, 1993) (See figure 1.4). Tomographic imaging techniques have shown lithospheric delamination to be an unlikely cause of the elevations seen in orogenic plateaux as there is little evidence of an abnormally thickened lithospheric root (Maggi and Priestly, 2005).

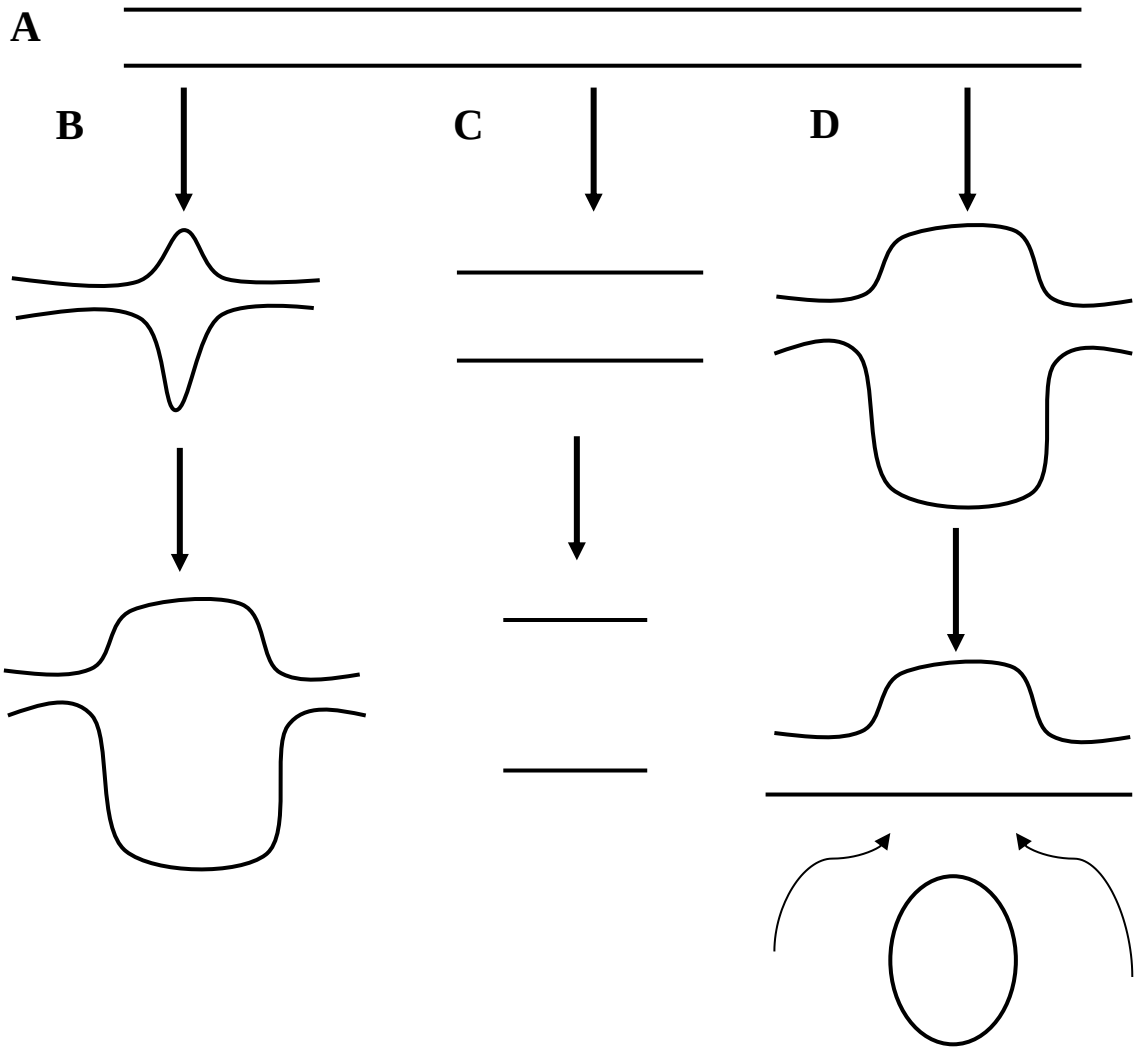

1.4 – Cartoon showing possible crustal thickening patterns for making an orogenic plateau. *Initially unthickened crust (A) can undergo shortening just at the margins of a plateau, with no further shortening within the plateau interior (B),This shortening could be achieved with seismic thrusting or ductile crustal shortening, depending on the rheology (and therefore depth). It could be uniformly thickened and shortened across the plateau region (C). Lithosphere, thickened enough by another process to become thermally instable detaches and moves downwards allowing buoyant asthenosphere to replace it, increasing the elevation of the crust above. This is a way of achieving elevations greater than those seen in seismically thickened regions.*

Rainfall is low within a plateau interior due to the orogenic rain shadow effect. The low relief means there are few steep gradients to drive air columns up, causing them to cool and de-hydrate. Furthermore, the high elevation means that much of the moisture in air columns has already dropped by the time they reach the plateau interior. The variation

in the climatic and tectonic parameters is somewhat discontinuous in nature (e.g. there is an observable cut-off of seismogenic thrusting between the relatively quiescent plateau interior and the actively thickening plateau margins). This discontinuity allows for the study of divergent settings next to each other, within the same geological terrane, allowing for the partial negation of lithology as a controlling variable, and also permitting a focus on the differences in fluvial systems due to changes in tectonics and climate.

Rivers draining from the plateau interior through the surrounding mountain ranges experience these varied tectonic and climatic settings. In this way orogenic plateau allow for the effect of different climatic and tectonic settings to be observed acting on the same river. Increasing rainfall towards the foot of these rivers is consistent with the assumptions underlying the smooth, concave-up longitudinal profile paradigm, but two things undermine this assumption; uplift is neither consistent along the river length, nor continuously increasing towards the river head. Examining how rivers behave across orogenic plateaux will help understand whether the concave-up form can be applied to such rivers. If not, a different paradigm for river form may be more appropriate.

Studying the drainage of an active setting has some distinct advantages over studying relict drainage. Active drainage can be directly correlated with the current tectonic and climatic settings, and while there is the response time of a fluvial system to take into account, the currently observed tectonic and climatic setting can be assumed to be close to that represented by the current drainage form. With an inactive drainage system, both the river forms and the conditions causing those forms are not directly available for observation. The river form has to be inferred from the sedimentary record and/or river terraces (Burbank et al., 1996; Jones et al., 1999; Maddy et al., 2005) and the controlling tectonic and climatic conditions inferred from old geomorphology or sedimentology, which also need dating to correlate. Furthermore, traces of inactive fluvial systems need to be deconvolved from the effects of later erosional modification to get accurate data about river forms in old tectonic and climatic settings. Active systems

remove a level of interpretation in collecting values describing river forms and the conditions that form them.

As well as providing a varied, yet connected, collection of settings to investigate their effect on river form, the evolution of orogenic plateaux is interesting and important in its own right, producing large topographical features that are controls on global air circulation patterns (Egger et al., 2000; Molnar et al., 1993; Raymo and Ruddiman, 1992). The balance of mass being removed from an orogen through erosional processes versus the influx of mass from tectonic advection processes controls the growth of the orogen. The presence of a plateau shows that over geological history the flux of mass into the region has been larger, but it is possible for that to not be the case at every point in its history with a plateau growing through cyclic periods of the flux of mass into and out of the region being larger in turn (Masek et al., 1994). Therefore the drainage of orogenic plateaux is a first order control on the topography of the plateaux as it is one of the major controls on the movement of mass out of the orogen.

Two different plateaux are used as study areas: the Turkish-Iranian and Tibetan plateaux. By using two orogenic plateaux and looking for common features in the fluvial geomorphology of the plateaux we can be surer that geomorphology ascribed to particular features of an orogenic plateau is a characteristic of orogenic plateaux in general (and presumably through time) and not particular to one locale. The Turkish Iranian and Tibetan plateaux are the only large scale orogenic plateaux caused by active continental collisions. The only other orogenic plateau comparable in size is the Andean Altiplano, but this is not seen as a good comparable case as it originates from an ocean-continent subduction zone, rather than a continent-continent collision zone.

1.4.1 The Turkish-Iranian plateau

The Turkish-Iranian plateau is an orogenic plateau formed by the collision of the Arabian and Eurasian plates. The suture between the two plates is located along the north eastern

boundary of the Zagros mountain range, which also approximately forms the southwestern margin of the plateau. The collision is active with a convergence rate between 18 and 28 (±2) mm/yr, with the rate being higher in the East as the Arabian-Eurasian Euler pole lies in the Mediterranean (Sella et al., 2002; Vernant et al., 2004a; Vernant et al., 2004b). The total area affected by this collision is in the region of 3 million km^2 (Allen et al., 2004) with 1.07 million km^2 of this being classified as the plateau interior (see following sections for how this number is reached). The plateau interior has elevation values mostly between 1 and 2 km, with occasional peaks reaching up to 2.5km. Pliocene-Quaternary volcanic summits are higher still with several summits over 5km (e.g. Ararat and Damavand).

Active thrusting is almost completely absent within the plateau interior, with little present day uplift observable (Allen et al., 2011b) Convergence occurs in the actively thickening and thrusting Zagros and Alborz mountain ranges. Further shortening is taken up in strike-slip 'escape' tectonics of Anatolia towards the Aegean (Purvis and Robertson, 2004) and rotational strike slip movement in the north eastern Kopet-Dagh (Allen et al., 2003; Jackson, 2001; Vernant et al., 2004b). Thrusting also occurs across the Greater Caucaus range. A thickened crust is observed throughout the plateau although is lower than might be expected under the Alborz mountains at the northern margin, where there is no thickening under the mountains relative to the adjacent basins (Radjaee et al., 2010).

Climate across the Turkish-Iranian plateau follows the pattern expected of an orogenic plateau (see figure 4.14). Desert (less than 200 mm/yr) precipitation levels are seen in the plateau interior with rainfall rising to > 900 mm/yr in the northern mountain ranges bounding the plateau (IMO, 1997). Rainfall levels are lower to the south, but are still higher than in the plateau interior.

A)

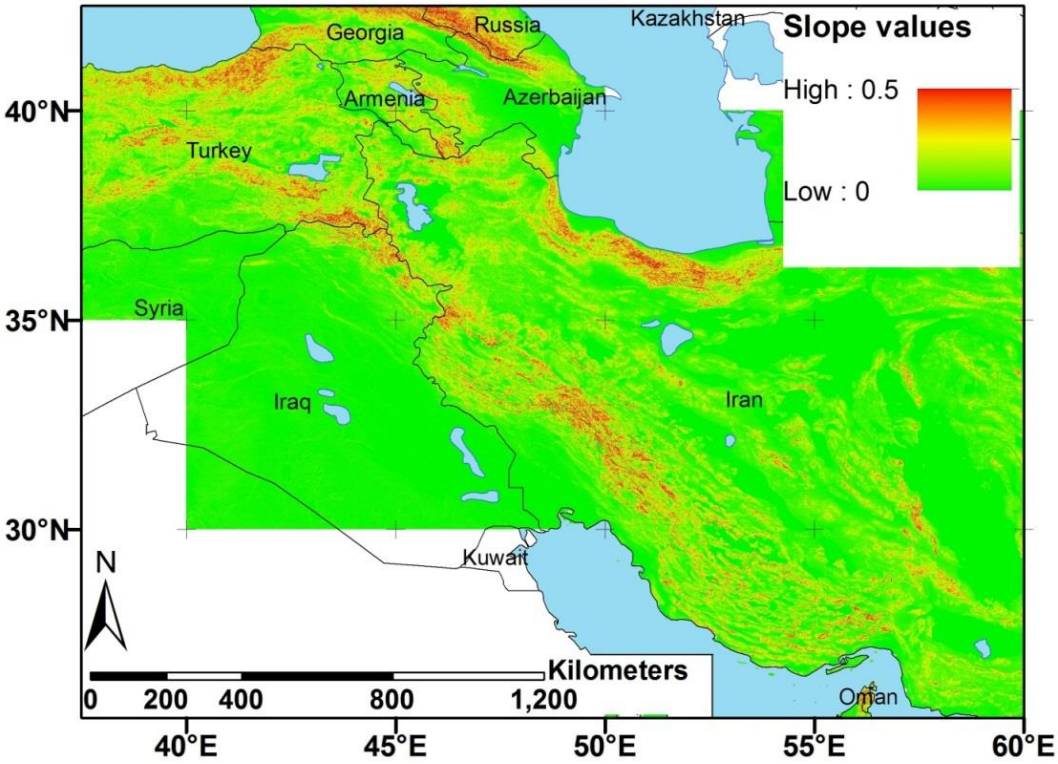

B)

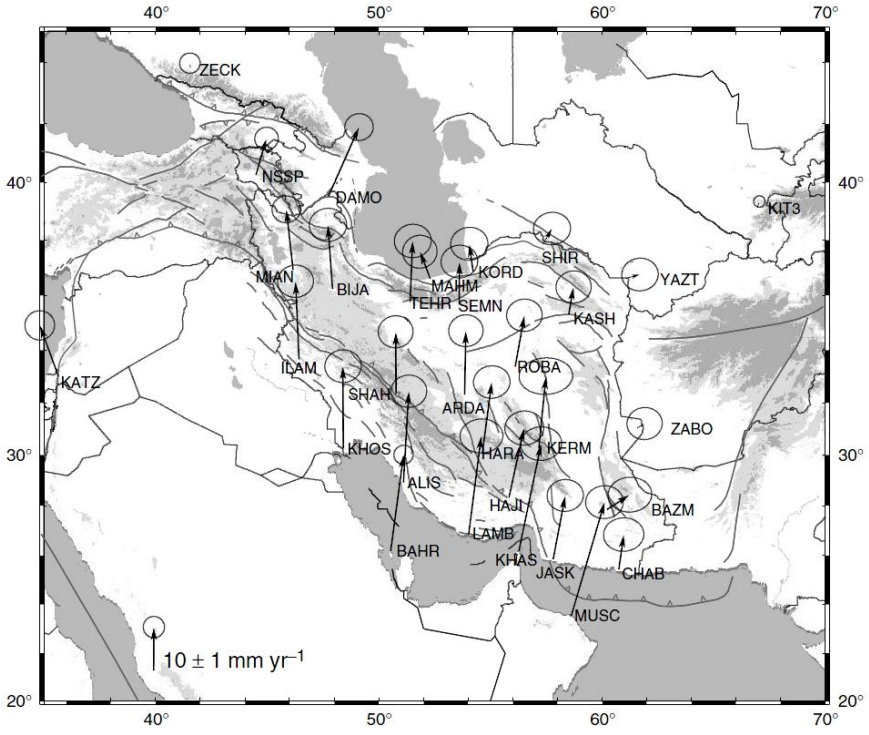

See over for caption

C)

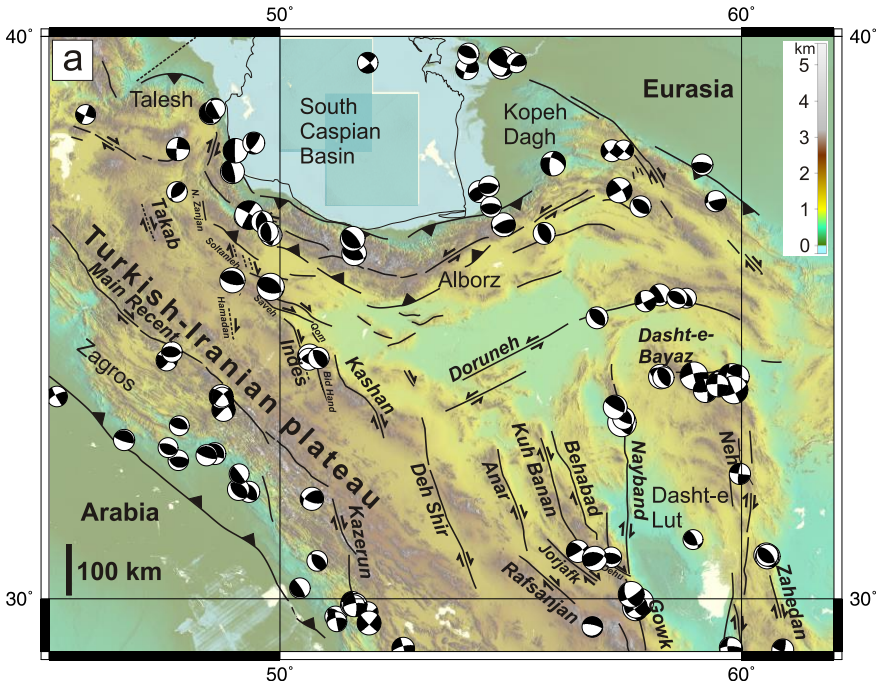

1.5 –Overview of the Turkish-Iranian plateau *Basic features of the Turkish-Iranian plateau: A) Slope values across the region. Note high slopes at the margins. B) GPS velocity field relative to Eurasia from (Vernant et al., 2004b). Uncertainties shown by ellipses. Text is codes for International GPS Service stations. C) Tectonic overview of the plateau, modified from (Allen et al., 2011a).*

1.4.2 The Tibetan plateau

The Tibetan plateau is an orogenic plateau formed by the collision of the Indian and Eurasian plates. Estimates for the initiation of collision range between 70 to 35 Ma (Aitchison et al., 2007; Hu et al., 2012; Searle et al., 2011; Searle et al., 1987; Yin and Harrison, 2000) and is currently active at a rate of roughly 40-50 mm/yr (Molnar and Stock, 2009; Patriat and Achache, 1984; Zhang et al., 2004). The shortening is accommodated in north dipping thrusting along the Himalayan and Karakoram mountain ranges, with further shortening taken up in thrusting and strike-slip movement in central and south eastern Asia (Armijo et al., 1986; Cook and Royden, 2008; Tapponnier et al., 1986). While shortening is occurring in a north-south orientation, the plateau is

undergoing east-west extension on a set of north-south orientated normal faults, mainly within southern Tibet (Molnar and Lyoncaen, 1989), this extension may represent the beginning of gravity driven plateau decay, although currently the plateau is still growing.

The Tibetan plateau is the largest and highest plateau on earth with a plateau interior size of ≈3.15 million km^2 and a height across the plateau of roughly 5 km above sea level. The high plateau is underlain by thick crust ranging from 60-80 km (Li et al., 2006). The thickest crust is found to the south of the plateau where the Eurasian plate is underthrust by the Indian plate.

Rainfall levels vary greatly between the low levels in the plateau interior and the maximum along the Himalayan mountains. The variation is from less than 400 mm/yr (Sobel et al., 2003) in the plateau interior to over 3000 mm/yr due to monsoon driven precision along the Himalayan rangefront (Bookhagen and Burbank, 2006; Wobus et al., 2008).

A)

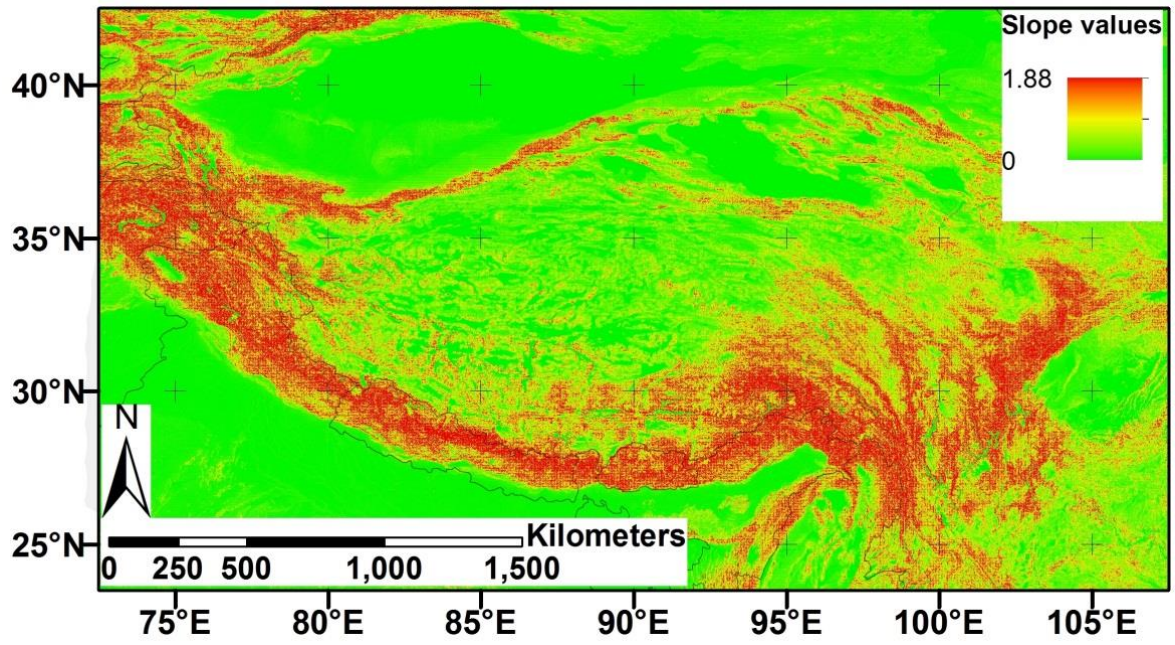

B)

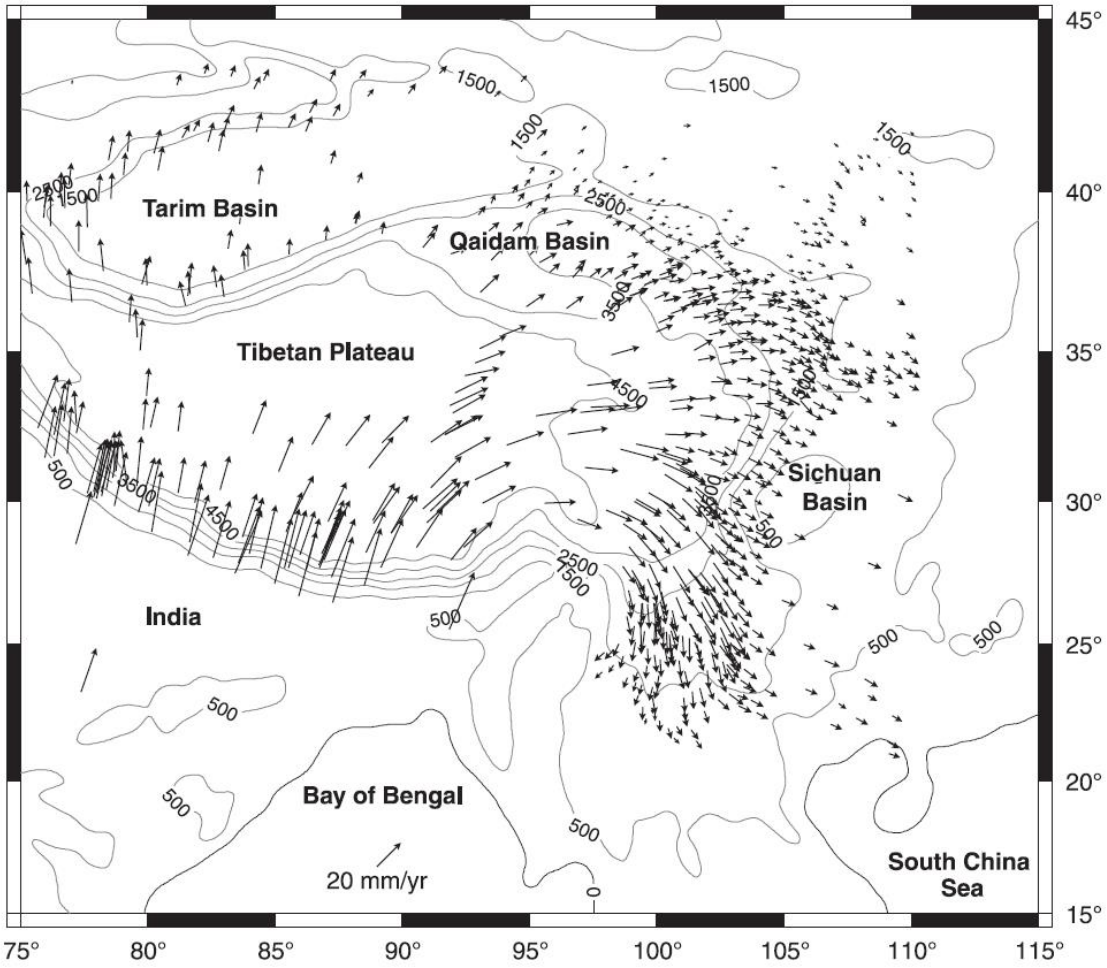

See over for caption

C)

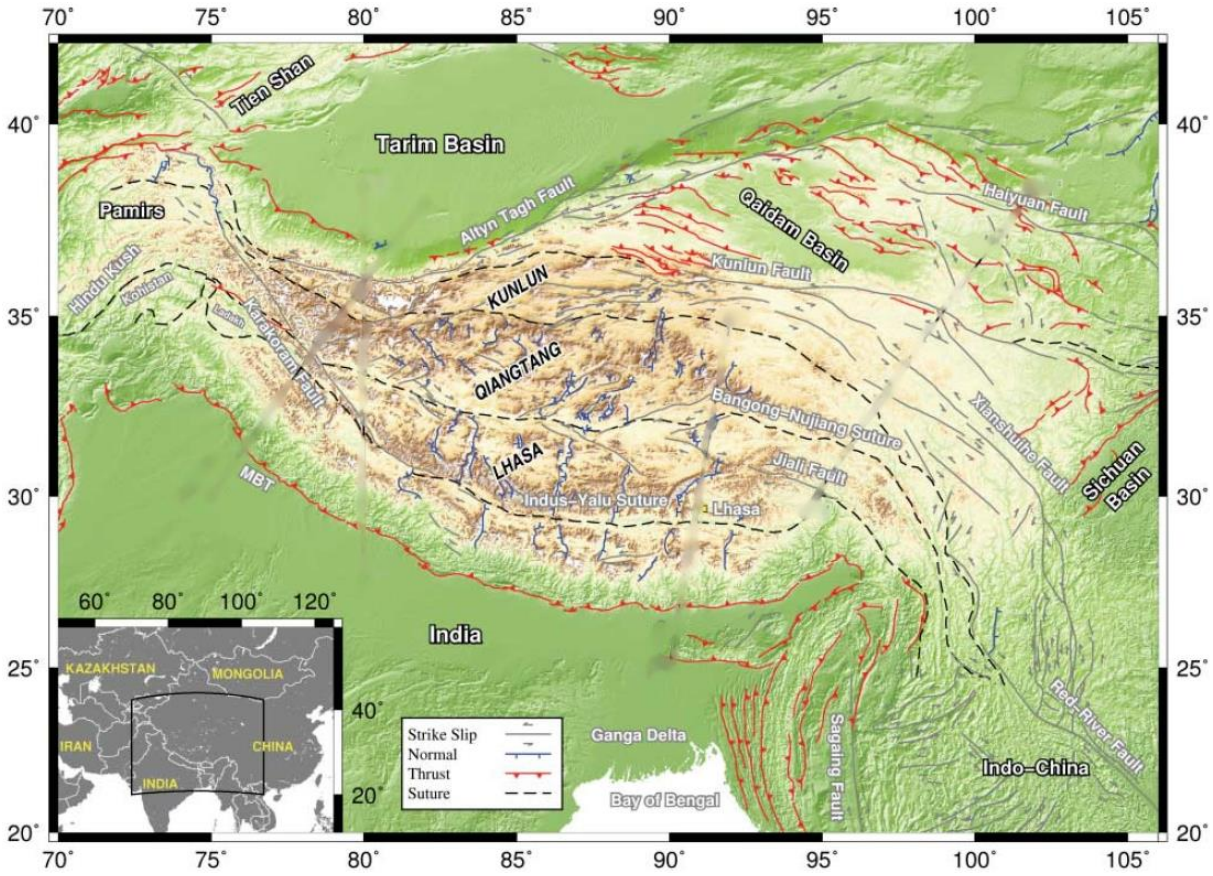

1.6 –Overview of the Tibetan plateau *Basic features of the Tibetan plateau are shown: A) Slope values across the region. B) GPS velocity field relative to Eurasia modified from (Gan et al., 2007) , the grey arrows show the velocity of India relative to Eurasia from (Sella et al., 2002). Ellipses show uncertainties in the GPs measurements. C) Tectonic overview of the plateau from (Searle et al., 2011).*

1.4.3 Delimiting plateau extent

Orogenic plateau regions can be split into several different areas. Primarily they consist of a low relief, high elevation plateau interior, a set of fringing mountain ranges and lowlands outside the mountain ranges that act as the sink for drainage that moves material from the plateaux interiors. These lowlands can also be water bodies that act as the termination point for plateau drainage.

It is useful to delimit the differences between these areas, so that the effect of different topographic, tectonic and climatic settings on plateau geomorphology can be

categorised and described. There are multiple ways of evaluating how the plateau extent can be designated These ways are described in the following sections, along with a consideration of which method is most appropriate to use in the studies that form the rest of this thesis. While other methods not mentioned below could also be used for designating the cut-off between the plateau interior and the surrounding mountain ranges (e.g. geological terrane changes), the options are limited to those that can be accomplished with the remote sensing methodology used in this thesis.

1.4.3.1 Seismicity delimitation

A seismicity delimitation of the plateau interior considers the difference between the plateau interior and the surrounding mountains based on the processes ongoing in the orogen, rather than the topographic approaches, which rely only on the expression of those processes in the resulting geomorphology. This approach highlights the contrasting seismicity properties of the plateau interior and the surrounding mountains. The conceptual model of a plateau used in this case is that the plateau is a relatively seismically quiescent region surrounded by actively thickening thrusting regions (to be more precise, the plateau interior could contain active strike-slip and extensional faults, but not thrusts). The plateau interior has been subject to thickening to form the high elevation (and thickened crust) that defines the plateau interior, but deformation moves outwards as a threshold thickness is reached where it becomes energetically unfavourable for thrusting to continue as compressional forces are balanced by gravitationally driven spreading forces. Thrusting then continues within the plateau margins until they thicken to the level of the plateau interior (Andronicos et al., 2007; England and Houseman, 1988).

This allows the difference between the plateau interior and the plateau margins to be defined by the tectonics in each region. In this situation the plateau interior is defined as the region where significant seismogenic thrusting is absent. As the thrusting stops due to excess thickening the boundary between the regions where thrusting is absent (interior)

and the thrusting is present (margins) should correspond to an elevation value, above which it is energetically undesirable for thrusting to continue. To carry out this division into plateau interior and plateau margin the location of seismic thrust events with Mw > 5.5 and with double couple values greater than 80% were plotted up for both the Turkish-Iranian and Tibetan plateaux. In both cases, the division between thrust events present or not lie at an elevation contour. The elevation is different between the Turkish-Iranian and Tibetan plateau, with the area above 1000 m being the seismically delimited plateau interior for the Turkish-Iranian plateau and the cut-off being 3500 m for the Tibetan plateau.

A)

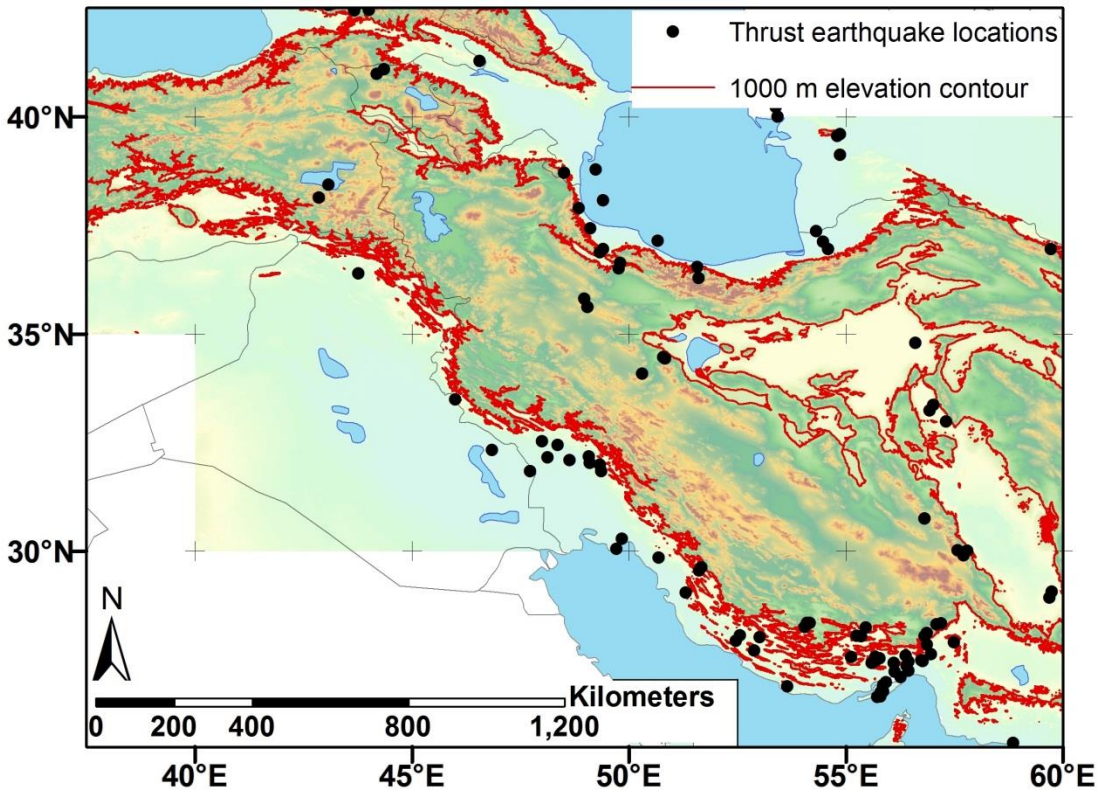

B)

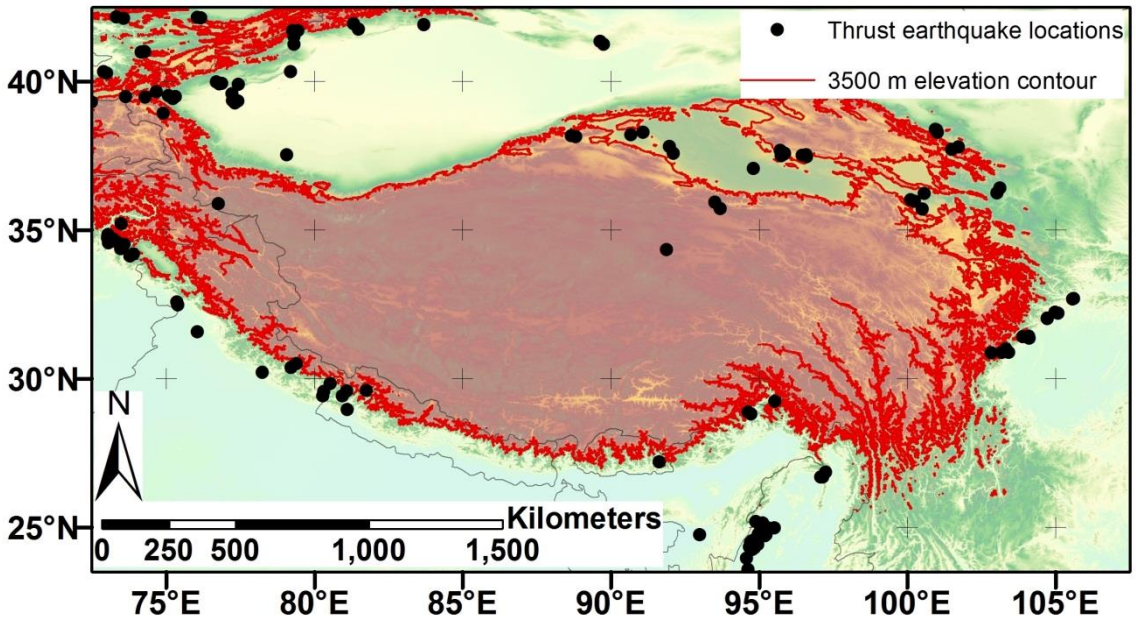

1.7 – Seismic delimitation of plateaux interiors *A) Turkish-Iranian plateau B) Tibetan plateau. In both cases note that the majority of the seismic thrust events lie below the elevation contour used to delimit the plateau interior (1000 m for the Turkish-Iranian plateau and 3500 m for the Tibetan plateau). Thrust events filtered to only include those with a magnitude over 5.5 and a double couple value of over 80% (Jackson, 2001).Earthquake locations from (USGS, 2010)*

The cut-offs for the two plateaux are different. This is due to the Tibetan plateau being capable of supporting greater thickening than the Turkish-Iranian plateau. This is caused by a combination of greater lithospheric strength and convergence rate in the Tibetan case (Copley et al., 2011; Maggi et al., 2000; Maggi and Priestley, 2005).

1.4.3.2 Topographic delimitation

Using the topography to delimit the plateau interior is the most intuitive way of identifying an orogenic plateau as a plateau is fundamentally a topographic feature. There are multiple ways of approaching this problem. (Masek et al., 1994) suggested that the edge of an orogenic plateau can be defined by identifying a high ridge around the plateau edge formed by the high mountain ranges that are diagnostic of the plateau margin. While the highest elevations in an orogen are found in the fringing mountain ranges, this definition does not hold up, as the overall elevation of the mountain ranges ringing both the Turkish-Iranian and Tibetan plateaux do not have average elevations that are larger than the average elevation of the plateau interior. They merely have larger relief (England and Houseman, 1988).

A more fruitful approach to plateau interior delimitation using topography considers the particular shape of a plateau. A plateau is a high elevation, low relief region of topography. This can be parameterised by dividing the average elevation of an area by the relief in that same area (Andronicos et al., 2007). This provides a ‘plateauness’ (ζR) value that can then be assigned to the point in the middle of the area. This window can then be swept over the study region to associate ζR values with all the points that make up the orogen. By defining a ζR cut-off, plateau interior regions can be distinguished from the plateau margins.

This approach can be susceptible to being influenced by the size of the moving window. Using GIS software to repeat the process with different sized windows, producing a raster of ζR values each time and then comparing these 3-D surfaces (with the

third dimension being ζR, rather than elevation) can show a range of window sizes where the variation is due to genuine changes in ζR, rather than changes in window size. If the difference between two rasters is low, than the variations in ζR values in those rasters are likely to be due to changes in plateau topography, rather than changes in window size, as both rasters will be displaying similar ζR values.

1.4.3.3 Plateau definition to be used and rationale

In general this thesis will use the seismic delimitation as the way of determining a cut-off between plateau interior and the surrounding mountains. Although there are cases where considering the topography of the plateau is more appropriate for classifying the observed geomorphological features (see chapter 4), if not specified for the rest of the thesis, it should be assumed that the plateau interior refers to a region within a particular elevation contour, where the elevation contour is a cut-off for plateau building thrusting.

This definition is chosen to help with addressing the first aim of the thesis. Using a seismic definition of a plateau gives a definition that is based around the forces driving plateau formation. As the thesis aims to investigate the connection between the tectonic (and climatic) setting of a plateau and the resulting geomorphology, a definition that can divide the plateau into regions with distinct forcing factors allows for a better investigation into how the topography responds to different inputs.

1.5 Data used

All the analysis of the plateau morphologies is done with remotely sensed data. Mostly this is done with digital elevation maps (DEMs) and satellite imagery. These data sources are complemented with some climatic data, primarily 30 years of precipitation data from the Iranian Meteorological Organisation.

1.5.1 Topographic data

The topographic data used in this thesis are DEMs derived as part of the Shuttle Radar Topogrpahy Mission (SRTM). This provides elevation data by timing radar returns from and to NASA's shuttle orbiter meaning the base data is in the form of radar phase differences assigned to each pixel in the DEM. This means that the data requires processing to produce a workable DEM. The pixel size of the DEMs produced is 90 x 90 m. The raw data needs careful processing as it is subject to multiple sources of systematic error. The radar reflection can be from objects that are not the ground surface, so areas of vegetation such as forests can artificially increase the apparent elevation of an area. Furthermore the radar signal is absorbed by water and does not return to the sensor if reflected at high angles. As a result lakes, seas and regions of high slope produce voids within the data.

To cover these voids the v.4 data from CGIAR (Howard and Kerby, 1983) was used. This dataset fills in voids within the SRTM data with data from other sources, mostly the GEOTOP 30 dataset. This is a DEM with a pixel size of 1km, as a result although the data files have a constant 90 m resolution across the area, some regions will have a data sampling resolution of more than that and the values provided by the data files are just interpolated.

1.5.2 Satellite imagery

The satellite imagery used is Landsat 7 Enhanced Thematic Mapper + (ETM+) data. The Landsat 7 ETM+ tool detects electromagnetic radiation reflected and emitted from the Earth, but unlike the SRTM, does not need to produce any signal itself. The ETM+ tool collects electromagnetic radiation in 7 distinct bands (see table 4.3) that correspond to different parts of the visible and infra-red regions of the electromagnetic spectrum. The intensities of the bands can be used to produce composite colour images from 3 bands by assigning red, blue and green intensities of the composite image to three of the 7 possible

bands. This produces false colour images as none of the Landsat 7 ETM+ bands perfectly align with RGB colour bands used to produce composite colour images. In the case of the images used bands 7, 4 and 2 are used as the red, green and blue bands respectively

The pixel size of the seven main Landsat 7 ETM + bands is 30 x 30 m. However the pixel size of the satellite images used in this thesis was 15 x 15 m. This is because the Landsat 7 ETM + tool also has a panchromatic band whose bandwidth is too large to produce useful images, but has a resolution of 15 m and so can be convolved with the multi band images to sharpen them.

1.6 Thesis Outline

The main body of the thesis is three chapters (2-4) detailing research describing geomorphology and comparing those features to the local settings. They all look at aspects of the linkages between the geomorphology and the tectonic and climatic drivers of a region, but use a variety of methods and study areas to do this. Chapter 2 evaluates the morphology of rivers crossing from the interior of an orogenic plateau to its margins. Chapter 3 builds on the work of chapter 2 by doing 2-D modelling of the formation of the river profile shapes seen in chapter 2. Being able to vary the parameters controlling the development of a river draining an orogenic plateau allows for an investigation into what factors control orogenic plateau morphology. Chaper 4 continues looking for linkages between climate, tectonics and geomorphology of orogenic plateaux. In this case the context is that of the large numbers of alluvial fans seen within the Turkish-Iranian plateaux.

Chapter 5 provides a synthesis of the key research findings derived from the previous three chapters. These findings are discussed and there is a consideration of where they fit into the wider context of fluvial and geomorphic plateaux. In addition, I outline on-going and potential future research projects resulting from the findings and techniques

of this thesis, highlighting the research questions that remain to be addressed. Finally, I provide a clear restatement of the main findings of these studies in chapter 6.

2. Morphology of river longitudinal profiles in orogenic plateaux and their margins

In this chapter, the forms of longitudinal profiles of rivers draining from the interior of the Turkish-Iranian and Tibetan plateaux to the respective plateau margins are quantified. Looking at the drainage of two orogenic plateaux (the Turkish Iranian and Tibetan plateaux) allows for a comparison between two similar tectonic and climatic settings. Features of the drainage from one plateau that are similar to the features of the other suggest that those features are diagnostic of plateaux in general, rather than being particular to an individual plateau. The observed morphologies are compared to theoretical forms of a river in topographic equilibrium (Begin et al., 1981; Knighton, 1998; Snow and Slingerland, 1987). This comparison allows for an understanding for a how a river is affected by the particular setting of flowing from a relatively stable and arid plateau interior through a deforming and relatively wet plateau margin. The tectonic and climatic conditions along the length of a river draining from a plateau interior to a plateau margin contrast with the modelled, measured and assumed conditions of previous studies (Amos and Burbank, 2007; Roe et al., 2002, 2003). In addition to the problem of how the river longitudinal profile is affected by particular conditions of an orogenic plateau, the feedback between this fluvial morphology and the driving factors is examined. This requires a consideration of the observed river form found in the studied plateau regions. The deviation of these long profiles from a theoretical shape has implications for the effect of the studied rivers on the continued growth of orogenic plateaux. Rivers draining from a plateau interior to the plateau margin show a sigmoidal longitudinal profile, meaning lower gradient headwater reaches when compared to a more typical concave-up river profile. This lack of gradient in the headwaters would correspond to a lack of incision in the plateau interior and a related lack of material removal from the plateau interior,

thereby not retarding lateral plateau growth, which would happen if the rivers were efficient agents of erosion.

2.1 Effect of drainage on plateau development

Drainage of an orogen is a first order control on the topography of the orogen (Ahnert, 1998; Allen and Allen, 2005; Ramsey et al., 2008). By acting as the base-level for hillslope erosion processes rivers directly influence the rate of surface material removal across an entire orogen. If a river's transport capacity is lower than the rate at which material is supplied by the adjacent hillslopes, through landsliding, slumping and soil creep processes (transport limited systems) (Allen and Hovius, 1998; Burbank et al., 1996), then sediment accumulates within and adjacent to the river, increasing the elevation of its long profile and reducing the gradient of the adjacent hillslopes. On the other hand, if the transport capacity of a river outpaces the rate of sediment supply then net incision occurs (a detachment limited case). In this case the river undercuts the local hillslopes, increasing their gradient. The rate of erosional processes is proportional to the gradient of the hillslopes, so rivers' affecting adjacent hillslope gradients translates to a control on local erosion rates (Allen and Allen, 2005; Larsen et al., 2010).

Controlling local erosion rates makes rivers an important control on the formation of the orogenic plateau they drain (Brookfield, 1998; Wobus et al., 2008). River incision and the resulting increase of erosion on the adjacent hillslopes works against geomorphic plateau formation processes. If the rate of erosion removing material from the plateau is greater than the rate of tectonic advection of material into the region, then river incision causes a retardation of the plateau (Garcia-Castellanos, 2007; Masek et al., 1994). Essentially, for a plateau to grow, rock uplift must be greater than the rate of incision along plateau-draining rivers. The form of a plateau-draining river is both indicative of and a control of incision along its length, as stream power (a measure of energy dispersion along the banks and bottom of a stream and therefore a first order control on the amount of

incision a stream can perform) is dependent on the gradient of a river at a given point. Therefore, understanding and quantifying the form of rivers draining orogenic plateaux can help to identify the loci of incision along their lengths. Knowing where loci of incision are along plateau-draining rivers is likely to help to understand current plateau growth/retardation processes (Clift et al., 2008; Korup, 2006; Whitehead and Clift, 2009). If there is considerable incision within a plateau interior, this suggests that plateau-draining rivers are retarding plateau growth by removing material from the plateau interior to the surrounding lowlands. If no reach within the river seems indicative of increased incision, or the loci of incision are within the plateau margins it suggests that the net effect of these rivers is not to retard growth of the plateau.

2.2 River networks extracted

To investigate the river networks draining the Tibetan and Turkish-Iranian plateaux, the form of these river networks was defined. To get three dimensional information on the long profiles of plateau-draining rivers, elevation values were extracted from SRTM (Shuttle Radar Topography Mission) DEMs (Digital Elevation Maps) (Jarvis et al., 2008; Jarvis et al., 2004). This requires knowing the path of plateau-draining rivers and then extracting the elevation values from each pixel of the DEM that coincides with the river path.

Using the SRTM data to derive elevation values along river profiles has some accuracy and precision issues:

1) The pixel size of the DEM is 90 metres, making this the smallest distance between sample points along the river profile. This sample spacing is not consistent as the pixels are square.

2) If the sampled elevations along a river are not adjacent to each other, but are arranged diagonally on the DEM pixel grid the sample spacing will be

90 m x √2 (127.3 metres). This discrepancy could be avoided by using a custom DEM based on regular hexagonal or triangular pixels.

3) The SRTM DEM data make it necessary to sample the river profile data along the horizontal, rather than using vertical sampling or sampling directly along the three dimensional length of the profile. This makes it possible to miss knickpoints whose elevation change is sufficiently small that when averaged over a 90 metre horizontal length scale they do not seem to have a gradient higher than the background gradient of the river. Missing knickpoints that are this small does not matter for the purposes of this study. These small scale increases in gradient can be attributed to local causes that do not represent the plateau scale river forms and processes this study investigates (Bishop et al., 2005; Miller, 1991; Wohl, 1993).

4) The elevation value associated with each pixel is an average of the elevation within that 90 metre x 90 metre area; this has implications for the detail of extracted river profiles. In many cases, the width of the investigated rivers is less than 90 m, this means that the elevation values extracted from the DEMs are overestimates. These oversized pixels convolve the elevation of the rivers and the adjacent banks, increasing the mean elevation value to higher than that of the actual value of the river surface. Near incised gorges this effect is pronounced as the contrast in elevation values between the river surface and adjacent riverbanks is larger. Many gorges are due to rivers responding to changing conditions by narrowing and increased incision (Tealdi et al., 2011; Wohl, 2000), this narrowing further distorts the elevation value assigned to a river profile as

more of the area of a DEM pixel will be composed of the river bank than the river surface if the channel width is narrower.

5) An additional error in the elevation values obtained from the SRTM DEMs is due to features that interfere with the radar signal getting to the ground surface. Examples of these include forested patches and buildings; these features increase the elevation value assigned to the DEM pixel they are within, causing a further overestimate of elevation values (Bhang, 2005; Jarvis et al., 2004).

Assigning elevation values to the length of a river is trivial for a single river, where its course can be determined relatively easily, but attempting to do this for the drainage of two orogenic plateaux and their surrounding margins, with an area of 3 million km^2 in the Turkish-Iranian case and 13.9 million km^2 in the Tibetan case, is much more difficult, requiring a greater investment of time and/or computational resources.

2.2.1 River networks derived from DEM data

One approach to acquiring the horizontal, plan-view locations of river networks is to use the DEM data to automatically generate river networks. The elevation values can be used to locate river locations using the D8 river routing algorithm (Tarboton et al., 1991). This algorithm simulates placing a unit of water on every pixel of a DEM. Starting with the highest elevation values, the pixel's unit of water is moved to the adjacent or diagonally adjacent pixel with the greatest elevation gradient between it and the source pixel (giving 8 directions for the water to be routed), adding to the unit of water already in that pixel, simulating run-off down the steepest local slope. This process is repeated, allowing water to accumulate in local lows and saddle points. The routing of the water stops when the flow accumulation reaches a pixel which is lower than all the surrounding pixels (a sink)

or the edge of the DEM. The implementation of this algorithm used is that found in the ArcGIS hydrological toolset.

After using local slope to determine how much water accumulates in each pixel, before the water moves onto a lower pixel, the pixels that are part of the river network need to be designated. To do this a value of flow accumulation is used as a cut-off, so that pixels with flow accumulation values above this are designated as being part of a river network.

The flow accumulation values used to determine whether a pixel contains a river or not are arbitrarily chosen. A suitable flow accumulation value could be chosen by an iterative process of altering the cut-off values until the represented drainage network is within a specified (although necessarily arbitrary) agreement with the actual drainage network within the study area. This approach would need prior knowledge of the existing drainage network, making the point of determining the position of the drainage network redundant. As will be seen, there are significant disadvantages with automating the finding of the location of the drainage network in this way, so if the cut-off used requires determination of the drainage locations anyway, it may as well be determined manually.

Determining the appropriate flow accumulation cut-off to use involves the following trade-offs. Setting the value too low preserves detail of the river networks, but highlights pixels as belonging to the drainage network that are not part of the area's river network. An overly low cut-off value also produces a drainage network that includes many rivers that are too small to be of interest when looking at plateau-wide drainage and that do not run from the plateau interior to the margins. If the cut-off value is set too high, although only the largest rivers are picked out (which are the ones of interest to this study), the uppermost reaches of the rivers do not get picked out, as the flow accumulation is lowest in the head waters where the effective drainage area is low (see figure 2.1).

A)

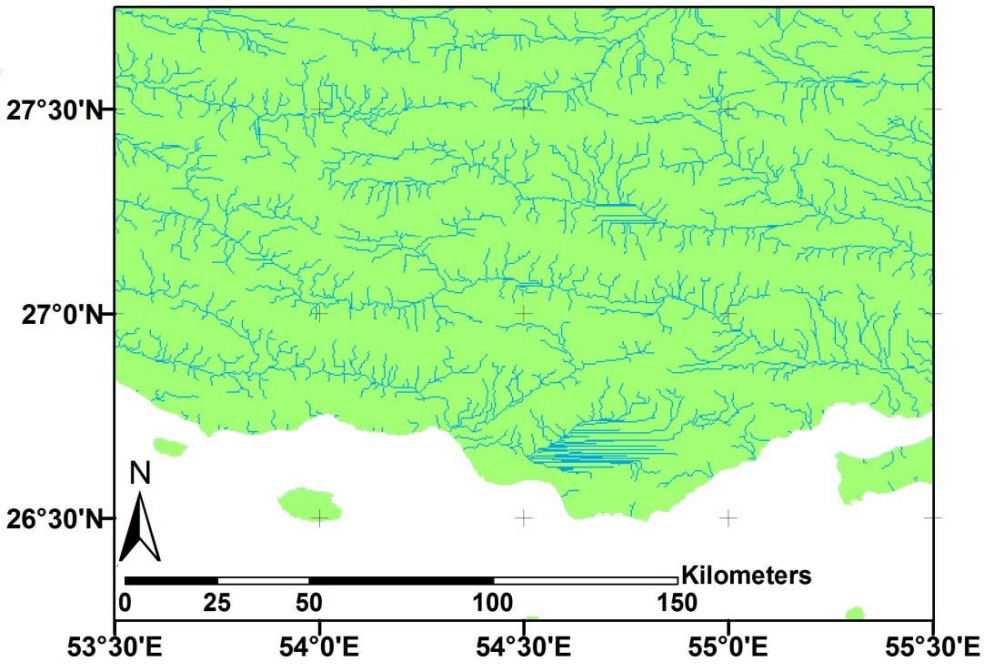

B)

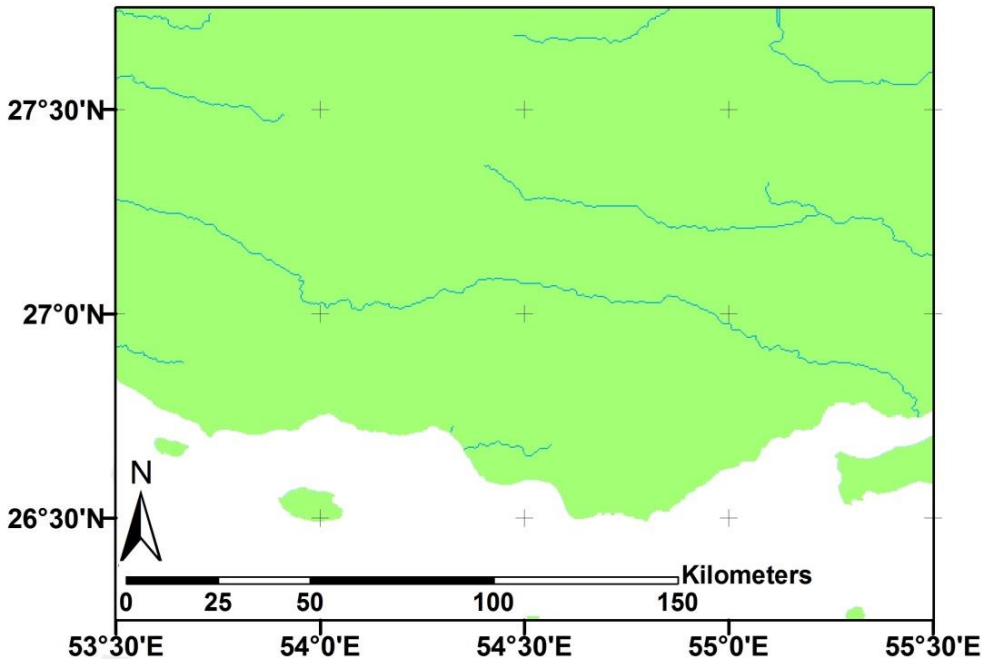

2.1 – Diagrams showing the effect of changing flow accumulation values. *A) A river network generated using a comparatively low value for flow accumulation (10 km^2). B) A river network generated using a comparatively high value for flow accumulation (1000 km^2). Although A) shows more detail in the river network, much is spurious and may not correlate with the drainage of the area. Note that the networks some completely straight sections. This is where conditioning of the DEM has caused the algorithm to fail. The examples here are taken from SE Iran.*

To produce useable river networks, high flow accumulation values were used which produce drainage networks that highlighted only the big rivers draining from the plateau interior to the plateau margins, while making sure that the value chosen was low enough to preserve most of the length of these rivers. The algorithm was run multiple times to find final values to use that produce traces of the main plateau-draining rivers whose lengths were within 10% of the length observed when low flow accumulation values are used, while still removing the spurious river traces seen in the low accumulation case. The flow accumulation cut-off values used correspond to a drainage area of 500 km^2 for the Turkish-Iranian plateau and 5000 km^2 in the case of the Tibetan plateau. While not too much can be read into the variation in these values as they are not calibrated to a particular drainage pattern or hydrological setting, the order of magnitude difference between the two plateaux is striking. While not investigated as part of this study, a difference of a factor of ten seems to fit well with the scaling differences between the two plateaux. The tectonic cut-off for the Tibetan plateau is set at 3.5 km elevation (using the elevation limit of seismogenic thrusting), while that for the Turkish-Iranian plateau is at 1 km elevation. This factor of 3.5 for a linear feature is approximately the square root of ten, the scaling factor for the 2-D variable of drainage area. Differences between the two plateaux could represent different climate between the two, with a drier climate in the Tibetan case requiring a greater drainage area for the creation of a plateau-draining river. Alternatively, this numerical difference could represent increased drainage capture having occurred in the drainage of the Tibetan plateau, resulting in larger drainage areas associated with the rivers draining this plateau, as the rivers with smaller drainage areas are just tributaries of these larger rivers.

Using the D8 algorithm to determine the location of the drainage network requires that the DEM is conditioned before the algorithm is run. This conditioning is needed as the algorithm terminates at pixels that are topographic sinks. Therefore, running it on an unconditioned DEM produces an unrealistic drainage network, where rivers are frequently

bisected by sink pixels that do not represent actual topographic features, but are present due to inaccuracies in the underlying DEM. The base SRTM data have a vertical accuracy level of 8m (Jarvis et al., 2004; Rodriguez et al., 2005). Thus, areas of low gradients, where this error is greater than the elevation difference between adjacent pixels, are particularly prone to sinks caused by inaccuracies in the data. This is exacerbated in rugged, mountainous regions (such as the gorges formed by plateau-draining streams) where the elevation error is often higher (ref Jarvis, 2004). The conditioning to remove these spurious sinks involves increasing the elevation values of the sink pixels to the lowest of their surrounding pixels. This is an iterative process, as after the first elevation increase is performed, the pixel is then evaluated to see if it is now part of a larger multi-pixel sink, in which case, this new sink is then raised until it is at the same elevation as the lowest surrounding pixel. This conditioning produces hydrologically sound DEM's but does not distinguish between sinks in the region due to DEM flaws, or those that represent the termination points of internal drainage. Much of the area of an orogenic plateau is internally drained, so removing real sink areas and forcing the entire plateau to be externally drained produces drainage networks that do not correlate well with the reality of the drainage networks of the studied orogenic plateaux (see figure 2.2). Useful drainage networks can still be derived automatically from DEM data, but that requires identifying real topographic sinks manually, by using other datasets to identify river termination points. However, if that is done, the river locations will have already been identified, making the point of using the DEM data to determine the form of the plateau-draining drainage network redundant.

A)

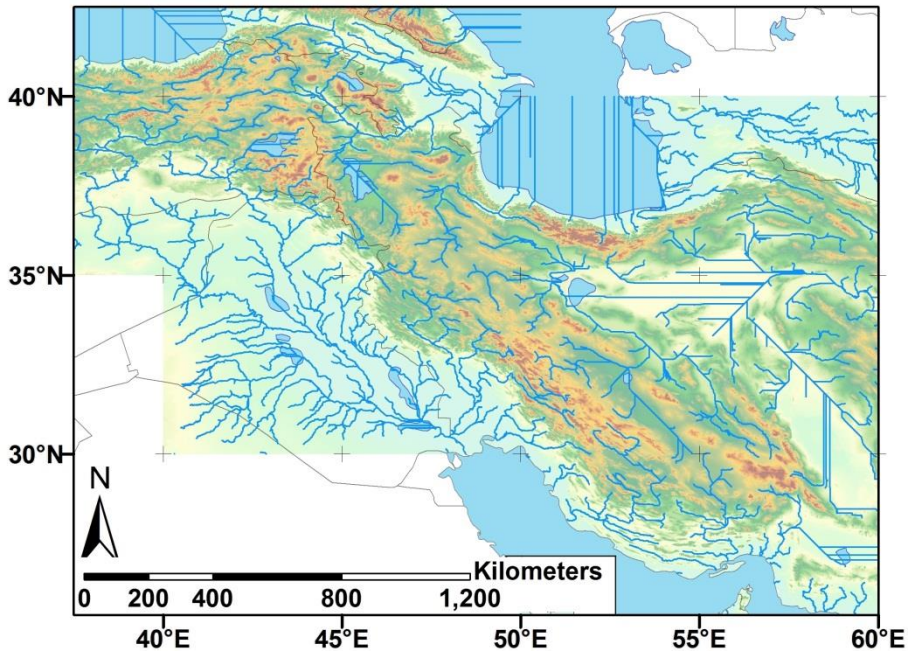

B)

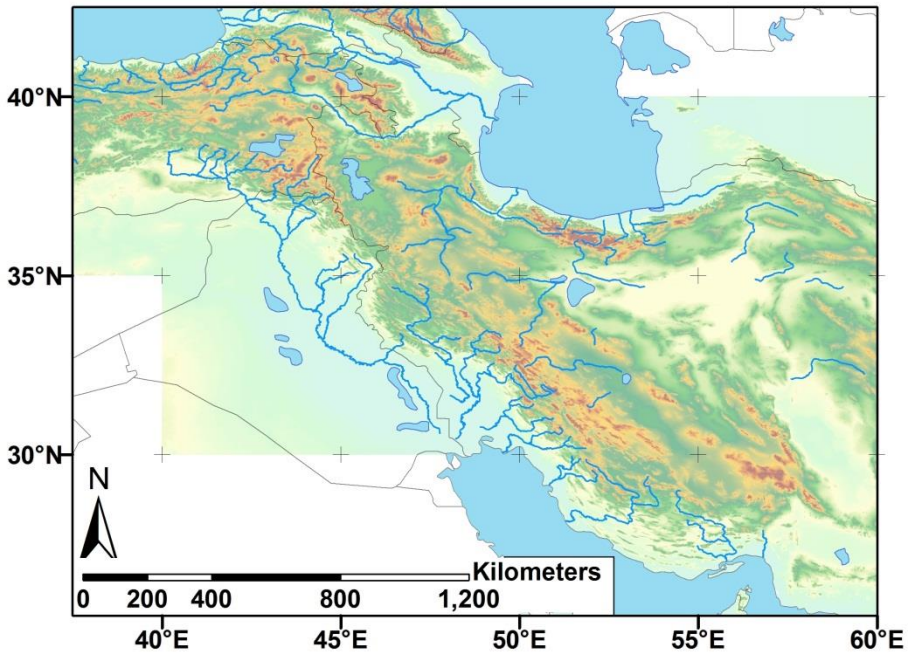

2.2 –Turkish-Iranian plateau drainage networks derived using the D8 algorithm and inspection of Landsat images. *A) Drainage network from D8 (Tarboton et al., 1991) applied to SRTM data. Conditioning the DEM causes the algorithm to fail in the plateau interior, producing perfectly straight traces. River sections are falsely connected by the algorithm. B) Network from inspection of river traces observed on Landsat 7 ETM+ images. This network is less comprehensive, with only rivers of interest. However, it is more accurate.*

The maximum lateral precision of a drainage network theoretically possible using the SRTM data is 90 m. The drainage networks derived using SRTM data for this study have less precision than this. This is because using the D8 algorithm over the extent of an entire orogenic plateau on the 90 m square pixels of the native DEM proved to be too computationally intensive. Instead the DEMs were resampled to 324 metre square pixels for the Turkish-Iranian plateau and 540 metre square pixels for the Tibetan plateau, representing the larger size of the Tibetan plateau. These pixel sizes are the smallest usable pixels that allow the computations to happen within available memory constraints.

2.2.2 River networks derived from Landsat 7 (ETM+) images

The other way to obtain the plan view position of river networks is to look at river traces on satellite images and digitise them into a georeferenced reference frame. The river traces can be identified by either manually scanning the images or using properties of river traces to pick out river locations. The Landsat 7 ETM+ images provide false colour information in a 24 bit format, where 8 bits are designated to each of the three colour channels, with red corresponding to medium wavelength infra-red radiation, green corresponding to short wavelength infra-red radiation and blue corresponding to the green part of the visible light spectrum. As the Landsat images provide colour information to be interrogated, any consistent spectral properties of river traces would allow the location of rivers to be automatically determined.

Two issues prevent the use of a spectral analysis approach to determining river locations using Landsat 7 ETM+ images. Firstly, there is a lack of consistent colouring of the observed river traces (see figure 2.3), making defining the spectral ranges to use in confining which pixels belong to rivers impossible. The natural variation in the displayed colours of the river traces is exacerbated by the number of ephemeral rivers that were dry at the time that the Landsat image was captured, changing their appearance relative to a filled river bed. Secondly, to produce a river profile a plan-view line, not an area, is

needed. Using the DEM driven method of automatically determining river position produces drainage networks with rivers that have to be one pixel wide, while picking out river pixels with a spectral analysis technique does not produce a line (and therefore one-pixel wide trace), but instead an area where the river is located. This is an issue in the case of wide rivers, where the area delimited as being part of a river is wider than one pixel. In these cases, the automated spectral analysis approach does not produce a definite path for the river.

A)

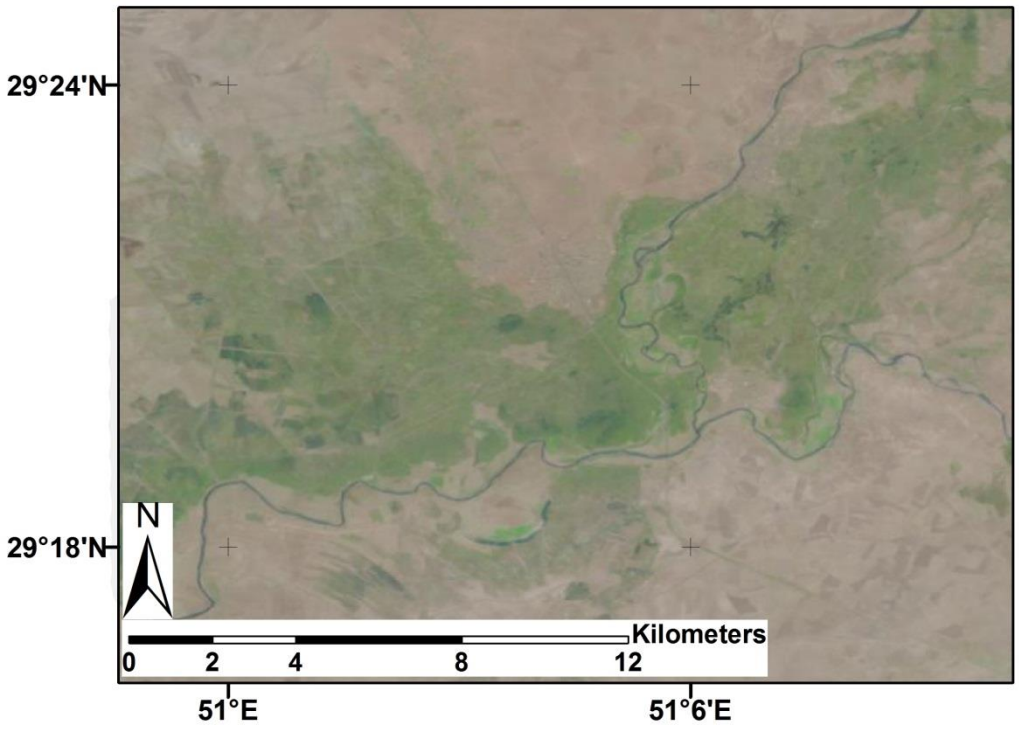

B)

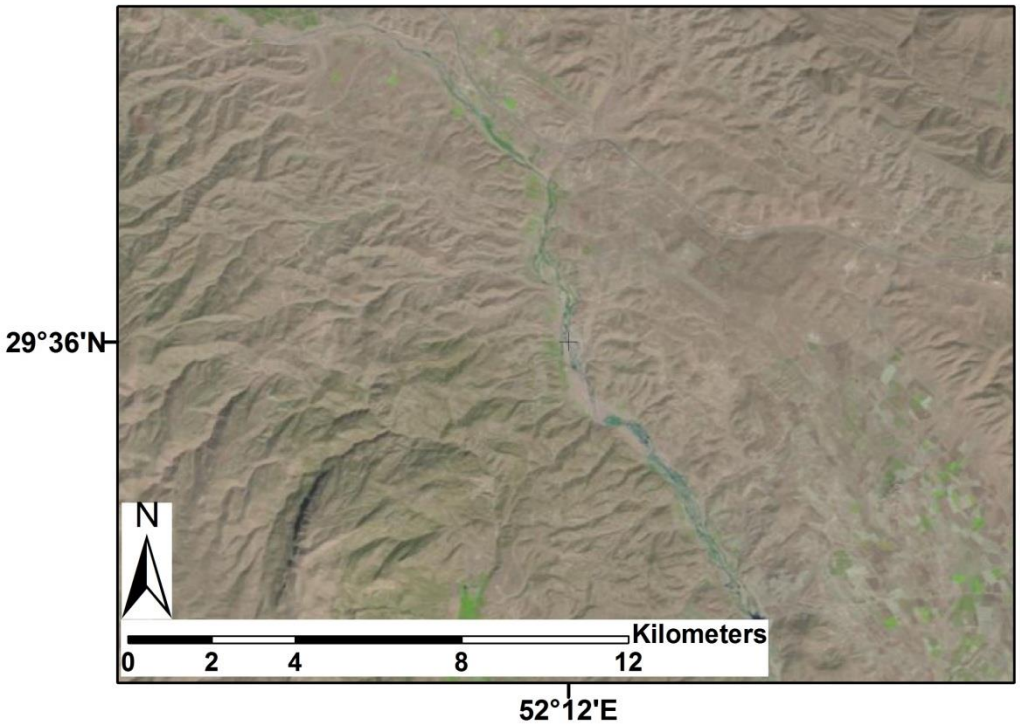

2.3 – Landsat 7 ETM+ images of observed river traces *A) A meandering river with a uniform blue colour. B) An anastomosing river with a lighter more varied colour. The variation in the pictures show the difficulties in automatically designating rivers from Landsat 7 ETM+ images.*

The long profiles extracted using traces determined from the Landsat 7 ETM+ images and then the elevation data from the spatially corresponding SRTM data are noisy. This noise comes from a variety of sources. Noise in the underlying data affects the vertical accuracy of the profiles, in a similar way to the profiles extracted using the D8 algorithm on the SRTM DEMs. This source of noise is particularly noticeable in rivers with widths less than 90 metres where the elevation values assigned to the pixels underlying the sampled river traces represent a convolution of the river elevation and the elevation of the adjacent river banks. Unlike river profiles obtained by using the D8 algorithm, river traces obtained using just the Landsat 7 ETM+ images do not 'snap-to' the topographic lows of the river courses. As a result both human error in digitising river traces, and reaches where the river trace from a Landsat image does not correlate perfectly with a topographic low in the underlying DEM, produce sections in the extracted long profiles where the elevation values are artificially high. These spikes in the profile represent pixels where the elevation of the landscape adjacent to the river has been sampled, instead of the river path itself. The noise due to the pixels' elevation values convolving both the river bank and the river path also manifests as positive spikes (see figure 2.4). The specific causes of noise in river long profiles extracted from using river locations extracted using Landsat 7 ETM+ data mean that unlike most noisy data where the noise causes the values to randomly fluctuate around the real values, the noise is expressed in the form of positive spikes, where the elevation values are artificially high.

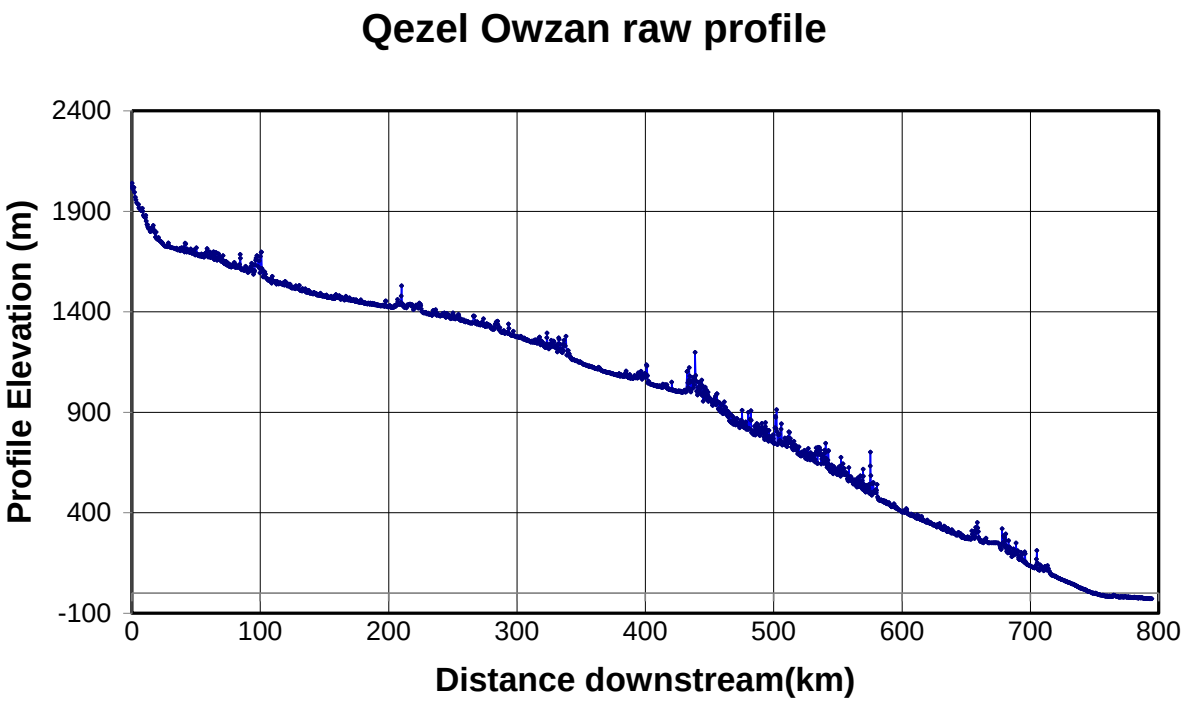

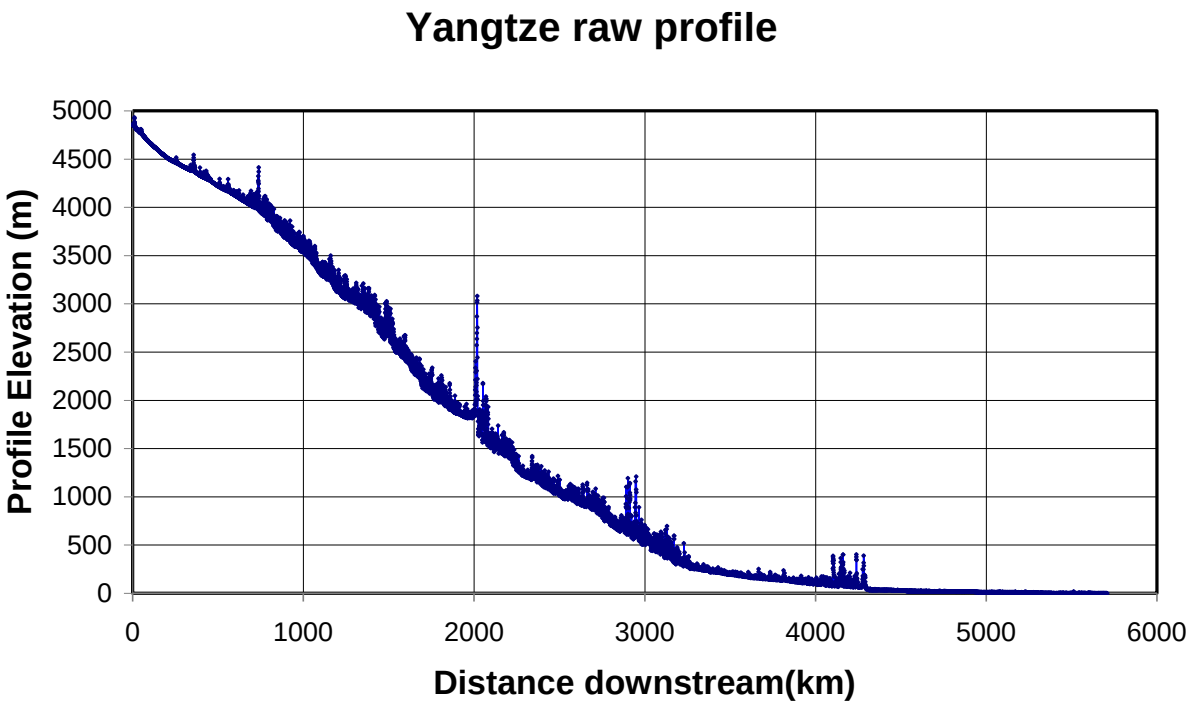

2.4 – Raw longitudinal river profiles extracted using SRTM elevation data with plan view river locations derived from inspection of Landsat 7 ETM+ images *These raw profiles show how the noise present in long profiles where the rivers are located using Landsat 7 ETM+ images is in the form of positive spikes superimposed on the actual long profile. See figure 2.9 for the location of the named rivers.*

Due to the nature of the noise, using a traditional filtering method on the raw long profiles will not produce a result that is close to reality. As the noise is positive, an averaging-based approach to filtering would produce a long profile with elevation values higher than reality. Instead an iterative approach was taken to remove sections of the profile that were part of a spike. Any points that are higher than both the points either side of them (the tips of the spikes) are identified and then removed. This moves the tips of the spikes, leaving other points to act as the tips and be removed in further passes (see appendix B for a full explanation of the method). This method has the fortunate side effect that it also removes any sections of the profile where the water appears to be flowing uphill, further increasing the realism of the final long profile.

2.2.3 Comparison of river networks derived manually and those derived automatically.

Although deriving river networks using the D8 algorithm is the fastest way of defining the plan view location of a drainage network, it is less accurate compared to manual inspection of Landsat images. Automated spectral analysis of the Landsat 7 ETM+ images proves to be impossible due to the lack of a consistent spectral pattern to the pixels making up river traces in the images.

Using the automatically generated drainage network comprehensively covers the study areas, whereas manually derived drainage networks depend on an observer locating all the rivers present in a region. A systematic approach to inspecting a region counteracts this weakness in the approach. In the cases of the orogenic plateaux studied this is achieved by going around the perimeter of the plateaux and digitising the rivers seen. This can lead to some of the rivers that are completely internal to a plateau being missed. As this study looks at rivers that drain from the plateau interior to the plateau margin, not digitising all the internal drainage does not matter. Furthermore the automatically generated drainage network is extremely poor at representing internal drainage, producing

straight lines that connect to the better represented external plateau drainage (see figure 2.3).

The data density in the river networks derived using the two approaches is different. The drainage network derived automatically samples the river elevations at every pixel underlying the derived paths, making the spacing of sample points 324 metres for the Turkish-Iranian plateau and 540 metres for the Tibetan plateau. In the case of a river trace going from pixel to pixel diagonally across the underlying DEM, instead of across adjacent pixels, the sample spacing increases by a factor of $\sqrt{2}$ to 458.2 metres and 763.7 metres respectively. Determining the location of the rivers through manual inspection has no computational limits, so the base pixel size for the underlying DEM of 90 metres can be used (127.3 metres when the river goes diagonally across pixels). In practice the sample spacing of the long profiles of manually derived rivers is less dense than this. Due to the removal of data points needed to remove spikes and smooth the profiles derived from manually determined drainage networks, the spacing of points that make up these long profiles is variable depending on how much erroneous data is removed. In the case of the studied rivers the sample spacing for the manually derived river profiles varies between 0.48 km and 2.79 km with a mean spacing of 1.46 km. The distribution of spacing values is roughly symmetrical with a median of 1.39 km.

The smoothing necessary to produce realistic long profiles from the manually derived drainage networks does not have to be done for the automatically generated data. As the automatically generated drainage network depends on water accumulating by flowing downhill, no smoothing is needed as the profiles can't have any spikes, as any sections where the water flows uphill, as either a spike or a sink, would bisect the profiles.

In order to examine the form of river profiles draining from plateau interiors to plateau margins the long profiles from the manually derived drainage networks are used. Despite the advantages of automatically derived drainage networks the inaccuracies of these networks make them too removed from the reality of the drainage network to be

used. These flaws are not just the obviously unrealistic straight rivers across the plateau interiors. The automatically generated drainage network for the Tibetan plateau had severe errors in the area eastern syntaxis (see figure 2.5). Due to the computational necessity of the large pixel size used the rivers merged and were diverted into false paths. Problems with automatically generating drainage networks for the Turkish-Iranian plateau have been previously noted in other work (Ramsey, 2006).

The D8 algorithm's inability to accurately position rivers in a plateau setting means that the automatically generated river networks are too unreliable to be used to evaluate the rivers' forms. One of the reasons the algorithm fails is that it does not accurately assign the right number of pixels to drain into each pixel associated with a river location. As such, it makes it unfeasible to assign a value for the total upstream drainage area at each point along the rivers. Although downstream distance can be used as a proxy for upstream drainage area (Knighton, 1991), analyses of the steepness and concavity of the studied rivers (see chapter 1 for details of these quantities), such as those seen in (Kirby and Whipple, 2001) are inappropriate.

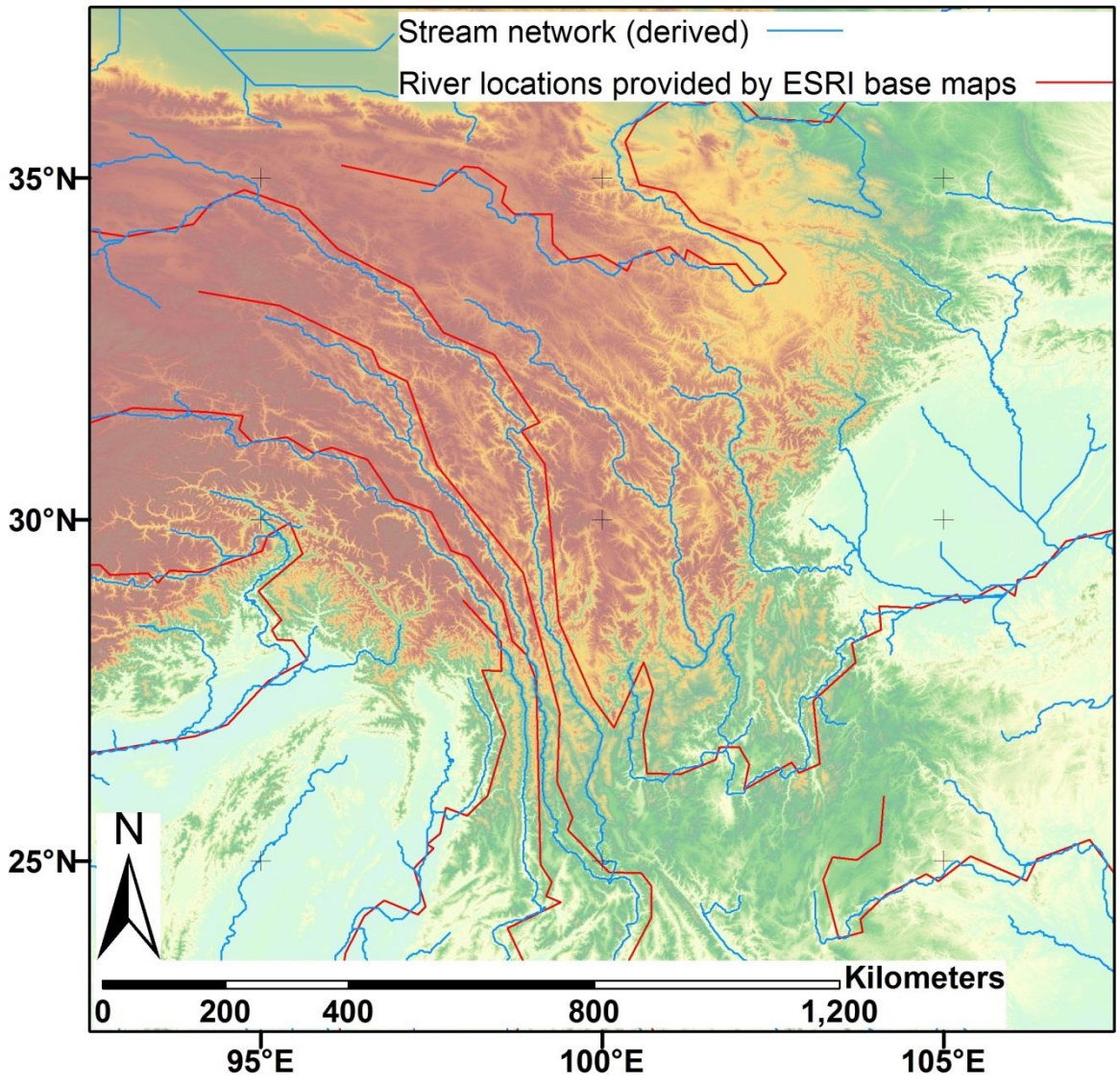

2.5 – Comparison of river paths derived using the D8 algorithm and mapped locations. *River locations derived from the topography using the D8 algorithm are shown in blue. The actual locations as provided by ESRI in their digital maps dataset (ESRI, 2010) are shown in red. Inaccuracies in the automatically generated river paths can be clearly seen. In particular the Yangtze river is shown to be incorrectly diverted to the south to join the Mekong, instead of heading east. Additionally the traces from the ESRI dataset show a lack of precision and are not perfectly aligned with the low topography of valleys in the SRTM data.*

2.3 Long profiles of plateau-draining rivers

The rivers examined in this study are those whose headwaters are within the interior of an orogenic plateau and drain externally across the boundary between plateau interior and plateau margin, before crossing the plateau margin region to the surrounding lowlands or

coast line. These rivers pass between the differing tectonic and climatic conditions of the plateau interior and the surrounding plateau margins. These rivers are the only ones that connect the sediment routing systems of both the plateau interior and the plateau margins. As such they are the only fluvial systems that can control large scale plateau development by moving material from the plateau interior to the surrounding regions. The only other significant mechanism for moving material from the plateaux interior and plateau margins is gravity driven flow. It is important to understand the form of plateau-draining rivers as they govern the main process working in opposition to tectonic advection of material into a plateau.

As plateau-draining rivers cross from the dry, low uplift setting of a plateau interior to the high uplift, wet setting of an active plateau margin, they experience contrasting controlling conditions along their length (Hessami et al., 2006; Masek et al., 1994). Investigating the forms of these rivers will look at how fluvial systems behave in unusual and varying climatic and tectonic settings.

In particular, the concave-up long profile that represents the minimum energy dispersal along a river's length is incompatible with the topography of an undissected plateau. A concave up longitudinal profile is the standard form assumed to represent a river whose profile is graded, meaning that there is no net incision or aggradation along its length (Goldrick and Bishop, 2007; Knighton, 1998; Schumm et al., 2000). The low relief topography of an undissected plateau interior cannot support this morphology. The headwaters of a plateau-draining river are in the plateau interior. This would juxtapose the highest gradient section of a concave up river with the low relief topography of the plateau interior. Moving outwards from the plateau interior, through the plateau margins, the relief and overall gradient of the topography increase, while a concave up river's gradient would be decreasing. The morphology of a concave up river, moving down from the headwaters is in opposition to the topographic changes observed moving from plateau interior to margins (see figure 2.6).

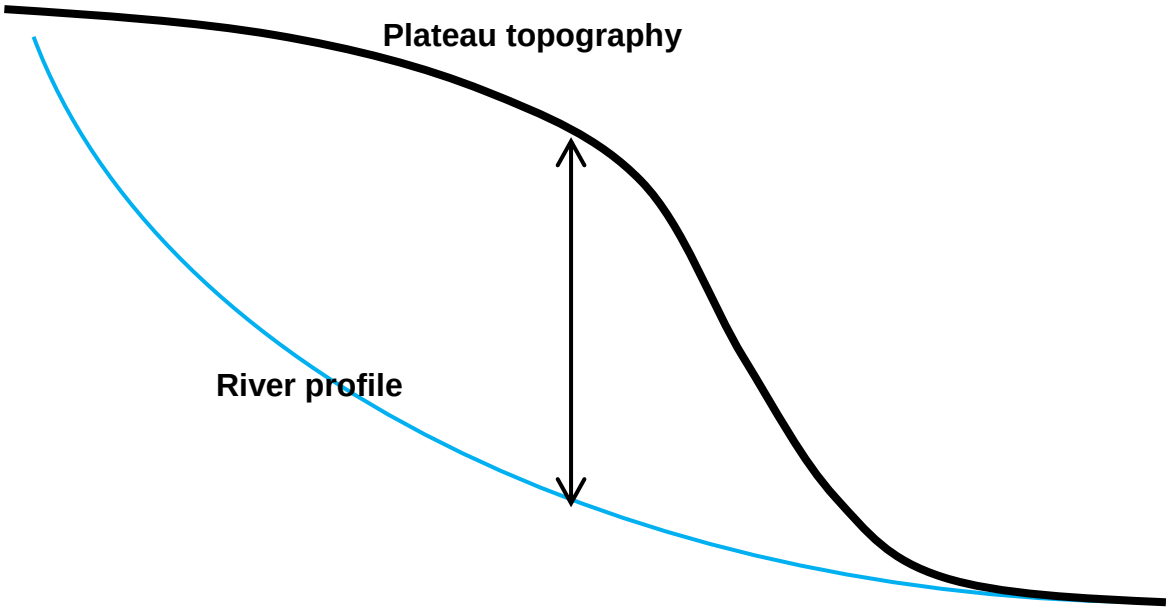

2.6 – Comparison of river longitudinal profiles and plateau topography. *A cartoon showing the mismatch between an idealised graded river profile and the topography profile from a plateau interior to a plateau margin. For a river running from a plateau interior to the surrounding lowlands, showing a concave up profile, the river would have to incise into the plateau, dissecting it.*

The only way a river could support this opposing morphology within a plateau setting is to not follow the topography it is sited within, but to carve out its own path through gorge forming processes, creating a dissected plateau. Investigating the long profile forms of the rivers draining orogenic plateaux will establish whether the rivers are assuming a morphology compatible with the large scale topography of a plateau or incising into the plateaux and evolving towards a concave-up longitudinal river profile. This is not to suggest that if rock uplift and incision are balanced, producing a river in topographic equilibrium, that it must have a smooth concave-up form (Finnegan et al., 2008; Hanmar and Clifford, 2007; Knighton, 1998; Larue, 2011), but variations from this shape along a river's length at least suggest variations in the tectonic and climatic setting.

Concave-up rivers are still a possible morphology in a plateau region if they are contained wholly within either the plateau interior or plateau margin. In the former case

the river may just have a low overall gradient compatible with the low relief of a plateau interior. If the river's headwaters don't extend into the plateau interior and it starts within a plateau margin the situation is similar to a more standard mountain river setting.

For the purposes of this study, the rivers investigated are those that are influenced by both the plateau interior and plateau margin settings. This limited the rivers to ones that have over 15% of their length either side of the plateau boundary as defined as an elevation contour (1 km elevation contour for the Turkish-Iranian plateau and 3.5 km elevation contour for the Tibetan plateau) (see chapter one for rationale). The rivers with a substantial part of their length either side of the plateau boundary are the ones that can move material from the plateau interior to the plateau margin and therefore control plateau evolution by acting opposite to the tectonic processes building the orogenic plateaux. The choice of 15% either side of the plateau boundary is an arbitrary one, but would need to be large enough that it excludes rivers that don't significantly link the settings of the plateau interior and the plateau margins. Some rivers that cross the elevation determined plateau interior boundary don't significantly connect the plateau interior and plateau margins and so don't play a part in moving material out of the plateau interior. Ultimately the rivers chosen need to be ones that are affected by the setting of both the plateau interior and the plateau margin. The most definite way of doing this is to characterise the effects on river form of both the plateau interior and plateau margin settings and analyse only rivers that have these characteristics. While this is a possible avenue of further study, in this case those characteristics are the focus of the investigation, so are initially unknown, and therefore the 15% length either side of the plateau boundary is a suitable criterion for river selection.

The other selection criterion for the rivers studied is those over 100 km in length. This is to make sure that form of studied rivers long profiles is not overly controlled by local factors, such as a fault cross cutting the rivers path or a single change in underlying lithology along the river length. Although such local factors definitely have an effect on

the long profiles of the plateau-draining rivers, by looking only at the longer rivers, overall patterns in plateau-draining river morphology can be seen. In smaller rivers their form can be influenced much more strongly by local, rather than plateau wide driving forces. 100 km is long enough to ensure the river profile is not entirely controlled by a single fault segment. The size of a single fault's influence would be expected to be roughly the same (Whittaker et al., 2007; Zhang et al., 2011) as the faults' down-dip size, with the maximum fault size constrained by the crustal thickness, which varies from a maximum of 80 km in the interior of the Tibetan plateau to around 30 km at the margins of the Turkish-Iranian plateau (Hatzfeld and Molnar, 2010; Maggi and Priestley, 2005).

Few of the rivers draining the plateaux meet both of these criteria, only ten in the case of the Turkish-Iranian plateau and seven in the case of the Tibetan plateau. Instead, most of the length of the drainage networks for both plateaux is in the form of rivers that drain to the surrounding lowlands/coastline, but do not extend into the plateau interior, or rivers that are wholly contained within the plateau interior. It seems that drainage that goes from the plateau interior across the plateau boundary is often partitioned by the rapid uplift at the plateau margin (Sobel et al., 2003; Walker and Fattahi, 2011) leading to the formation of disconnected drainage systems. The rivers that do maintain a connection between plateau interior and plateau margin are those that would have large enough stream power that their rates of incision at the plateau boundary are high enough to keep pace with the rapid uplift present in that zone. This would largely be accomplished through increased discharge along the rivers, compared to the rivers in a similar setting that would get dissected by the plateau margin uplift. Although only a small number of rivers extend significantly into the both the plateau interior and the plateau margins, these rivers do have a significant control on the drainage of the plateau regions. Likely due to the large discharge needed for a river's incision to keep pace with the rock uplift at a plateau margin, the rivers studied have large drainage areas, which account for significant

percentages of the drainage area for each orogenic plateau, 53% of the Tibetan plateau's area and 40% of the Turkish-Iranian plateau's area.

Initial observation of the long profiles of all rivers in the plateau regions shows many to have long wavelength (> 50 km) convex-up reaches along their longitudinal profiles (see figure 2.7). This was noticed in rivers that did not meet the plateau interior-plateau margin connectivity criteria outlined above as well. The long wavelength convex up reaches gives these rivers long profiles a sigmoidal form.

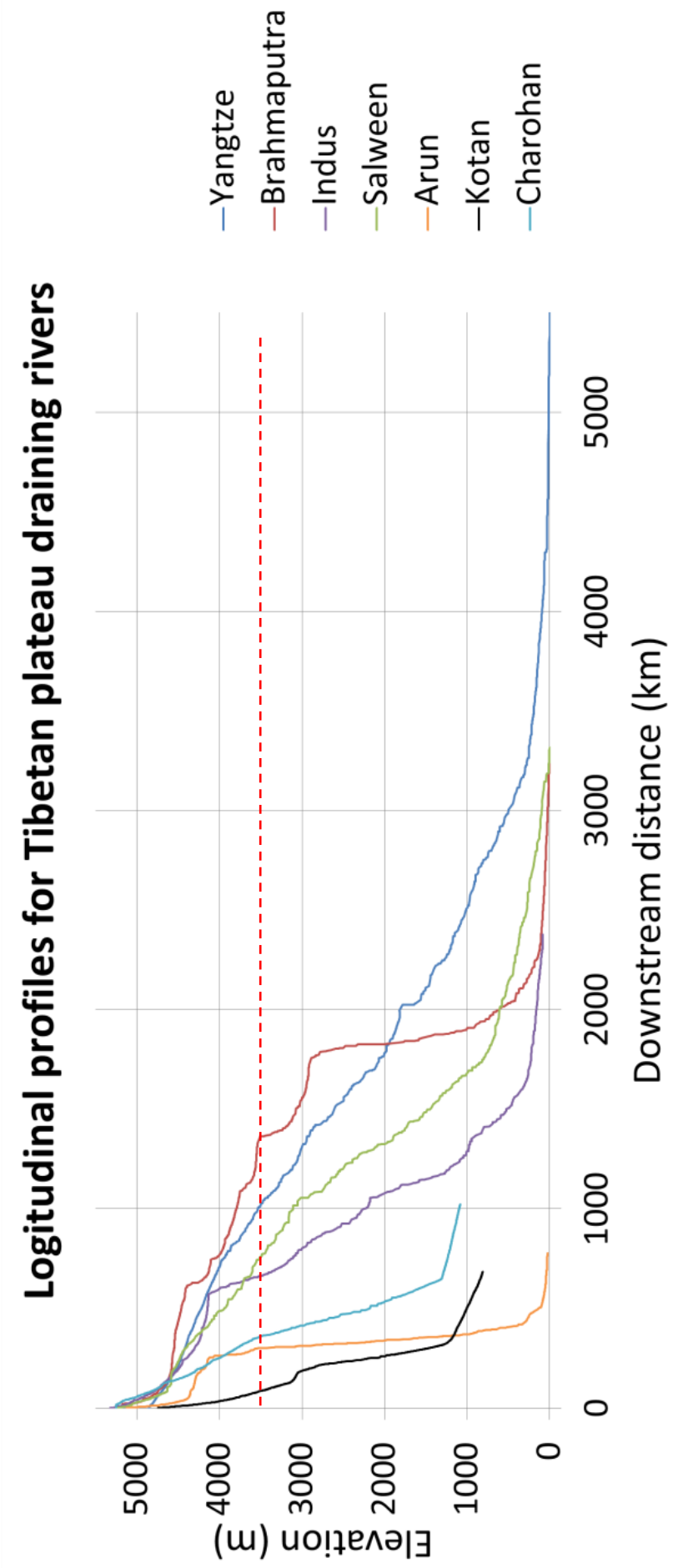

See over for caption

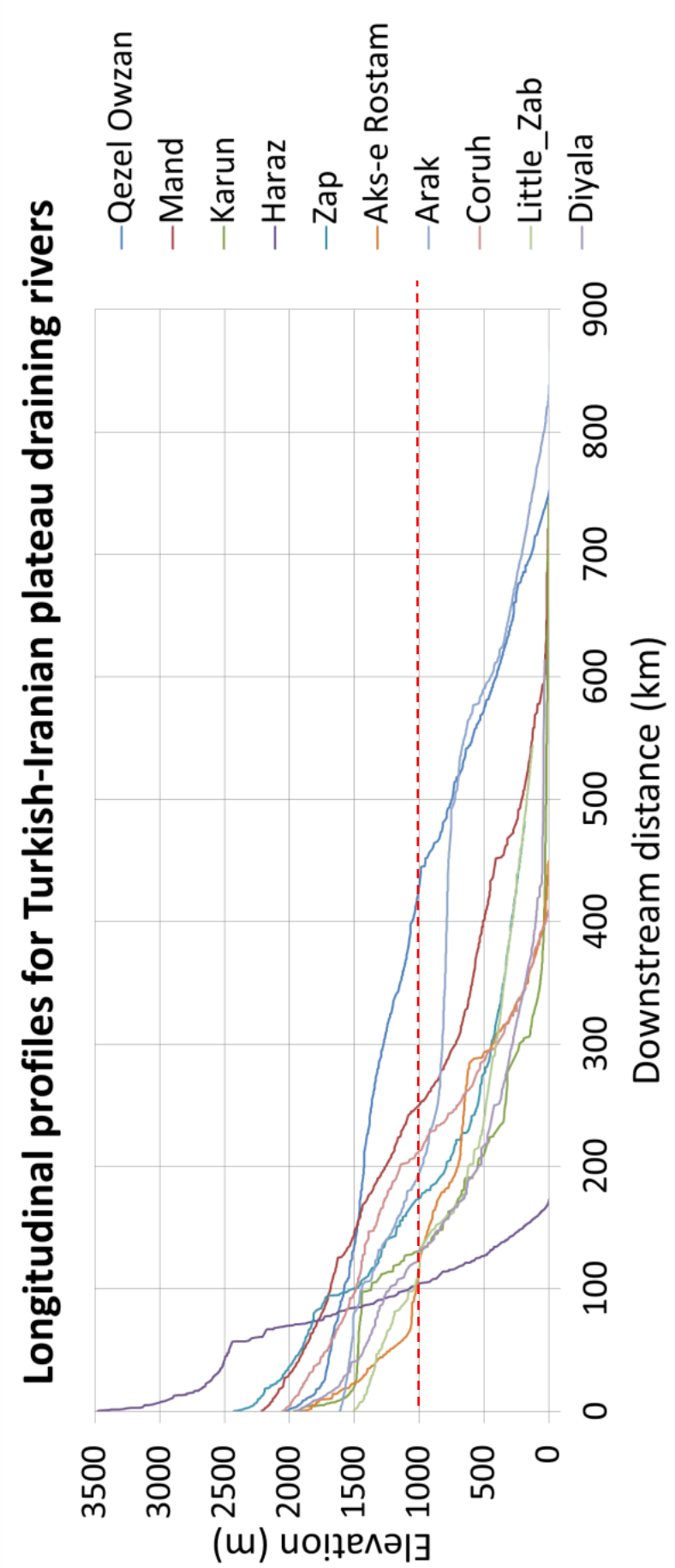

See over for caption

2.7 – Long profiles of rivers draining the Turkish-Iranian and Tibetan plateaux. *These long profiles are taken from sampling DEM data along river courses. The noisy profiles are then smoothed (see appendix C). Dashed red lines show the elevation used as the seismic cut-off between the plateaux interiors and margins. The profiles show long wavelength (>100 km) convexities, primarily at elevations above the elevation that corresponds to the cut-off for seismic thrusting in the plateaux. The convexities vary in magnitude but are seen in many rivers draining the plateaux. Taken as a whole the longitudinal profiles have sigmoidal shapes. River locations seen in figure 2.9.*

Convex up reaches in rivers are not uncommon, and have been associated with a variety of driving factors. These include movement of faults that cross cut the river path (Devi et al., 2011; Whittaker et al., 2007), juxtaposition of lithologies of varying resistance underlying the river (Ramsey et al., 2008; Wohl, 1993), changing climate along the rivers length (Kobor and Roering, 2004; Roe et al., 2002, 2003) and increased infiltration of ground water toward the rivers head (Bouwer, 1978; Huang and Niemann, 2006; Rorabaugh, 1964; Walvoord and Striegl, 2007).

A number of factors make it unlikely that these convexities are local features with local controls. Firstly the size of these convex reaches is larger than would be expected if they were fault controlled. Secondly the convexities are noticed in rivers throughout both plateaux, suggesting a common factor controlling them that is related to the plateau setting, rather than merely local controls. Additionally, the location of the convex reaches shows no correlation to changes in lithology of the plateau (see figure 2.8).

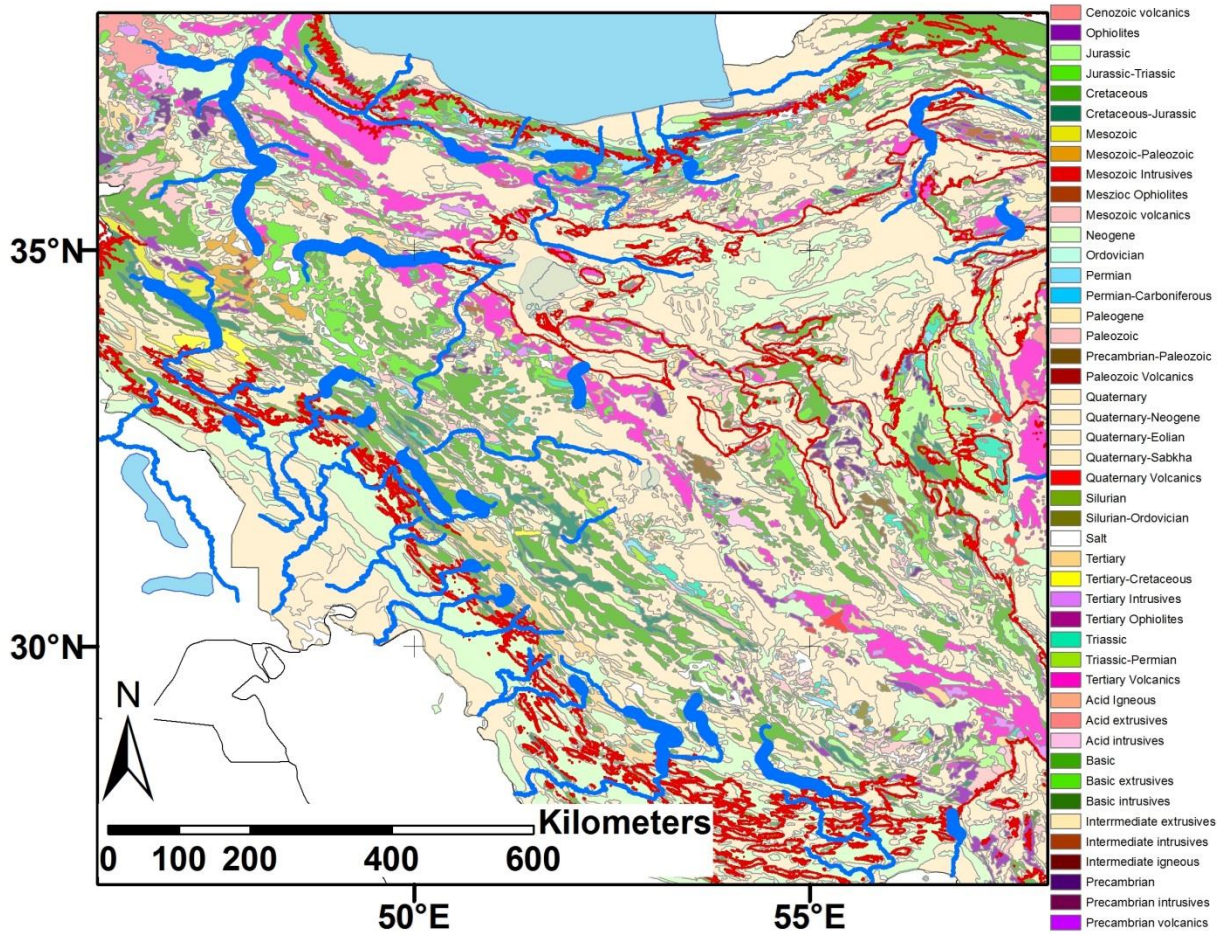

2.8 – Location of observed convex reaches of rivers draining the Turkish-Iranian plateau *The paths of the rivers whose long profiles were observed are shown by a thin blue line. The thick sections are convex reaches manually picked out within these river profiles. The underlying geological map of the area shows that there is no correlation between these convexities and lithological changes along the river lengths. Particularly noticeable is that the convex reaches are present above the 1km elevation contour (shown in red) that represents the cut-off of seismogenic thrusting around the plateau. Geological map from (Pollastro et al., 1999).*

Finally, the location of the convex reaches in the case of both the Turkish-Iranian plateau and the Tibetan plateau shows a correlation with the elevation value used to define the plateau interior boundary. For rivers draining the Turkish-Iranian plateau, convex reaches can be seen in the river profiles at elevation values around 1 km, while the same is true for rivers draining the Tibetan plateau at elevation values of about 3.5 km (see figure 2.7).

2.3.1 Identification of anomalous sections within longitudinal profiles

The first step in understanding how the convexities observed in plateau-draining river profiles record plateau formation events and/or can influence further plateau formation is to quantify these observations. Locating anomalous reaches purely by manually picking out convexities in the river profiles without a predetermined criteria for locating these reaches can lead to observation bias towards more obvious convexities and/or picking out reaches that don't actually represent an anomaly in the river form, but are merely small-scale knickpoints. A more systematic approach to finding reaches that represent a significant deviation from a graded state is needed. This section goes into detail about how an objective way for locating non-equilibrium forms in plateau-draining rivers was derived, and then used.

To look at the plateau-draining rivers that control movement of material between plateau interior and plateau margin, only rivers that met the >100 km length and >15% of their length either side of the plateau interior boundary criteria, as detailed previously, were investigated (see figure 2.9).

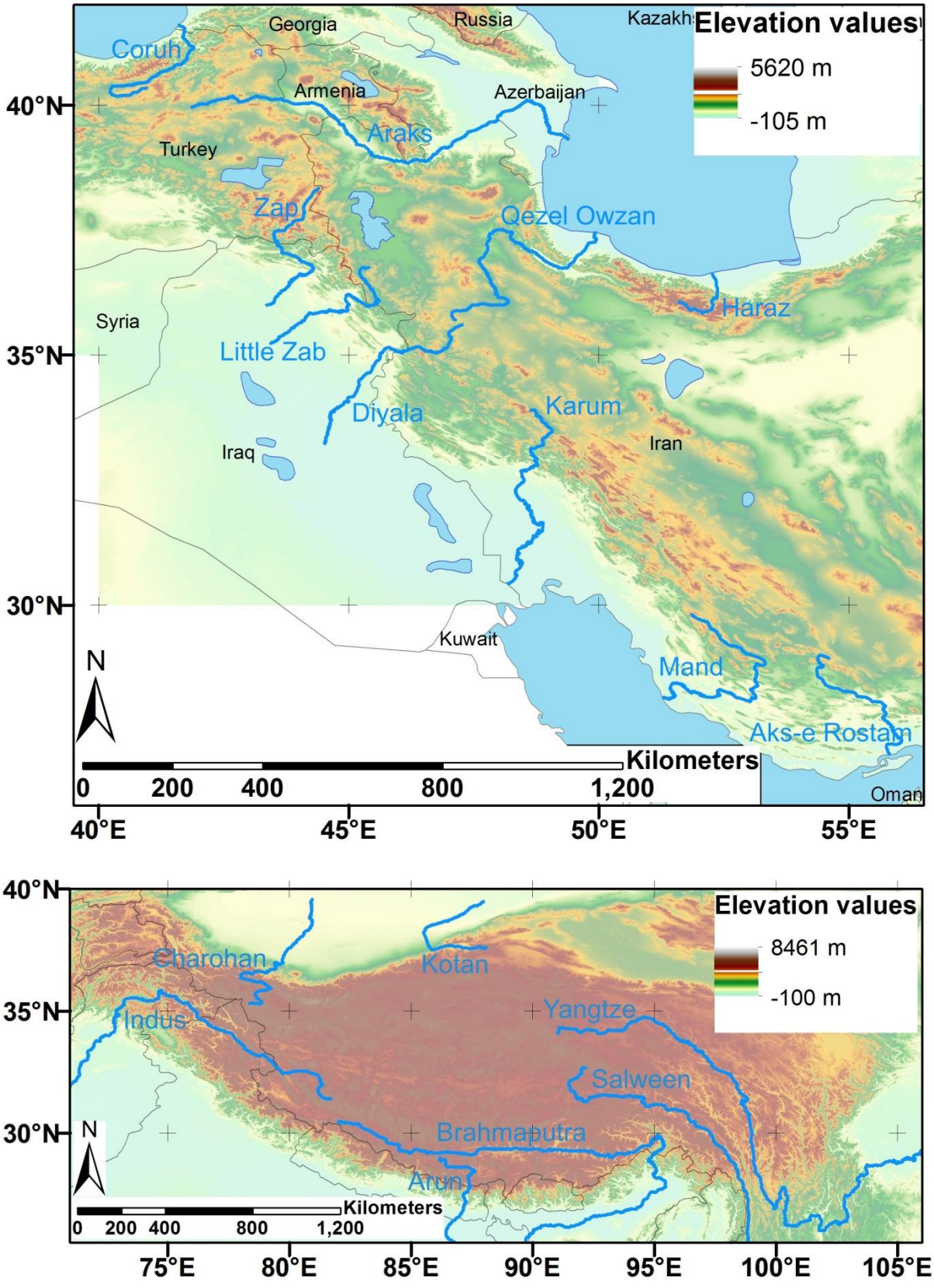

2.9 – Locations of plateau-draining rivers *Locations of rivers longer than 100km with more than 15% of their length either side of the elevation contour representing the margin of the studied plateaux. End points of the Karum, Diyala, Little Zab and Zap rivers are where they join the Tigris.*

To locate and quantify anomalous reaches in rivers that connect plateau interior and plateau margin, the long profiles of these rivers are investigated as to whether they are in equilibrium or not. Knowing about equilibrium along river length is useful for understanding how the plateau-draining rivers can affect plateau evolution. Reaches out of equilibrium represent loci of incision and deposition along river length. While it is possible to use the form of the drainage to estimate the incision taking place along each river, independent uplift rates along the rivers' lengths are not available, making it impossible to directly ascertain if the rivers are in topographic equilibrium or not. The approach used to determine if the rivers are in equilibrium is based on the ln of slope versus ln of downstream distance (DS) form of a longitudinal profile (Bishop, 2007; Goldrick and Bishop, 2007; Larue, 2011). This form describes an equilibrium river profile using the equation:

$$\ln S = \gamma - \lambda \ln D \qquad \textbf{(1)}$$

Where: S is the local slope

D is the downstream distance

λ is the exponent in the power law relationship between downstream distance and water discharge ($Q = lD\lambda$)

γ is $\ln RI_{grade} / il$

γ contains influences on river form from lithological variations, variations in catchment size and infiltration of water downstream as R is dependent on lithological resistance to erosion, I_{grade} is the level of incision when a river is graded, i is the proportion of stream power expended in incision and l is the coefficient of the downstream distance against water discharge relationship. Using the DS relationship includes the often used SL relationship between river slope and distance downstream as a subset of the DS

relationship (Goldrick and Bishop, 2007; Hack, 1973; Hack and Young, 1961; Knighton, 1998), merely being the case for the DS relationship where λ is equal to 1. For an equilibrium river equation ***(1)*** shows the relationship between the ln of downstream distance and the ln of local slope should be linear, meaning a graph of ln S against ln D should plot as a straight line (Goldrick and Bishop, 2007; Wohl, 2000). The DS approach allows for the identification of the type of disequilibrium sections by the way these sections diverge from the straight line trend of a river in equilibrium. Knickpoints show as peaks in the line and a gradient change due to an adjustment to a different equilibrium (such as a change in underlying lithology) displays as a parallel shift up or down in the line. By looking at equilibrium along the length of the rivers, instead of just highlighting convex reaches, this approach also identifies sections that are not in equilibrium, but don't show as easily observed long wavelength convexities. This approach will also show parts of the convex reaches that still represent an equilibrium form.

To use the DS approach graphs of lnD against lnS are plotted for the studied rivers (see figure 2.10).

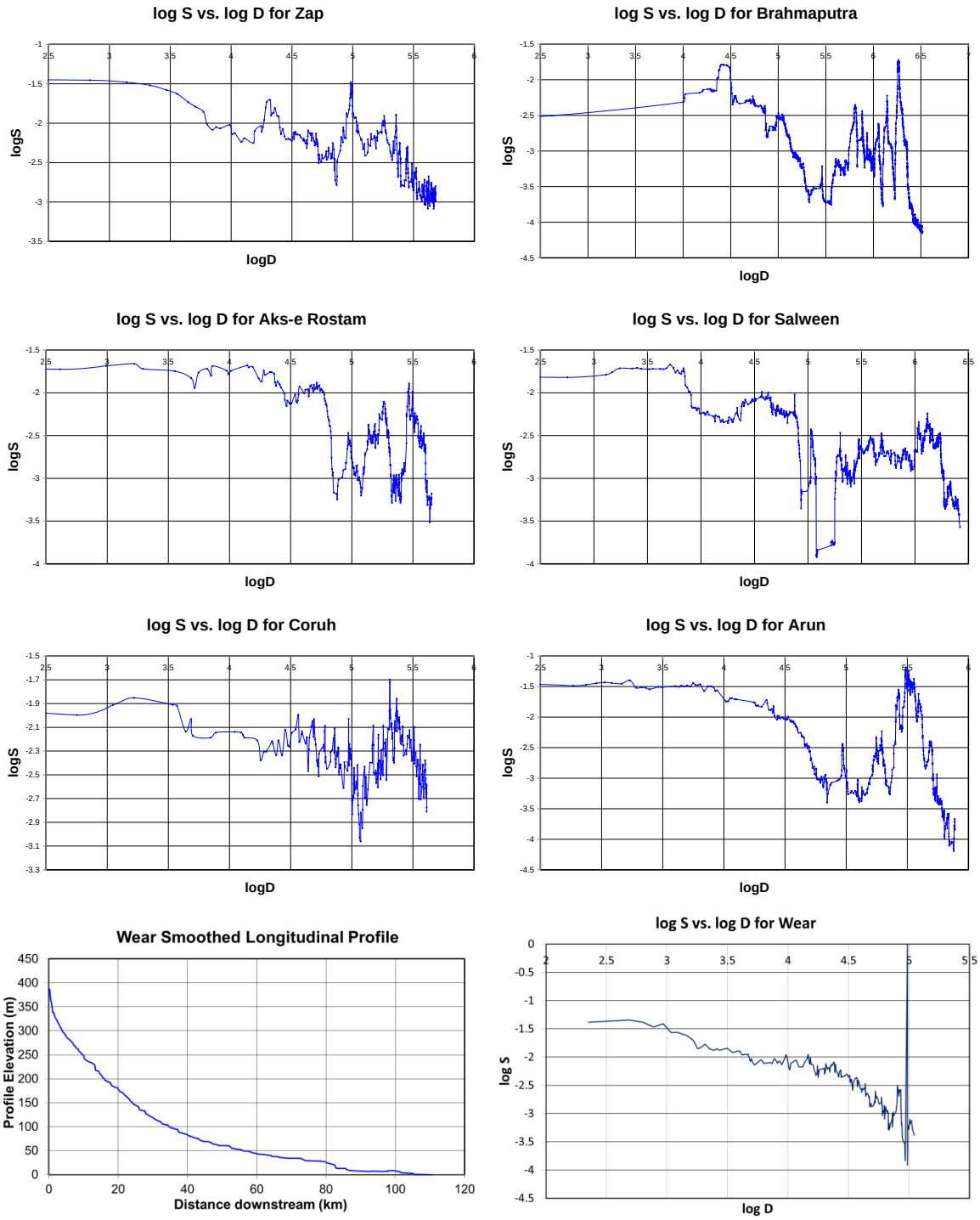

2.10 –Representative graphs of lnS against lnD for plateau-draining rivers *ln of local slope (S) plotted against ln of downstream distance (D) for plateau-draining rivers. The graph traces show no systematic deviation from a straight line. Locations for the rivers found in figure 2.9. For comparison, the longitudinal profile and lnS vs. lnD graphs for the river Wear from the north east of England are shown as an example of a river with a concave up profile that is closer to the idealised graded form of a river. The lnS vs.ln D graph follows a simpler trace that is closer to linear, with one spike representing the knick point that can be seen in the profile.*

Observation of the lnD vs. lnS graphs shows the plateau-draining rivers have a chaotic trace on these graphs. None of the graphs show the constant gradient pattern of a river in equilibrium, making it impossible to pick out sections that have a systematic deviation from an equilibrium gradient. The chaotic forms of the graphs means that most of the sections of the graphs have a gradient that varies significantly from the linear line of best fit to the graph data. Rather than merely declaring that the graphs are chaotic and don't represent a river in equilibrium, the distribution of lnS versus lnD gradient values along the river lengths are analysed to look for patterns in which sections are out of disequilibrium and how the distribution of the disequilibrium reaches relates to the plateaux topography.

Firstly, for each point of the graphs of the rivers the gradient (δlnS/δlnD) is calculated. Next, for each river the mean δlnS/δlnD value along the river is calculated. This average value is used as a constant gradient to reference the lnS/lnD gradients against. In an equilibrium situation the δlnS/δlnD value should remain constant along the river's length, so the mean value is used as a proxy for this value. Although variation along the river lengths would be expected for any real data set, significant deviation of the δlnS/δlnD values from the mean would represent a section in disequilibrium. To locate the disequilibrium sections along a river, points where the δlnS/δlnD values are more than one standard deviation from the mean value of the river are highlighted ('disequilibrium points') (see figure 2.11). The points with δlnS/δlnD values more than one standard deviation higher than the mean are differentiated from those with δlnS/δlnD values more than one standard deviation lower than the mean. This is done for each studied river. Choosing one standard deviation as the amount a δlnS/δlnD value has to differ from the mean before it is declared in disequilibrium is an arbitrary amount, but is based off the distribution of values along each river, rather than choosing a single value that is then applied to each river, whether it is appropriate or not.

A)

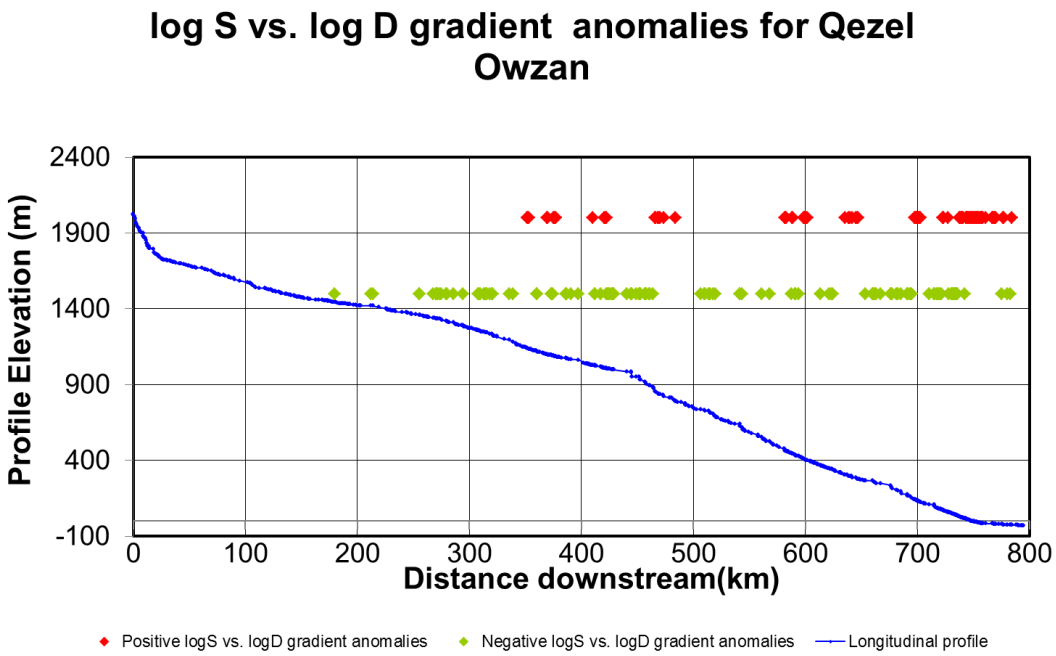

B)

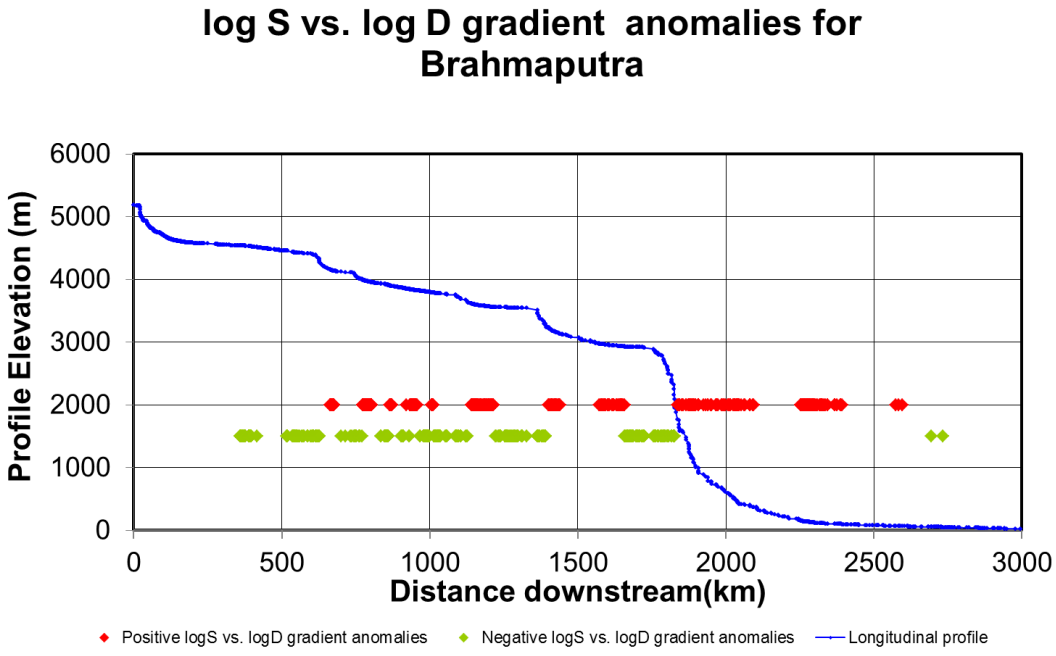

2.11 – Plateau-draining rivers with disequilibrium points highlighted *A) Qezel Owzan draining the Turkish-Iranian plateau B) Brahmaputra draining the Tibetan plateau. Locations where the δlnS/δlnD values are greater than one standard deviation above the mean values of the river shown by a red dot. Points where δlnS/δlnD values are more than one standard deviation lower than the mean value for the river are shown by a green dot. Positive and negative disequilibrium points are intermingled. The density of a particular type of points shows the larger patterns of disequilibrium along the river lengths.*

The δlnS/δlnD value is a measure of the curvature along the river as it looks at how quickly the slope of a river changes with distance downstream. High curvature values, likely to be associated with above average incision (Howard et al., 1994; Turowski et al., 2008) have high δlnS/δlnD values. Conversely, low curvature values likely to be associated with lower levels of incision have low δlnS/δlnD values.

Picking out single points that have δlnS/δlnD values more than one standard deviation from the mean δlnS/δlnD value of a river does not provide information about the large scale form of the river. Isolated individual points are likely to represent small knickpoints with local controls, rather than larger patterns in plateau-draining rivers' morphology. Locating individual disequilibrium points can be useful in determining the position of local controls such as lithological changes, joining of a tributary, etc. However the individual disequilibrium points do not indicate anything unusual about the total morphology of a river, as roughly one third of the points would be expected to have a δlnS/δlnD value more than one standard deviation from the mean. This prediction depends on the δlnS/δlnD values for each river being roughly normally distributed (see figure 2.12).

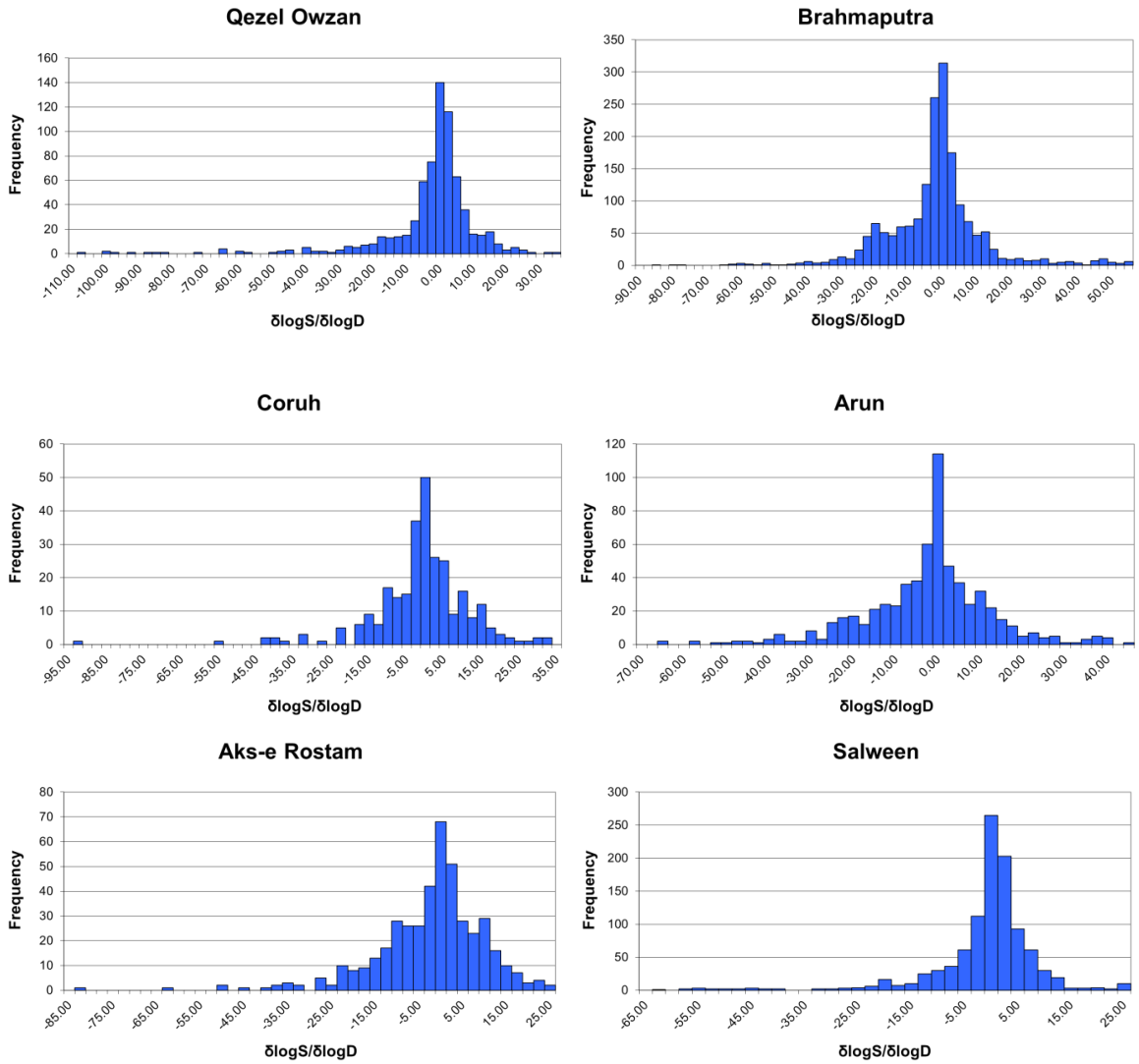

2.12 – Histograms of δlnS/δlnD values *Frequency distributions of δlnS/δlnD values for representative plateau-draining rivers. The frequency distributions show high Kurtosis, but are approximately normally distributed. This shows that the assumption that one approximately one third of the values would be expected to lie more than one standard deviation from the mean is reasonable. River locations are in figure 2.9*

To use δlnS/δlnD values to examine the features of plateau-draining rivers the density of disequilibrium points along river length is calculated. This allows for the identification of clusters of similar disequilibrium points and therefore river reaches with an unusually high or low curvature. The method used to identify river reaches with unusually high or low curvature values is as follows:

1) A window with a length of 2% of the river's length is moved along each river.

2) Each time the midpoint of the window aligns with a sample point along the river length, the number of sample points and the number of disequilibrium points in the window is counted.

3) Disequilibrium points within the same window where the δlnS/δlnD value is more than one standard deviation above the mean value are cancelled out by points where the δlnS/δlnD value is more than one standard deviation lower than the mean value on a one to one basis, and vice versa. This allows for the identification of areas that have consistent patterns to their disequilibria points, rather than just highlighting reaches with intermingled high and low curvature sections.

4) The net number of disequilibrium points is divided by the total number of points within the 2% window. This ratio represents the density of disequilibrium points and is assigned to the sample point at the mid-point of the moving window.

5) If there are more points with δlnS/δlnD values more than one standard deviation lower than the mean than points with δlnS/δlnD values more than one standard deviation higher the disequilibrium density point value is negative. This differentiates these samples from those where the number of points with δlnS/δlnD values greater than one standard deviation above then mean outnumber the points where the δlnS/δlnD values are more than one standard deviation lower than the mean.

   Classifying the points as within a section of negative or positive disequilibrium does not mean that they are actually in a state of negative disequilibrium (as that doesn't actually mean anything), instead the negative/positive values are just used to distinguish between disequilibrium caused by reaches with low curvature or high curvature, respectively

The disequilibrium points where the δlnS/δlnD values are more than one standard deviation above the mean cancel out those in the same sampling window where the values

are more than one standard deviation lower than the mean, and vice versa. They are cancelled on a one-to-one basis. By having these values cancel out, only reaches where there is a consistent pattern in the type of disequilibrium points are highlighted. This cancelling out removes reaches where high and low curvature disequilibrium points are heavily intermingled. These reaches do not represent a consistent pattern of either high or low curvature in the plateau-draining river morphology. Instead, these reaches are those with multiple small, inconsistent deviations from equilibrium, which in total do not form a larger scale part of the river form. The final results of this analysis give every sample point along the plateau-draining rivers a disequilibrium percentage that ranges from +100% to -100%. +100% assigned to a point means every sample point within a distance of 1% of the river length has a δlnS/δlnD value more than one standard deviation above the mean δlnS/δlnD values for the river. -100% assigned to a point means every sample point within a distance of 1% of the river length has a δlnS/δlnD value more than one standard deviation below the mean δlnS/δlnD values for the river.

Looking at δlnS/δlnD values along river lengths is an objective way of looking for non-equilibrium forms of plateau-draining rivers. It avoids the subjective judgments that are made in just identifying unusual convex-up reaches in these rivers. Although the actual δlnS/δlnD values vary considerably from river to river, looking for clusters of disequilibrium points along each river allows for the forms of these rivers to be usefully compared. Another advantage of the δlnS/δlnD analysis performed is that is treats rivers as entire entities, avoiding the need to break rivers into distinct reaches, which would bring another subjective step into the analysis.

2.3.2 Anomalous sections within plateau-draining rivers

The distribution of high and low densities of points whose δlnS/δlnD values are more than one standard deviation from the average for a river can be seen by plotting those values on a map along the studied rivers (see figure 2.13).

A)

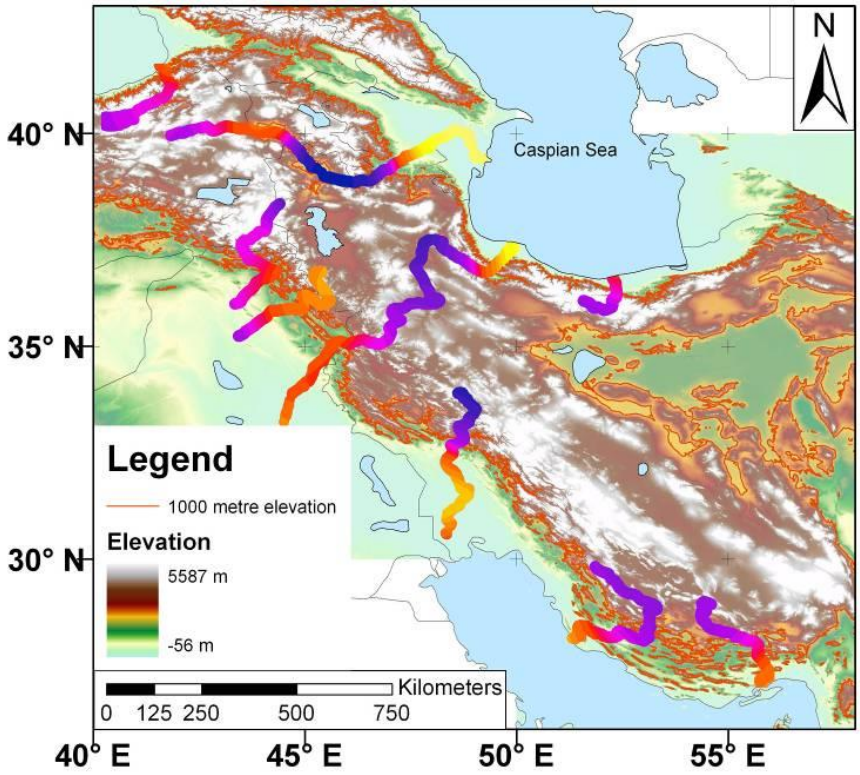

B)

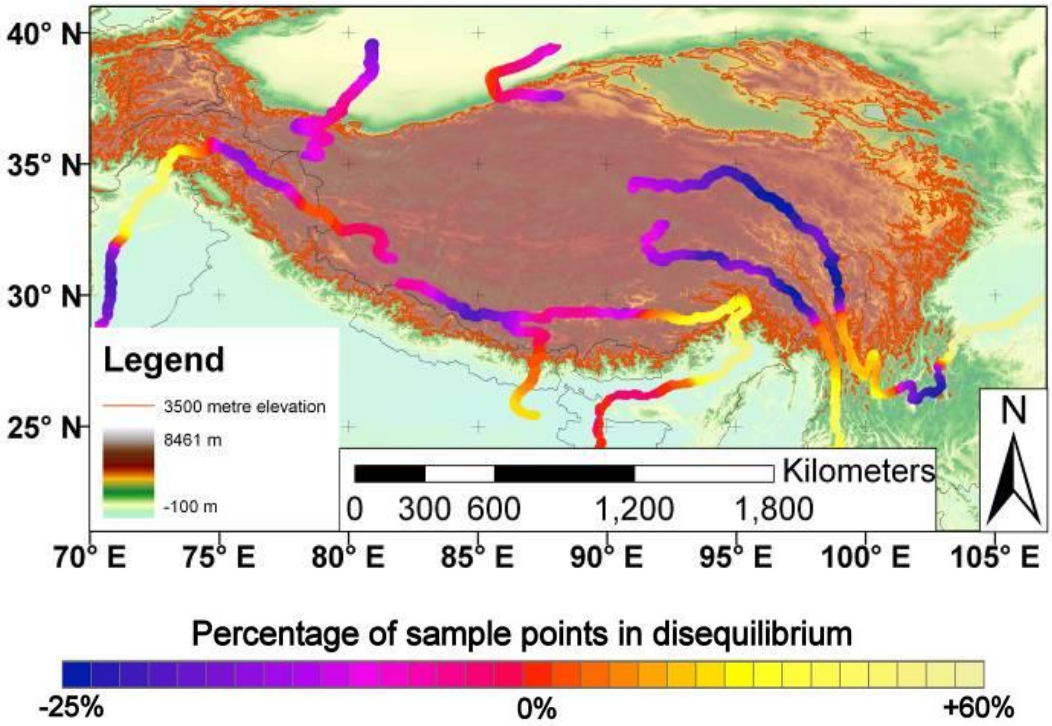

2.13 – Density of disequilibrium points along plateau draining rivers *A) Turkish-Iranian plateau. B) Tibetan plateau. Densities of δlnS/δlnD values more than a standard deviation from the mean are shown. Concentrations of values more than a standard deviation higher than the mean are shown in orange/yellow, while concentrations of values more than a standard deviation less are purple.*

The location of reaches with high densities of points whose δlnS/δlnD values are more than one standard deviation from the mean for that particular river shows a definite pattern in their distribution. Reaches with a high density of δlnS/δlnD values more than one standard deviation above the average are arranged around the edge of the plateau interiors (where the boundary of the plateau interior is defined by an elevation contour, above which plateau-thickening thrusting is absent – see chapter 1). Reaches within the plateaux interiors have a high density of δlnS/δlnD values more than one standard deviation lower than the mean.

Referring back to figure 2.7 illustrates what these deviations from equilibrium mean for the morphology of the river profiles. Reaches with a high density of high value δlnS/δlnD points have a high curvature. These reaches are incising reaches that pass through the plateau margins, forming the high gradient front of the sigmoidal shape seen in plateau-draining rivers. The reaches within the plateau interior with a high density of points with low δlnS/δlnD values are relatively flat reaches that form the low gradient, high elevation part of the sigmoidal longitudinal profile.

Particularly noteworthy is that the changeovers between reaches with a high concentration of δlnS/δlnD values above the mean and reaches with a high concentration of δlnS/δlnD values below the mean are located near the elevation contours that designate the boundaries of the orogenic plateaux (see figure 2.7 and chapter 1). This is the case for both the Turkish-Iranian and Tibetan plateaux. Seeing the same pattern for both plateaux suggests that this distribution of disequilibrium reaches is a factor of plateaux drainage, not particular to one particular setting.

Deviations from a graded profile are often attributed to movement of faults that intersect with a river's path (Schumm et al., 2000; Seeber and Gornitz, 1983; Whittaker et al., 2007), varying lithologies underlying the river (Duval et al., 2004; Ramsey et al., 2008; Seidl et al., 1994), increased sediment supply to the system (Schuerch et al., 2006) or changes in local base level over time (Begin et al., 1981; Blum and Tornqvist, 2000).

These factors do not seem to be the causes of the disequilibria reaches seen in these plateau-draining rivers. The location and size of the identified disequilibria reaches have no correlation with the underlying geology (see figure 2.8).

Furthermore the morphology of the plateau-draining rivers is not consistent with that of rivers perturbed by flowing over multiple lithologies. That type of perturbation produces a knickpoint formation response and while knickpoints are present within the studied river profiles, the large-scale disequilibria patterns in the rivers are not knickpoints. The disequilibria reaches not having a knick point morphology also makes changes in local base-level an unlikely candidate for the cause of the observed disequilbria reaches. Changes in local base level tend to produce propagating knickpoints, in contrast to the long wavelength convexities seen in the studied rivers. Additionally, If base level change was the control on the disequilibria section of the studied rivers it would be unlikely that the position of the disequilibria sections would correlate to the tectonic cut-off that demarcates the boundary of the orogenic plateaux. This suggests that despite the variety on the lengths of rivers studied, the propagation speed of the base-level change effects was somehow tuned so that the resulting morphologies all ended up near the plateau boundary by this point. In addition, the consistent patterns of river disequilibria would have been controlled by more than one base level. In both the Turkish-Iranian and Tibetan cases the plateau-draining rivers do not all terminate at the ocean. To the north of the Tibetan plateau rivers drain into the Tarim basin and rivers draining north from the Turkish-Iranian plateau terminate in the Caspian Sea. The coincidence of river disequilibria reaches with the plateau boundaries also makes a large sediment pulse an unlikely cause of the large wavelength convexities seen in the rivers. If these disequilibra were caused by sediment pulses it seems unlikely that they would all have progressed to the same relative place along the rivers. Furthermore, increased sediment supply causing an increase in the elevation of the river bed suggests that the studied rivers are transport limited. This is unlikely, given the high incidence of gorge forming seen, particularly as

the rivers pass through the plateau fringing mountain ranges. If the disequilibrium reaches were being controlled by fault movements they would be local to the faults and less pervasive in nature. Displacement along a river length due to fault movement has a wavelength roughly the same as the size of the fault that is moving (Gardner, 1983; Miller, 1991; Wohl et al., 1994). The larger scale patterns in disequilibria are longer than the likely sizes of the faults at the plateau margin that they cross.

It is notable that disequilibrium reaches are present in areas where the rivers go through a significant gorge (see figure 2.13b). The juxtaposition of convexities in the river longitudinal profiles and adjacent gorges show that the morphology of the rivers does not merely follow the topography of the orogenic plateaux. Instead the morphologies of the plateaux draining rivers represent an intermediate morphology between concave-up rivers that form gorges to maintain the shape of their longitudinal profiles and the sigmoidal shape of an elevation swath moving out from the plateau interior.

2.4 Discussion

Looking at the longitudinal profiles of plateau-draining rivers gives an opportunity to study rivers long profiles in tectonic and climatic settings that are very different from that of a more typical graded river, or the simpler disequilibrium profiles of a river in a less developed orogen. Rivers draining orogenic plateaux experience a low uplift, low discharge regime in their headwaters. The uplift the river experiences is at a maximum in the middle reaches of the rivers where they flow through the plateaux ringing mountain ranges., this is also where the orogenic rain shadow is at its minimum, increasing the discharge to the rivers. At the reaches to the end of the rivers, in the surrounding lowlands, rock uplift is again negligible and rainfall has not been enhanced by topographically enhanced uplift of the moisture column. Having tectonics and climate that vary along the length of the river contrasts with a lot of the settings that river profiles are studied in which assume either roughly uniform rock uplift along the river length, uplift increasing

towards the river headwaters (representing the centre of an orogeny that has not grown a plateau) or uplift concentrated at a fault that crosses the river path (Densmore et al., 2007; Masek et al., 1994; Wobus et al., 2006). This study therefore presents an investigation of river profiles experiencing a particular set of conditions. Examining the long rivers that drain from the plateau interior to the surrounding lowlands as a whole, instead of dividing them into arbitrary reaches to be investigated individually allows for the differences in morphology along the river length to be more naturally extracted and related to the features of the underlying plateaux.

The widespread presence of disequilibria reaches within plateau-draining rivers aligned to the edge of orogenic plateaux shows the systematic effect draining an orogenic plateau has on the shape of river longitudinal profiles. The δlnS/δlnD methodology does not specifically highlight a particular form as it is just designed to show deviations from the forms of rivers in topographic equilibrium, but when combined with inspection of the longitudinal profiles of the studied rivers (see figure 2.7) it can be seen that the rivers have a sigmoidal shape, which is then highlighted by the δlnS/δlnD method. Some rivers show more of a double concave-up form than a sigmoid, due to high gradients in the (possibly colluvial) headwaters where the rivers are getting established in rougher sections of topography left isolated within the larger expanse of low relief topography that characterises the plateaux. The longitudinal profiles of plateau-draining rivers show a consistent shape with a flat section at high elevations and a higher curvature and higher gradient section within the plateau ringing mountain ranges, before flattening out again as the river passes through the surrounding lowlands (see figure 2.13).

The uniformity in the pattern of disequilibrium of the plateau-draining rivers suggests this is a persistent part of plateau-draining river morphology. If the observed longitudinal profiles represented a transient adjustment to the local topographic, tectonic and climatic setting, then it is unlikely that it would be consistently found across plateau-draining rivers and the two orgogenic plateaux studied. This is not to suggest that the

longitudinal profiles themselves are persistent. If the profiles were persistent while the orogenic plateau grows laterally, the change over point between reaches with high δlnS/δlnD values and those with low δlnS/δlnD values would be located further and further back into the plateau interior as the orogeny continues. This would be associated with gorge forming as the plateau moved outward, dissecting the plateau. Gorge formation does occur in some places, especially the eastern side of the Tibetan plateau, but in many other plateau margins it is not pronounced. Even the large gorges at Tibet's eastern margins are associated with rivers showing the sigmoidal longitudinal forms associated with the other plateau-draining rivers, suggesting that there is still not enough incision happening to completely retard the plateau growth and the change over point is likely to have been moved laterally outwards to some degree. As gorge topography is not universally seen, it suggests that the longitudinal profiles of the plateau-draining rivers are typically adapting to the orogenic plateaux growing laterally, by changing their longitudinal profiles so that the change-over remains close to the edge of the plateau. This sets up a situation where incision along the plateau-draining rivers is working in opposition to the lateral growth of the plateaux. The lack of widespread plateau dissection and closeness of the changeover between high δlnS/δlnD values and low δlnS/δlnD values and the plateau edge suggests that the rivers do little to retard the plateau growth, instead the longitudinal profiles of the rivers have been pushed out as the plateaux evolve.

Quantifying the amount that incision along the river length retards plateau growth is not possible with the method used for identifying disequilibrium reaches. As the method only uses the morphology of the river's longitudinal profile as its data source, it doesn't look at the balance of rock uplift and river incision along the river length. Studying this balance, which would be necessary to provide a definite answer as to whether the plateau is undergoing net retardation by river driven incision or net lateral progradation due to tectonically driven rock uplift at the plateau margins.

The method used to quantify the nature of the plateau-draining rivers' longitudinal profiles is good at locating anomalous reaches that appear not to be in equilibrium. Looking at the density of disequilibrium points, rather than just highlighting spikes or gradient changes in a lnS versus lnD graph allows for the location of larger scale features, that may have less extreme topographic traces but describe the form of a river over longer distances than a local knickpoint or change in the underlying lithology. It is particularly tuned to find long wavelength anomalies in the river longitudinal profiles (where long is defined relative to the spacing of sample points along the river length). However, the method is less good at characterising the indentified disequilibrium reaches. Identifying an unusual rate of change in slope with respect to downstream distance flags up unusual curvature along a river's longitudinal profile, but what counts as unusual curvature is dependent on the local value of downstream distance and the slope at that point. Near the mouth of rivers, the lower gradients found there and the greater distance downstream means that a smaller change in the value of local curvature is needed in absolute terms to produce a greater proportional change. As the definition of anomalous, disequilibrium reaches is relative to the mean $\delta lnS/\delta lnD$ value along the rivers' length this greater proportional change is measured. The upshot of this quirk of the method used is that patterns of anomalous $\delta lnS/\delta lnD$ values seen upstream represent larger morphological changes than those seen downstream (although not necessarily more significant ones).

This method provides a tool for looking at non-plateau-draining rivers as well. Analysing the form of any river's long profile in this manner allows an assessment of whether it is in equilibrium as a whole without effects of local knickpoints affecting the results. It would work well in tandem with analysing how perpendicular the plan view path of a river is to the topographic contours it crosses, which is a way of seeing how much the plan-view profile of a river has adapted to changing topography (Ramsey et al., 2008).

Analysing the form of the plateau draining rivers shows the sigmoidal longitudinal profiles associated with plateau drainage, but does not explain why plateau-draining rivers assume this shape, instead of a more conventional concave up shape. The main feature that needs to be explained is the low gradient at the headwaters (in contrast to the model of a graded river, which has its highest gradients at the head of the river). Possible candidates for the low headwater gradients are lack of uplift in the plateau interior, low rainfall in the plateau interior, increased resistance to incision of the lithologies underlying the upper river reaches and groundwater infiltration in the upper reaches of the rivers (Bouwer, 1978; Huang and Niemann, 2006). That the positioning of the unusual forms of the plateau-draining rivers shows a correlation with the plateaux edges and not the underlying lithologies makes a lithological control unlikely (Figures 2.13 and 2.8). Similarly, groundwater sapping would be primarily controlled by the underlying lithologies and is unlikely to be affected by the growth of the plateaux, so is not a realistic suggestion for controlling all the plateau-draining rivers. Lack of uplift and an orogenic rain shadow within the plateau interior are both part of the evolution of an orogenic plateau. These linked tectonic and climatic signals would provide the conditions for low gradient river headwaters by not providing either rock uplift or discharge needed to incise along the river. As a result high gradient reaches could not be maintained. The change to a higher rainfall, higher rock uplift setting at the plateau margins would contrast to the plateau interior setting allowing for the highest gradients to be found as the rivers pass through the plateau margin mountain belts, rather than at the headwaters as in a typical concave-up river.

Splitting the input of the tectonic and climatic controls within the plateau interior that lead to the unusual river longitudinal profiles of the plateau-draining rivers is difficult. The two factors are linked, a dry plateau interior climate being controlled by the rain shadow effect of the tectonically built, high, flat plateau topography, while the lack of rock uplift in the plateau interior is enhanced by the low levels of net erosion from the

plateau interior, due to the low rainfall there. See chapter 3 for an attempt to model these effects on plateau-draining rivers' longitudinal profiles.

2.5 Implications for orogenic plateau development

Plateau-draining rivers are a first order control on the development of orogenic plateaux (Liu-Zeng et al., 2008; Masek et al., 1994) as they are the main method of removing material from the plateau interior out of the orogegnic zone. If they incise enough that the rate of material removed is greater than the rate that material is tectonically advected into the orogen, then lateral plateau growth will be retarded. This retardation would be observed in the longitudinal profiles of the plateau-draining rivers as the relatively high levels of incision along the river length would allow it to counteract the underlying rock uplift to move towards the concave-up longitudinal profile that represents a graded river. Gorge-forming would be a natural consequence of this incision. The other end of the spectrum would be a plateau draining river with little incision along its length. In this case the river would follow the underlying topography and not incise its own path. The upshot of this would be a river whose longitudinal profile would follow the sigmoidal form of the topographic transect from plateau interior to the surrounding lowlands.

That the analysed plateau-draining rivers have sigmoidal forms shows that they have not completely retarded the growth of the orogenic plateaux. However there is gorge forming along the lengths of some of the plateau-draining rivers (particularly noticeable in the region where the Yangtze, Salween and Mekong rivers leave the plateau at roughly 100^{o}N and 30^{o}E – visible in figure 2.13). This suggests that the plateau draining rivers longitudinal profiles do not represent either end case scenario, where they are not completely retarding plateau growth, but there is some incision opposing the growth of the plateaux. In this situation the location of the long wavelength convexity that gives a river's longitudinal profile a sigmoidal shape is of interest. In the case of the rivers studied, the low curvature, low incision part of the profile changes over to the high curvature, high

incision reaches at the edge of the plateau (see figure 2.13). By not biting back into the plateau, they show that the rivers are not producing a net retardation of plateau growth.

The sigmoidal forms of plateau-draining rivers are a consequence of the tectonic and climatic setting of an orogenic plateau, however if autocyclic processes within the rivers were able to resist the lateral progradation of the plateau and maintain a concave-up longitudinal profile the lateral growth would be retarded. It is only due to plateau-draining rivers assuming the form they do (particularly the low gradient, low discharge, low incision headwaters) that allows plateau interiors to grow to a height where tectonically driven thickening and compression is balanced by gravitationally driven spreading, necessitating a lateral movement of the zone of deformation (England and Houseman, 1988; Molnar et al., 1993; Molnar and Lyoncaen, 1989; Rey et al., 2001).

Although plateau-draining rivers represent the main erosive connection between the plateaux interiors and the surrounding regions, the form of plateau draining rivers within the plateau interiors means they transport far less material than if they had a more conventional concave up shape. This allows more large quantities of material to be trapped within the plateau topography, which could conceivably be liberated if the forms of the rivers returned to a concave-up shape.

3. 2-D modelling of the development of river longitudinal profiles in plateau settings

The previous chapter shows that non-standard longitudinal profiles are found in the rivers draining the Turkish-Iranian and Tibetan orogenic plateaux. These profiles have a sigmoidal shape with low gradient headwaters and the highest gradients at the boundary between the plateau interior and the plateau margin. These shapes contrast with the concave-up shape taken to represent a graded river (Hack, 1973; Hack and Young, 1961; Knighton, 1998). Although movement on underlying faults (Allen and Densmore, 2000; Seeber and Gornitz, 1983; Whittaker et al., 2007), changes in the lithology underlying the river course (Ramsey et al., 2008; Wohl, 1993), variations in climatic conditions along the river length (Kobor and Roering, 2004; Roe et al., 2002, 2003) and shifts in local base level (Begin et al., 1981; Blum and Tornqvist, 2000) can allow for a non-concave-up equilibrium river shape as the drainage form alters to a new equilibrium to compensate for these factors, the observed sigmoidal forms need to be explained in terms of more widespread, external forcing factors.

As the sigmoidal profile form is present in the plateau-draining rivers of two separate orogenic plateaux and in the vast majority of all the rivers over 100 km in length and with more than 15% of their length either side of the plateaux boundary, these sigmoidal longitudinal forms seem to be a near universal feature of rivers that drain from a plateau interior across the plateau boundary and through the thrust zones at the plateau margins. Thus, while individual, local forcing factors have undoubtedly affected the rivers longitudinal profiles, causing knickpoints and regions of abnormally high or low gradients, for them to be controlling the form of plateau-draining rivers long profiles in the same fashion around the borders of two orogenic plateaux would represent an enormously unlikely coincidence.

Consistent with the model of orogenic plateaux being formed from linear mountain ranges, which have reached a height where tectonically driven thickening is balanced by gravitationally driven spreading, leading to lateral building of the plateaux (England and Houseman, 1988; Rey et al., 2001), the sigmoidal profile of the plateaux draining rivers is assumed to have evolved from a mostly concave-up form draining the antecedent mountain belts. To move from a concave-up river shape to a sigmoidal longitudinal profile requires a change to the river's controlling parameters. Two hypotheses for this change in shape are:

1) Lack of rock uplift at the head of rivers within the forming plateau interior. Lack of uplift at high elevation in the plateau is consistent with the observation of seismic thrusting being limited to low elevation in the plateau regions studied (See chapter 1 for a fuller description of possible uplift scenarios). Should the modelling be unable to recreate the observed pattern in river longitudinal profiles, this may indicate that the assumption does not hold. Lack of uplift at the head of the river would not allow for the maintenance of high gradients at the rivers' heads, thereby reducing incision within the plateau interior and leading to a shape that follows the underlying terrain more than incising its own path.

2) Low rainfall within the plateau interior and so within the catchment area feeding the head of the rivers. This would reduce discharge along the river in the plateau interior, in turn reducing incision in the higher reaches of the river. Low rainfall within the plateau interior would be consistent with an orogenic rain shadow effect (Roe, 2005).

It is important to note that these hypotheses are not mutually exclusive. Attributing lack of rainfall (hypothesis 2) to an orogenic rain shadow effect requires the beginning of a plateau to be formed to produce the rain shadow in the first place. In this case, the lack of rainfall would be a positive feedback factor in enhancing the formation of sigmoidal rivers in a plateau setting. Conversely, low rainfall in the plateau would hinder the removal of material from the surface of the plateau. This would hinder rock uplift in the region due to isostatic compensation, thereby enhancing the processes of hypothesis 1.

Ultimately, both hypotheses describe ways of reducing the transport and incision capacity of the upper reaches of plateau-draining rivers. By having less ability to incise into the underlying rock, autogenic controls on the river longitudinal profiles become less important, and so instead of being able to adapt to local conditions and maintain a graded shape, the long profiles experience more control by allogenic factors. This manifests itself in the shape of the rivers' long profiles as a sigmoidal form that is similar to a topographic swath from a plateau interior to the surrounding lowlands, as the rivers' forms are determined by following the underlying topography, instead of incising their own path into the underlying material.

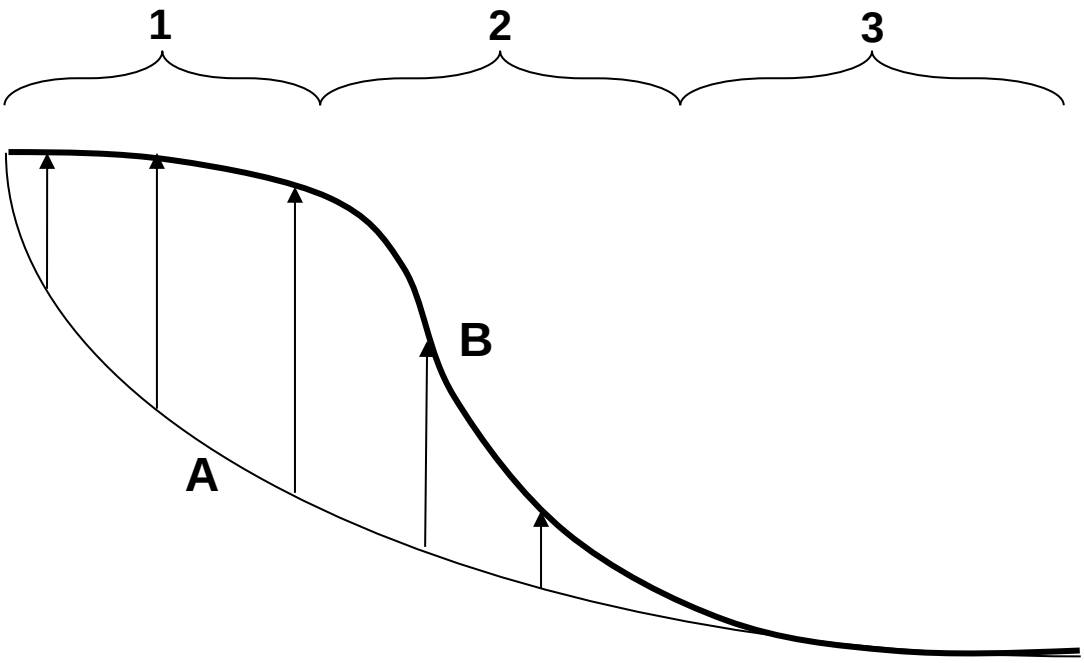

3.1 – Conceptual model for the formation of sigmoidal longitudinal river profiles *As a plateau develops, the rivers draining from the plateau interior (region 1) to the surrounding lowlands (region 3) change from a graded profile (A) to a sigmoidal form (B). This is done by uplift in the plateau until an elevation is reached where crustal thickening by compression is balanced by gravitationally driven spreading. Within region 1 the lack of incision leads to a reduction of the rivers' gradients. Incision can be maintained within the surrounding uplifting mountain ranges (region 2), allowing it to connect the reaches in regions 1 and 3, while the lack of uplift in region 3 leaves the form of the river in this region mostly unchanged.*

To try and unpick the controls on river long profiles in a plateau setting numerical modelling was carried out. This modelling aimed to show the relative importance of the tectonic (hypothesis 1) and climatic (hypothesis 2) controls on the rivers. It would also show how differing conditions along the length of a river profile can lead to the formation of the observed sigmoidal forms. Modelling allows the controls on river longitudinal profiles to be quantified in a way that is not possible simply by observation of sigmoidal longitudinal profiles in reality. By its nature a model requires the tectonic and climatic conditions driving the resulting geomorphology to be defined and quantified. The advantage of having complete knowledge of the driving conditions in a model is balanced by uncertainty in how to set up the model to ensure it represents reality. In this study the

ability to control and define driving parameters of the model is used to quantify the relative importance of climatic and tectonic factors and demonstrate how the combination of those factors can derive rivers with sigmoidal longitudinal forms from graded, concave-up rivers. This is done in two steps:

1) First the set-up of a model that can produce sigmoidal longitudinal profiles from concave-up rivers is described. This will go some way towards explaining the mechanisms driving this change.

2) The sensitivity of the model to changes in the driving conditions is examined. Each variable in the model is altered and the range of values that still allows the model to produce sigmoidal longitudinal profiles is recorded. This range of 'sigmoid possible' values is then compared to a realistic range for the value and the percentage of real world variation that still results in sigmoidal river profiles calculated. The values with a smaller 'sigmoid possible' percentage will be the variables that the model is most sensitive to if the terrain is to support a sigmoidal longitudinal profile for a plateau-draining river.

3.1 Model set up

The model aims to only explain the development of sigmoidal river longitudinal profiles, not the plan-view form of plateau-draining rivers so a 2-D (not including time) model was used, where the dimensions are distance downstream and elevation above sea level. The model set up has a 1000 independent points, where a line joining them represents a river's longitudinal profile. The points are evenly spaced horizontally, but can move up and down vertically at each time step. The model evolves in discrete steps, representing the progress of time. At each time step the magnitude of erosional incision along the river and

tectonically driven rock uplift is calculated for each point in the model. The incision value is taken away from the elevation at each point and the rock uplift is added to the elevation value. This produces new elevation values for each point, to give the profile at the next time step. At each time step the new elevation values are then used to calculate the incision and uplift values for the next timestep. This last point is particularly important, as it means that uplift and incision through time are not defined and imposed upon the model, instead the dependency of those parameters on topography set and the uplift and incision are free to change through time with the model. Being constructed of evenly spaced points, whose elevation is free to move, imposes some limitations upon the model. Primarily, this set up prevents modelling a situation where a river extends laterally, either through incision at the headwaters moving the head of the river back into the orogen (Craddock et al., 2010), or deposition at the toe of the river, producing a delta/fan that extends the river's termination point away from plateau being drained. Both headward incision and river lengthening at the toe reduce the overall gradient of the river, particularly at the ends of the profile, increasing its sigmoidal nature. Therefore, a model set up where this isn't possible represents a high gradient, low sigmoidal version and the combination of parameters needed to produce a sigmoidal long profile in this case would be more stringent than may be the case in reality.

The initial state of the model, before incision and deposition is imposed on the longitudinal profile, is that of an idealised graded river. This smooth, concave-up profile is intended to represent drainage that is adapted to a linear mountain range setting, where the elevation of the mountains are at the maximum supportable by the orogen. After building up the mountains to their maximum elevation the orogen evolves by forming a plateau, extending laterally (England and Houseman, 1985; England and Molnar, 1997; England and Houseman, 1988). This is when sigmoidal longitudinal forms are hypothesised to form from antecedent graded rivers. Setting time step zero for the model at the point where a plateau begins to be formed avoids having to additionally model the whole history

of the orogen. It also ensures that the initial river longitudinal profile that the sigmoidal forms evolve from is a smooth graded profile, giving an interpretation that is as generalised as possible, providing the most useful basis for describing the formation of sigmoidal longitudinal profiles.

The choice of mathematical function to produce the initial smooth curve is not simple. There is no agreement about what function best describes a graded river's longitudinal profile. Curves suggested in the literature include negative (decaying) exponentials, power law curves and negative logarithms (Knighton, 1998; Snow and Slingerland, 1987). All of these curve types can be seen to fit real river longitudinal profiles, with conflicting descriptions of the dependence on the setting the rivers are within. The initial river longitudinal profile chosen was a power law form as suggested in (Goldrick and Bishop, 2007; Hack, 1973; Hack and Young, 1961; Knighton, 1998; Montgomery and Dietrich, 1992). This form has some mechanical rationale, beyond just having a close fit to some observed river profiles. In Hack's case this was derived from the assumption that river profile slope and downstream distance were related by the following power law:

$$S=kL^{n}$$

Where: S is the river slope

L is the downstream distance

And k and n are both empirically derived constants that can be tuned for each river or population of rivers investigated.

In this equation n is an index of river concavity and must be negative to produce a concave-up longitudinal profile. For a graded river where stream power is as evenly dispersed as possible along its length, the reduction in river slope with downstream

distance is a reasonable assumption, as this is a compensation for the increase in drainage area and therefore water discharge along the river profile. Substituting $\delta H/\delta L$ (where H is elevation) for S and then integrating gives the following equations for a river profile:

$$H = H_1 - k\ln L \quad \text{when } n = -1 \quad \text{or:}$$

$$H = H_0 - (k/n+1)L^{n+1} \quad \text{when } n \neq -1$$

Where: H_0 is the elevation when L=0

And H_1 is the elevation when L=1

The power law form is more generally applicable than the logarithmic form, which only applies when n = -1, so is chosen as the graded river starting point for the model.

Once the form of the initial profile is decided upon, scaling issues need to be considered. A dimensionless approach to setting up the model, with a river '1' high and '1' long was rejected as it is desired to have the sensitivity variables with the same magnitude and units as real, observable variables. This allows for an easier extrapolation of the models results to the controls on real rivers. As the modelling developed from previous work on the rivers draining the Turkish-Iranian and Tibetan plateaux, these two settings are possible exemplars for the scaling used in the model. The Tibetan case was used to determine the scaling of the initial model profile. Tibet is more studied than the Turkish-Iranian plateau, meaning that possible values for the models controlling parameters are better known, allowing for the investigation of sensitivity variables to focus on those variables that actually control the formation of sigmoidal long profiles, instead of those that are just unknown. As the first step is to represent drainage from the mountain range antecedent to the Tibetan plateau, just before it starts growing laterally into a plateau, the drainage at the model's first step should be comparable in scale, although not form, to the current drainage. Therefore, the form of the drainage for the first

time step is a smooth, concave-up power law curve, where the height is set to 5107 m and the length is set to 2452 km. These two values are the average of the heights and lengths of the rivers draining from the Tibetan plateau interior to the surrounding lowlands, that were studied in chapter 2.

After setting the initial river form, the initial uplift and incision parameters are defined and then they are allowed to evolve over the following time steps. Those conditions and how the inputs change are detailed in the next two sections. This is an unusual approach, particularly with regards to uplift. Uplift in landscape evolution models is often externally defined from the first time step onwards (Codilean et al., 2006; Kooi and Beaumont, 1996; Masek et al., 1994).

The size of the time step was kept as small as possible. Having a smaller time step gives a smoother transition from river profile to river profile at each step, reducing the chance of a large incision or uplift amount destabilising the model in a physically implausible way, before the negative feedbacks in the model can show the river profile correcting itself. The constraint on how small the time steps can be is the computational time and space available. If the time steps are kept too small, the small changes from one profile to the next mean that interesting changes in the profile over time are not seen before the limit in the number of time steps is reached. The time step length chosen was 1 million years. While this is a relatively long time, giving the model a coarse temporal resolution, it is comparable to the response time of large rivers (0.25 – 2.5 Ma) (Whipple, 2001), so represents long term change to river form, rather than just temporary fluctuations as rivers readjust (although such fluctuations would only be modelled if a higher density of time steps was being used to capture the change in river form more frequently). Looking at changes on this timescale also looks at changes that are meaningful on the timescale of formation of the Tibetan plateau that the model is patterned on (Harrison et al., 1992). As the model simulates a river longitudinal profile

changing as the orogen evolves from a linear mountain range to a plateau, having a time step long enough to capture that change is important.

The lithology underlying the modelled river was considered, however lithology did not seem to be a control on the form of plateau-draining rivers in reality (see chapter 2). As such, variation in lithology along the length of the river was not modelled at all. Variation in the erodability of different lithologies is contained in scaling of the incision applied at each time step.

The uplift function was subjected to a scaling factor, as the variation in uplift along the length of the river was described in relative rather than absolute terms (explained in section 3.1.1). The scaling was set based on the first time step, after that the uplift and incision functions were allowed to evolve freely, based on the topography of the previous time step. The scaling factor was set so that the average incision and uplift at the first time step were roughly equal, this was to represent a near graded state for the river draining the linear mountain range assumed to be the fore-runner for the orogenic plateau being modelled. While the total uplift and incision were set to be the same, the variation along the river length between the two variables does allow the river form to change in further time steps.

The 2- D model does not take into account changes that take place out of the plane of the model. This places certain limits on the model. Firstly, it disregards material moving laterally. This situation is a good fit for a river draining the middle section of an orogen where material spreading out of the plane of a river profile, due to a build-up of topography, is compensated by the comparably high topography either side. At the ends of an orogen, where the topography falls off, gravitationally driven spreading from higher to lower topography is a significant factor on the evolution of the topography (England and Molnar, 1997; England and Houseman, 1988; Rey et al., 2001). A second limit is an inability of the model to take into account river response by a change to channel width. This is a common way for river to adjust to changes in water discharge along its length

(Amos and Burbank, 2007; Knighton, 1998; Wohl, 2000), but was badly constrained in the dataset of real rivers that the model is intended to represent. The topography of the rivers studied in chapter 2 are constrained by SRTM data, which has a pixel size of 90 m x 90 m, this is often wider than the river width, particularly in the sections of rivers draining through the mountain ranges surrounding an orogenic plateau. Another way that rivers adjust to changes in their forcing conditions is to alter the amount of meandering along the river course. This effectively changes the local length of the river and so therefore the local gradient (Knighton, 1998; Xu, 2002). While the length change is not modelled the gradient change response is part of how the model evolves. Finally, a 2-D model of a river profile does not explicitly model the shape of the adjacent interfluves. The shape of the interfluves is important as local gradient and elevation determine both rainfall (and so water discharge and incision) and local rock uplift.

In this model the profile of the river is used as a proxy for the elevation and gradient values that control uplift and rainfall. This assumption is one of the largest in the model, but is justified by rivers working as a base level for adjacent interfluves (Harkins et al., 2007; Wohl, 2000), so it is reasonable to assume that plateau topography would track river morphology, showing similar changes in elevation and gradient, moving from the plateau interior to the surrounding lowlands.

To make a computationally feasible 2-D model of a complicated 3-D system a set of assumptions was necessary (see table 3.1)

3.2 – Table of assumptions made in the construction of the river evolution model

Assumption	Justification
Movement of mass into or out of the plane of the model is negligible.	Except for at the end of an orogen, the flux of mass perpendicular to the direction of orogen driving convergence is negligible as there is no relative elevation difference or gradient of convergence velocity to drive mass movement.
The elevation of the interfluves is comparable to the topographic trace of the adjacent rivers.	Interfluve topography would track river topography as the rivers act as a base level for the adjacent interfluves. This is especially true for a detachment-limited stream that is capable of maintaining interfluves at the angle of repose.
The model can't adjust the river's horizontal length.	Imposed as a computational necessity. However increasing length would only allow for the extension of the river into the low-lying areas or the low relief plateau interior. As such, a river that could extend its length would only display a more pronounced sigmoidal form.
The river does not adjust by changing its width.	This change is not captured in the model. However, the formula representing incision along the river does not have the channel shape as part of its governing parameters so does not have to take channel shape into account.
No change in rock resistance to erosion along river length.	Previous work (chapter 2) shows that lithological changes were not correlated to the form of the river.
Elevation scales proportionally to crustal thickness.	This allows elevation to be used as a proxy for crustal thickening. Good correlation is seen between maps of crustal thickness and elevation in plateau regions (see appendix C).

3.1.1 Rock uplift

Rock uplift is applied to each point along the river profile at each time step. The uplift amount represents the tectonic effects on the elevation of the river profile. In the approach used in this chapter, the rock uplift function has two parts, which are then multiplied by a scaling factor outlined below. The first is crustal thickening due to lateral convergence of the orogen. The second is a negative section that represents crustal thinning due to gravitationally driven spreading. Removed from tectonic driving forces the crust will move towards a uniform thickness as it spreads. This gives a formulation for rock uplift like this:

$$\Delta h(x) = k\Delta t(U - T)$$

Where: h is the elevation

x is the horizontal distance along a river's longitudinal profile

k is a scaling factor

Δt is the timestep

U is the uplift rate due to orogen forming convergence

T is the rate of crustal thinning due to gravitationally driven spreading

For the purposes of the model there is assumed to be a linear relationship between crustal thickening and rock uplift at the surface. A close correlation between plateau elevation and crustal thickness can be observed, suggesting that this is a reasonable assumption to make for the construction of this model (see appendix C). This means that modelling factors that affect crustal thickening can be turned into rock uplift for the purposes of modelling river evolution. Convergence and gravitationally driven spreading both affect crustal thickness. To convert crustal thickness into changes in rock uplift it is

assumed that changes in crustal thickness are isostatically compensated. This allows for changes in surface elevation to be directly determined from changes in crustal thickness by assigning values for the density of the crust and the mantle. The conversion factor between surface uplift and crustal thickening is given by:

$$\frac{Increase\ in\ surface\ uplift}{Increase\ in\ crustal\ thickening} = \frac{\rho_c - \rho_m}{\rho_m}$$

Where: ρ_c is the density of the crust and

ρ_m is the density of the mantle

This conversion factor is not directly used in the model. The model uses an approach seen in (Masek et al., 1994), where the absolute size of rock uplift is not analytically derived from functions for rock convergence and gravitationally driven spreading. Instead the distribution of these parameters along the river length is calculated and then they are multiplied by a scaling factor so that the first timestep has a realistic magnitude for the uplift. The uplift is then free to evolve in the following timesteps. Crustal and mantle density are assumed to not vary with position along the river profile and are not needed to be kept as separate variables. They are not part of the tectonic and climatic variables that are to be investigated as to their effect on the formation of sigmoidal longitudinal profiles. Due to this, the conversion factor between crustal thickening and rock uplift is included as part of the scaling factor applied to the rock uplift function.

The uplift calculation assumes that lateral movements at the surface are represented by the movements of the crust as a whole, and that there is no significant divergence between lateral surface movements and lateral movement of the crust as a whole, meaning no significant shearing occurs between the top and bottom of the crust. On the scale of an orgoen, the shearing that can be seen in field observations is small

compared to the large scale movements that construct the orogen (England and Houseman, 1988). The rheology of the crust, and therefore its strain response to stresses imposed on it, is approximated by a simple power law form as seen in (England and McKenzie, 1982, 1983). This form is:

$$\dot{\varepsilon} = (\bar{\tau}/B)^n$$

Where: $\dot{\varepsilon}$ is strain rate

$\bar{\tau}$ is average stress

B is a constant that represents the vertically averaged structure

n is a constant that represents the strain response

n has a value of 1 in the case of a Newtonian fluid and represents materials experiencing increasingly plastic behaviour as the value increases.

The first part of the uplift function, that due to collision is caused by the relative movement of vertical sections of material, where the relative movement is towards each other, thickening occurs. To quantify this, the convergence of lateral velocity vectors of the land surface needs to be calculated. The convergence of the velocity is important when calculating crustal thickening. It does not matter how fast a column of crust is moving laterally, but how fast it is moving compared to the surrounding crust. If all the crust is moving with the same velocity, there will be no thickening as the lack of convergence means the crust won't 'pile up'. Once the convergence of lateral velocity vectors has been calculated, the next step in calculating the rate of rock uplift is to multiply the convergence by local crustal thickness. The thicker the crustal thickness, the greater the absolute increase in crustal thickness due to velocity convergence (England and McKenzie, 1982, 1983). For a 2-D model where movement of material in or out of the plane of the model is

disregarded, calculating the convergence of lateral velocity vectors simplifies to differentiating the function for lateral surface velocity with respect to horizontal distance along the length of the river. This involves the assumption that the modelled river is draining perpendicular to the structural strike of the orogen. Obviously the plan view shape of a real river would never follow a perfectly straight line from plateau interior to plateau margin, but this assumption removes any need for an arbitrary definition of how the river path compares to the direction of convergence for the orogen and therefore gets rid of the need for any geometrically based correction to the surface velocity function along the river length. Thus, the expression for the change in crustal thickness is:

$$\frac{ds}{dt} = s\frac{du}{dx}$$

Where: *s* is crustal thickness

t is time

u is the lateral surface velocity at a point along the river

x is horizontal distance along the longitudinal profile

u is the function for velocity along the length of the modelled river. It is produced by simplifying a 3-D function for surface velocity in the interior of an orogen, formed by a relatively rigid indenter colliding with a larger landmass, down to a 2-D function for the change in velocity along the path of the modelled river (England and Houseman, 1985; England and Molnar, 1997; England and Houseman, 1988).

The expression used for *u* is:

$$u(x) = U_0 e^{-(x\sqrt{n\pi/2D})}$$

Where: U_0 is the velocity at the head of the river profile

x is the horizontal distance along the profile

n is the exponent in the power law rheology assumed for the crust

D is the length scale of the indenter forming the orogen

U_0 is the lateral velocity at the locus of two colliding landmasses. As this is the location that is first to experience uplift it is taken as the position that is highest in the modelled linear mountain range that is starting to form an orogenic plateau. While this may not be the case for a real mountain range, the region of maximum uplift will be the position of maximum convergence in lateral surface velocity, as detailed in the above relationships. The highest point in an orogen is a topographic positive inflection point and so will represent a watershed. Taking the watershed to be the head of a river is an obvious assumption to make, that is used here due to the model focusing on the longitudinal profile of the river, rather than modelling the geometry of the entire basin. In reality, there would be a distance between a catchment's watershed and the head of a river where sediment transport is carried out by non-fluvial processes, until water discharge collects to a level where a stream can form.

The second part of the rock uplift function is actually a crustal thinning term that represents thinning driven by gravitationally driven spreading (see figure 3.3). Contrasts in the gravitational potential energy of adjacent regions lead to material moving from the regions with the highest gravitational energy (England and Molnar, 1997; England and Houseman, 1988; Rey et al., 2001). Assuming the regions to be in isostatic equilibrium,

this corresponds with movement from higher to lower elevations. This is parameterised as being proportional to the difference between the square of the crustal thicknesses of the two areas (England and Molnar, 1997). This is then scaled by a separate parameter that combines all the constants that represent the orogenic plateau's rheology. As such, this parameter works as a proxy for the Argand number, which is a variable that is the ratio between the buoyancy stress resulting from differences in topographic equilibrium and the stress required to deform the orogen. The proxy used in this case combines the effects of the Argand number and the conversion from stresses to the rate in elevation change, without having to have a detailed knowledge of the rheology of the modelled area. A large value represents a relatively weak rheology, unable to support sizable changes in elevation of adjacent regions. Combining this with the first part gives an expression for the rock uplift calculation at each timestep as follows:

$$\Delta h(x) = k\Delta t\left(U_0 e^{-(x\sqrt{n\pi/2D})} - A\frac{h^2}{dx}\right)$$

Where: *h* is the elevation

x is the horizontal distance along a river's longitudinal profile

k is a scaling factor

⊿t is the timestep

U_0 is the velocity at the head of the river profile

x is the horizontal distance along the profile

n is the exponent in the power law rheology assumed for the crust

D is the length scale of the indenter forming the orogen

A is the Argand number proxy

The Argand number proxy is not a free parameter. Instead it is set to a value that ensures that the uplift at the head of the river at the first time step is ≈ 0. This represent the case of an orogen that has just assumed its maximum height before starting to expand laterally, so uplift has just switched off at the orogen's peak and is moving to the energetically more favourable lower elevation regions.

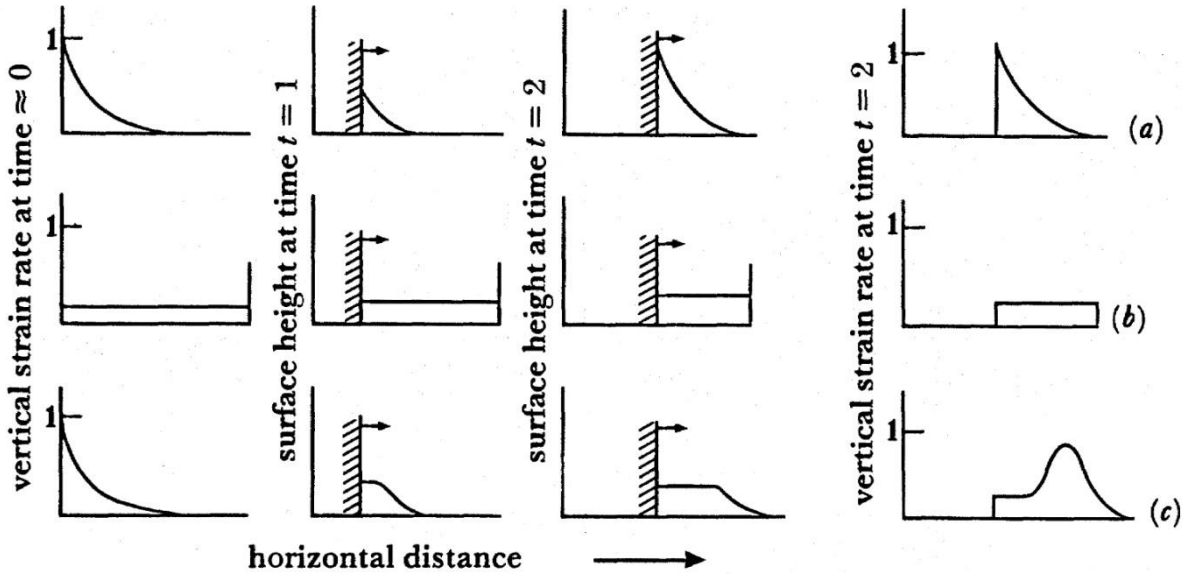

3.3 – Cartoon of the effect of both buoyancy forces and convergence on rock uplift on plateau evolution *(a) is the situation where the argand number is low so lithospheric strength is high. (b) is the situation where the argand number is high so lithospheric strength is low. (c) represents an intermediate case. In (a) the strength of the lithosphere allows for changes in elevation to be maintained over time, the low influence of buoyancy forces means that there is no change in stresses due to convergence over time. In (b) the weak lithosphere can't support changes in elevation so a perfectly flat plateau just thickens and shortens. In (c) the plateau shortens and thickens until a threshold elevation is reached where convergence and buoyancy forces are balanced and then uplift moves outwards, peaking in the plateau margins. Based on (England and Houseman, 1988).*

This final formulation for the uplift applied at each point along the river profile evolves at each time step, based on the profile at the previous time step. While the parameters can be set so that the uplift at the first time step is defined, by not defining the uplift at each further time step and allowing it to be determined based on the profile topography the model produces a more realistic representation of river evolution than one

that just applies predefined uplift values along the river profile at each time step (Roberts et al., 2012).

3.1.2 Orogenically driven precipitation

Working against rock uplift is incision driven by the action of the river being modelled. This is controlled by the local gradient at each point and the water discharge upstream of those points. Variation in water discharge along the river length is controlled by the changes in precipitation from the plateau interior to the surrounding lowlands. Therefore to accurately model the effect of plateau topography on the continued evolution of a river profile the model includes an expression for the precipitation levels along the river length. The variation in precipitation is dependent on the elevation and local slope of the terrain. As this model equates the gross topography of the plateau to the morphology of the river profiles, this produces a feedback within the model. Elevation and gradient values are modified by precipitation driven incision and then these values control the amount of precipitation at a point.

To understand the control of topography on precipitation the appropriate conceptual model is to imagine a column of air that has picked up moisture over a water body or the sea and is moving perpendicular to the structural strike of orogenic features, from the surrounding lowlands, to the higher reaches of an orogen. The moisture carrying capacity of an air column is dependent on the temperature of the air, higher temperatures enhancing the moisture carrying capacity of the air. As the air is forced upwards by the topography of the orogen it cools adiabatically, reducing its carrying capacity. Eventually the carrying capacity of the air body is less than the moisture volume being carried and so excess water is precipitated over the landscape. (Roe, 2005) High gradients cause an increase in precipitation as the column of air cools quicker moving over steeper terrain and higher elevations receive less precipitation as the air column is carrying less moisture by the time it reaches higher elevations. This results in a precipitation pattern over orogenic

plateau regions where rainfall is concentrated at the margins of the plateau and lacking within the plateau interiors. This control on precipitation by topography can be seen from a simple examination of the rainfall patterns over the Turkish-Iranian plateau and comparing them to the topography of the region.

A)

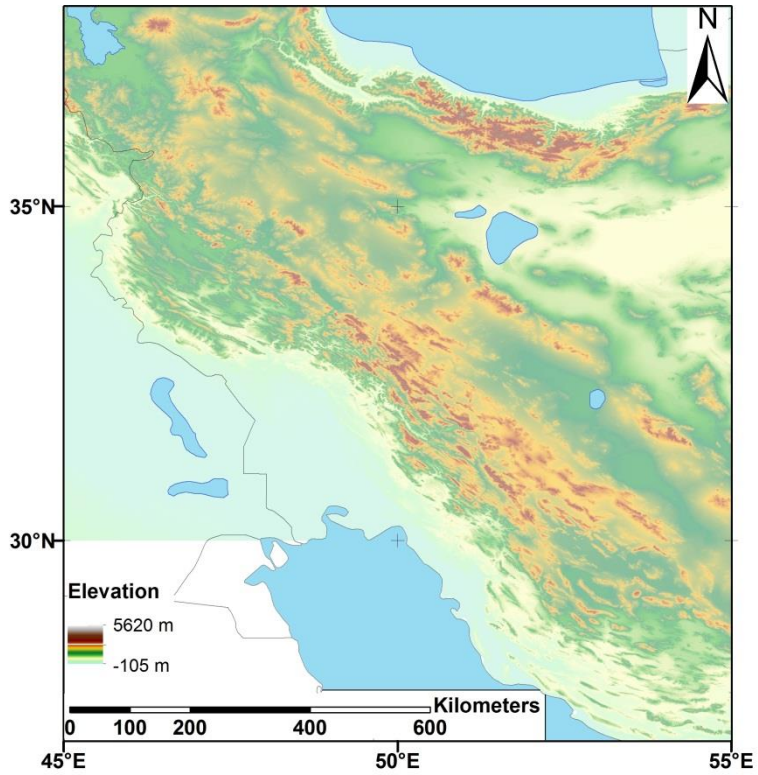

B)

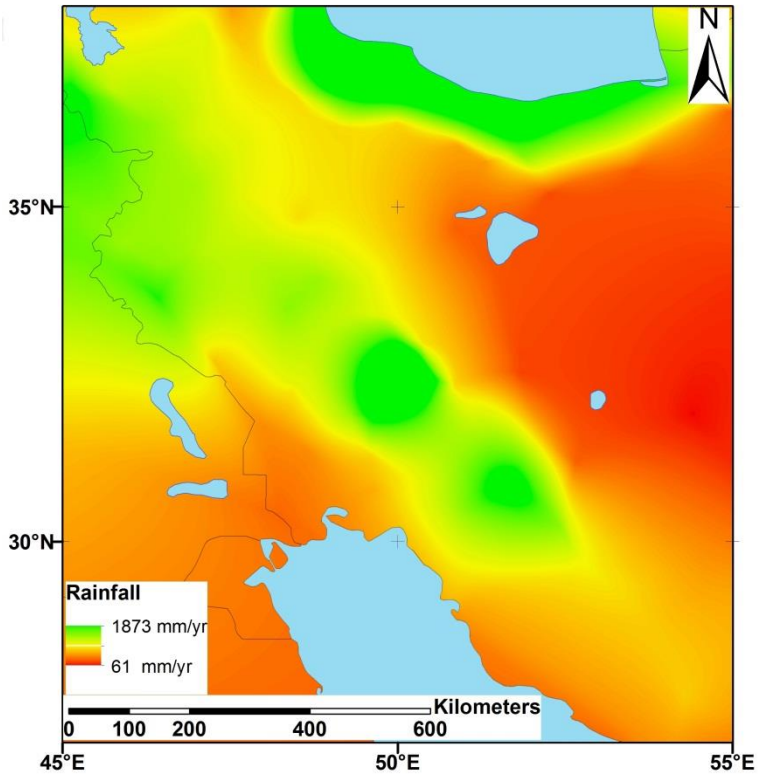

3.4 – Comparisons of topography and rainfall in the Turkish-Iranian plateau *A) Topography of the Turkish-Iranian plateau. B) Rainfall over the Turkish Iranian plateau (IMO, 1997)*

To model this changing precipitation along the river length the following formulation is used (Roe, 2005; Roe et al., 2002, 2003; Sinclair, 1994):

$$\nabla F = \left(a_0 + a_1 u \frac{dh}{dx}\right) E_0 e^{\left(AT_s - Lh(x) \middle/ B + T_s - Lh(x)\right)}$$

Where: ∇F is the atmospheric moisture convergence rate at a point

a_0 is the background moisture convergence in the absence of varying topography

a_1 is a scaling factor for the moisture convergence due to the effects of topography

u is the regional windspeed driving moisture convergence

h is local elevation

x is the horizontal distance downstream.

E_0, *A and B* are constants that form part of the Clausius-Clapeyron equation

T_s is the surface temperature at sea level

L is the temperature lapse rate in ^{0}C/km

E_0 A and B are set at 6.112, 17.67 and 243.5 ^{0}C respectively (Bolton, 1980; Emanuel, 1994). a_0, a_1, u and L are free parameters, while T_s is set at 20 ^{0}C.

After calculating ∇F values along the river length a Gaussian smoothing function needs to be applied to represent variations in windspeed over time and a moving moisture columns ability to move over discontinuous topography. Doing this allows for a more realistic, more continuous variation in precipitation levels along the river and prevents any artefacts due to a sudden change in gradient along the river. For ease of computation this

Gaussian smoothing is approximated by repeated passes of a running average (Akansu and Haddad, 2000; Nixon and Aguado, 2012).

This function is designed to calculate precipitation from the input of topographical elevation and surface gradient. When applying this to a 2-D model that is only modelling a river profile it does not correspond exactly. However one of the assumptions of this model is that the elevation of the river profile can be taken to be representative of the adjacent interfluve. Although there will be an obvious mismatch between the elevation along a river and the adjacent interfluve it can be assumed that they are likely to track each other. This is particularly applicable in the case of a detachment limited stream where the rock strength of the interfluve and the interfluve spacing are the controls on the interfluve topography, rather than the rate of material removal from the interfluve. In the region of most interest for the formation of sigmoidal longitudinal forms (the plateau interior) it is reasonable to assume that the rivers are mostly detachment limited (Wohl, 2000) while draining through high elevation regions with low rainfall and erosivity. Assuming that adjacent interfluves track river shape, the mismatch in elevation between river and interfluve is not too important as the relative shapes will be similar, so the pattern of precipitation change along the river length will still be represented.

In a similar fashion to the formula for calculating rock uplift along the river length the formula for precipitation is controlled by the topography along the model at each time step. This means that precipitation does not have to be manually determined at each timestep, and so this allows the model to be used to demonstrate how the interlinking between tectonics, topography and climate can allow for the evolution of a sigmoidal longitudinal river profile.

3.1.3 River incision

As noted above, the modelled river is assumed to be detachment limited, rather than transport limited. This is a reasonable assumption for a model concentrating on a

mountain river draining from the high regions of an orogenic plateau. Such a river is likely to have a high enough gradient and a low enough total of liberated sediment (particularly in its upper reaches) that this assumption is valid except for in certain limited situations, such as damming of the river due to landsliding from seismic or storm events (Allen and Hovius, 1998; Dadson et al., 2004; Hovius et al., 1997; Schuerch et al., 2006). Such events are transitory, meaning the assumption is even more valid when considering the system over geological timescales. As such the model does not explicitly model depositional processes, although increases in elevation along the river bed are still represented in the rock uplift function.

In these circumstances, local incision at each point along the river can modelled by values derived from the stream power incision law. A value for incision rate is determined at each point along the river profile, this is then multiplied by the time step and taken away from the elevation values along the river profile. The standard form of the incision law that is used is (Howard and Kerby, 1983; Stock and Montgomery, 1999; Whipple and Tucker, 1999):

$$E=kA^{m}S^{n}$$

Where: *E* is the incision rate

A is the drainage are upstream of the point being investigated

S is the local slope

k, *m* and *n* are empirically defined constants

This function uses drainage area to represent the influence of stream discharge on river incision. This assumes a direct correlation between catchment area and stream discharge, therefore suggesting a uniform precipitation across the catchment area. Furthermore this formulation ignores the effects of armouring of the river bed and

assumes the passage of a river over the landscape always causes some incision. In reality, only stream power that is excess to that needed to transport the river's sediment load will be used to incise into the underlying substrate.

The first assumption is corrected for by using a different formulation where discharge is represented by the average precipitation upstream of the sample point multiplied by the upstream drainage area. This ignores precipitation that does not reach a region's drainage network due to infiltration, transpiration and evaporation. These quantities are prohibitively difficult to quantify without extensive field work along the type of plateau-draining rivers being modelled. Furthermore, this correction assumes that average precipitation values over time are a good representation of waters erosive potential. The way that an amount of water is precipitated over time is also important when ascertaining how much that water can drive incision once it reaches an area's drainage network. A large, yet irregular (flashy) precipitation event can cause more incision than the same amount of water deposited at a constant rate over a longer period of time (Dadson et al., 2003; Lague et al., 2005; Palmer and Ralsanen, 2002). Quantifying this is again prohibitively difficult to do in a realistic way. However, by treating discharge as the drainage area multiplied by the precipitation, the effect of the orogenic rain shadow effect can be incorporated into the model and investigated. Using the formula for precipitation given in the previous section the formula for incision becomes:

$$I = \Delta t k \left(\int_0^x p(x) \frac{A(x)}{dx} dx \right)^m S^n$$

Where: I is the incision undertaken at each time step

p(x) is precipitation along the river length (represented by the smoothed ∇F values)

Assuming that there is always some incision when a river passes over a landscape is a reasonable assumption in the detachment limited case. It could be corrected for by adding a parameter to the end of the incision formula, but that would merely add an unconstrained parameter to be arbitrarily decided on ,without altering the relative pattern of incision along the river length, so wouldn't help with the investigation into how the changes in conditions along the river profile allow for the production of a sigmoidal form.

As this is a 2-D model there is no way to directly represent the changes in the drainage area that inputs to each point along the river. Drainage area is instead represented by $A=x^2/3$ ((Montgomery and Dietrich, 1992).

The final factor integrated into the incision part of the model is a restriction to prevent incision below sea level (h=0). This prevents the nonsensical situation where a river erodes below the level it flows into.

3.2 Conditions leading to the formation of sigmoidal longitudinal profile forms

Using intermediate values of the free parameters in the model (see figure3.6) produces a graded river that moves into a more and more sigmoidal form over successive time steps (see figure 3.5). This is notable as none of the free parameters in the model had to be specially tuned to produce a sigmoidal river shape. Instead, the sigmoidal longitudinal profiles came about as a natural response to the set-up of a model to represent the evolution of an orogenic plateau.

The model uses a fairly standard approach to modelling incision, but is unusual in the uplift being initially set to represent a laterally expanding orogenic plateau, rather than just imposing a uniform uplift along the river length. The precipitation is also responsive to changes in topography at each time step allowing for an approach to modelling river profiles that parameterises the effects of the shape of a drainage area, not merely its size. That this set up produced sigmoidal profiles without additional tuning suggests that

drainage from a plateau interior to its margins is likely to be naturally sigmoidal in form. Further sensitivity testing ascertains whether the ease of sigmoidal profile formation is just restricted to default values of the free parameters or are available to a wider range of values.

Another interesting point about the modelling is that later time steps show the model starting to destabilise. This is due to some of the constraints of the way the model is constructed. The model is stopped from eroding lower than sea level. Nor can the river length extend beyond the length of the initial set. These constraints can lead to sections where consecutive points all have elevation values of 0. The resulting lack of gradient makes local incision zero and so only uplift is applied to those points at the next time step. In later time steps this can produce a discontinuous step in the elevation giving high gradient (and therefore precipitation and incision) values at the discontinuity for the next time step. Such high incision can then reduce the elevation at the points back to 0. This sets off a continuing cycle of increasingly large oscillations at the toe of the profile. While not undermining the observed changes seen in the profiles, this undesirable effect could be reduced with increasing computational input being used to reduce the size of and increase the number of time steps. Smaller time steps would mean smaller changes in elevation at each step, preventing the over correction from zero incision or one in which gradients at discontinuities give overly high incision. Having the model improved by smaller time steps is a natural consequence of any model that is discontinuous through time.

A)

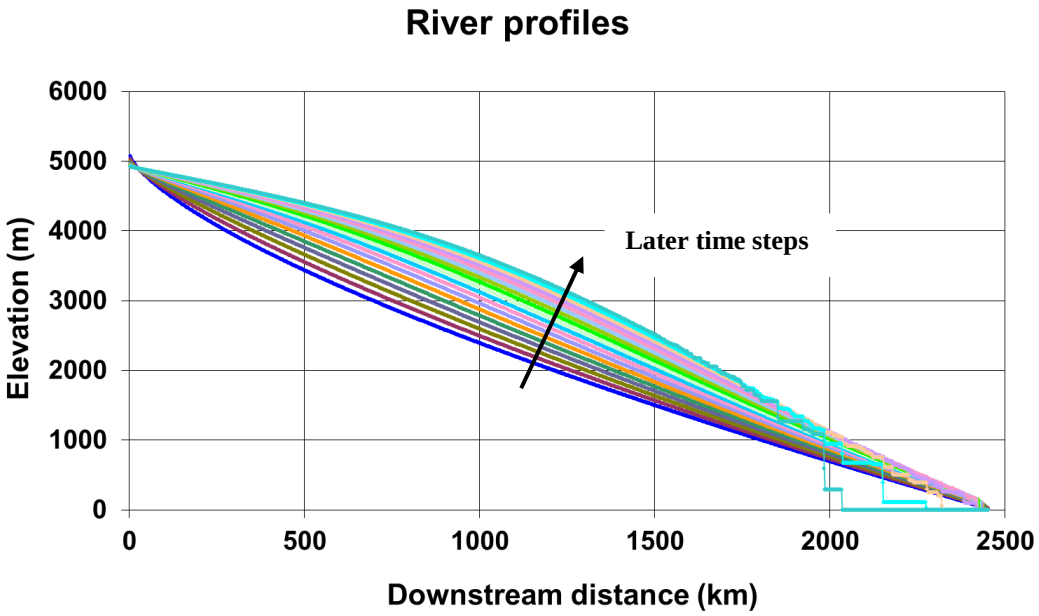

B)

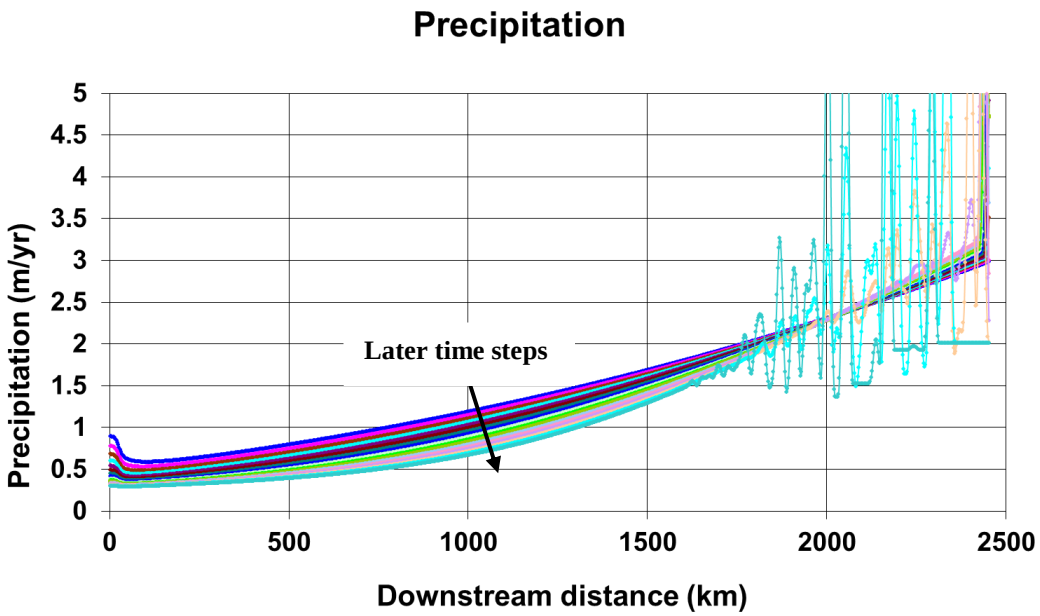

See over for caption

C)

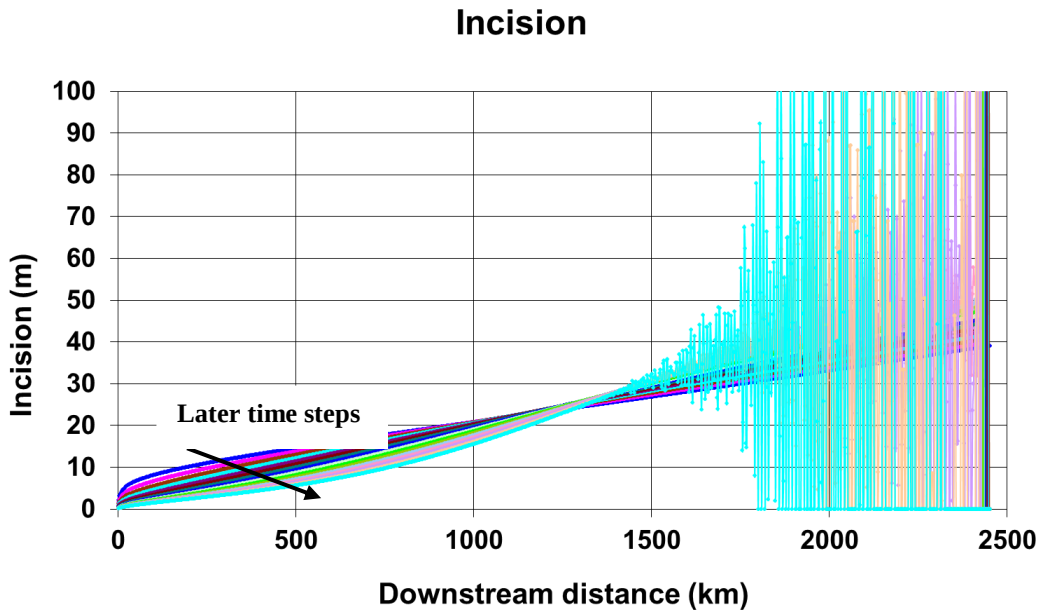

D)

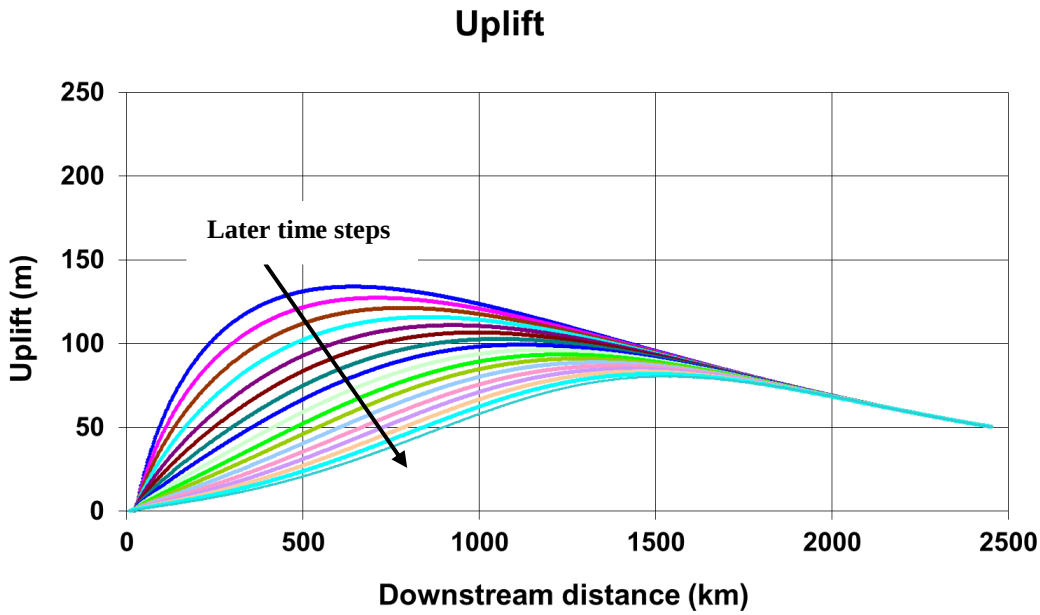

3.5 – Model outputs and inputs at each timestep *Evolution of the model at successive time steps. Arrow shows progression in time steps. A) Longitudinal profiles – These change to sigmoidal form through time, with a lower gradient headwater and increasing gradient downstream. B) Precipitation- The plateau becomes more arid, with the rainfall concentrating at the plateau margins. C) Incision – The same pattern is seen as in precipitation D) Uplift – Uplift dies off in the plateau, moving to a value set only by the tectonics of the orogen at a distance progressively further away from the initial peak of the orogen.*

3.3 Model sensitivity to climatic and tectonic conditions

To see what range of parameters can lead to rivers with sigmoidal forms, each free parameter was varied until the model failed to produce a sigmoidal shape. These ranges of the variables were compared to realistic ranges of the values. By seeing what proportion of the realistic range is compatible with the formation of sigmoidal river profiles a sensitivity value can be calculated for each variable. If the ranges are the same, then it doesn't matter what value is chosen in the model when producing a sigmoidal form, so the sensitivity is 0%. If only one value produces a sigmoidal river shape then the sensitivity is 100% (see figure 3.6). Looking at the range of 'sigmoid possible' values compared to the possible range for each value is a better way of comparing the model's sensitivity to each parameter than a direct comparison. Just comparing the 'sigmoid possible' ranges of different variable would mean nothing without normalising them to the realistic ranges of those variables as they all represent different quantities and are often measured in different units.

The sensitivity values can then be used to get an idea of what the controls are on the sigmoidal river forms observed in chapter 2. This allows for the identification of how tectonics and climate combine to control river form and see which factor is more important in the creation of sigmoidal river longitudinal profiles.

3.6 – Table of model parameters *This table lists all the parameters used in the construction of the model. Parameters not flagged as free are constrained to set values to allow for the modelling of an orogenic plateau setting. Where a parameter is flagged as being free, the effect its variance has on river profiles can be investigated. For these parameters the range of values that can produce a sigmoidal river profile outcome is compared to a realistic range for the parameter in all settings, allowing for the calculation of a sensitivity percentage. (values in brackets are the 'default' values used for the initial model run showing how the model could produce a sigmoidal shape from a graded river). The notes column will show whether a parameter is mostly associated with tectonic, lithological or climatic control on the river profile form.*

Parameter	Free	Possible range	Range for sigmoidal rivers	Sensitivity	Notes
Height	**N**	5107m		**N/A**	Height is the average height of rivers draining the Tibetan plateau.
Length	**N**	2452km		**N/A**	Length is the average length of rivers that drain from the interior of the Tibetan plateau to the plateau margins.
River steepness	**N**	0.12		**N/A**	This is the coefficient of the power law that describes the initial graded river profile. It is set ensure that the river toe is close to sea level.
Length/Slope exponent (n)	**N**	0.6 (Knighton, 1998; Maritan et al., 1996)		**N/A**	This is used to set the initial graded river shape.

m (Stream power incision law)	**Y**	0.25 – 1 (Howard et al., 1994; Howard and Kerby, 1983; Wohl, 2000)	0.45 - 0.57 (0.5)	**84%**	Primarily climatic variable. This represents the influence of discharge on river incision and so the supply of water to the system. Tectonics can influence the catchment shape and so this variable. Often empirically determined. m/n should be kept to roughly 0.5 (Whipple and Tucker, 1999).
n (Stream power incision law)	**Y**	0.66 – 1 (Howard and Kerby, 1983; Sobel et al., 2003; Wohl, 2000)	0.85 – 1 (1)	**55.9%**	Primarily tectonic variable. This represents the influence of local slope on river incisions and so the effect of tectonic forcing of the shape. Internal feedbacks (partially climate driven) can also effect the local slope. Often empirically determined. m/n should be kept to roughly 0.5

a_0	**N**	0.086		**N/A**	Effects the background rainfall levels present if there were no change in topography across the orogen. Initial value for precipitation variables set so that rainfall in the plateau interior was close to modern day values of <500 mm/yr (Sobel et al., 2003).
a_1	**N**	3		**N/A**	Effects the orogenic precipitation function's sensitivity to topography. Initial value for precipitation variables set so that rainfall in the plateau was close to modern day value of <500 mm/yr (Sobel et al., 2003).
Average windspeed (u)	**Y**	1.5-15 (Egger et al., 2000; Jiang et al., 2010)	1.5 - 15 m/s (10) (Roe, 2005)	**0%**	Climatic variable.
Temperature at sea level (T_s)	**Y**	0 – 30 (Peixoto and Oort, 1992)	0 – 30 ^{0}C (20) (Roe, 2005)	**0%**	Climatic variable. The possible range represents the range of average sea level temperatures between the equator and 60^{0}N/S
Temperature lapse rate (L)	**Y**	5 - 9.8 ^{0}C (Essenhigh, 2006)	5 - 9.8 ^{0}C/km (6.6)	**0%**	Climatic variable. The high value for the lapse rate represents a dry adiabatic lapse rate, while the lower bound is a saturated lapse rate.

Time step	**N**	100000 yr		**N/A**	The size of the time step is limited by the total number of time steps possible to compute. Smaller values reduce destabilising effects in the model.
Incision coefficient (k)	**Y**	$1.3x10^{-3}$ - $1x10^{-7}$ (Sobel et al., 2003; Stock and Montgomery, 1999)	$2.8x10^{-4}$ - $3x10^{-6}$ ($1.5x10^{-4}$)	**47.8%**	Primary lithological variable. k is usually inspected in log-log space, so for sensitivity testing this is also done to prevent getting unrealistically high sensitivity values for a value that varies by several orders of magnitude.
Uplift scaling coefficient	**N**	0.008		**N/A**	Set so that the mean uplift and incision at the first time step are approximately equal, to model the river starting off in a graded state.
Collision velocity (U_0)	**N**	50 mm/yr (England and Houseman, 1988)		**N/A**	Change in collision velocity would change the scale of the maximum elevation, also scaling with plateau rheology (n and Argand number).

n - rheology	**Y**	1-10 (England and Houseman, 1988)	1-10 (3)	**0%**	Lithological variable. 1 represents a Newtonian fluid
Collision length scale (D)	**Y**	0-20000 km	2750 – 20000 km (5000)	**13.75%**	Tectonic variable. No real reference scale for indenter scale range. The top end of the ranges is set by ≈½ Earth circumference.
Argand number proxy	**N**	$6x10^{-17}$		**N/A**	This is set so that the uplift at the river head in the first time step is close to zero (representing a plateau beginning to expand laterally as it reaches its maximum height).

The ranges that produce sigmoidal rivers in this model set up cannot be taken as a catalogue of values that the parameters describing an orogen must lie between if sigmoidal rivers would be observed to be draining an orogenic plateau. This is because most of the parameters described above are not completely independent and their effect on the system is influenced by both the scale of the system and the values of the other parameters. This is why the sensitivity of the model to changes in the variables is more valuable than the exact values themselves.

The sensitivity analysis shows that the only variables that the model is sensitive to (as long as the values are limited to realistic ranges) are the parameters controlling the stream power incision law. The one exception to this is a low level of sensitivity to the length scale of the collision, where if the length scale is too small compared to the plateau-draining rivers, incision dominates and the rivers rapidly incise all the way down to the base level. In essence, this says that large rivers on small orogens have incision that

completely overwhelms the tectonic advection of material into the orogen, dissecting and destroying it. The geological implications of this are that in the orogens investigated the drainage has scaled with the orogen, as would be expected. If orogenic processes act on an area with large antecedent drainage systems they are unlikely to be able to cause plateau formation.

The lack of model sensitivity to climatic (temperature and wind speed) and rheological parameters suggests that sigmoidal river forms would be a factor of all orogenic plateau drainage and are not specific to just the two plateaux studied. All orogenic plateaux through geological history would be expected to be drained by sigmoidal rivers. A plateau forming uplift function is necessary to form the sigmoidal rivers observed, but once this type of uplift is imposed on a graded river a sigmoidal river forms. This highlights the combined work of climate and tectonics in forming sigmoidal rivers. Even when the effects of orogenic rain shadows are fully taken into account the pattern of uplift seen in an expanding plateau is still a necessary condition.

The only parameters that the model shows significant sensitivity to are the parameters controlling the stream power incision law. This may be partly enhanced by the interdependence of these factors, the m and n values are frequently discussed as controlling river form by their ratio, rather than their individual values. This ratio is taken to represent different stream incision processes, with an m/n ratio of 0.5 indicating that incision is proportional to basal shear stress and a ratio of 1 representing incision rates proportional to specific stream power (Howard et al., 1994; Howard and Kerby, 1983; Stock and Montgomery, 1999). None-the-less, k m and n roughly correspond to a lithological, climatic and tectonic control on the steam incision respectively.

The k value in particular can be taken as a proxy for erodability of different lithologies (Sobel et al., 2003; Stock and Montgomery, 1999), as it is the linear scaling of a mountain river's incision through bedrock. The model shows the formation of sigmoidal rivers to be sensitive to this parameter, but to a lesser degree than the other parameters

controlling river incision. This corresponds to the results seen in chapter 2 where there was no correspondence seen between the pattern of disequilibrium in plateau-draining rivers and the underlying lithologies.

The next variable is m, the exponent of area in the stream power incision law. This can be considered as the most climatically influenced of the three variables that parameterise the stream power law. This variable controls the sensitivity of the stream power incision law to the drainage area and precipitation levels of the catchment feeding the incising streams. In this way it represents the sensitivity of incision to the climatic variable (precipitation) effected by the topography of an orogenic plateau (due to rain shadow effects). This parameter shows the greatest sensitivity in different model runs, with a smaller relative window of values that produce sigmoidal profiles than any other variable. This suggests that stream incision's sensitivity to precipitation and discharge changes is the most crucial factor in forming sigmoidal drainage of an orogenic plateau (assuming the pattern of uplift particular to a laterally expanding orogenic plateau is present in the first place).

Second to m in sensitivity is the exponent of slope in the stream power incision law, n. This variable controls the sensitivity of a stream's incision to changes in slope along its length. As the slope is created by the plateau forming tectonics this is the most tectonically influenced of the three variables. However, similarly to the way that m cannot be simply considered as just the climate sensitivity variable, n is not just the tectonics sensitivity variable. The processes of incision act to change the slope of the incising streams, so n represents the streams sensitivity to not just the tectonically created topography, but also its own erosional processes.

Taking both the m and n values together, the ranges that are compatible with sigmoidal river profiles give m/n ratios of approximately 0.5, which would mean that the incision was approximately proportional to basal shear stress along the stream. This is consistent with most investigations of rivers thought to be closer to a graded state ((Seidl

and Dietrich, 1993; Stock and Montgomery, 1999; Whipple and Tucker, 1999), suggesting that unusual conditions are not needed to make these unusual river profiles.

3.4 Conclusions

The conclusions drawn from this modelling are shaped by the two ways this model was intended to be used outlined by the first part of this chapter. Firstly it was to be used to demonstrate how the tectonic and climatic setting of an orogenic plateau can lead to sigmoidal longitudinal profiles of the rivers draining from the plateau interior to the plateau exterior. Secondly the sensitivity of the model to changes in its controlling variables was investigated to try and see if tectonic or climatic factors have more control.

The model does not deviate from common descriptions of river incision (Knighton, 1998; Seidl and Dietrich, 1993; Wohl, 2000), basing that on the stream power incision law. Neither does it specify a particular pattern of precipitation to drive the incision law. Changes in precipitation along the river length are purely driven by the topography of the river and are not pre-determined to produce a sigmoidal profile outcome. The only unusual part of the modelling is imposing the particular uplift pattern of a plateau that is expanding laterally. Forming a sigmoidal longitudinal profile from a model where the inputs at each time step are so responsive to the outputs at the previous time step, without any specific tuning suggests that sigmoidal longitudinal profiles are normal reactions of drainage systems to orogenic plateau formation. Two parts of the sensitivity testing back up this conclusion. Firstly the sensitivity of the model to many of the free parameters was zero, suggesting that as long as the setting combined to form an orogenic plateau a sigmoidal river shape was likely. Secondly, the range of values compatible with sigmoids for the m and n exponents of the stream power law gives m/n ratios of approximately 0.5, consistent with many investigations into rivers in more standard settings. This further reduces the need for unusual processes to cause sigmoidal river profiles.

The parameters of the model that did show some sensitivity were those controlling the stream power law. The model seemed most sensitive to the parameter representing sensitivity to climatic fluctuation and least sensitive to the variable representing lithological changes, with the variable representing sensitivity to tectonics being intermediate. Changes in the way the river responds to climatic variables are most likely to prevent a plateau-draining river from displaying a sigmoidal longitudinal profile.

The conceptual model of longitudinal profile form arising from this is concave-up graded rivers being shaped into sigmoidal forms by plateau growth. Plateaux display a sigmoidal topographic transect from the plateau interior to the surrounding lowlands and as they grow they make the rivers draining them follow the same shape. The role of climate is 'permitting' this change to happen by not allowing too much incision along the river length to retard this growth. Ultimately the factors are working together to produce the river forms seen. Coupling of tectonic and erosional systems is an important part of any model hoping to realistically replicate observed topography (Allen, 2008; Allen and Allen, 2005; Codilean et al., 2006). Only if the rivers display a large sensitivity to the water discharged along them do they incise enough to retard the plateau growth and maintain a concave-up shape.

4. Features of alluvial fans in orogenic plateaux interiors

4.1 Summary

This chapter aims to show alluvial fans in orogenic plateau interior settings differ from those located in the related climatic and tectonic setting of the active fold-and-thrust belts found at the margin of a plateau. A secondary aim of this chapter is to use identified differences between fans in clearly defined active or plateau interior settings to characterise the fans located in intermediate settings, whose tectonic, climatic and geomorphic characteristics are intermediate those of the plateau interior and active margin settings. (see chapter 1 for a discussion of how to determine the boundary between the plateau interior and the deforming thrust belt surrounding it). This secondary aim relies upon the findings of the first to provide a framework for characterising the fans in intermediate areas.

The study area used for this work is the Turkish-Iranian plateau and its northern margin, over the Alborz mountain range. This is a large study area that incorporates both an actively thrusting mountain range and the relatively quiescent plateau interior. Datasets interrogated to identify characteristics of alluvial fans are the Shuttle Radar Topography Mission (SRTM) Digital Elevation Maps (DEMs), Landsat 7 Enhanced Thematic Mapper (ETM)+ imagery and annual rainfall data from the Iranian meteorological survey (IMO, 1997; Jarvis et al., 2008; Pollastro et al., 1999; USGS, 2008, 2010). Data processing is done with ArcGIS, Global Mapper and Excel.

Using these datasets multiple parameters (e.g. Fan area, fan surface gradient, fan volume etc.) of numerous fans are measured. These parameters are then compared to the setting of each fan. Variables used to categorise the setting of the fans are:

1) The distance between the fan head and the seismogenic thrusting zone
2) The ζR ('Plateauness', defined as elevation/relief (Andronicos et al., 2007; Formento-Trigilio and Pazzaglia, 1998) (see chapter 1)) value at the fans' head.
3) Annual rainfall at the fans' head.

For the rest of the chapter the two groups of parameters are referred to as either setting variables, if they are controlling variables that drive fan geometry or fan parameters if they are parameters that are measured to define fan geometry. The relationships between setting variables and fan parameters are determined in two ways. Firstly, the fan parameters are compared to these tectonic and climatic setting variables. Secondly, the fan population was divided into thirds, and the fan parameters of these three sub-populations compared. The three sub-populations of alluvial fans are based on the setting variables that are compared to the fan parameters. The first third comprises the fans that are closest to the seismogenic thrusting zone. These fans represent those that are most likely to be influenced by the active deformation at the plateau margins. The second third are those that have the highest ζR value at their head. These fans are those whose setting is most like a typical plateau interior. The final third are the fans that don't meet the two previous criteria and so represent an intermediate population, which is inspected to see how they relate to the previous, more tightly defined, sub-populations. Dividing the fans into three sub-populations like this is somewhat arbitrary, but allows for the two aims of the study to be addressed. An arbitrary division is a necessary compromise in a study that aims to characterise the difference between fans in regions. A suitable follow up would be to investigate how the distinguished differences between the fans in the regions successfully categorise a separate fan population, but this is beyond the scope of this work.

It is concluded that alluvial fan parameters can distinguish between populations of fans in an actively thrusting setting and fan populations in the tectonically quiescent plateau interior. But, the change in fan parameters between fans in the actively thrusting and plateau interior settings is gradual, indicating that no threshold is crossed from one setting to the other that has a drastic effect on morphology.

This is a large and spatially distributed dataset, which provides a catalogue of fan morphology parameters in differing tectonic and climatic settings. As a result, there are direct implications for using it to calibrate numerical models producing artificial topography as they simulate past climatic and tectonic conditions.

4.2 Introduction

4.2.1 Alluvial fans within a plateau setting.

Alluvial fans are associated with tectonic settings that provide accommodation space for fan growth (e.g. rift settings and thermally subsiding basins) (Densmore et al., 2007; Dorn, 2009; Ferrill et al., 1996; Hartley et al., 2010; Viseras et al., 2003; Waters et al., 2010), despite orogenic plateaux interiors not actively subsiding, alluvial fans are common in this setting, with 57.6% of the Turkish-Iranian plateau surface being covered by alluvial fans (this value is calculated by totalling up the area of Quaternary alluvial sediments identified and dividing it by the total study area) (Pollastro et al., 1999). One factor providing conditions suitable for alluvial fan formation are an arid to semi-arid climate leading to fluvial systems that are transport limited and so form depositional systems. Uneven temporal variation in precipitation leads to occasional higher levels of discharge along fluvial systems in plateau interior settings, allowing for the transport of material from proximal catchments to alluvial fans. Additionally, large parts of the plateau are internally drained, in part because of tectonic uplift at marginal thrust belts and the formation of an orogenic rain shadow in the plateau interior defeats drainage systems that drain from the

plateau interior to the surrounding lowlands (Metivier et al., 1998; Sobel et al., 2003). These internal fluvial systems have a low gradient, due to the lack of tectonic uplift and resulting lack of gradient along the length of the fluvial system. Such low gradients contributed to the transport-limited nature of the river systems and enhance sediment deposition. Established internal drainage means that transported sediment stays in the receiving basin, lowering gradients along the fluvial system and setting up a positive feedback system where these reduced gradients enhance further sediment deposition (Sobel et al., 2003). This feedback mechanism within internal drainage, distributing material within a plateau setting to the lowest elevation regions, is one of the methods that plateau topography smoothes out as an evolving orogenic belt becomes a plateau.

4.2.2 Alluvial fans as an indicator of tectonic and climatic conditions

Changes in the topography of the landscape require tectonic movement, erosion or deposition. As a result, geomorphology acts as a record of the tectonic and climatic influences on a landscape.

Using geomorphology as a way of understanding the tectonics and climate of a region is complicated by the fact that the landscape reflects the influences of conditions leading up to the present day, not just current conditions. While geomorphology tends to have geologically quick response times (0.25 – 1.5 myr for fluvial systems (Whipple, 2001) tectonic and particularly climatic driving conditions can also change on these relatively rapid timescales. A further complication, particularly associated with the geomorphology of fluvial systems, is that geomorphological features can represent the tectonic and climatic setting of a different area, due to sediment transport processes moving material resulting from a particular setting to another setting (Frostick and Jones, 2002).

Alluvial fans are a good example of geomorphological features that can be used to understand the tectonics and climate of an area (Bahrami, 2012; Dade and Verdeyen,

2007; Jones, 2004; Quigley et al., 2007; Waters et al., 2010). Their catchment areas tend to be adjacent to their deposition areas, reducing the problems of long-distance sediment transport making correlation between tectonic and climatic setting and the resulting geomorphology difficult. Many fans are also still active (as seen by the presence of a fluvial system connected to the fan head and active channels visible on the fans' surfaces) (See figure 4.1). Active channels in eastern Iran have been dated as being established after the Last Glacial Maximum, in the region of 10,000-12,000 years before the present (Le Dortz et al., 2011; Walker and Fattahi, 2011).

A)

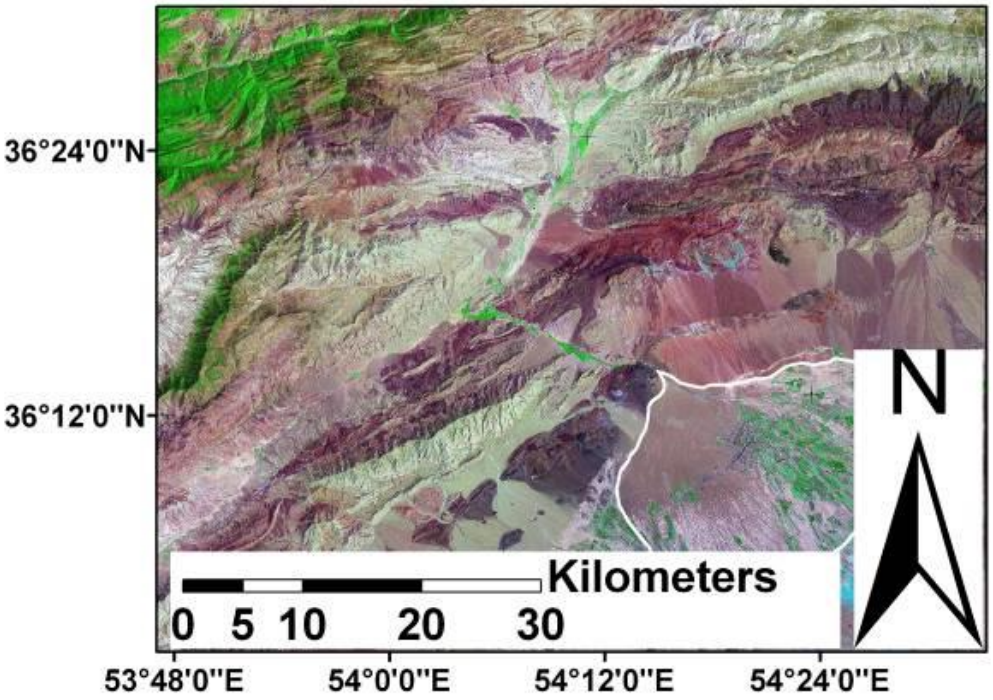

B)

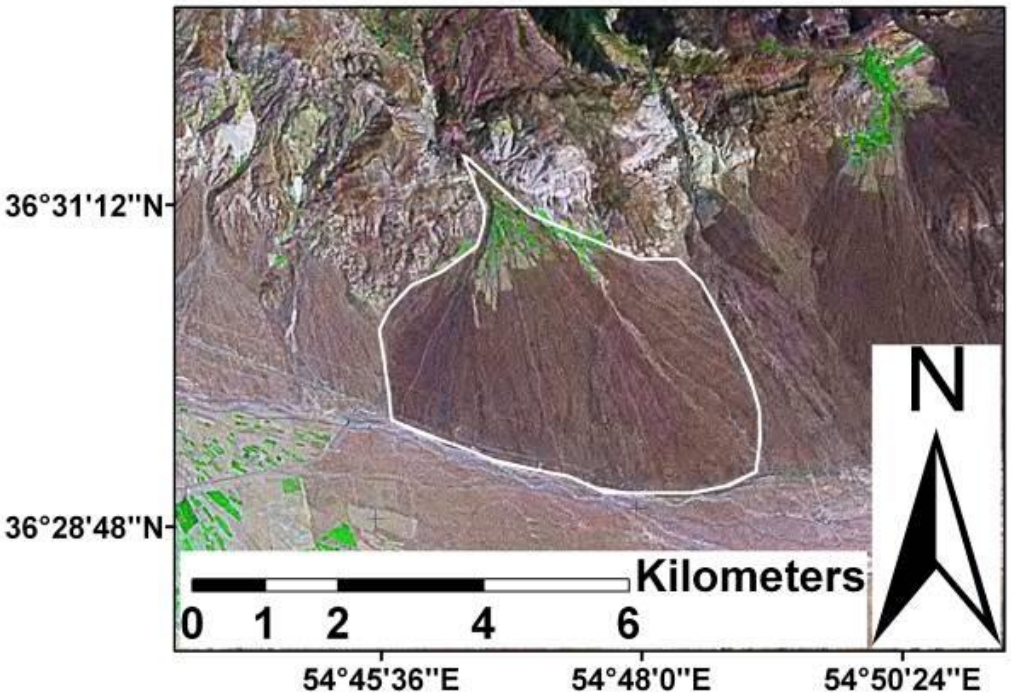

Diagram 4.1 – Images showing alluvial fans that are currently active: *A) An alluvial fan with a current river connecting to the sediment distributing alluvial fan. B) Active channels visible on an alluvial fan surface.*

Active fans are definitely currently responding to present climatic and tectonic conditions. While knowledge of a fan's response time would be needed to ascertain how a fan's geomorphology corresponds to the present tectonics and climate, as opposed to recording delayed responses to previous conditions, being active shows there is some correlation. The response time of fluvial systems is rapid (Frostick and Jones, 2002; Quigley et al., 2007; Whipple, 2001) compared to the formation time of an orogenic plateau (Ahmadhadi et al., 2007; Allen et al., 2004; Guest et al., 2006) effectively allowing alluvial fans to sample the recent conditions of an orogenic plateau.

Fluvial system responses to tectonic and/or climatic forcing are in the type (grain size, composition etc.) and amount of sediment supply and changes to the accommodation space receiving this material. Rapid relative tectonic uplift produces more sediment supply and more accommodation space. Tectonics provides the accommodation space and gradient necessary for any fan, and ultimately control their location (Allen, 2008; Allen and Hovius, 1998; Jones, 2004), but tectonic processes work in tandem with climate. More rainfall means more sediment liberated and transported, enhancing fan progradation and increasing a fan's areal extent, but a persistently wet climate will promote a river with increased transport capacity that effectively by-passes and incises the fan: the fan will turn in to a floodplain. An exception is where a fan terminates at a lake margin. However, higher rainfall levels will control fan extent by raising lake heights and preventing fan expansion beyond the lake margin. As both these factors can both enhance and retard fan progradation, describing the linkages between fan morphology and fans' climatic and tectonic setting is complex.

This study uses remote sensing to look at the morphology of alluvial fans. This provides only information about the surface of alluvial fans, so stratigraphic detail about fans is unavailable. However, knowing about the fan surface provides information about the balance of sediment supply and accommodation area over the lifetime of the fan.

When sediment supply rate is high compared to accommodation space production, fans prograde over a larger area.

4.2.3 Questions to investigate

This study uses the previous rationale for a correlation between fan morphology and the tectonic and climatic setting of the fan as the basis for asking two questions:

1) How do the surface characteristics of an alluvial fan correlate to the known tectonic and climatic variables of a region?

2) Can the surface characteristics of an alluvial fan allow the tectonic and climatic variables of an area to be deduced?

These two questions are the reverse of each other. To attempt to answer them validly it is important not to engage in circular reasoning where the characteristics of an alluvial fan population that correlate with particular tectonic and climatic variables are then used to deduce those tectonic and climatic variables that have been seen to correlate to that alluvial fan morphology. Instead different fan populations, or sub-populations of the total fan population studied, need to be used for the separate questions.

The second question has implications for using fan characteristics to constrain the tectonic and climatic setting of an area, when other data is unavailable. In particular a specific sub set of the question is, ‘can fans be used to show that an area is tectonically active in areas where there is no observable or seismogenic tectonic movement?’ Fans present in an area where there is no other evidence for tectonic movement show there must have been some tectonics to provide the accommodation space and gradient necessary for fan formation, but not necessarily that they are still current.

4.3 Alluvial fan features detectable from remotely sensed datasets

The remotely sensed datasets used are SRTM DEMs and Landsat 7 ETM+ images of the Turkish-Iranian plateau. The DEMs provide infomation about the morphology of the fan surface, while the Landsat images provide false colour data related to electromagnetic radiation reflected and emitted from the fan surface.

Fans were located using the Landsat 7 ETM+ data, rather than the SRTM DEMs. The Landsat images were more suitable for delimiting the boundary between fans and the background landscape, due to the large contrast between them. SRTM data prove unsuitable for defining fan boundaries as the gentle gradients of most alluvial fans provides little contrast between the fan surface and the background landscape (see figure 4.2). The Landsat images have a large amount of contrast between fan areas and background areas, due to lithological differences and reworking of the sediment in the fan itself.

A)

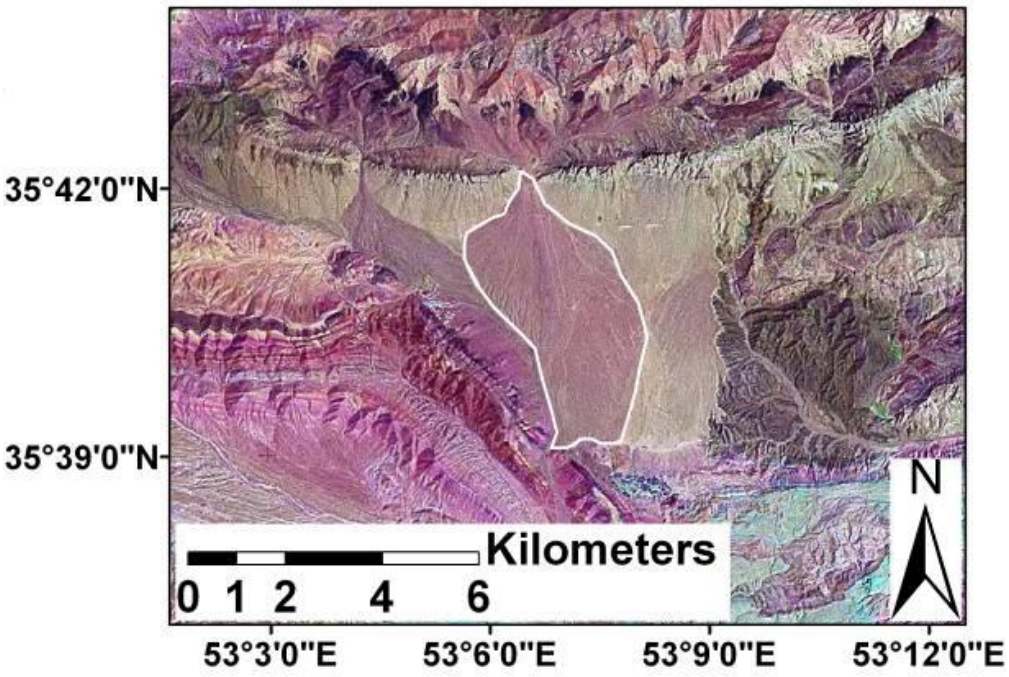

B)

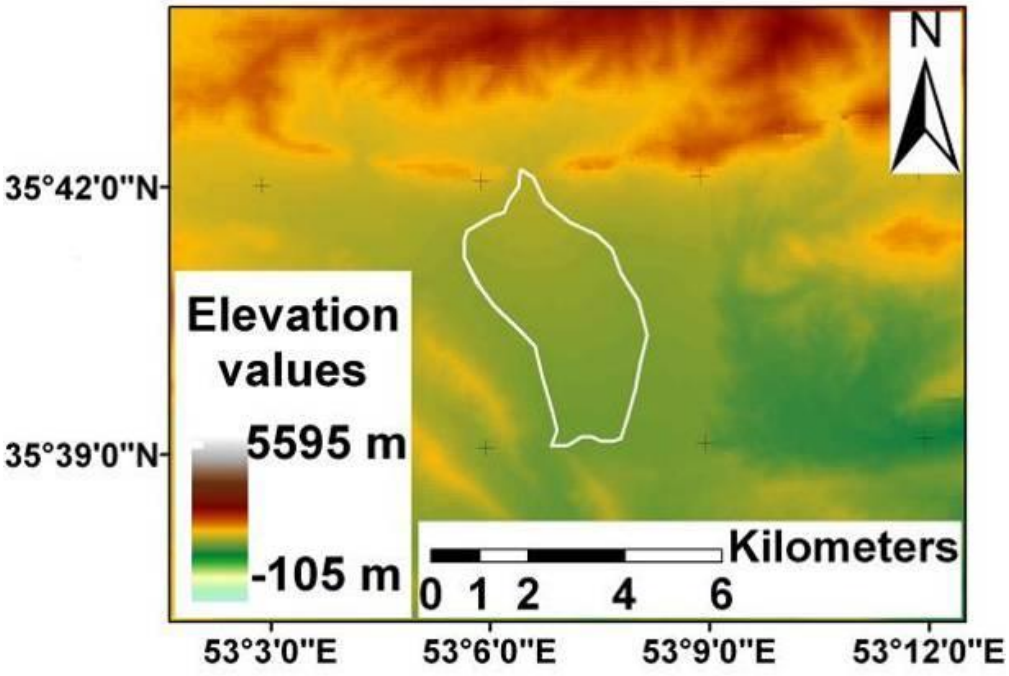

Diagram 4.2 - Images showing the difference in contrast between alluvial fans and the surrounding area for both SRTM and Landsat 7 ETM+ data: *A) A fan shown using landsat 7 ETM+ data. B) The same fan shown with SRTM data. The fan is far more visible in A) due to greater contrast between the fan area and the background region.*

4.3.1 Landsat 7 Enhanced Thematic Mapper + data

The Landsat 7 satellite provides imagery collected by the ETM+ instrument mounted aboard the satellite. The instrument records the intensities of electromagnetic radiation in the visible and infra-red parts of the spectrum that is reflected by the Earth. It samples it with a 30 metre resolution at the Earth's surface, which can be sharpened by a panchromatic band with a 15 metre resolution (See table 4.3.1a).

The parts of the dataset used in this study are provided in the Geocover product from EarthSat, which consists of bands 7, 4 and 2 each sharpened to have a 15 metre resolution. Band 7 measures the intensity of medium wavelength infra-red radiation and is designed to be useful in discriminating mineral and rock types. Band 4 measures short wavelength infra-red intensity and is used to estimate biomass and separate water bodies from vegetation. Finally, band 2 collects the green part of the visible spectrum and is tuned to match the peak electromagnetic emittence of vegetation and is useful for distinguishing plant types and extent (Masek et al., 2006; USGS, 2008). Each pixel of the satellite images used has 24 bits of information associated with it, 8 bits for band 7, which produces the intensity of red in the images, 8 bits for band 4, which produces the intensity of green in the image and 8 bits for band 2 which produces the intensity of blue in the image. Combined, these produce the false-colour images used in this study.

Landsat 7 ETM+ band	Wavelengths of electromagnetic radiation sampled (m x 10^{-6})	Description of wavelength range	Resolution (m)	Uses of this wavelength range
1	**0.450 – 0.515**	**Blue-Green**	**30**	**Penetrates water and distinguishes between forest types.**
2	**0.525 – 0.605**	**Green**	**30**	**Matches the green reflectance wavelength of vegetation.**
3	**0.630 – 0.690**	**Red**	**30**	**Matches the wavelength of light absorbed by chlorophyll.**
4	**0.775 – 0.900**	**Near IR**	**30**	**Used to estimate biomass and discriminate soil moisture.**
5	**1.550 – 1.750**	**Mid IR**	**30**	**Penetrates atmospheric haze, discriminates roads, bare soil and water.**
6	**10.400 – 12.500**	**Thermal IR**	**60**	**Intensity corresponds to the heat radiated. Related to soil moisture.**
7	**2.090 – 2.350**	**Mid IR**	**30**	**Discriminates between mineral and rock types and soil moisture.**
8	**0.520 - 0.900**	**Panchromatic**	**15**	**Wide spectral band with high resolution used to sharpen imagery.**

Table 4.3 - Table of Landsat 7 ETM+ bands: *The table shows the wavelength of electromagnetic radiation sampled by each band and its intended uses.*

These images were used in two ways. Firstly, the false-colour images often showed a high level of contrast between alluvial fans and the background surface, so they were more useful than the SRTM images in delimiting the extent of the fans. Although Landsat images don't give any information about the shape of the fan surfaces, as they don't contain any elevation data, by allowing for a more accurate delimitation of the fan extent than SRTM data, they can provide plan-form morphological data, such as fan area, fan perimeter and progradation length.

Secondly, the band 7 data was used for its ability to distinguish between mineral and rock types. While not able to provide absolute information on rock types without ground truthing, and subject to interference from non-mineralogical variance that can also affect the reflectance and emittence of infra-red radiation, reducing its precision, it was used to provide a numerical way of distinguishing the lithological composition of alluvial fans.

4.3.2 Shuttle Radar Topography Mission Digital Elevation Maps

The base SRTM data collected is the phase difference between two radar returns at two radar antenna mounted 60 metres apart on the shuttle orbiter. This Interferometric Synthetic Aperture Radar (InSAR) technique allows for these phase differences to be turned into elevation values, producing the DEMs used in this study (Jarvis et al., 2008).

The radar returns do not always represent ground surface as vegetation can provide a surface for radar reflection, meaning heavily vegetated areas, particularly in humid areas where water covering enhances the effect, can produce spurious results, where the elevation values are artificially increased (Rodriguez et al., 2005; Rodriguez et al., 2006). Furthermore, radar returns are prone to excessive scatter in area of high surface gradient and at water surfaces, such as lakes. This leads to voids within the SRTM data, where no values are present. This problem is more of an issue in orogenic plateaux margins, where high relief values cause more shadowing, preventing radar returns.

The dataset used is provided by the Consultative Group on International Agriculture Research's Consortium for Spatial Information (CGIAR-CSI) and is their fourth version of the SRTM dataset (Jarvis et al., 2008). In this they try to address the inaccuracies and voids in the original SRTM dataset by removing obvious pits in the surface, caused by inaccuracies in the SRTM data and filling the voids with DEM data from alternate data sources (Jarvis et al., 2004; Reuter et al., 2007). Where alternate DEMs are not available, the elevation values are interpolated from the surrounding terrain. This results in void-less data, although the accuracy of the data is reduced in high relief areas.

DEMs are useful in providing information about the 3-D shape of the fan surface. This gives more insight into fan volume and so the sediment stored as an alluvial fan, in contrast to the Landsat images providing information about the areal extent of the fan and therefore the balance between sediment supply rate and accommodation space formation.

Additionally, DEM data allows for the investigation and delimitation of the morphology of the catchments feeding alluvial fans. Unlike the fan area delimitation, catchment areas have very little contrast with the background landscape on Landsat images. DEM data allows for this delimitation to be done in two ways. Firstly, applying the D8 algorithm (Tarboton et al., 1991) to a DEM allows for the construction of a drainage network, from which hydrological properties such as catchment area extent can be derived. This method proves unsuitable for accurately delimiting catchment areas as the algorithm fails in producing an accurate drainage network. The algorithm fails in dealing with internal drainage. To avoid drainage terminating at individual pits (cells whose elevation values are lower than the eight around it) DEMs are conditioned before running the algorithm. This conditioning involves raising the elevation of pits to the lowest elevation value of the surrounding cells. Doing this stops drainage terminating artificially at individual pits, but also prevents internal drainage being properly represented, as the termination points for all internal drainage networks are removed. Instead DEMs can be used to delimit fan catchments because the boundaries of catchment areas are ridges. This

topography can be easily highlighted by changing the hillshade values of the display in the global mapper software. By setting the hillshade values to simulate light from directly perpendicularly above the map surface, ridges become highlighted as they are the parts that reflect the most light back to the viewpoint directly above the map. Being able to detect ridges allows for much easier definition of catchment areas. The appropriateness of using these highlighted lines as catchment area boundaries is also checked by looking at the elevation values underlying the lines, ensuring they do represent ridges, and checking that there are no higher elevation values within catchment areas that would bisect the delimited catchments.

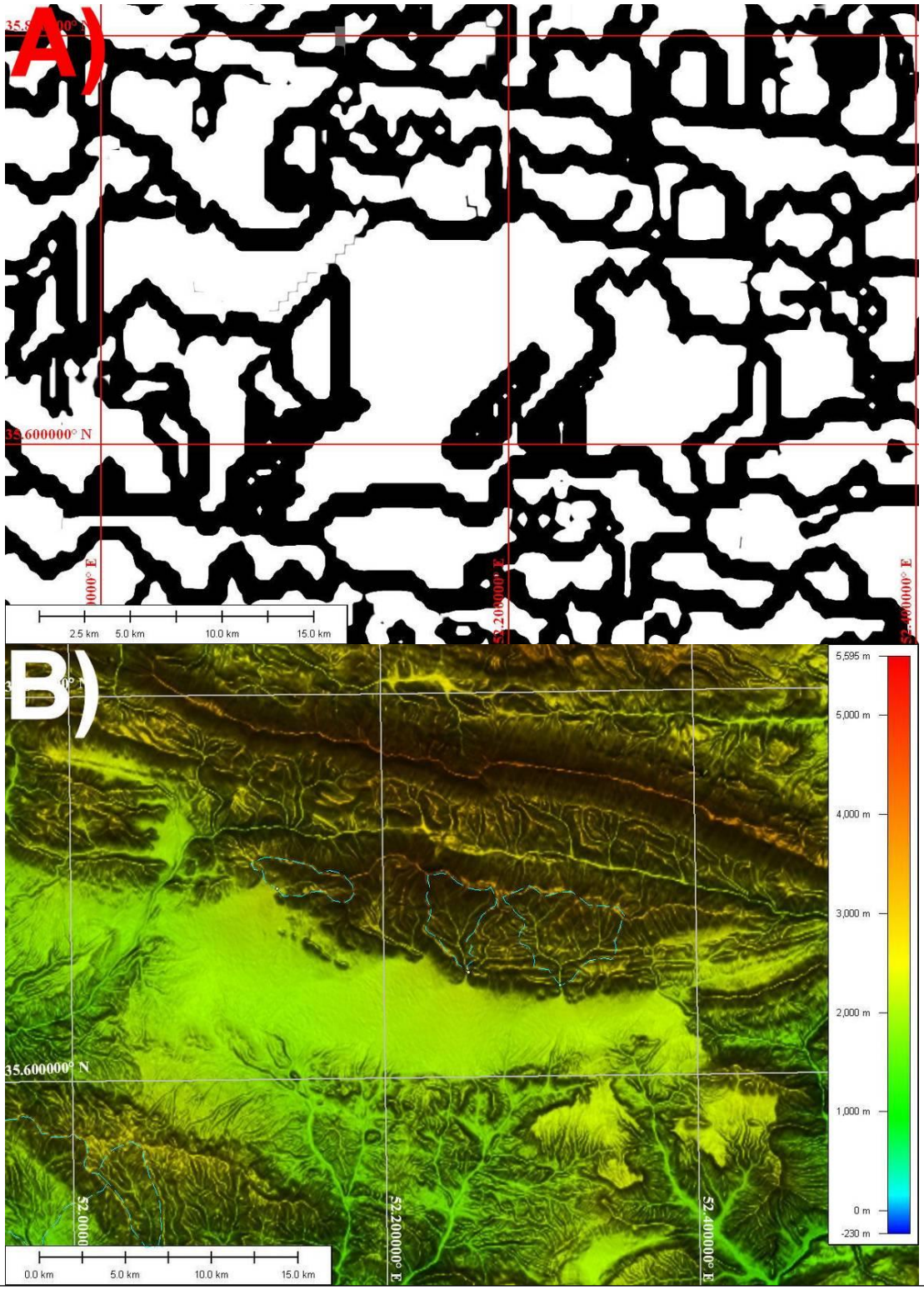

Diagram 4.4 – Diagram contrasting catchments delimted by the D8 algorithm and using the hillshade method: *A) Catchments delimited using an automated method based on drainage networks derived using the D8 algorithm. These catchments are artificially small as the drainage network is bisected by pits within the base DEM. Filling in the pits removes internal drainage completely. B) Catchments delimited using the hillshade method. Catchments indicated by a dashed blue line. Hillshade values are set up to represent a light source directly overhead, this highlights the ridges that are the boundary of catchments and rivers running in catchments.*

4.4 Parameters of measured alluvial fans

Various parameters of alluvial fans can be measured using remotely sensed data. Using these parameters, an alluvial fan can be characterised and the effect of differing tectonic and climatic settings on the fan's characteristics can be assessed. Having a defined list of fan parameters to measure allows for an objective way of characterising the alluvial fans studied. Previous work on alluvial fans has identified a standard selection of fan morphology parameters to measure (Carretier and Lucazeau, 2005; Dade and Verdeyen, 2007; Harvey, 2012; Harvey et al., 2005; Ritter et al., 1995; Stepisnik, 2010; Wang et al., 2008). These include fan area, source catchment area and the ratio between the two; fan progradation length; fan thickness; fan volume and gradient on the fan surface. Additional fan morphology parameters were also observed to more fully describe the shape of the fans, these are detailed below and are mostly derived, unit-less parameters that are scale-independent and so are used to measure the fan shape, without being influenced by the fan size. Choosing to measure these extra parameters was done specially for this study to obtain as comprehensive a dataset of fan morphology as possible.

4.4.1 Derived versus directly observed parameters

Some of the parameters used in characterising alluvial fans are not directly measured from the remotely sensed images, instead they are combinations of the values of directly observed parameters for the fan in question. This category of derived fan parameters includes all the scale-independent parameters. The parameters are those with no units, because they combine multiple scale-dependent parameters in such a way that the units cancel. A commonly used example of this type of parameter is the gradient of a surface, which is not measured directly, but is the fall in elevation from one point to another, divided by the horizontal distance between those two points (Assuming a uniform surface, so there being no need for a more complicated differentiation of the ground surface with respect to horizontal distance). Scale-independent parameters measure the geometry of

fans (or their catchments), rather than an element of their size, this makes them useful for seeing if the form of a fan changes with its setting, even if the sediment supply to accommodation space ratio (and so therefore the fans' areal extent) is different.

4.4.2 Scale dependent parameters

Fan Area is one of the most basic and useful scale dependent parameters measured. It is measured directly and does not have to be derived. This parameter is obtained from the Landsat 7 ETM+ images, where the boundary of the alluvial fan can be identified due to the high contrast between the background landscape and the fan surface. The boundary for each fan is digitised using the Global Mapper software, which then automatically produces a value for the area enclosed. Fan area is a parameter used as a measure of the size of the fan. It is not as good a measure of the sediment balance in a fan as the fan's volume, but can be measured more accurately as there are no assumptions that have to be made in obtaining this value. This parameter represents the balance of sediment flux to a fan over its lifetime against the rate of accommodation space formation.

Catchment area is a similar parameter to fan area; again it is measured directly and does not have to be derived. Identifying the boundary of a catchment area is more complicated than in the case of fan area, but when the boundary of a catchment is identified, the area is digitised and measured in the same way as for fan area. Identifying catchment areas using SRTM data is detailed in section 4.3.2. Catchment area has a control on fan development as is determines the area that material to make up the fan can be derived from. It is not enough to give an idea of sediment flux to the fan, as erosion rates across the catchment would also need to be known, but this temporal information can not be extracted from the data available.

Fan perimeter is a scale-dependent length parameter that is also automatically obtained from the Global Mapper software when alluvial fan extent is delimited. On its own fan perimeter is a measure of the fan's size and so does not provide more information

about how fans vary with tectonic and climatic setting variables than other measures of fan size, such as fan area and fan volume. Fan perimeter is useful in characterising fans when combined with other parameters that also measure fan size. Used in this way it can provide information about the plan-form morphology of a fan.

Fan progradation length is measured from the fan head to the furthest point on the fan perimeter. This represents the furthest displacement of material along the fan. Unless the fan is symmetrical, this is rarely along the central axis of the fan. Progradation length provides information about the efficiency of sediment transport along the fan and how the rate of accommodation space creation compares to the sediment supply rate. If the sediment supply rate is greater than the accommodation space creation rate, the progradation length is likely to be larger as the sediment is distributed over a larger area, due to lack of accommodation space.

Fan volume is the best measure of a fan's absolute size, being the summation of the sediment fluxes and erosion occurring on the fan over its history. However, except in a few cases (Hjelstuen et al., 1996) area is used to measure a fan's size instead, as it is much easier to measure. Volume is derived using the SRTM DEM data to define the 3-D surface of each fan. This comes from the elevation values of the SRTM data of pixels that correspond with the previously delimited fan area. This allows for the extraction of 3-D surfaces whose areal extent is the same as the fans'. To use these surfaces to derive fan volumes the bottom surface of each fan needs to be known and then the volume lying between the two surfaces calculated. Deriving fan volumes this way is non-trivial because of the dependence on knowing the form of fans' lower surfaces. Remote sensing cannot acquire data that isn't related to the ground surface so an assumption has to be made as to the topography of the lower fan surfaces. The assumption used is that the lower surface of a fan is a horizontal plane whose elevation is at the same height as the lowest point on an alluvial fan's perimeter. This assumption has obvious flaws. Firstly it ignores the relict topography the alluvial fans will have been laid over, as this topography is unlikely to be

completely planar. Secondly, even if the lower fan surfaces were planar, they are unlikely to be completely horizontal; the subsidence pattern of the depositional basins for the fans will set the geometry of these lower fan surfaces. It is also impossible to guarantee that using the lowest point on a fan's perimeter will give an elevation value representative of the mean elevation of a fan's lower surface; however the fan lower surface will contact the fan perimeter, so using this as a reference point is valid. Thirdly, fans are commonly deposited in subsiding areas, where there is enough accommodation space for the fans to build up (Allen and Hovius, 1998; Harvey et al., 2005). In these cases, the calculated value for volume is likely to be an underestimate, which does not account for the extra buried bacterial that makes up the fan. Despite the assumptions made in deriving geometry for fans' lower surfaces, this method provides workable data that allows for comparisons of fan volume that are as accurate as possible without the ability to section the fans to get volume estimates. The values for volume for steep fans in topographically steep regions are likely to be an over estimate as the topography underlying the fan head is likely to be at a higher elevation than the fan toe. In fault bounded fans the horizontal lower fan surface assumption is likely to lead to an underestimate of fan volume as the elevation under the fan head is likely to be lower than the elevation at the fan toe. By sampling a large number of fans, these opposing errors are likely to cancel out over the entire population of fans.

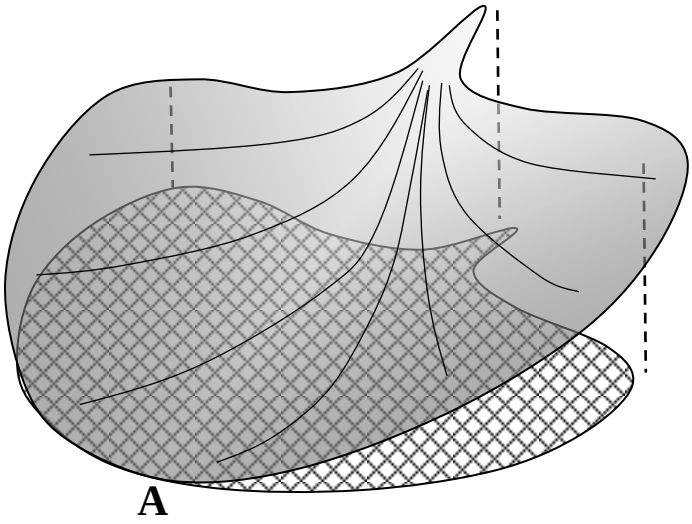

4.5 - Diagram showing how fan volume is calculated: *Fan volume is derived as being the volume between the 3-D surface of the fan(shaded) and a horizontal surface with the same areal extent as the top surface (crosshatched). The height of this horizontal surface is set at the lowest elevation found at the fan perimeter (A). Two sources of error are present: a) discrepancies in the fan surface due to errors in the DEM used and the limited resolution of the DEM (90 meter square pixel size). b) Uncertanties in the topography of the fan's bottom surface, a horizontal plane is used, but is unlikely to be correct.*

Compared to area, fan volume is more directly influenced by the sediment supply to the fan and so may be more useful as a way of looking at climatic inputs to the system as changes to the proximal climate can influence the sediment supply, but not the accommodation space available. However measuring volume in the way used in this study is subject to more errors than the measurements of fan area.

Fan thickness is derived using measures of fan volume and fan area. The fan volume is divided by the fan area, to give a value of mean thickness across the fan area. Like fan area, fan thickness is a convolution of sediment flux to the fan and the rate of accommodation space creation. High sediment supply, with a high rate of accommodation space creation allows for the development of thick fans.

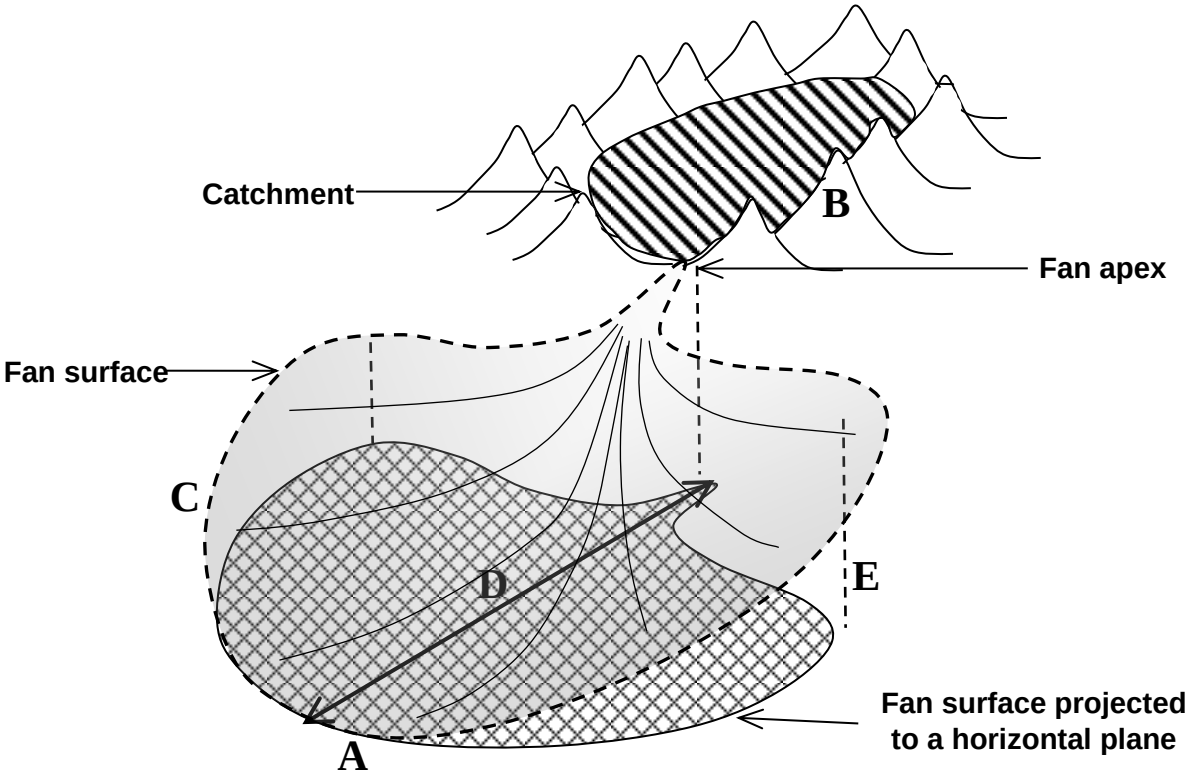

4.6 - Diagram showing scale dependent parameters of alluvial fans: A; *Cross-hatched region is fan area* ***B;*** *Striped region is catchment area* ***C;*** *Fan perimeter (dashed)* ***D;*** *Fan progradation length* ***E;*** *Fan thickness*

4.4.3 Scale-independent (geometric) parameters

Scale independent parameters are measured to see if alluvial fans in differing tectonic and climatic settings have varying geometries. Scale dependent parameters can see if alluvial fan size varies and give information about the relationship between sediment supply with accommodation space. In contrast, scale independent parameters measure the shape of an alluvial fan and provide information on how the sediment that makes up the fan is deposited.

Scale-independent parameters are usually made scale-independent by normalising a measured parameter. The parameters are usually normalised to either fan area or catchment area, depending on whether the parameter in question is related to the fan catchment or the fan itself. With many parameters, normalising to fan or catchment area

does not provide a dimensionless quantity that is truly scale-independent. In these cases the quantities are normalised to the square root of either catchment area or fan area.

The other way of producing a scale-independent parameter is to compare a parameter from the catchment area to a parameter associated with a fan. This category of parameters provide information about the transport of sediment from the catchment area to the fan.

Fan gradient is a scale-independent parameter that has not been normalised. It is a measure of the gradient of the fan surface from the fan head to the fan toe. To get a value for the fan surface gradient, several steps of derivation have to be performed. Just extracting and averaging slope values for each pixel of the fan surface does not give an indication of fan head to fan toe surface gradient. Many of the pixel slope values will not be aligned along the fan head to fan toe axis, so averaging those values gives an inaccurate value that convolves the gradient of the fan in directions that are not from fan head to fan toe. The other simple way of extracting a fan gradient value would be to calculate the gradient, relative to a horizontal plane, of a line between the fan head point and the fan toe point (defined when calculating progradation length as the point on the fan perimeter furthest from the fan head point). This method does not take into account the shape of the fan surface, which is rarely a linear line between those two points. To get a single value for fan surface gradient that acknowledges the geometry of the fan, the mean thickness value of each fan was divided by the fan progradation length. As this uses the mean thickness of the fan, and the progradation length represents the maximum distance travelled by material during the fan's formation, this proxy for gradient more accurately takes into account the fan geometry (see figure 4.7).

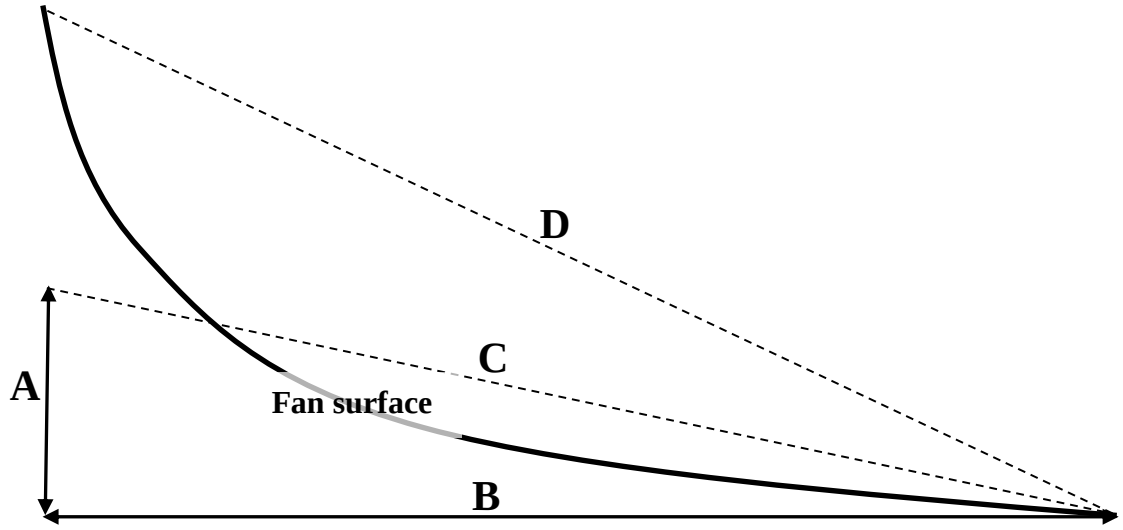

4.7 – Diagram showing the calculation of a proxy for fan surface gradient: *Fan surface gradient is defined as the mean fan thickness (A), divided by the fan progradation length (B). Using average fan thickness provides a more representative value of gradient (C) than getting the gradient of the line from fan head to fan toe (D). Using mean fan thickness takes into account the topography of the fan surface.*

Fan surface gradient is related to transport processes along the fan. Steeper gradients will allow for a greater rate of sediment transport, depending on the associated drainage network, this could mean greater sediment-bypass of the fan.

Fan area divided by catchment area is measured by taking previously extracted values of fan area and catchment area for each fan and dividing the former by the latter. This is a simplication of the power law relationship between fan area and catchment area identified in previous geomorphological studies (Bull, 1977; Hooke, 1968; Lecce, 1990). This parameter provides information about the relative efficiency of the erosive effects that release the material that makes up an alluvial fan and the depositional processes that form it. When this parameter is large, this suggests accommodation space is formed slowly compared to the rate of erosion in the catchment, suggesting either high levels of erosion or a low rate of accommodation space creation.

The square root of fan area divided by progradation length is a measure of the scale-independent planform geometry of an alluvial fan. This is also derived from the

scale dependent parameters, whose derivation was explained earlier. The higher this measure, the shorter and wider the fan's planform geometry is. This is partly related to the fan's setting as the longer, thinner fans that make up bahadas (Meyer et al., 2005; Vita-Finzi, 1968) would have small values for this perimeter.

The square root of fan area divided by fan perimeter length is another parameter used to characterise the planform geometry of alluvial fans and derived from the scale dependent parameters whose measurement was described earlier. As the smallest perimeter that encloses a given area is a circle, this parameter is a measure of a fan's roundness, where bigger values, represent a more circular fan.

The square root of catchment area divided by catchment length is directly comparable to the square root of fan area divided by progradation length, but just applied to the delimited catchment areas, rather than fan areas. Smaller values represent longer, thinner catchments, these catchments would have greater transport distances, so represent increased fluvial transport before deposition on an alluvial fan surface.

Similarly, **the square root of catchment area divided by catchment perimeter length** is comparable to the square root of fan area, divided by fan perimeter length. As a measure of catchment geometry it can be approximated to a measure of catchment roundness with bigger values, meaning a more circular fan.

Parameter	Use
fan surface gradient	**Gradient controls fluvial transport processes on the fan surface**
Fan area/catchment area	**Helps quantify the relative efficiency of erosional and depositional processes**
√fan area/fan progradation length	**Measure of fan planform geometry, particularly the aspect ratio of the fans**
√fan area/fan perimeter	**Measure of fan planform geometry, particularly the roundness of the fans**
√catchment area/catchment length	**Measure of catchment planform geometry, particularly the aspect ratio of the catchment**
√catchment area/catchment perimeter	**Measure of fan planform geometry, particularly the roundness of the fans**
4.8 – Table of sampled scale-independent fan parameters: *This table shows the scale-independent fan parameters and information they provide.*	

4.4.4 Parameters which are undetectable using remotely sensed data

There are certain parameters of alluvial fans that are related to their development and are likely to be controlled by the fans tectonic and climatic setting, but which are not able to be sampled by the remote sensing techniques used. As previously mentioned, one of the obvious omissions of this method is its inability to provide information about the development of alluvial fans through time. Instead the relatively rapid response time of fans is used as a justification for correlating observable tectonic and climatic conditions and fan characteristics. Despite this, it is acknowledged that the fan characteristics measured in this study represent the aggregate of all the tectonic and climatic settings the fan has experienced as it was formed.

Using remote sensing it would be theoretically possible to detect the amount and form of channelization upon the fans surface. This information would provide information

about how the fan's respond to climatic conditions in particular, as incised channels dissect alluvial fans, retarding their growth. However two problems make this impractical to do. Firstly the 15 metres pixel size of the Landsat images used is too large to identify many fan-surface channels, whose width is less than this. Even when channels can be identified by a contrasting pixel colour, assigning 15 metres as the channel width is likely to overestimate the channel width, as the channel may be a smaller feature with a pixel that has just changed the colour of that pixel, relative to the background colour. This pixel size problem is further exacerbated by the 90 metre pixel size of the underlying DEM, which makes extracting 3-D information even more problematic. Secondly, channels on the fan surface (especially those whose width is less than the 90 metre resolution of the SRTM data) can only be identified by contrast between pixels in a Landsat image that correspond to the river location and those of the background landscape. However, there is no consistent shift in colour that corresponds to fan-surface channels. This makes identifying channel location and morphology non-trivial and something that can't be automated.

Lithology is another parameter that can't be directly measured using remotely sensed data. As a proxy for lithology, the band 7 data from the Landsat ETM+ images can be used. Band 7 measures the intensity of medium wavelength infra-red radiation. This band of infra-red radiation was selected to differentiate between different mineralogies. While it is not calibrated to correlate particular values to specific mineralogies, differences in the intensity of this band can be used to highlight variation in lithology. To use band 7 intensity as a proxy for lithology, the mean value of band 7 intensity (measured on a linear scale of 0 – 255, as the data is held in an 8 bit format) for all the pixels that correspond to a fan is calculated and assigned to that fan, this is then done for each fan.

4.5 Study area

To look at the change in the fan parameters defined above with the climatic and tectonic settings associated with orogenic plateaux, the Turkish-Iranian plateau is used as a study area. In particular, the fans studied are located north of the Zagros suture. This area includes the plateau interior and the Alborz mountain range. By restricting the studied fans to those north of the Zagros suture, the geology underlying the fans is part of the same terrane (Pollastro et al., 1999), thereby limiting litholigical differences as a factor controlling fan morphology (see figure 4.9).

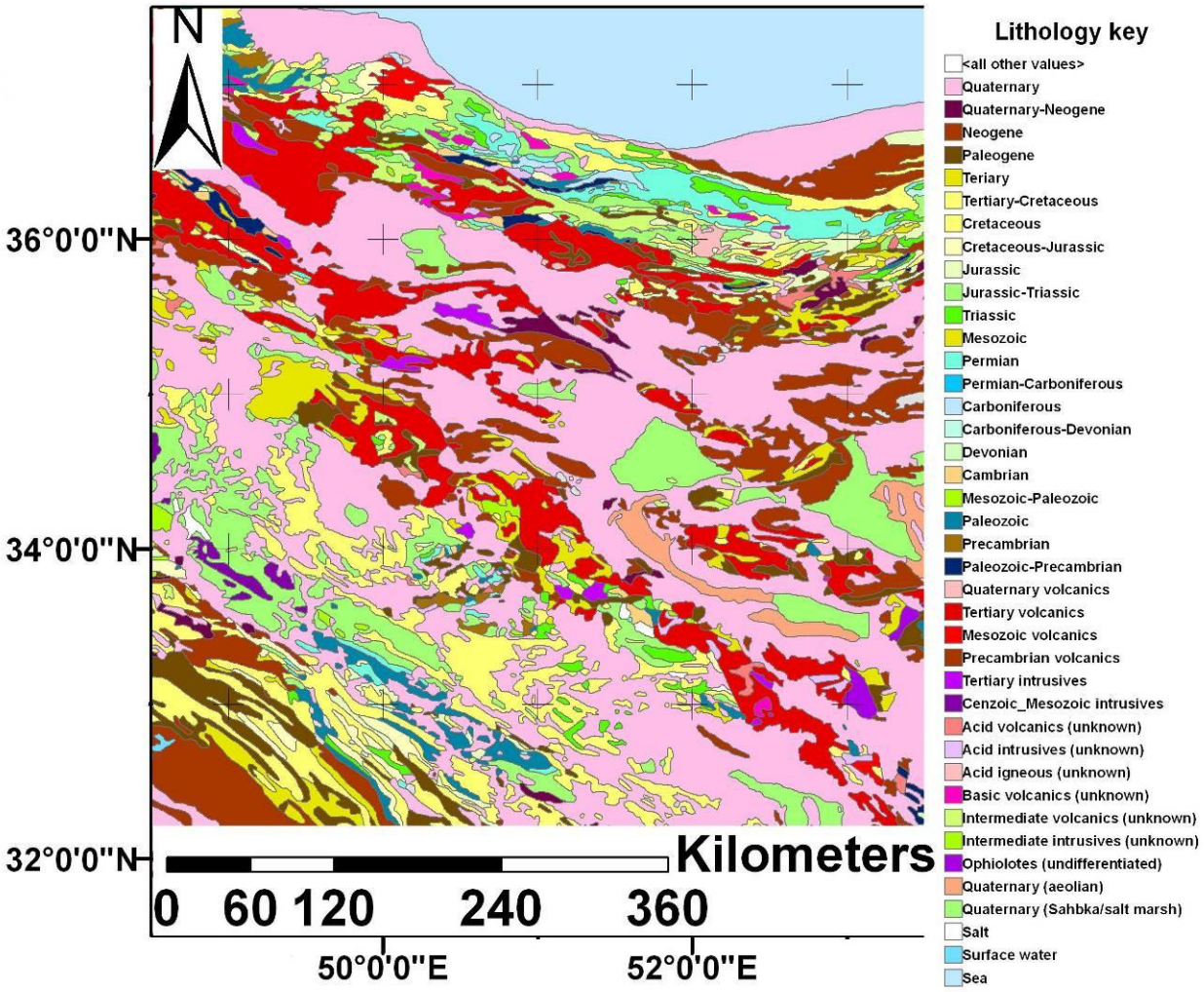

4.9 – Geological map of the Turkish-Iranian plateau and Alborz mountains: *This map shows the similarity of lithologies in the plateau interior and the Alborz mountains. Particularly noticeable is the large amount of area defined as 'Quaternary' (coloured pink) this represents the majority of the alluvial fan deposits in the plateau and demonstrates the lack of definition in the lithology of the fans (Pollastro et al., 1999).*

The study area includes both the plateau interior and an active thrust belt, where the deformation across the orogen is being taken up and the crust is actively thickening (Allen et al., 2004; Axen et al., 2001). Studying the alluvial fans of an orogenic plateau allowed for a comparison of fan properties in contrasting settings. The orogenic plateau setting also differs from previous studies of alluvial fan properties, which are often in extensional, rather than compressional, settings as they provide the accommodation space for alluvial fan formation (Ferrill et al., 1996; Jones, 2004; Leeder and Gawthorpe, 1987).

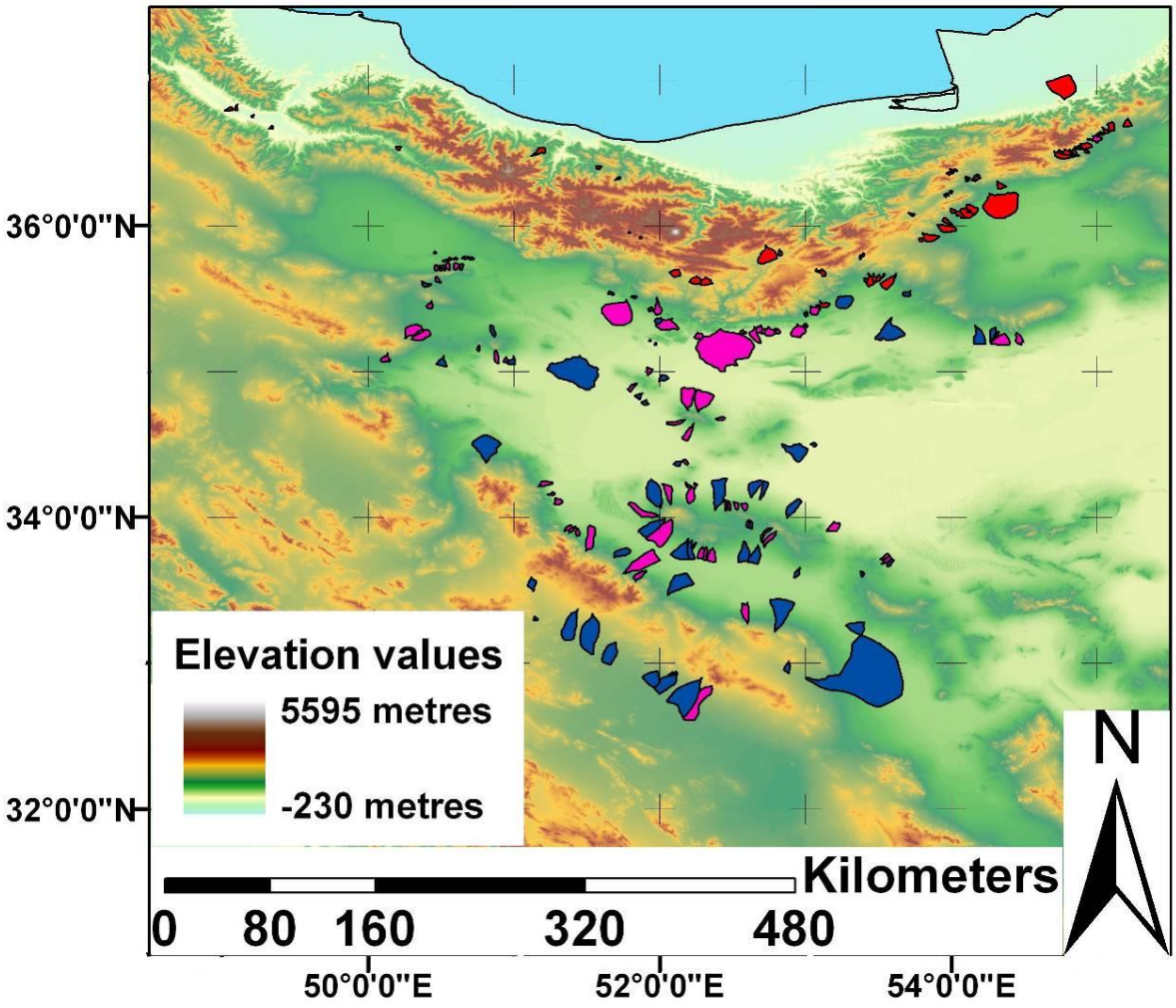

4.10 – Map of studied fan locations: *This map shows the delimited areas of the fans used in the study. The fans are colour coded by which sub-population they are assigned to. The third of fans nearest the 1000 metre elevation contour are red, the third of fans with the highest ζR values at the fan head are in blue and the intermediate sub-population fans are purple. The higher ζR fans and the intermediate sub-population are intermingled, although, as a whole population the high ζR fans are further from the plateau margins and further into the plateau interior. The shading under the fan areas represents the elevation of the landscape.*

4.5.1 Division of study area by tectonic and topographic properties

The stated question, 'How do the surface characteristics of an alluvial fan correlate to the known tectonic and climatic variables of a region?' has to be narrowed in focus to the orogenic plateau study area. This requires dividing up the study area into distinct categories (see chapter one for a further discussion on defining an orogenic plateau). These categories represent defined tectonic and climatic settings that allow the characteristics of the sub-population of fans that are found in each setting to be compared.

The divisions chosen were selected to give one sub-population of fans that represented the plateau interior, one sub-population that represented fans near the siemognic thrusting zone at the plateau margin and one sub-population that was undefined and intermediate to these two divisions. The settings of the first two divisions were designed to be better defined than the latter division; by comparing the fan characteristics of the alluvial fans in these two divisions, the difference in fan morphology between fans in the plateau interior and fans near the seismogenic thrusting zone could be observed, helping answer the first aim of this study. The latter division is used to address the second aim of the study. By characterising the fans in this division, these fans could be compared to the characteristics of the fan in the seismogenic thrusting and the plateau interior divisions. This would allow this intermediate division to be characterised as representing either a tectonically active, thrusting setting or a more stable, low relief plateau setting.

The sub-population of alluvial fans closest to the seismogenic thrusting zone are defined using the seismic cut-off definition of a plateau outlined in chapter one. There, the plateau regions are split into two sections, one is the plateau margins which are undergoing deformation and taking up convergence by active thrusting, while the second section is the plateau interior, which is no longer experiencing significant thrusting and is tectonically quiescent compared to the margins. Seismogenic movement in the plateau interior is more likely to be strike-slip movement, as either convergence is taken up in a manner that does not create excess topography, due to gravitational buoyancy forces

preventing the creation of further elevation, or the strike-slip movement is part of plateau decay as gravitationally driven spreading forces reduce the plateau topography. The cut-off between these two sections aligns closely with an elevation contour, in the case of the Turkish-Iranian plateau, this contour is at 1000 metre elevation. It is posited that this elevation value represents the point where compressional forces are balanced by gravitationally driven spreading of the thickened crust, so thrusting ceases and deformation is instead taken up by thrusting within lower elevation topography (England and McKenzie, 1982, 1983; England and Houseman, 1988; Houseman and England, 1986). Higher elevations within the plateau suggest some other processes must have acted on the topography to increase its elevation, but the lack of seismic thrusting suggests that they would have less effect on the local tectonics that govern alluvial fan formation and morphology. Defining the seismogenic thrusting zone as the topography on the outside of the 1000 metre elevation contour encircling the plateau allows for a definition of the sub-population of fans affected most by an actively thrusting tectonic setting. The definition for this sub-population is the third of the sampled fans whose heads are closest to the 1000 metre elevation contour. The fan head is chosen as the point to measure from because it marks the cross-over between the fan's catchment and its depositional area. As both have an effect on the characteristics of the fan and both are affected by the tectonic and climatic settings they find themselves in (Carretier and Lucazeau, 2005; Dade and Verdeyen, 2007; Harvey et al., 2005; Jones, 2004; Ritter et al., 1995), this works as a compromise location. Using a third of the sampled fans nearest the 1000 metre contour is an arbitary amount. In order to make sure that the sub-population most accurately represents fans affected by the plateau forming thrusting, the cut-off should be determined as the fans whose characteristics are different from the rest of the fan population due to their setting, rather than arbitrarily setting it at one third of the fan population. Defining the sub-population this way would be circular reasoning, however. The characteristics for determining which

fans have been most affected by an actively thrusting setting can only be done after that characterisation has been done.

For defining which fans represent the plateau interior setting, the cut off of a third of the sampled fans was used again. The definition used was based on the topographic description of the plateau. The fans defined as representing the plateau interior are the third with the highest ζR values at the fan head. ζR is a measure of how much local topography is representative of a plateau, where a plateau is understood to be a region of high elevation and low relief. ζR is calculated as the mean of local elevation divided by local relief, building on work in Tibet and the Rocky Mountains from (Andronicos et al., 2007; Formento-Trigilio and Pazzaglia, 1998). The use of ζR in this study expands on those works by looking at the variation of the measure with differing sampling radii being chosen. Furthermore this measure is chosen as a representation of plateau-like topography as a direct correlation to the topographic definition of a plateau as it is the simplest way of highlighting high, low-relief regions. This contrasts to the use of the parameter in (Formento-Trigilio and Pazzaglia, 1998), where it is used as a proxy for the level of drainage integration, with the assumption that fluvial incision scales with elevation and over time, thereby increasing relief as an orogeny grows. This is obviously unsuitable for a plateau situation, where the low relief interiors are also the topography whose elevation increased first. This value shows high values within the plateau interior, showing it's applicability to defining a sub-population of fans that represent the plateau interior (see figure 4.11).

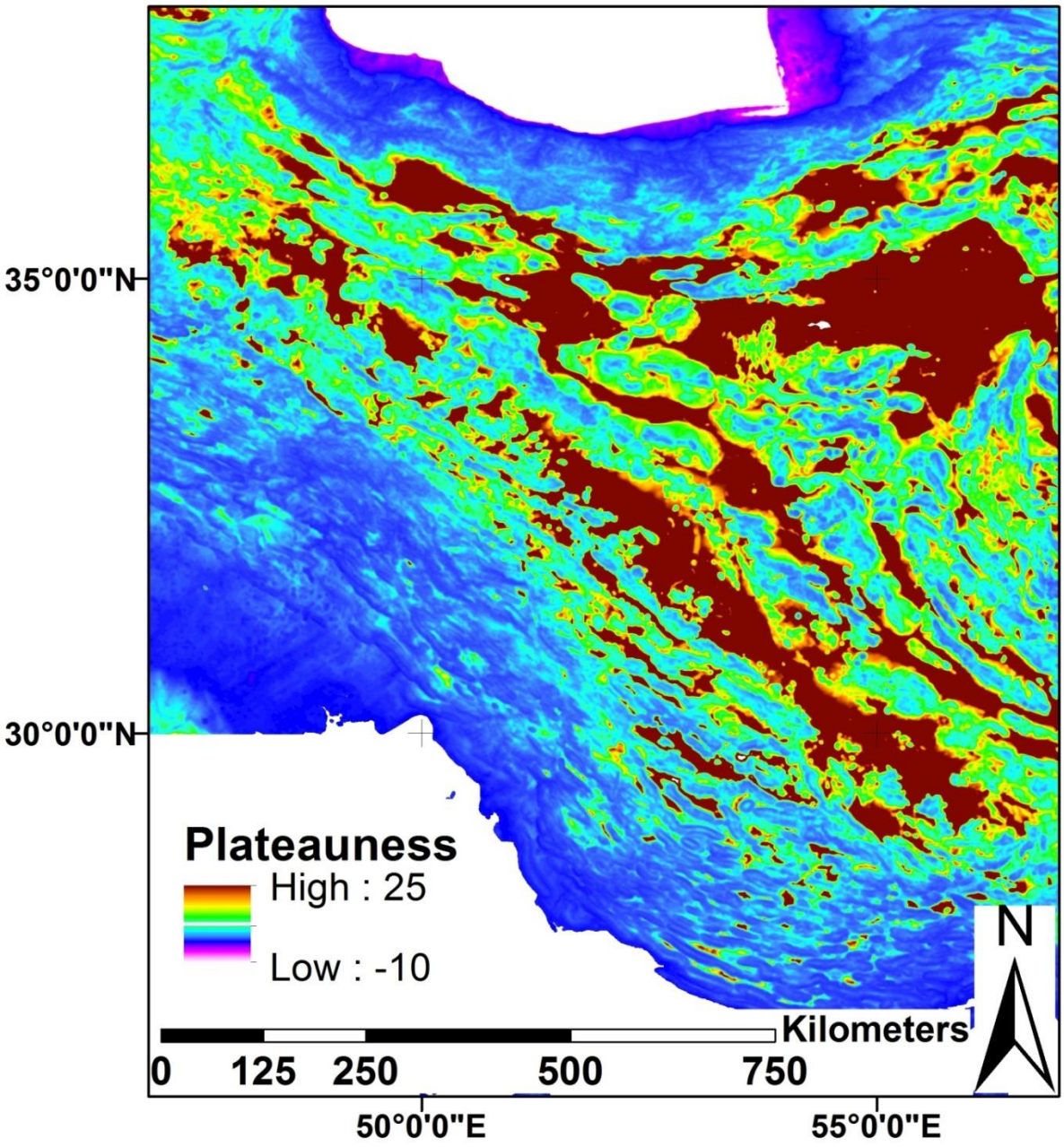

4.11 – Map of the distribution of ζR values over the study area: *The ζR value is calculated over a 2000 metre radius for this map. Brown represents high ζR values while dark blue represents the low values. This map clearly shows the high ζR values are within the plateau interior.*

The areas over which mean elevation and local relief are calculated are kept the same. In the case of this study, the areas are circles whose centre point is where the ζR value is assigned to. The radius of the circles is an arbitrary value, so the effect on the value of choosing different radii was investigated. ζR calculated over different radii values (500 metres, 1000 metres, 2000 metres, 2500 metres and 4000 metres) show a good correlation to each other. The correlation is higher when the radii values are closer, as is to be

expected, but even with radii values that are quite far apart the same pattern of ζR values is seen (see figure 4.12).

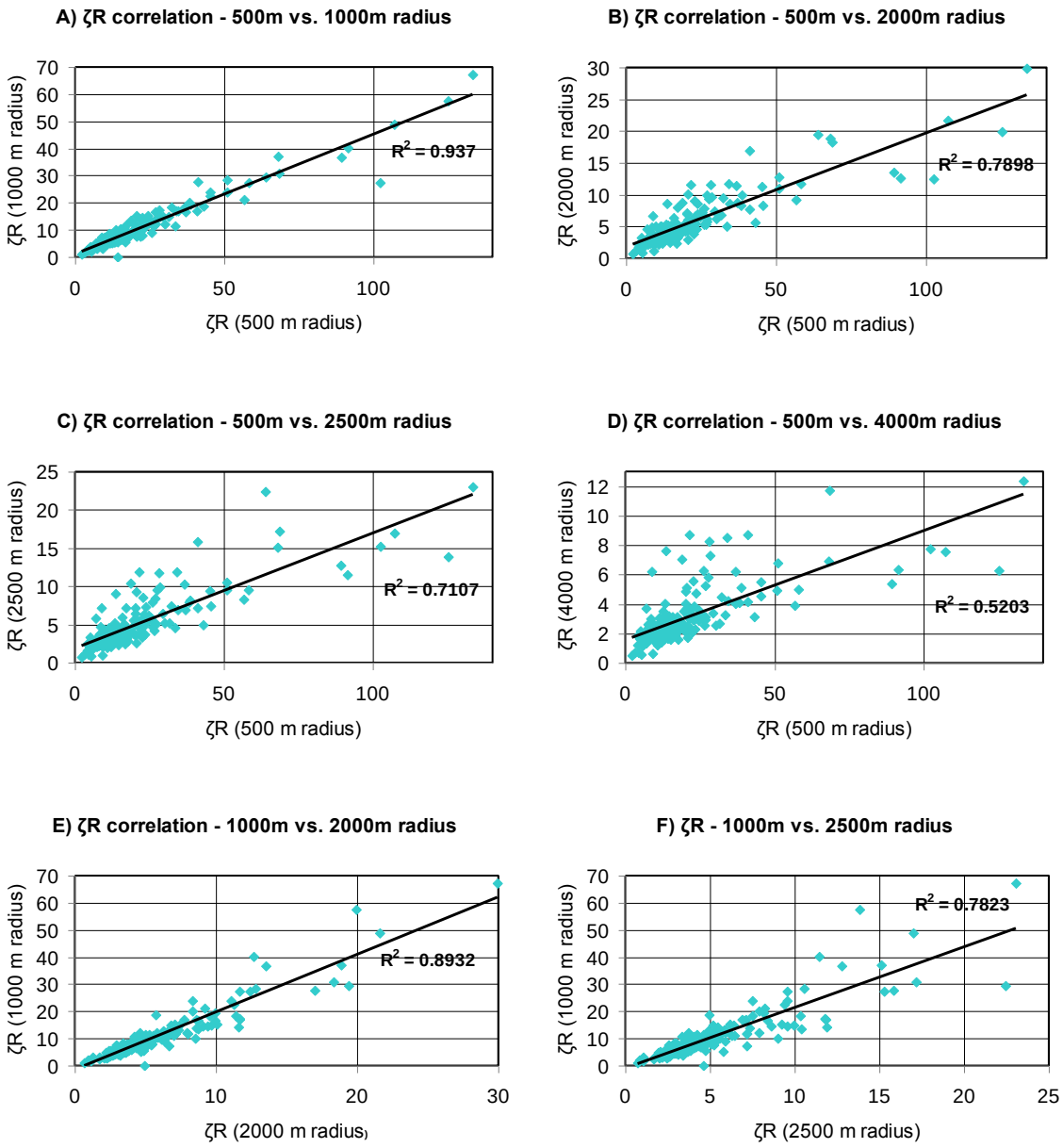

Caption on next page

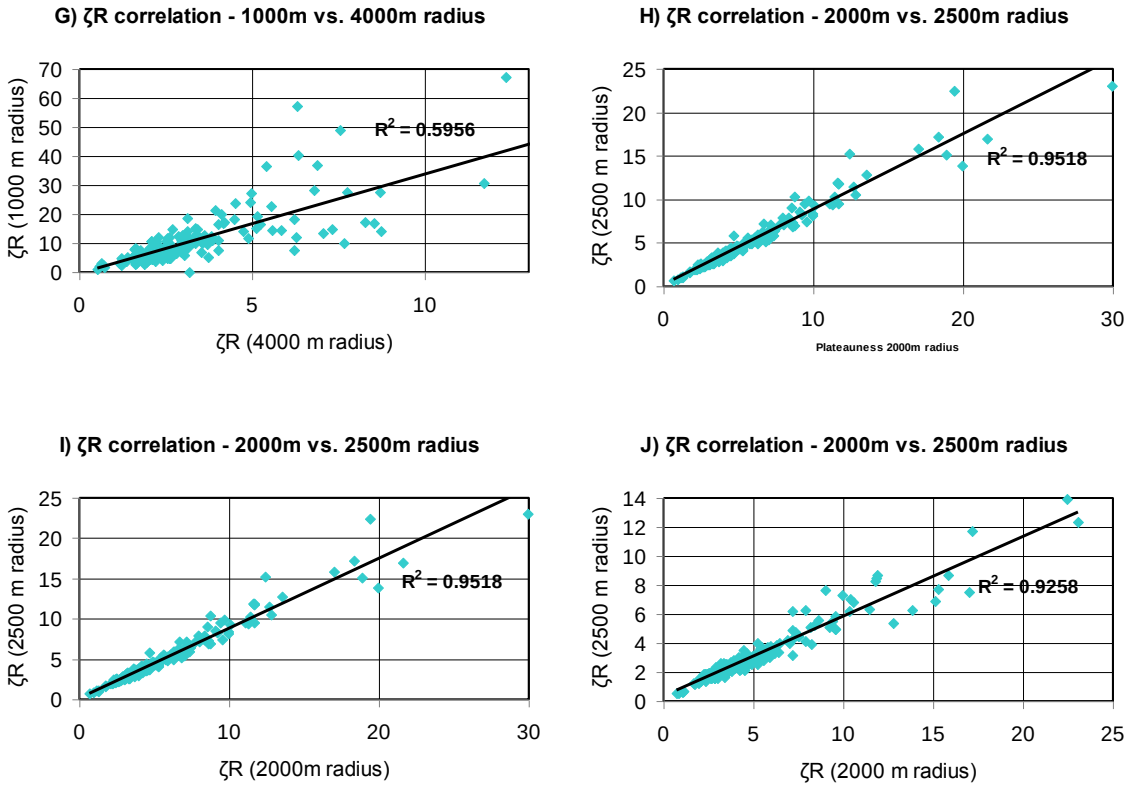

4.12 – Graphs of correlation between ζR values calculated over areas of different radii: *A) ζR value for a 500m radius against ζR for a 1000m radius. B) ζR value for a 500m radius against ζR for a 2000m radius. C)) ζR value for a 500m radius against ζR for a 25000m radius. D) ζR value for a 500m radius against ζR for a 4000m radius. E) ζR value for a 1000m radius against ζR for a 2000m radius. F) ζR value for a 1000m radius against ζR for a 2500m radius. G) ζR value for a 1000m radius against ζR for a 4000m radius. H) ζR value for a 2000m radius against ζR for a 2500m radius. I) ζR value for a 2000m radius against ζR for a 4000m radius. J) ζR value for a 2000m radius against ζR for a 4000m radius. All the graphs show a linear relationship between ζR values measured over different radii (trend lines and R^2 correlation coefficients are shown).*

For the purposes of this study a radius of 2000 metres is used. This value is intermediate of the values calculated and shows a reasonable correlation between all the radius values. A 2000 metre radius is also a larger sample area than many fans. This makes it more likely that the ζR value assigned to a point is not representative of a fan topography, but of a larger topographic setting that a fan can find itself in.

The intermediate sub-population of fans is just the remaining fans that don't meet the criteria of the previous two sub-populations. As this sub-population is used to address

the question of whether the surface characteristics of an alluvial fan allow for the inference of the tectonic and climatic variables of an area's setting, it is left undefined with respect to tectonic and climatic setting. By having this sub-population undefined, the parameters of its fans can be compared to the parameters of the fans from the more defined sub-populations, to infer which sub-population's tectonic and climatic setting corresponds better to the intermediate population.

Although the division of the total fan population into thirds is an arbitrary decision, it does appear to reflect genuine differences in the factors controlling the fan formation. Comparing values of a proxy for stream power (Catchment area multiplied by the gradient value) (Cohen et al., 2008; Lague and Davy, 2003; Tucker and Bras, 1998) at the fans' head for the three different sub-populations, shows the three sub-populations to be distinct (see figure 4.13). The 25^{th} -75^{th} percentiles of the stream power proxy for fans near the seismogenic thrusting zone and those in the plateau interior show no overlap showing these to be very distinct populations. The intermediate sub-population of fans has a considerable overlap in the 25^{th} -75^{th} percentile with the high plateauness fans, but with values that are a bit higher (and therefore moving towards the higher values seen in the sub-population near the seismogenic thrusting zone.). The big difference between these sub populations is in the mean value, which is much higher than that of the high ζ_R fan population.

The stream power at the head of a fan is a first order control on the amount of sediment delivered to the fan from its catchment. Having a higher stream power means the system is capable of delivering more sediment to the fan. As the three populations of fans show a variation in this controlling factor, it can be assumed that they are actually distinct sub-populations.

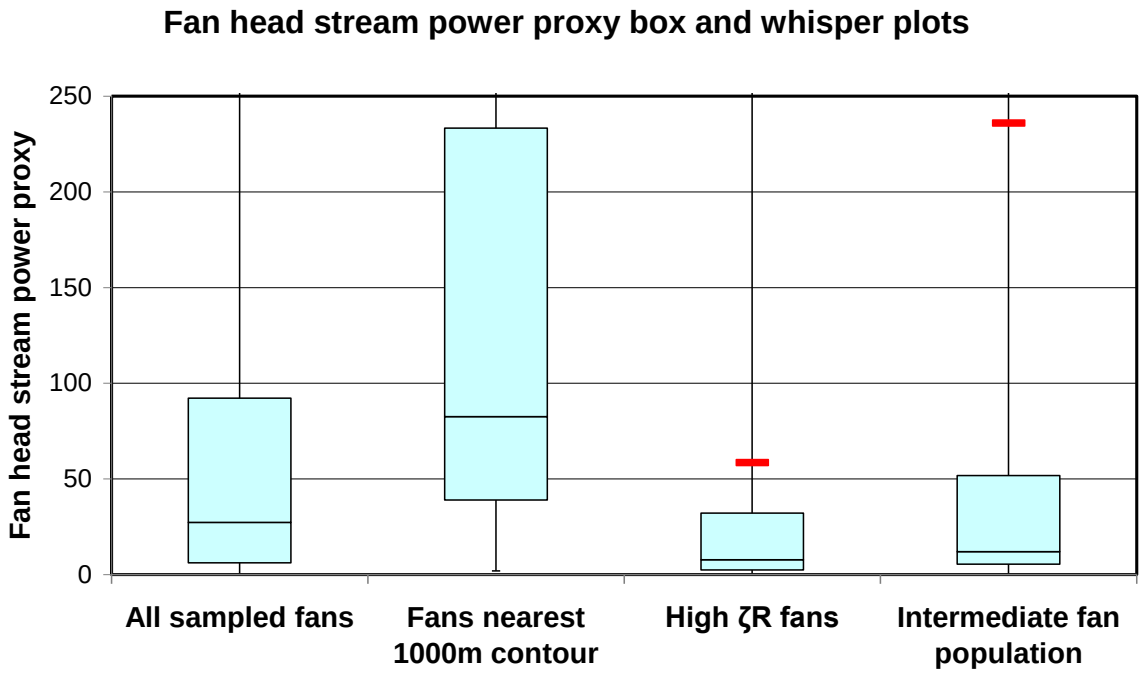

4.13 – Box and whisker diagrams of stream power for fan sub-populations: *The lines show the entire range of values of the sub-population. The top and bottom of the box represents the 75th and 25th percentile respectively. The line across the middle of the box is the median and the thick red line is the mean. The boxes show distinct differences between the stream power of the sub-populations.*

4.5.2 Location and sampling of alluvial fans

Alluvial fan areas were sampled by picking them out from satellite images. For time purposes, not every fan present in the study area was delimited, instead a sample of 206 alluvial fans was parameterised. The sampling was not truly random, as that would have required knowing the location and extent of every alluvial fan in the area and then selecting the fans to be parameterised randomly. As locating and defining the extent of the fans accomplishes much of the parameterisation of the fans and takes much of the processing time for each fan, this was not a practical approach. Instead, a semi-random approach was taken where a randomly chosen part of the study area was selected and then searched for an alluvial fan, then this was repeated for each subsequent fan. This approach

is subject to several sampling biases, but does allow for a spread of fans across the area, allowing for fans near the seismogenic thrusting zone and those in the plateau interior to be compared.

Larger fans and those whose surface has a contrast in colour (or topography) with the background landscape are more likely to be selected as they stand out more while manually scanning an area for a fan to select. While this selection bias has to be recognised, trying to avoid it is just as likely to produce a bias towards lower contrast fans. There is also a bias towards currently active fans; dead fans can be partly covered by subsequent deposition, making them more difficult to identify, the lack of reworking of the surface sediment also reduces the fans' contrast with the background landscape. The increased contrast of active fans makes identifying the full extent of a multi-lobed fan difficult. Sometimes only the active lobe is identified.

4.6 Characteristics of alluvial fans in differing tectonic and topographic settings

The fan parameters measured are compared against the variables used to characterise the tectonic, climatic and topographic settings across the orogenic plateau. This is done in two ways. Firstly, the distribution of the fan parameters among the three previously defined sub-populations of alluvial fans is compared using box and whisker diagrams. These diagrams allow the distribution of parameters in different populations to be compared. They highlight the 25^{th} percentile, 75^{th} percentile, median and mean of the sub-populations' values. Secondly, fan parameters are plotted against ζR values and the distance of the fans heads from the 1000 metre elevation contour. Comparing fan parameters directly to the variables used to define the plateau settings allow for an investigation of direct correlation of fan parameters against tectonic and climatic setting variables, while the box and whisker diagrams are better for comparing populations against each other, in the situation where populations of alluvial fans can be distinguished,

even if there is no direct correlation between a plateau setting variable and a fan parameter.

4.6.1 Parameters controlling alluvial fan morphology

The variables used to define the tectonic, climatic and topographic settings of the fans are;

1) The distance from the fan head to the 1000 metre elevation contour. This is used to characterise the tectonic influence upon the fan setting as the 1000 metre elevation contour corresponds to the cut-off between the seismogenically thrusting plateau margins and the plateau interior. Fans whose heads lie outside the 1000 metre contour are given a negative value, while those inside have a positive value for the distance from the 1000 metre elevation contour. Tectonics controls fan morphology by providing the gradient and accommodation necessary for alluvial fan formation.

2) The ζR value at the fan's head. This is a measure of the topographic setting the fans are within. This is formed by the tectonics and climate the fans are set within, but does more than just reflect the tectonics and climate. The topography shapes the accommodation space available for the fans to form within and can confine fan's areal extents.

3) Annual rainfall at the fan's head. This is derived from 30 year averages provided by the Iranian meteorological society (IMO, 1997) for selected points. These points are then contoured in the ArcGIS software using an inverse distance weighted method. This value is used to represent changes in the climate across the plateau. The geologically short period of time the rainfall is measured over means these values are unlikely to represent climatic conditions through the history of the alluvial fans as climate changes rapidly compared to fan response time and provides very little information about temperature

conditions across the study area. However as this study does not aim to provide a mechanical link between particular climatic conditions and fan morphologies, this measure of climate works to distinguish between different climatic conditions across the plateau region.

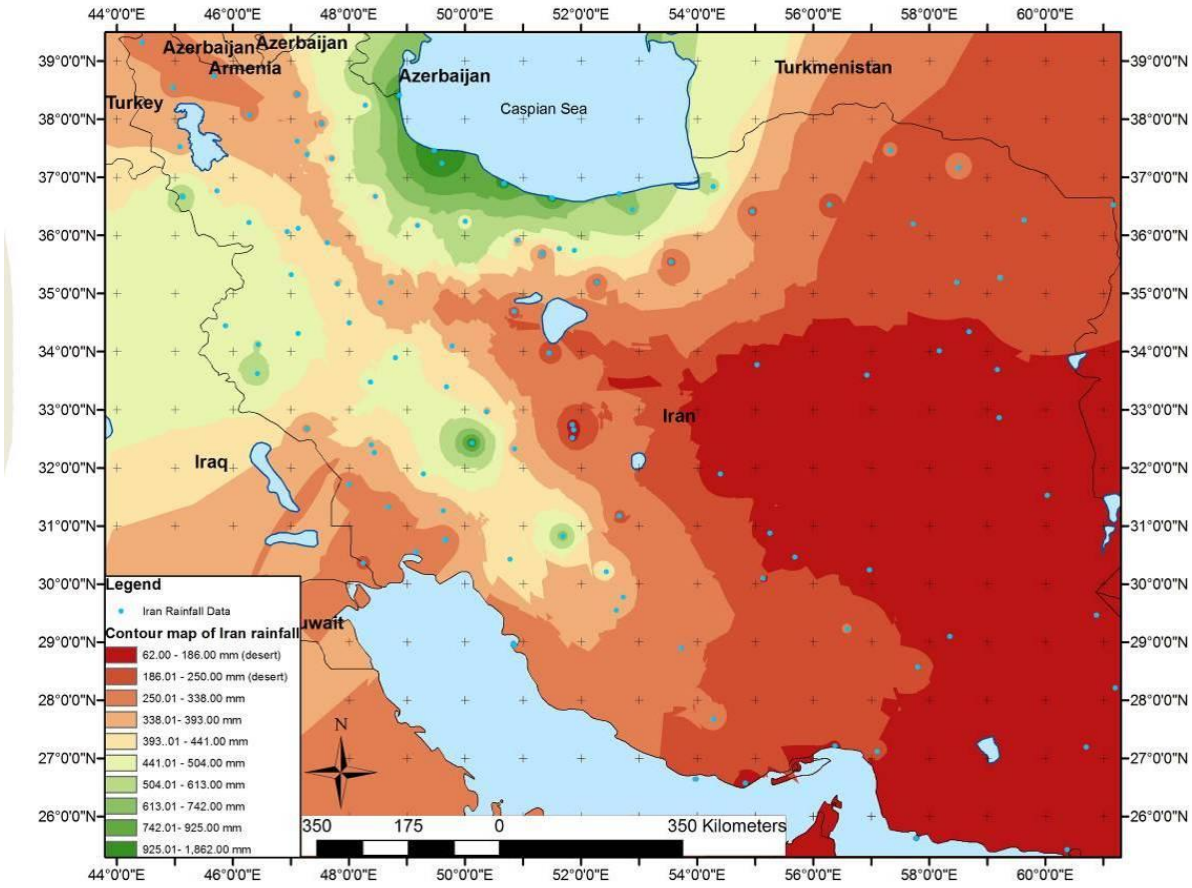

4.14 – Map of annual rainfall values across the Turksh-Iranian plateau: *Annual rainfall values are averaged over a 30 year period. Values are contoured between sampled points using the inverse distance weighting method*

4) Lithology of the catchment area. This is quantified by taking the mean band 7 values for each pixel of a Landsat ETM+ image that corresponds to a fan area. This affects the amount of material available to make the fan by affecting the rate of erosion in the fan catchment. The variation in this parameter is minimised by looking at fans north of the Zagros suture and therefore sourced from the same terrane. Obviously, this doesn't completely eliminate lithological variation, but helps to limit the range of lithologies.

Section 4.6.3 further shows that lithology has very little correlation with change in fan parameters in any case.

4.6.2 Comparison of fan parameters in different settings

To compare different sub-populations of fans, box and whisker diagrams were used. These diagrams allow the distribution of data within each sub-population to be assessed, allowing for a better comparison between populations than just providing a single number to represent each population. Furthermore by comparing the values and range of the middle 50 percentile (the inter quartile range), the effects of a few very large or very small values, that do not represent the setting they are within, are reduced.

Scale dependent parameters (fan area, fan perimeter, fan volume, progradation length, catchment area and catchment length) show consistent patterns in how they vary among the three sub-populations of fans defined earlier. The sub population of fans whose heads are closest to the 1000 meter elevation contour have the smallest values while the sub-population with the highest ζR values are the largest. The intermediate sub-population fans have intermediate values and do not align themselves with either of the other two sub-populations. The spread of values in the fan sub-populations also follows this pattern with the greatest variation being in the high ζR population and the smallest spread being in those fans closest to the 1000 metre elevation contour. All three sub-populations of fans show pronounced skewing of the distribution of scale-dependent parameters. The mean values are uniformly higher than the median values, this shows the scale-dependent parameters do not have a Gaussian distribution, but instead have a long tail towards the larger values.

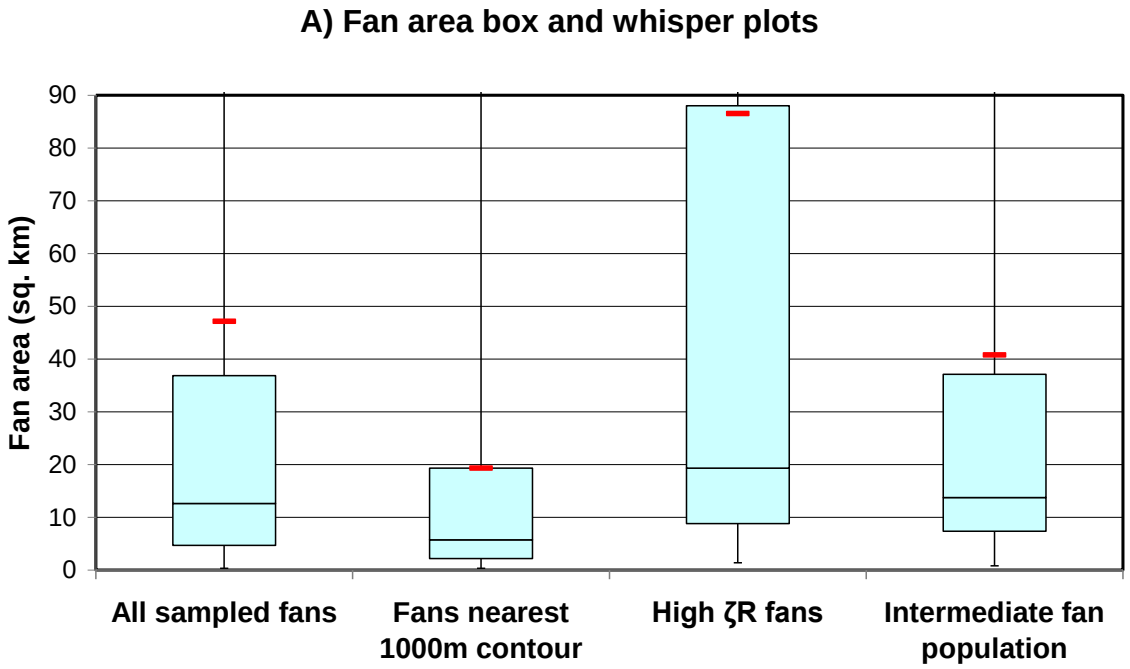

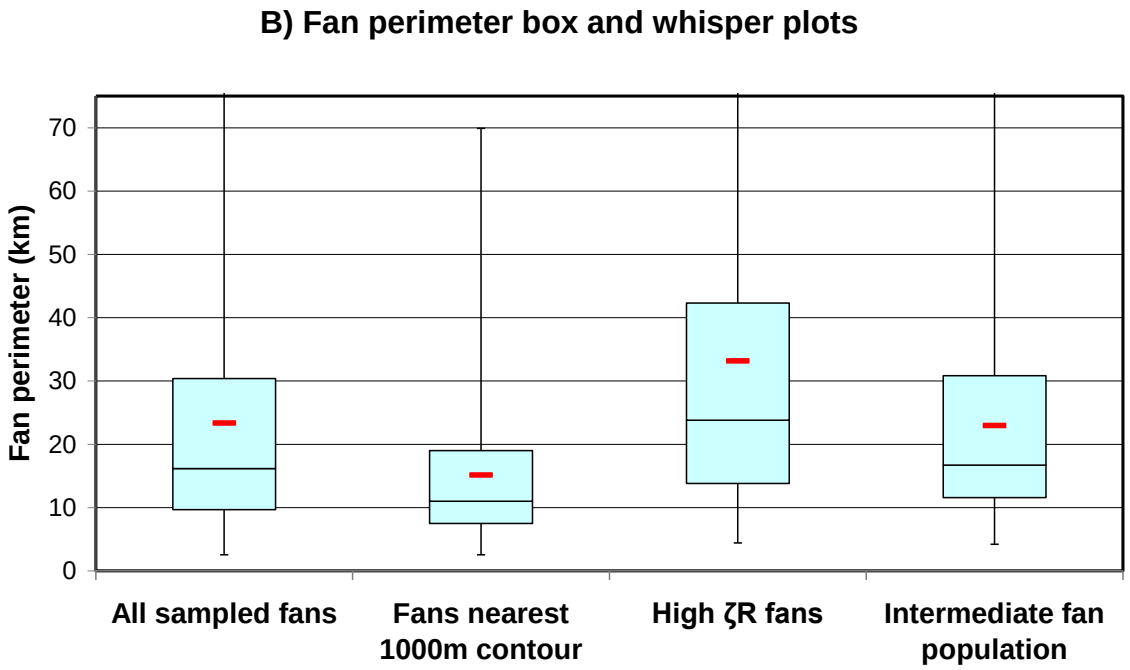

See over for caption

C) Fan volume box and whisper plots

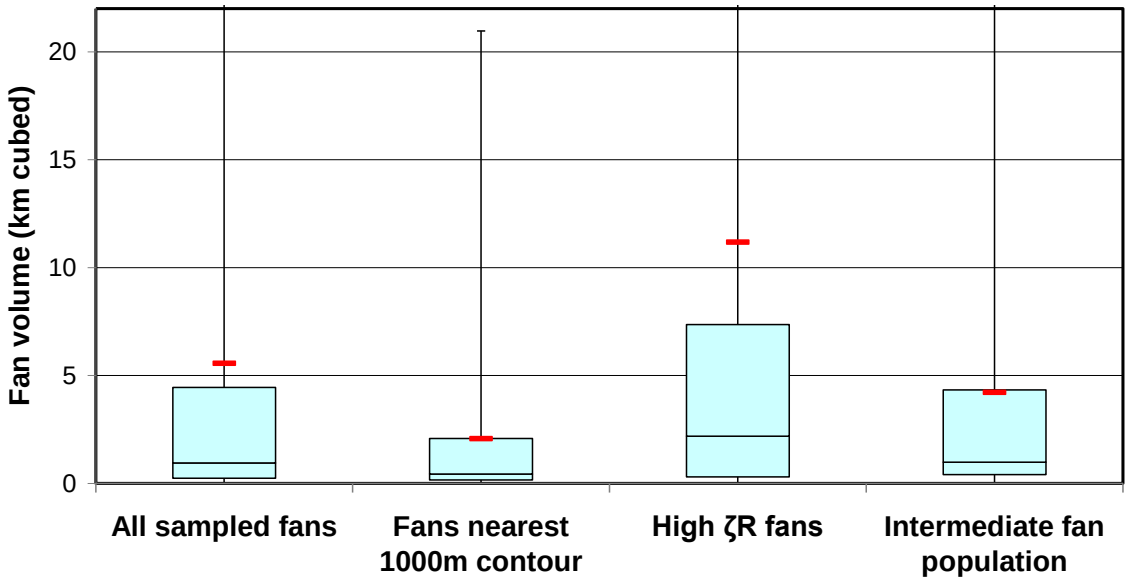

D) Fan progradation length box and whisper plots

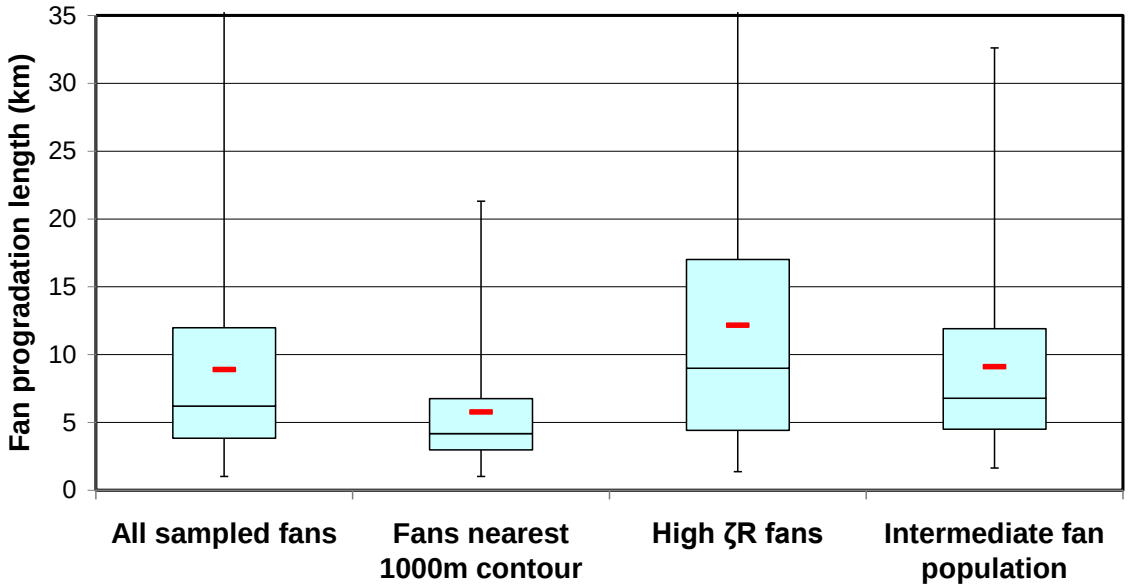

See over for caption

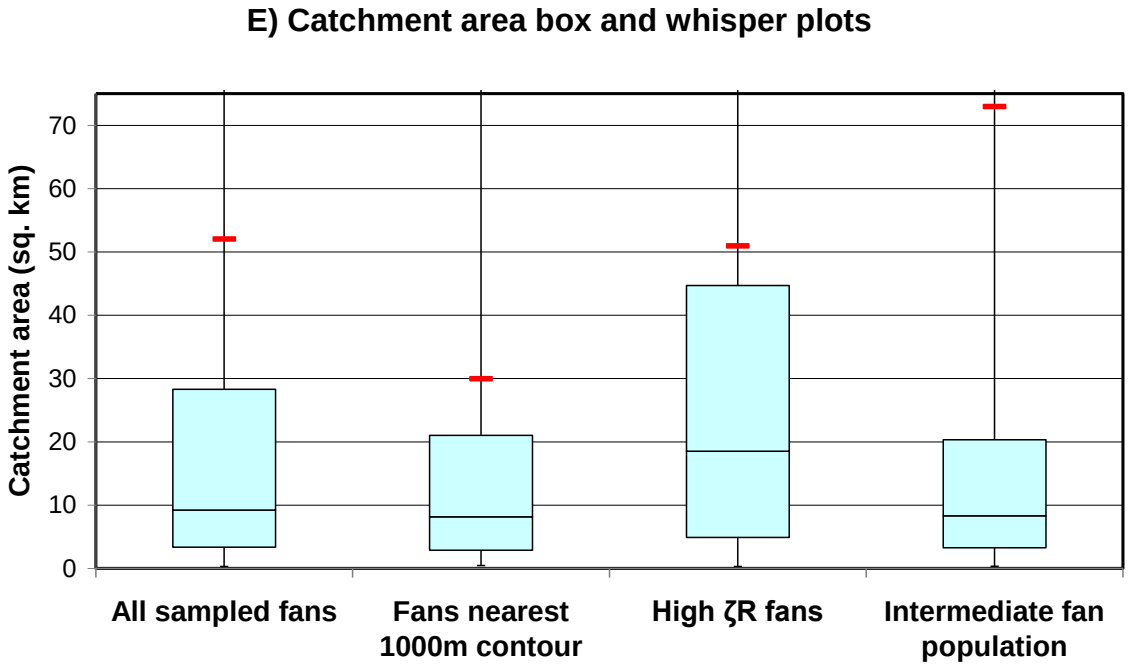

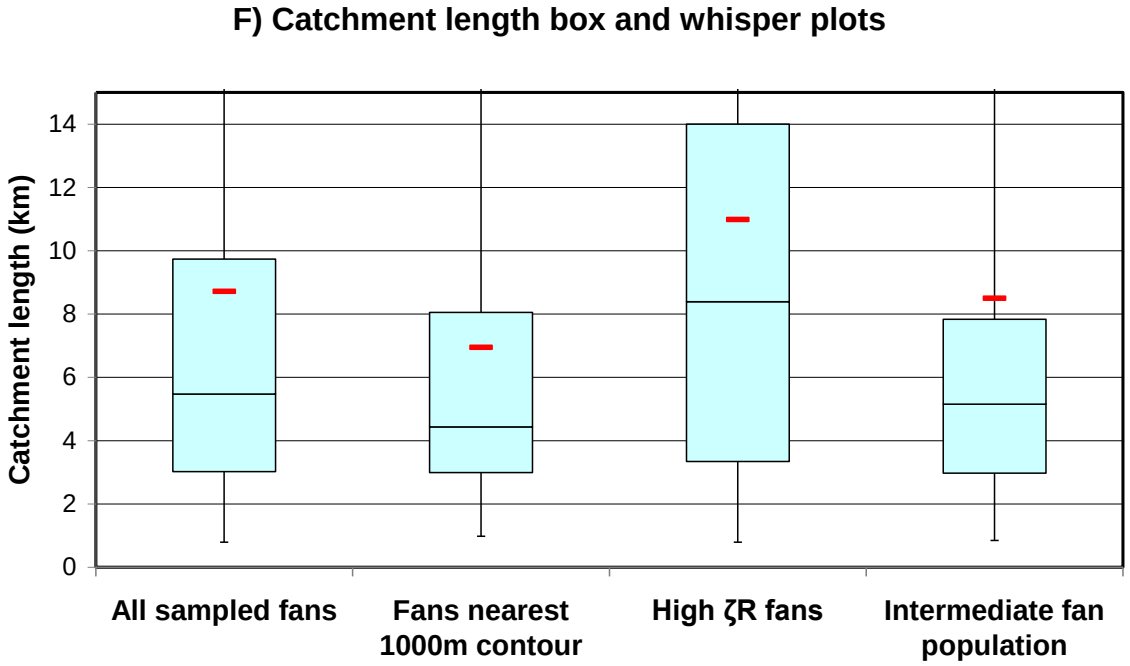

4.15 – Box and whisker plots of scale dependent fan parameters for different alluvial fan sub-populations: *A) Fan area B) Fan perimeter C) Fan volume D) Progradation length E) Catchment area F) Catchment length. In all the plots the mean value for the population is shown by a thick red line. All these plots show a similar pattern of having larger values for fans in the sub-population of fans associated with high ζR values and smaller values in the sub-population of fans closest to the 1000 metre elevation contour.*

The scale-independent parameter of fan area divided by catchment area shows similar results to the plurality of scale dependent parameters shown in figure 4.15, with high values in the high ζR sub-population and low values in the sub-population of fans closest to the seismogenic thrusting zone. One noticeable difference is that the intermediate sub-population has a range of values close to those of the high ζR sub-population.

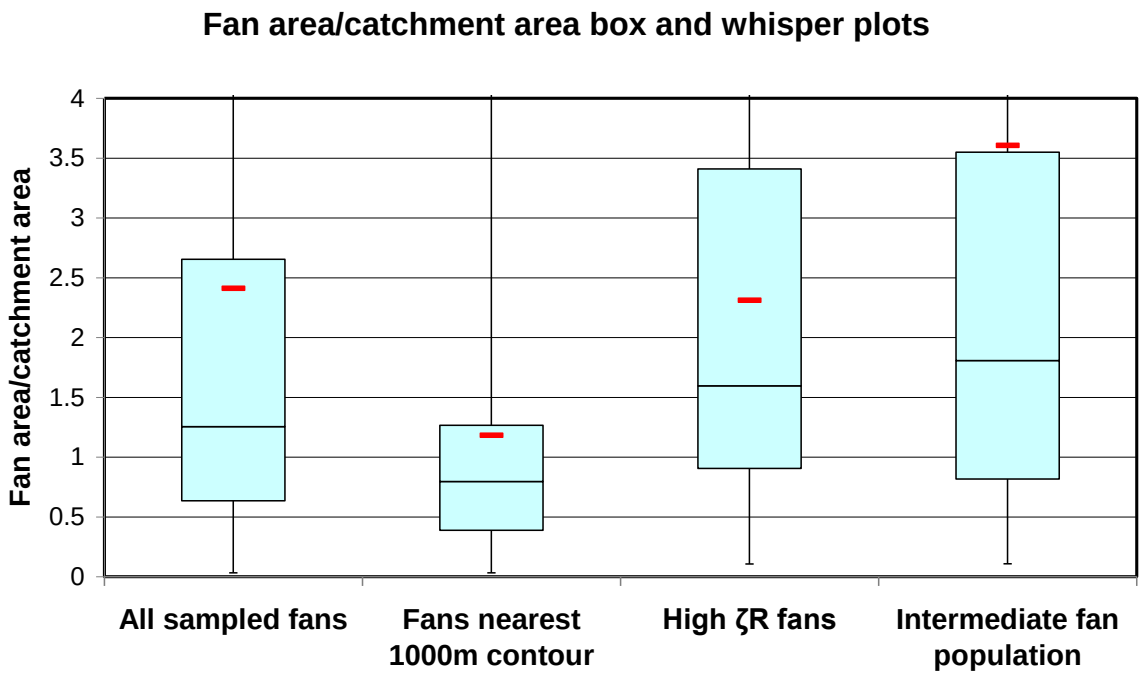

4.16 – Box and whisker plots of fan area/catchment area for different alluvial fan sub-populations: *In all the plots the mean value for the population is shown by a thick red line.*

Fan gradient shows the opposite pattern. The sub-population of fans nearest the seismogenic thrusting zone have the highest gradients, while the fans from the plateau interior are those with the lowest gradients (figure 4.17).

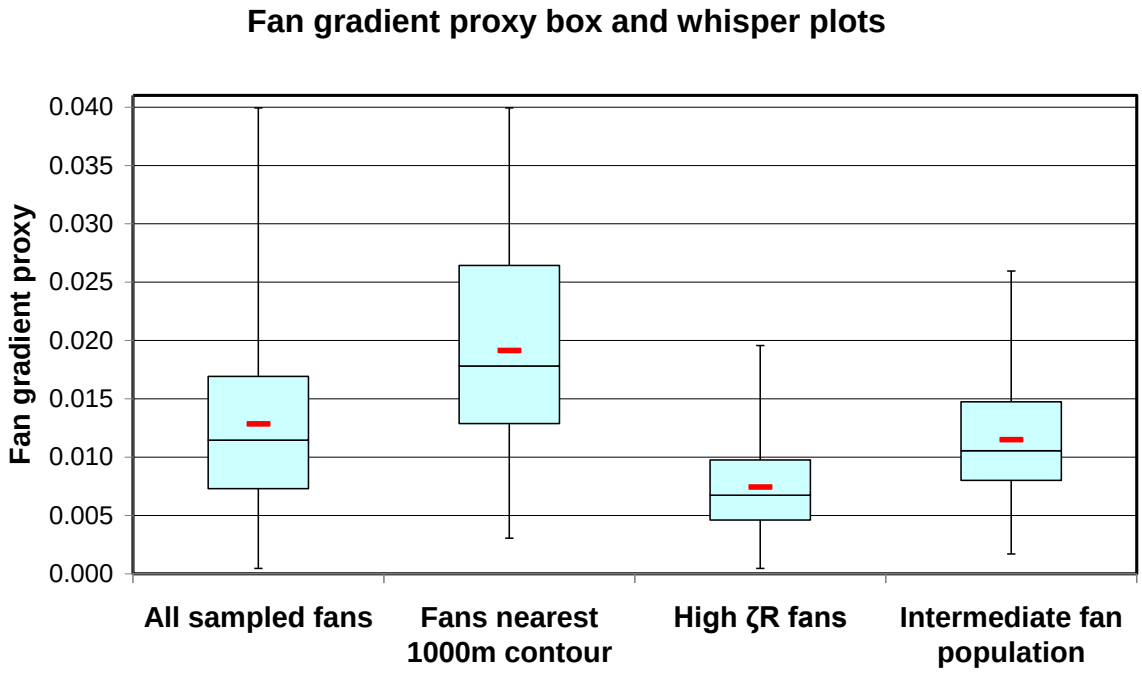

4.17 – Box and whisker plots of fan gradient for different alluvial fan sub- populations: *The mean value for each sub-population is shown by a thick red line. The fans near the seismically thrusting zone have the highest values, while the lowest values are those in the population of fans in the plateau interior.*

Scale-independent parameters that are related to alluvial fans' and their catchment's planform geometry (square root of fan area/progradation length, square root of fan area/fan perimeter, square root of catchment area/catchment length and the square root of catchment area/catchment perimeter) show very little difference in the values associated with the three alluvial fan sub-populations (figure 4.18).

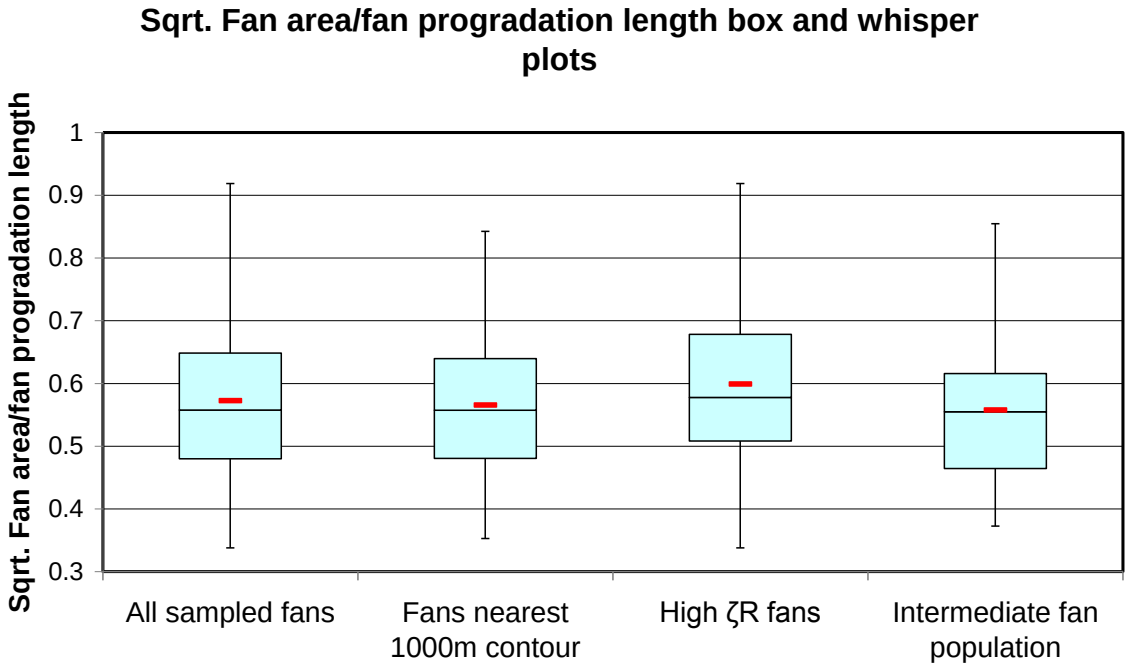

See over for caption

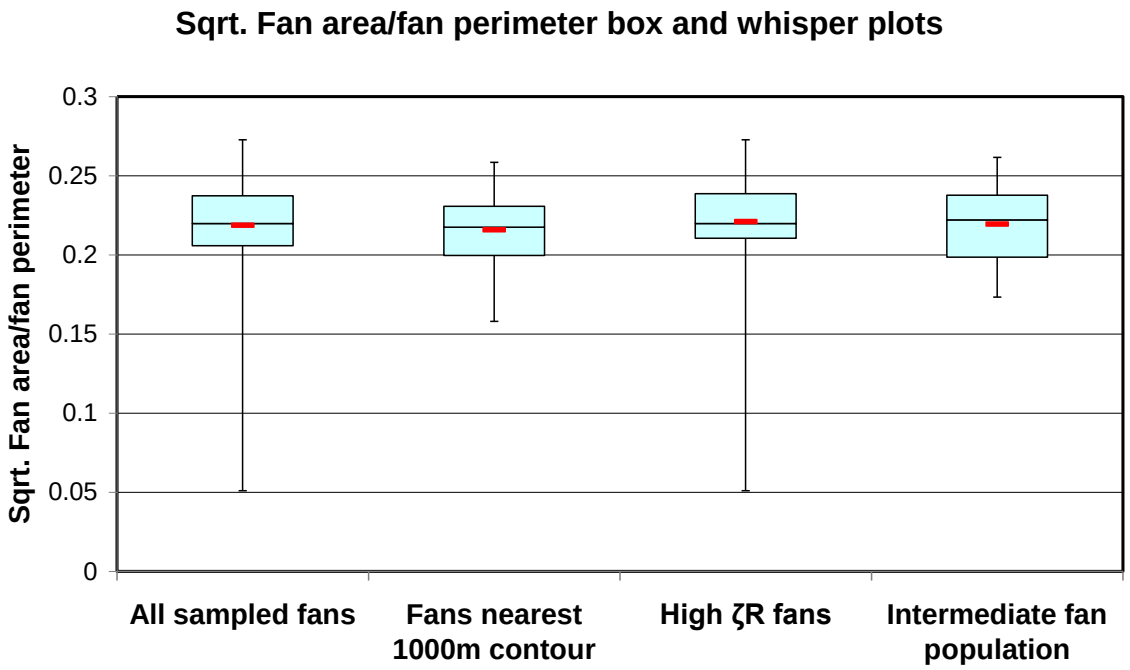

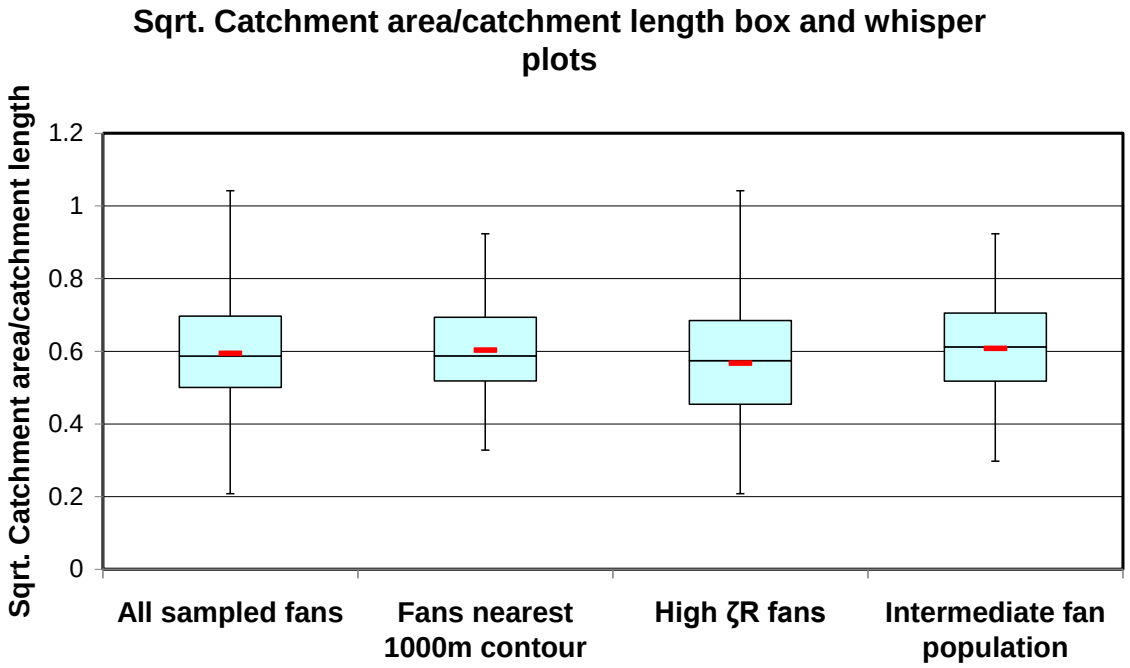

See over for caption

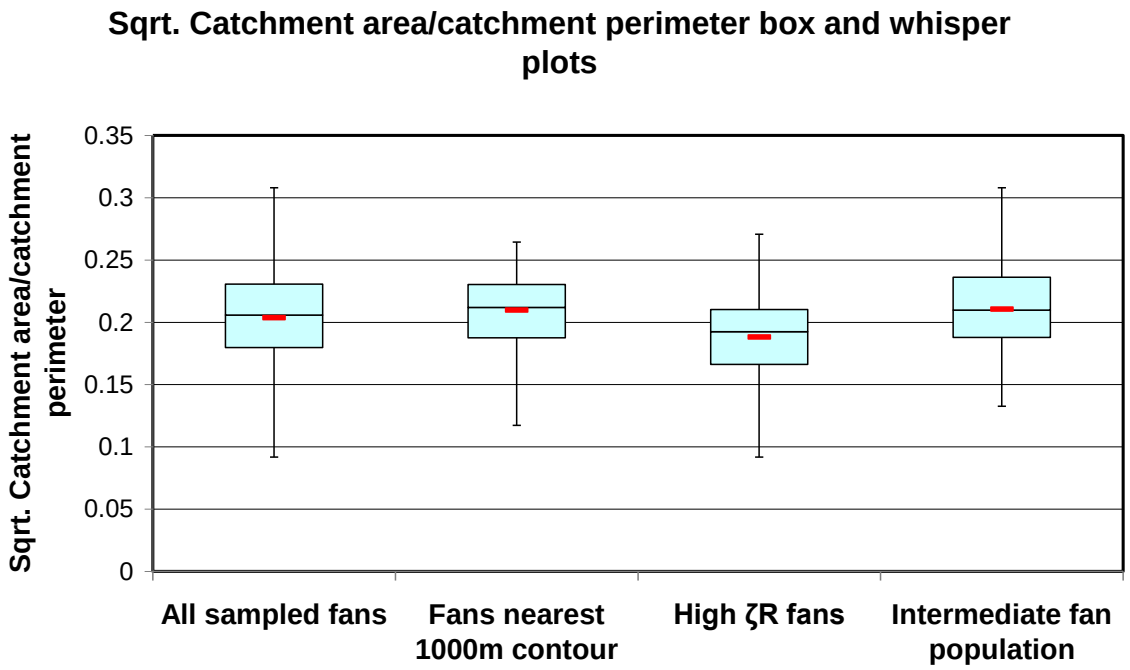

4.18 – Box and whisker plots of planform geometric parameters for different alluvial fan populations: *A) Square root of fan area/fan progradation length B) Square root of fan area/fan perimeter C) Square root of catchment area/catchment length D) Square root of catchment area/catchment perimeter. The mean value for each sub-population is shown by a thick red line. These graphs show there is very little difference in the planform geometrical parameters of fans in different settings.*

Graphs of catchment area against fan area for all the alluvial fan sub-populations show a power law relationship as would be expected for the relationship between these two parameters (see figure 4.19). The power law relationship is in the form:

$$F=cA^n$$

Where *F* is the fan area, *A* is the area of the catchment feeding the fan and *c* and *n* are empirically determined constants that represent that represent the erosivity of the climate and tectonics, the provision of accommodation space by tectonics and the erodability of the lithologies in the catchment area.

Such a power law is often used to relate the size of alluvial fans and the size of the controlling catchment (Bull, 1977; Harvey et al., 1999; Lecce, 1990; Mather and Hartley, 2005; Whipple and Trayler, 1996). This shows the non-surprising result that in general, larger catchments produce larger fans. The fact that relationships between fan area and catchment area can be extrapolated and that the fan sizes don't just reflect fans at different stages of growth suggest that some form of steady state is reached between sediment input into and sediment removal from the fans (Denny, 1965; Fraser and DeCelles, 1992; Hooke, 1968). The differences between these power law relationships for the different fan sub-populations are fairly small with a shift towards larger fan sizes for the trend line of the sub-population of fans with a high ζR value. Correlation to the line of best fit is highest for the fan with highest ζR values. This suggests that the controlling tectonic and climatic conditions are most consistent at an individual fan scale within the plateau interior. This intuitively makes sense as the tectonic controls that form the topography, and therefore help control the climate, of the seismogenic thrusting zone are discontinuous in nature. When compared to the relatively quiescent plateau interior, these discontinuous tectonics will lead to a greater variety of settings for individual fans than the more homogenous plateau interior.

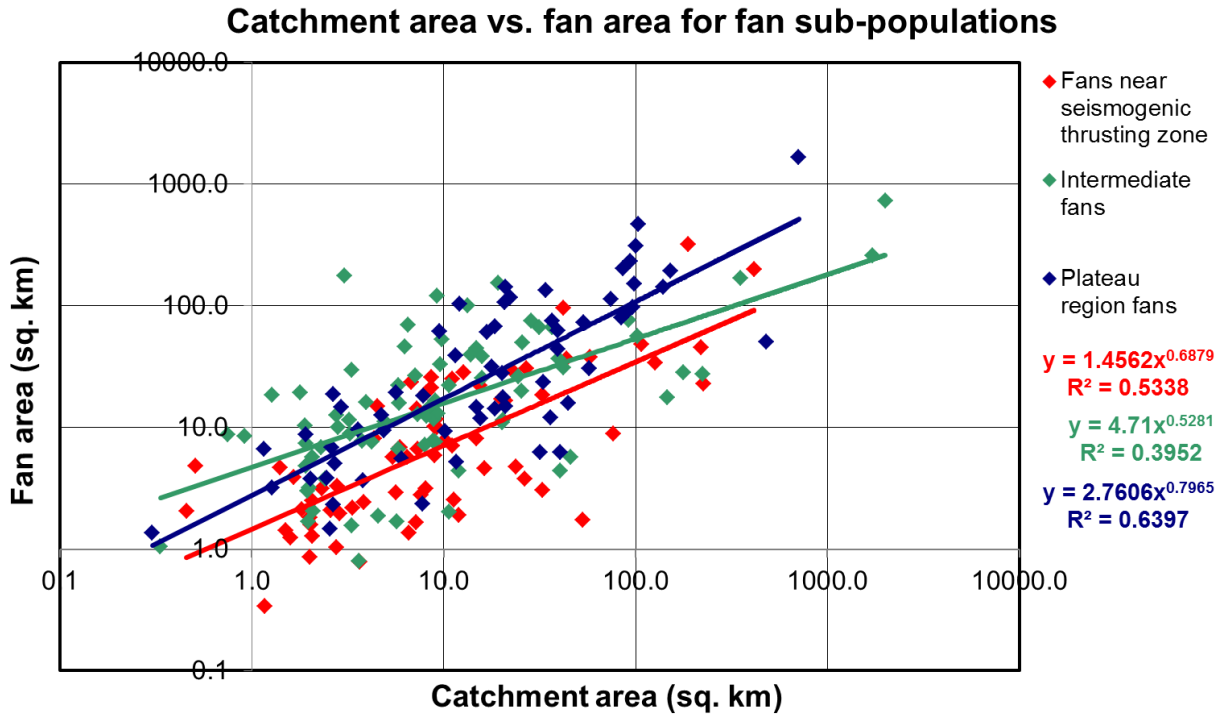

4.19 - Graph showing the relationship between catchment area and fan area for different fan sub-populations: *Data for the sub-population of fans near the seismogenically thrusting margins are shown in red, data for the fans with high ζR values at their head are shown in blue and data for the intermediate sub-population is shown in green. The form of the power law relationship between catchment area and fan area for the seismically thrusting area, the intermediate region and the plateau interior is shown.*

Graphs showing the relationships between fan area and fan gradient show a weak negative relationship (figure 4.20), with larger fans having flatter fan surfaces. This is as an intuitively reasonable result as fans that are not topographically constrained are likely to spread out further and so reduce in gradient. Both the distribution of the data points and the trend lines differentiate between the three sub-populations defined earlier. The sub-population of fans from the plateau interior have higher fan areas and lower fan gradients, while the opposite is true for the fans near the seismogenic thrusting zone. The intermediate fan sub-population has values that are intermediate to the other two sub-populations, rather than aligning with one group or the other.

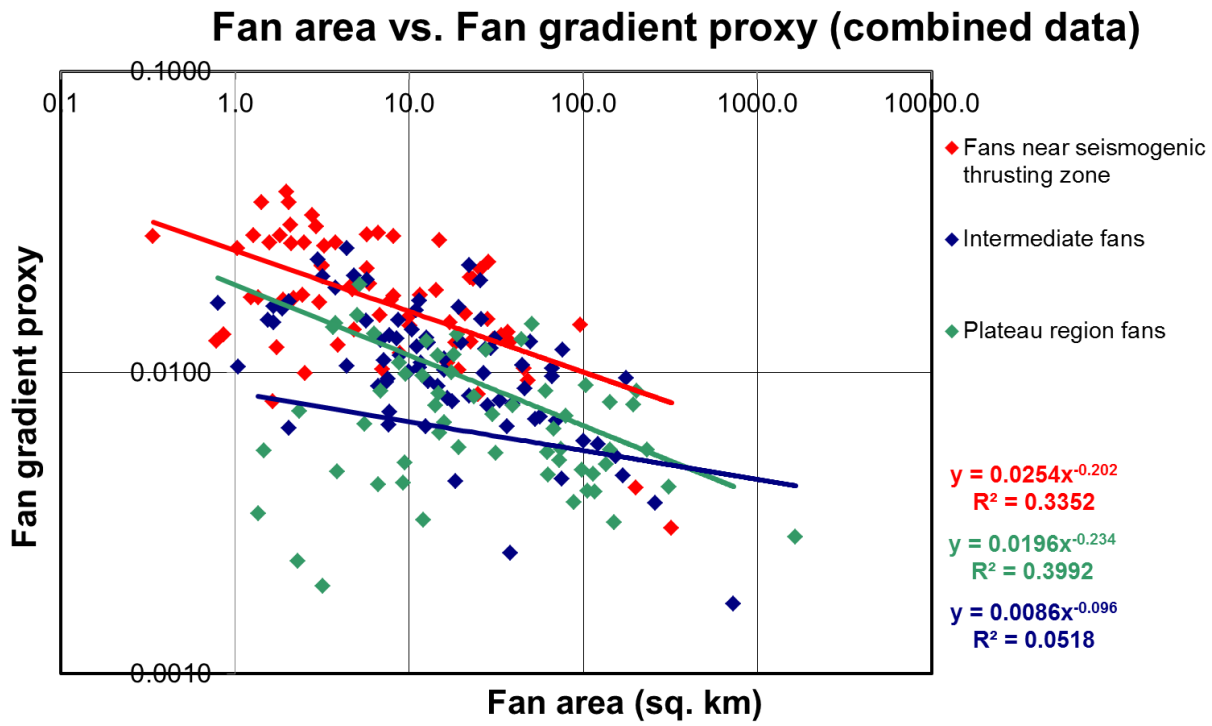

4.20 - Graph showing the relationships between fan area and fan gradient for fan sub-populations: *Data for the sub-population of fans near the seismogenically thrusting margins are shown in red, data for the fans with high ζR values at their head are shown in blue and data for the intermediate sub-population is shown in green. The form of the power law relationships between fan area and fan gradient for the three sub-populations of fans are shown. Also shown are correlation coefficients for these relationships. The graph shows limited overlap between the data points for the plateau interior fan sub-population and the fans near the seismically thrusting region.*

4.6.3 Variation of fan parameters with lithology

To look at the variation of fan characterisitics with the lithology the alluvial fans are derived from, the lithology needs to be parameterised. This is done by looking at the band 7 intensity of pixels from Landsat 7 ETM+ images that correspond to the alluvial fan locations (see section 4.4.4). In this approach each fan has a landsat band 7 value assigned to it, to represent the lithology of the fan. This value is the mean of the Landsat 7 ETM+ band 7 values for the pixels of the fan surface. Using these values to parameterise lithology works better than just assigning each fan a code based on the lithology of the fan indicated on a geological map. This is because many of the fans picked for this study are shown as being made up of alluvial fan deposits on the geological maps provided by the

national Iranian oil company (Pollastro et al., 1999), avoiding using this obviously circular definition is desirable. Furthermore the band 7 numerical value is more than just a coding system, it has some basis in the physical properties of the fan surface (in this case, it is a measure of the intensity of the infra-red radiation emitted/reflected by the ground between the wavelengths of $2.08x10^{-6}$ and $2.35x10^{-6}$ metres). Using the mean value allows the lithological make up of an alluvial fan to be parameterised with one value. A more complete useage of the Landsat 7 band 7 data would be to describe the distribution of values present in each fan area, but that would not allow for the lithology to be parameterised by a single number that could be compared directly to the fan values.

Looking at the distribution of the lithology proxy values (figure 4.21), between the three sub-populations of alluvial fans, shows that it is ill-suited for distinguishing between them. The distribution of Landsat 7 ETM+ band 7 intensity values is very similar for each of the sub populations.

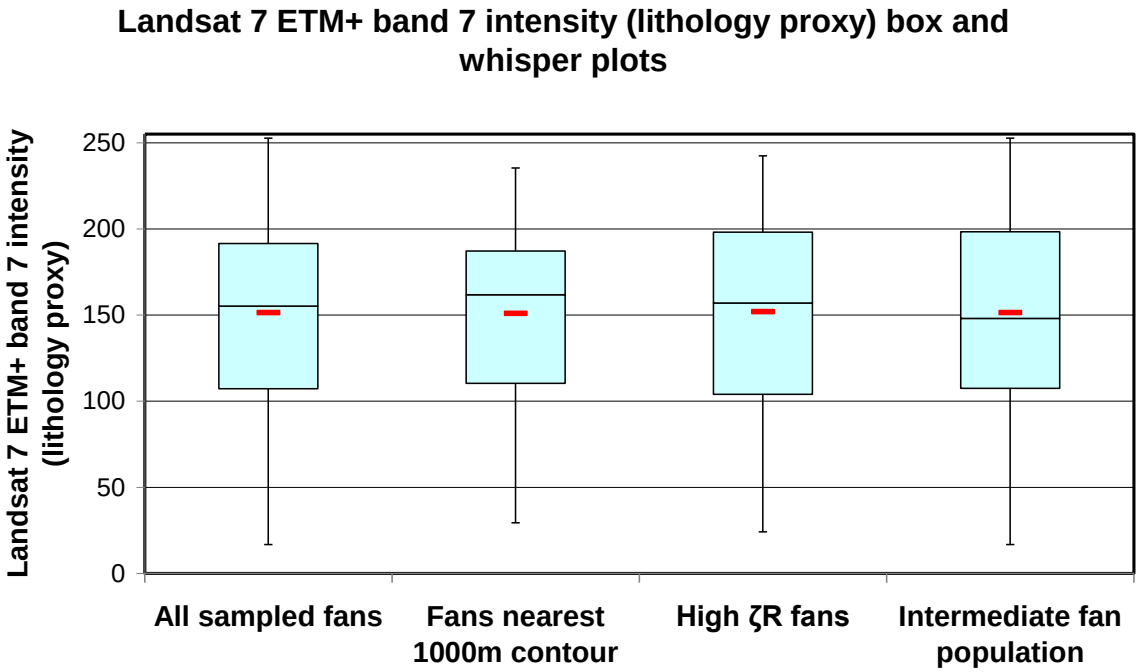

4.21 - Box and whisker plots of the lithology proxy for different alluvial fan populations: *The Landsat 7 ETM+ band 7 intensity can be used as a proxy for different lithologies. These plots show that the distribution of these values between the fan sub-populations near the seismically thrusting zone, within the plateau interior and in between show limited differences.*

To see if lithology is a control on fan characteristics, independently of the three defined sub populations, fan parameters were plotted against lithological proxy values. These plots show that there is no systematic variation of fan parameters with lithological proxy values.

A) Landsat 7 ETM+ band 7 intensity (lithology proxy) vs. fan volume

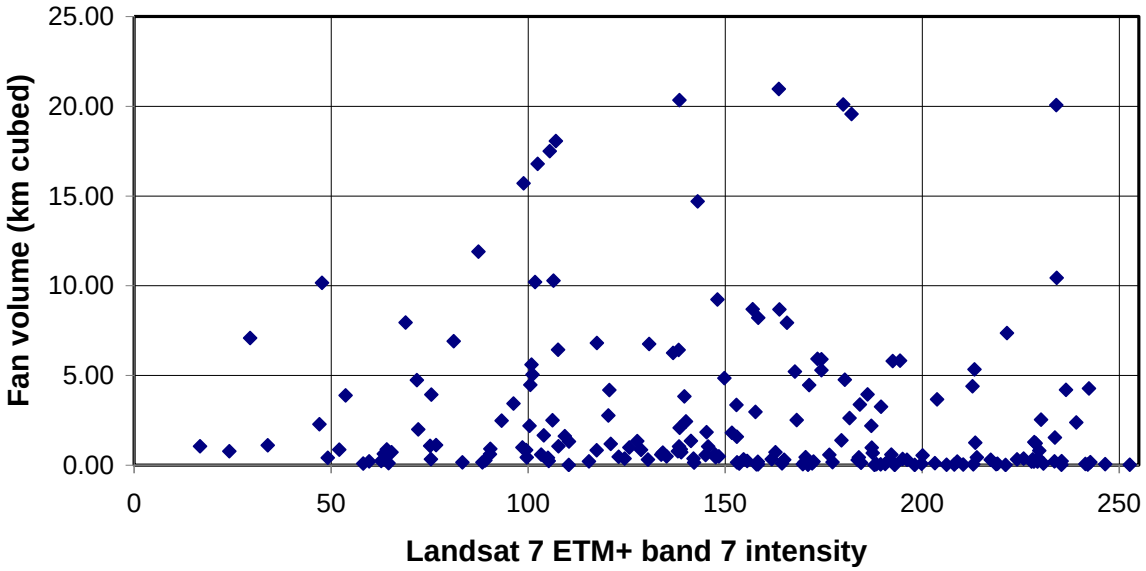

B) Landsat 7 ETM+ band 7 intensity (lithology proxy) vs. catchment area

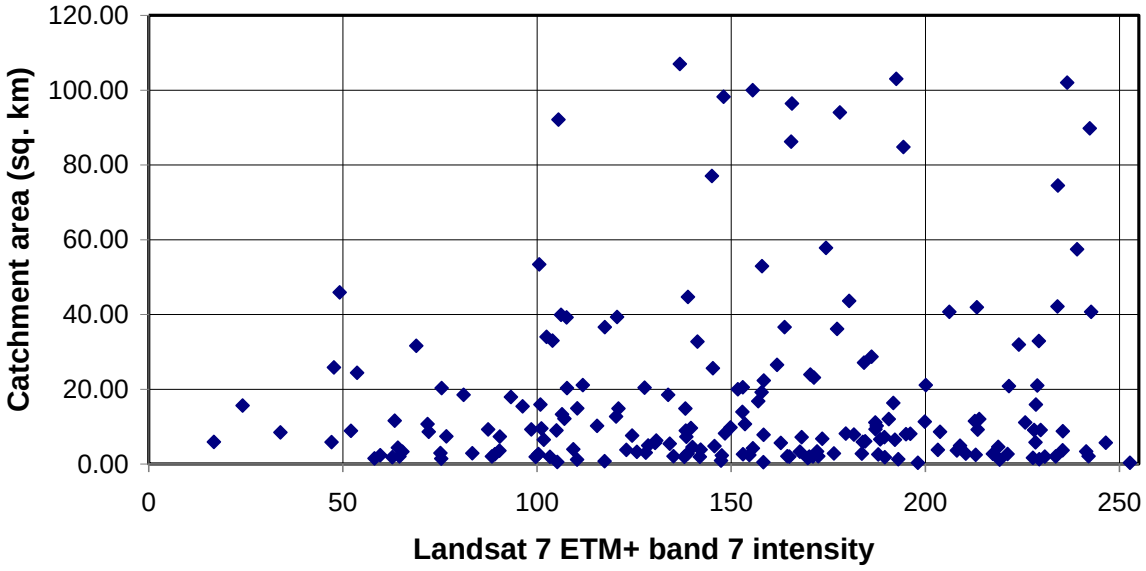

See over for caption

C) Landsat 7 ETM+ band 7 intensity (lithology proxy) vs. fan gradient proxy

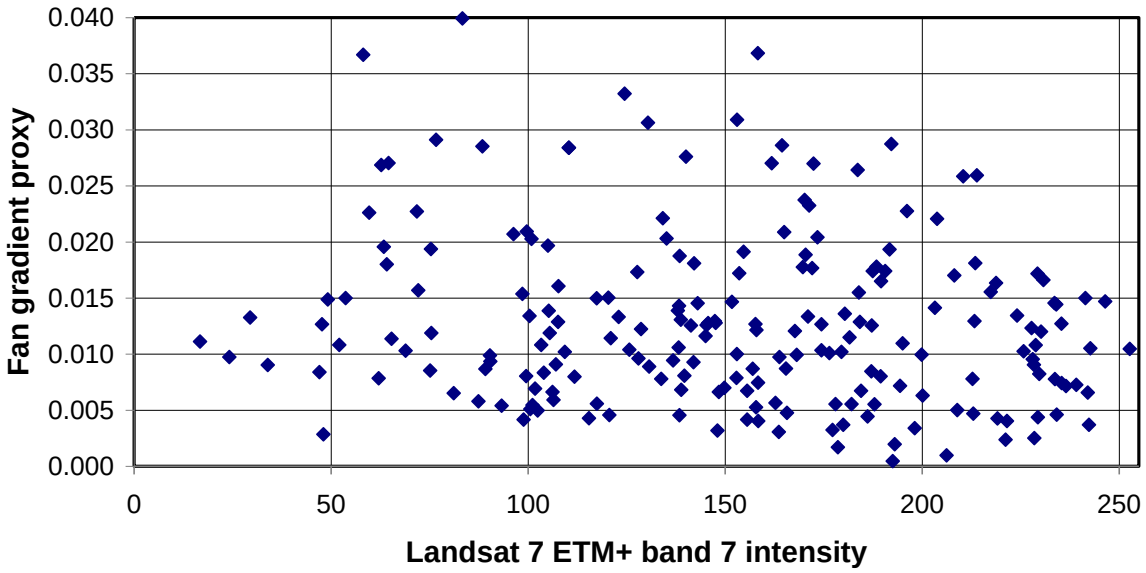

D) Landsat 7 ETM+ band 7 intensity (lithology proxy) vs. Fan area/catchment area

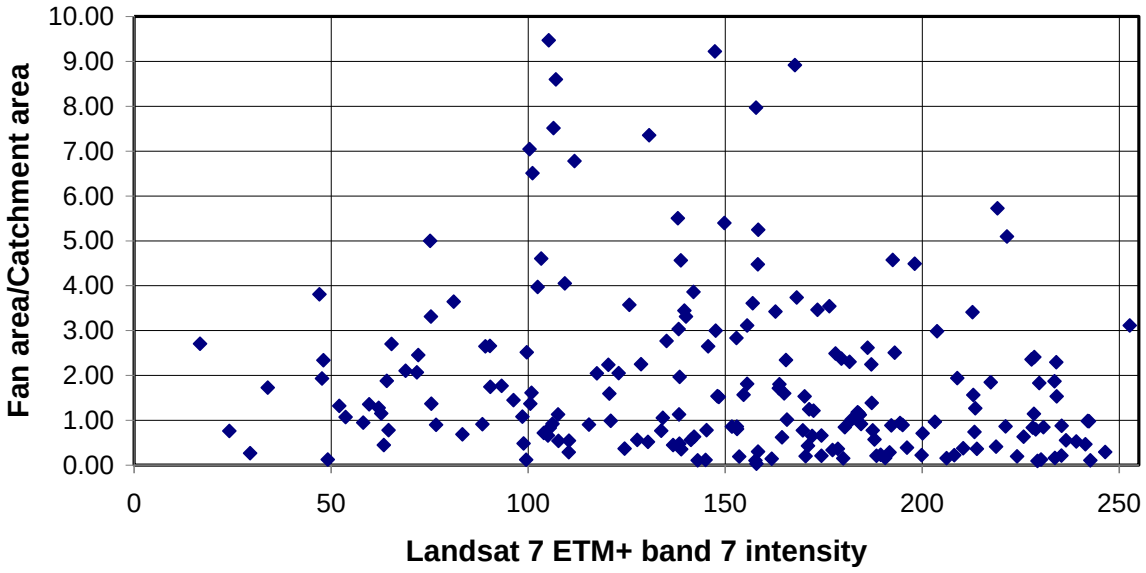

4.22 – Graphs of fan parameters against lithological proxy values: *A) Lithology versus fan volume B) Lithology versus catchment area C) Lithology versus fan surface gradient D) Lithology versus fan area/catchment area. These graphs show that parameters that are different between the different fan sub-populations show no systematic variation with the lithology proxy.*

4.6.4 Variation of fan parameters with distance from seismic thrusting zone

The 1000 metre elevation contour marks the boundary between the seismogenic thrusting zone and the non-thrusting plateau interior. The distance from this contour is used as a measure of how much influence thrust tectonics has on the setting of an alluvial fan. Fans that are positioned toward the plateau interior inside the contour are assigned a positive distance from the contour, while those positioned outside the contour are given a negative value.

Scale-dependent fan parameters increase in value the further the fan is from the 1000 metre elevation contour (see figure 4.23), this is consistent with the results from comparing fan parameters in the three sub-populations of fans, where the sub-population of fans closest to the 1000 metre elevation contour have the smallest scale dependent parameter values. While this is a weak relationship, the general pattern is that larger fans are present further from the 1000 metre elevation contour.

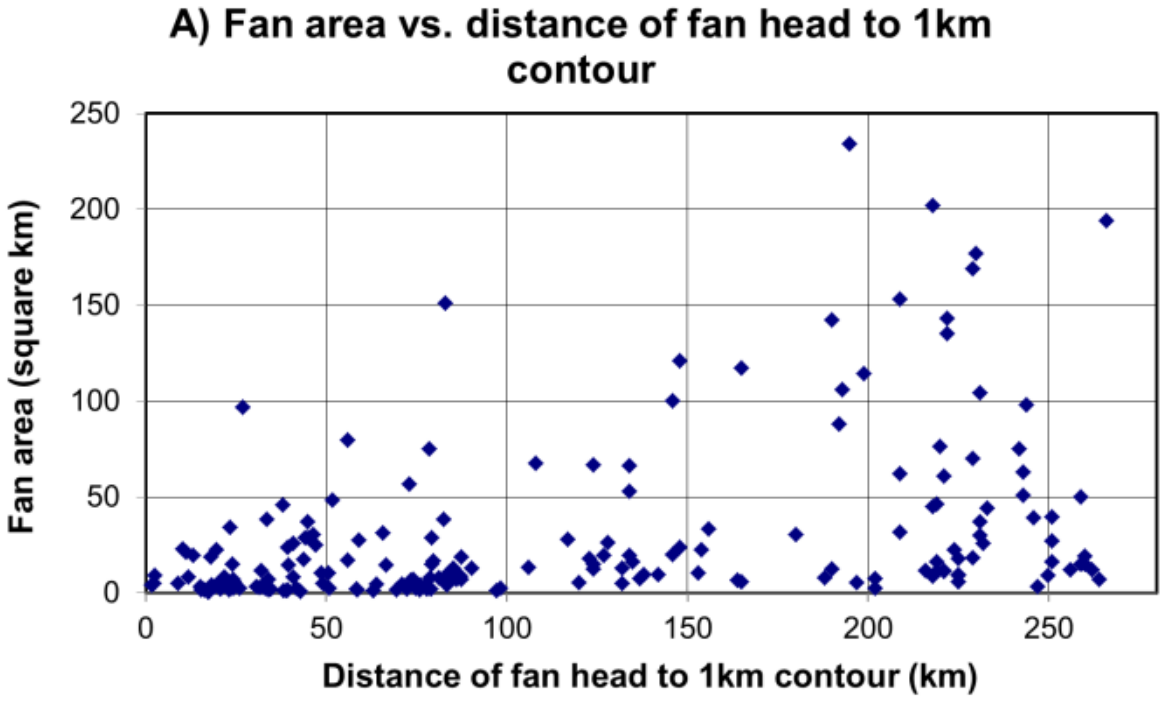

See over for caption

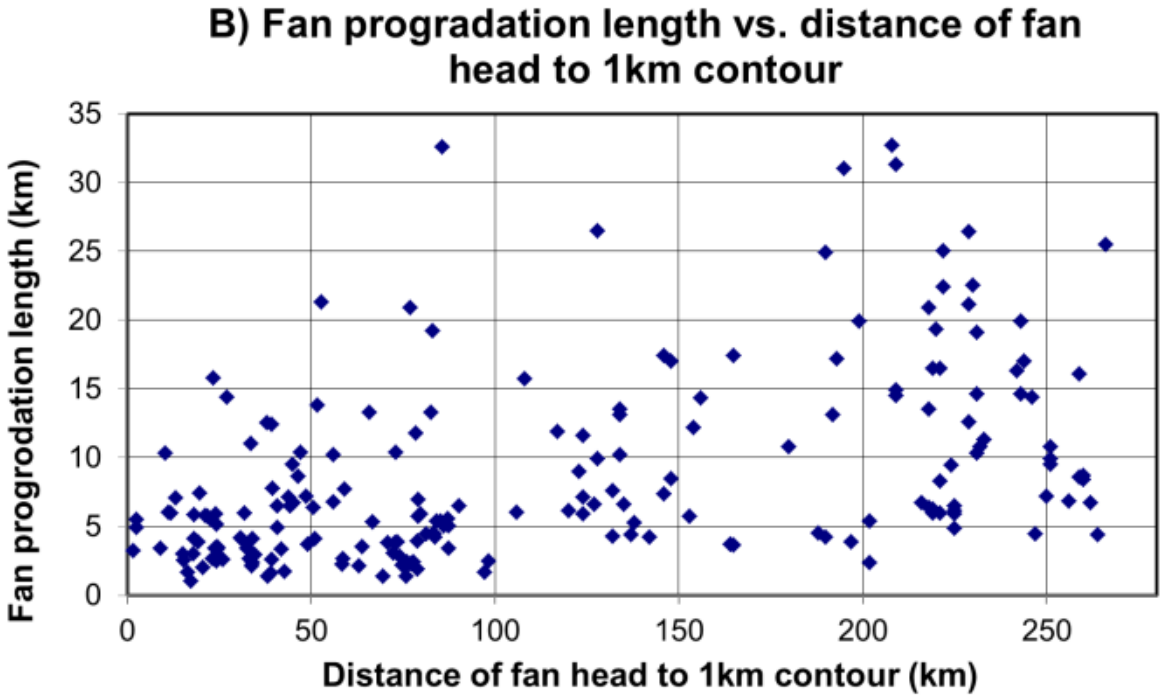

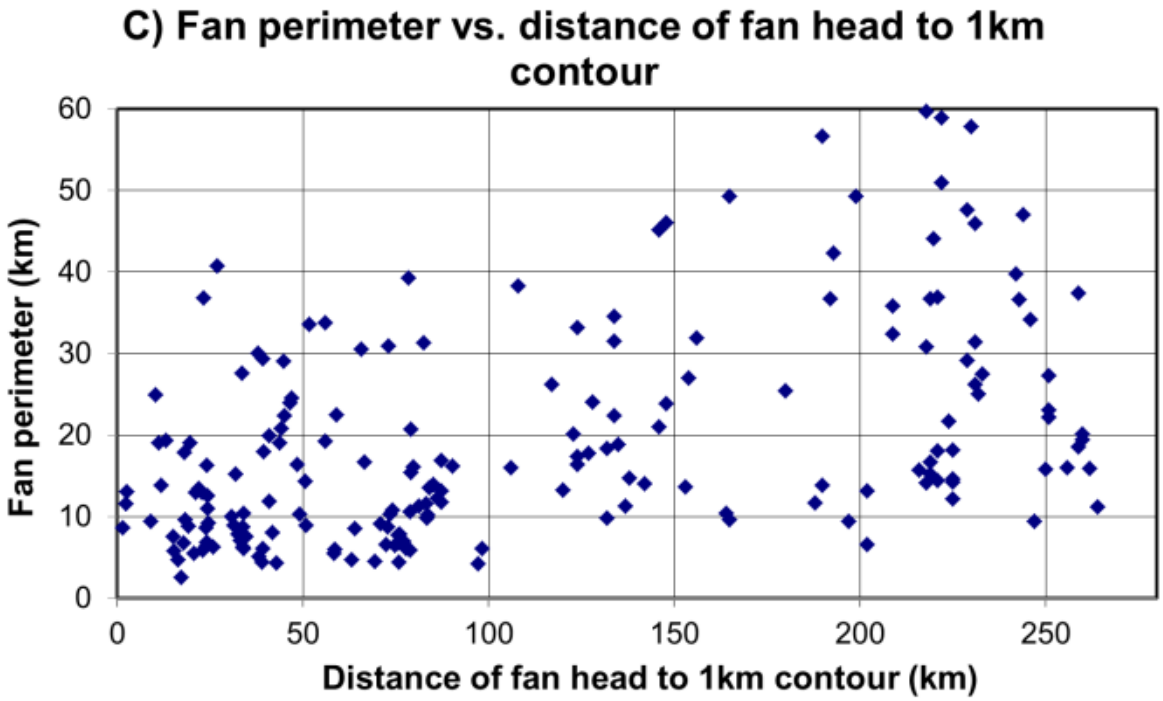

See over for caption

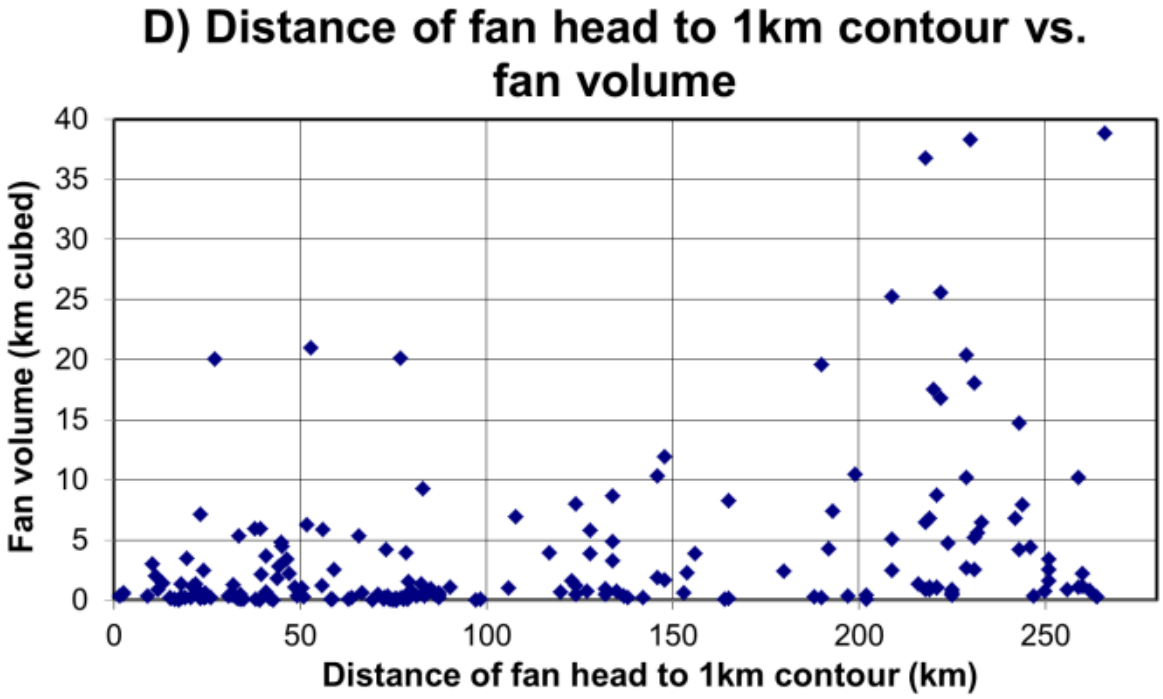

4.23 – Scale dependent fan parameters against distance between fan head and the 1000 metre elevation contour: *A) Distance of fan head to the 1 km elevation contour versus fan area. B) Distance of fan head to the 1 km elevation contour versus fan progradation length. C) Distance of fan head to the 1 km elevation contour versus fan perimeter. D) Distance of fan head to the 1 km elevation contour versus fan volume. These graphs all show a weak positive relationship, fan parameters measuring fan size get larger the further the fan is from the 1000 metre contour.*

The variation of scale-independent parameters that measure the planform geometry of the alluvial fans, with the distance of the fan heads from the 1000 metre elevation contour, is also consistent with the analysis of fan parameters within the three alluvial fan sub-populations. The planform geometry parameters show no systematic variation with the distance from the fan head to the 1000 metre elevation contour.

A) Distance of fan head to 1km contour vs. sqrt. fan area/progradation length

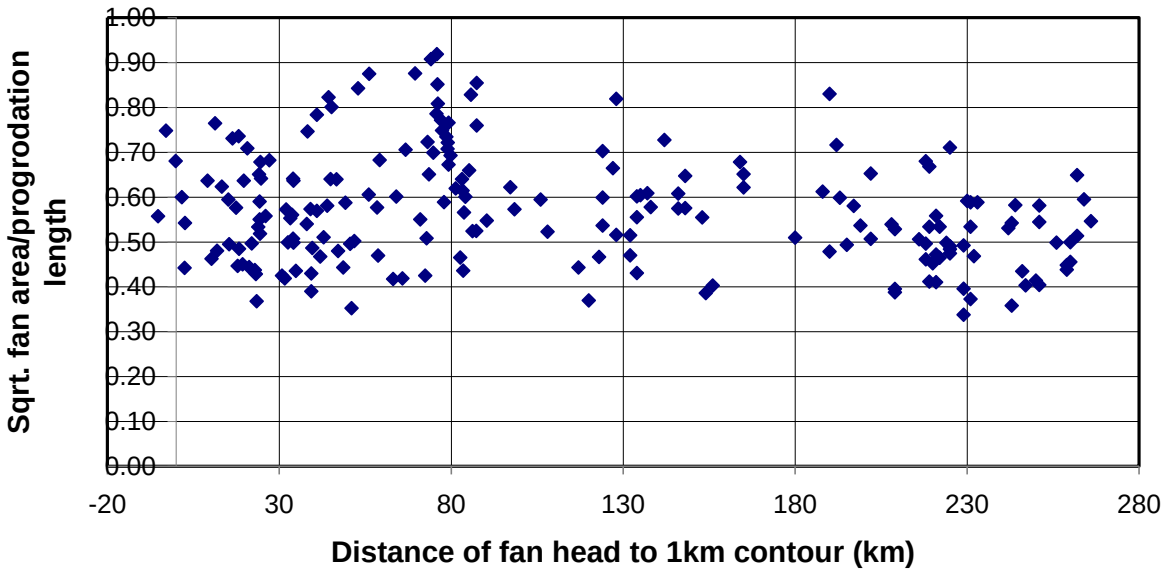

B) Distance of fan head to 1km contour vs. sqrt. fan area/perimeter

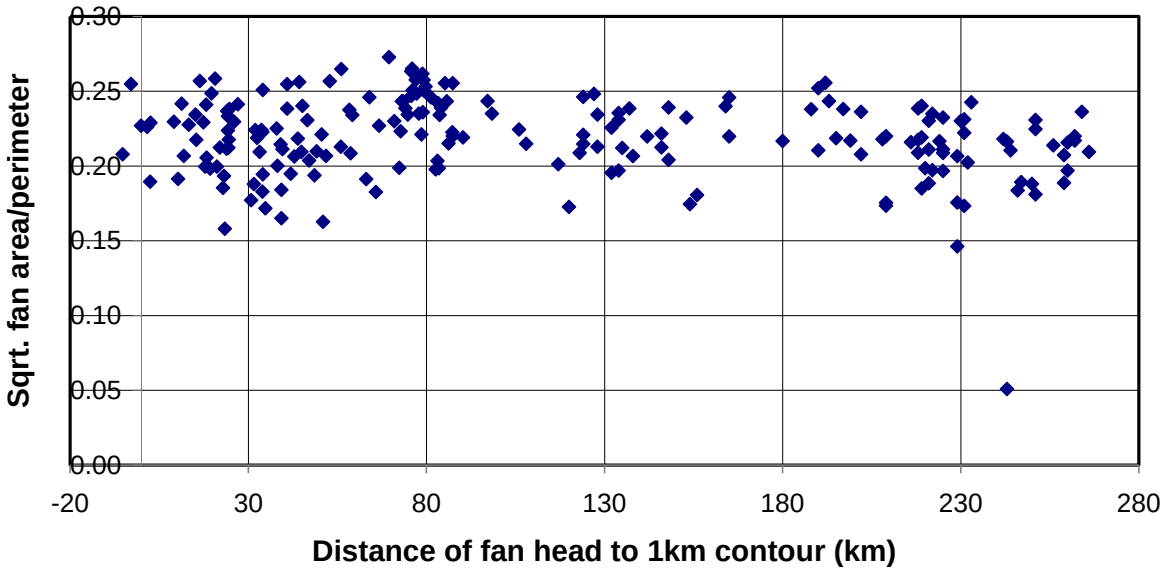

See over for caption

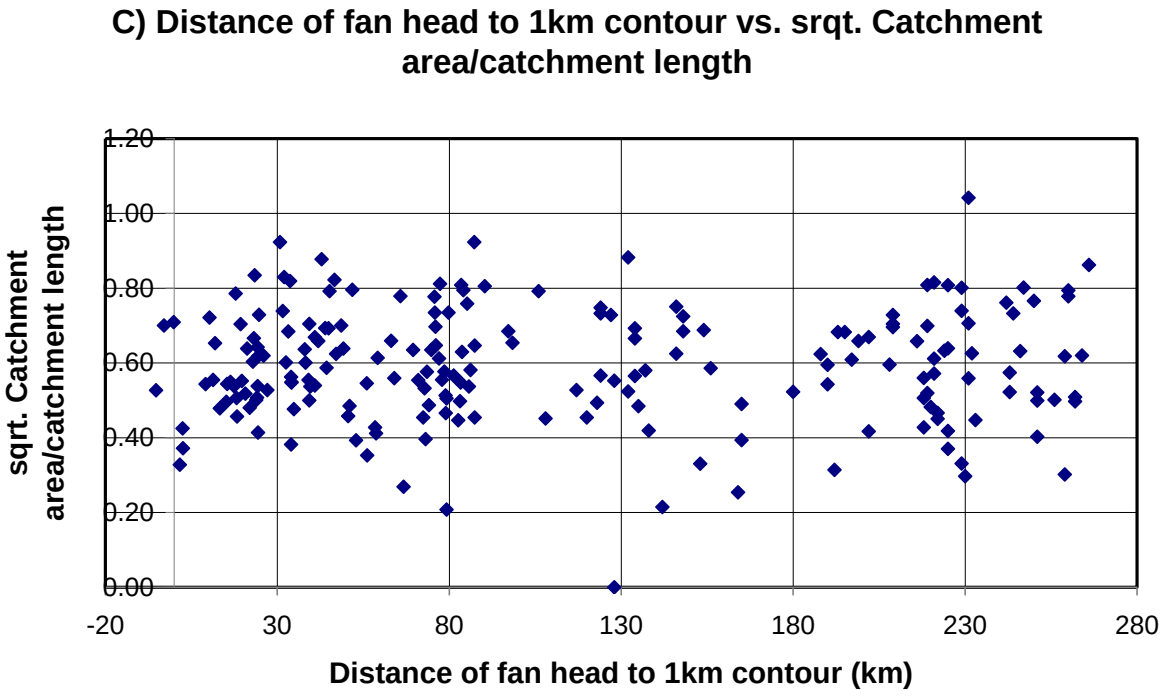

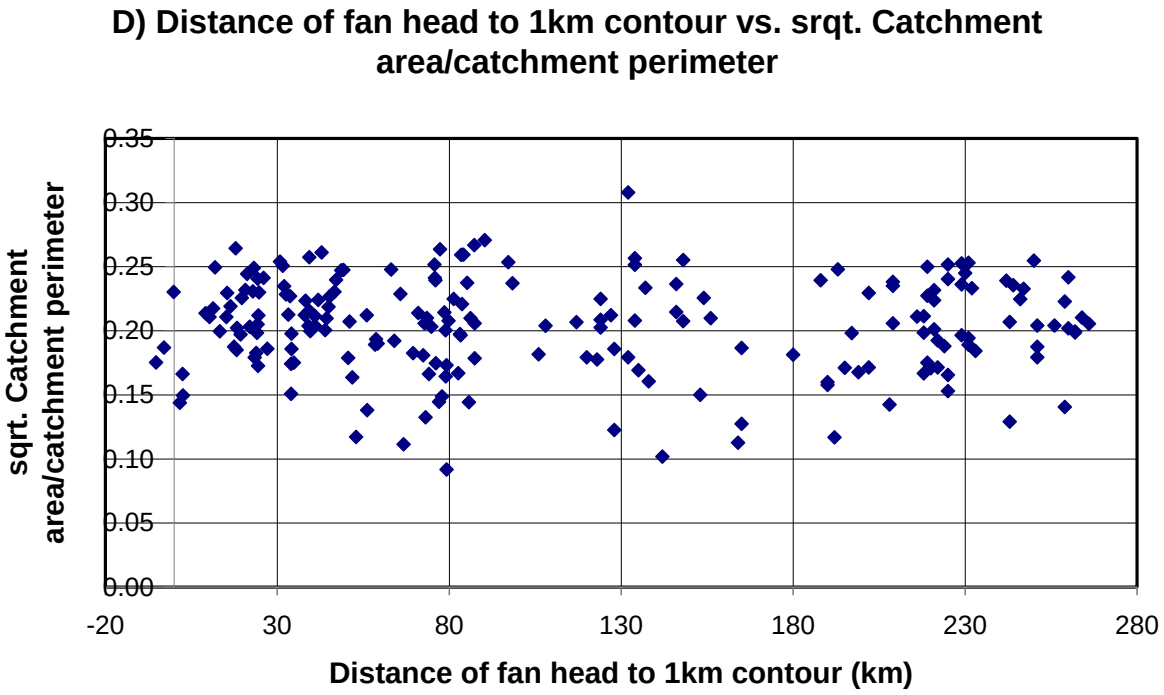

4.24 – Scale-independent fan parameters against distance between the fan head and the 1km elevation contour: *A) Distance to the 1 km contour vs. root of area divided by progradation length. B) Distance to the 1 km contour vs. root of area divided by perimeter. C) Distance to the 1 km contour vs. root of catchment area divided by catchment length. D) Distance to the 1 km contour vs. root of catchment area divided by catchment perimeter. There is no relationship between the distance from the seismic thrusting zone and the scale-independent measures of morphology.*

4.6.5 Variation of fan parameters with measures of ζR

ζR is a measure of local topography. It is calculated by dividing local elevation by local relief (see section 4.5.1). Figure 4.11 shows that high values of this variable correlate well with the plateau interior, making it a useful measure of 'plateauness'. Alluvial fans that have a high value of this variable at their heads are defined as having a topographic setting that most represents a plateau. Figure 4.11 shows that the ζR variable does not completely divide the study area into distinct regions, although fans with high values of ζR trend away from the seismogenic thrusting plateau margins.

Values for the fan gradient proxy reduce with increasing values of ζR. The relationship is not a straightforward correlation, instead the data points plot within an envelope where high values of fan gradient are not present at high values of ζR (see figure 4.25).

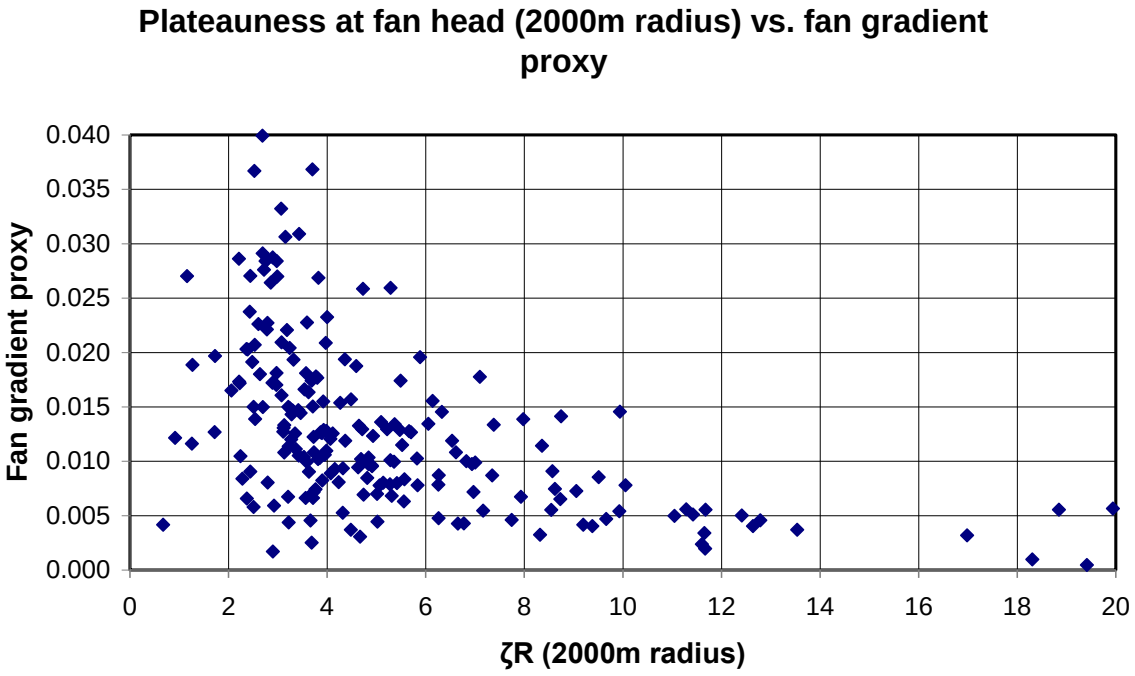

4.25 – Graph showing the relationship between the fan gradient proxy and ζR: *Data points plot within a declining envelope, where high values of the fan gradient proxy are only present at small values of ζR.*

The scale-independent fan parameters that measure the planform geometry of the alluvial fans show no relationship with the ζR variable, similarly to those parameters relationship to the distance from the 1000 metre elevation contour.

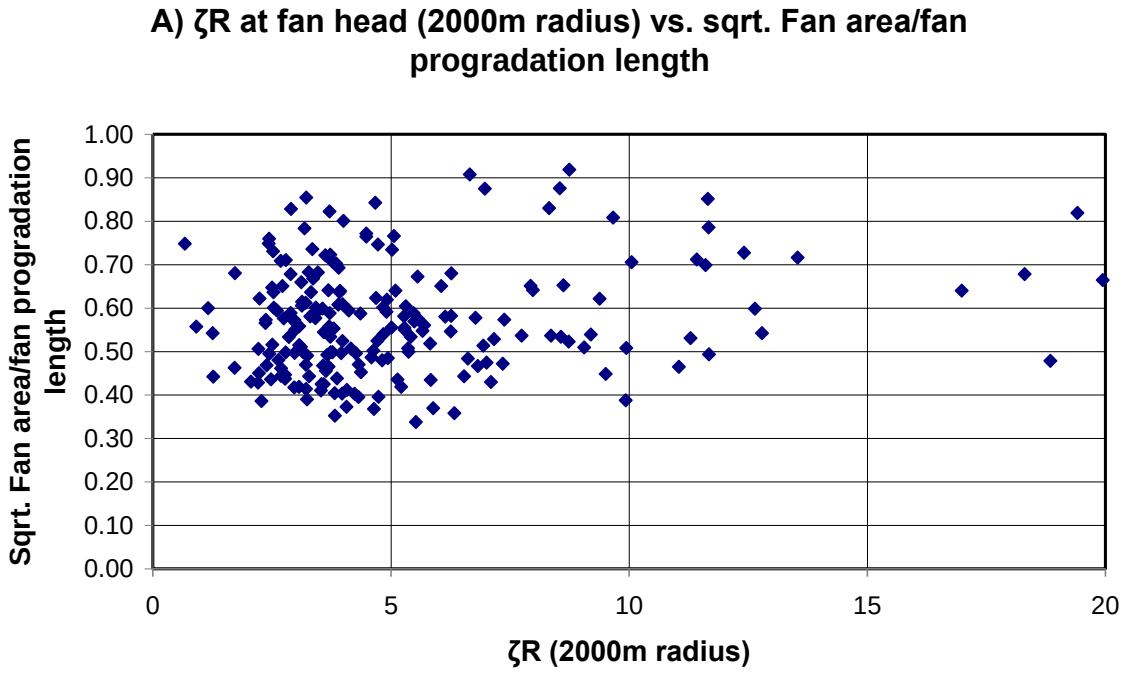

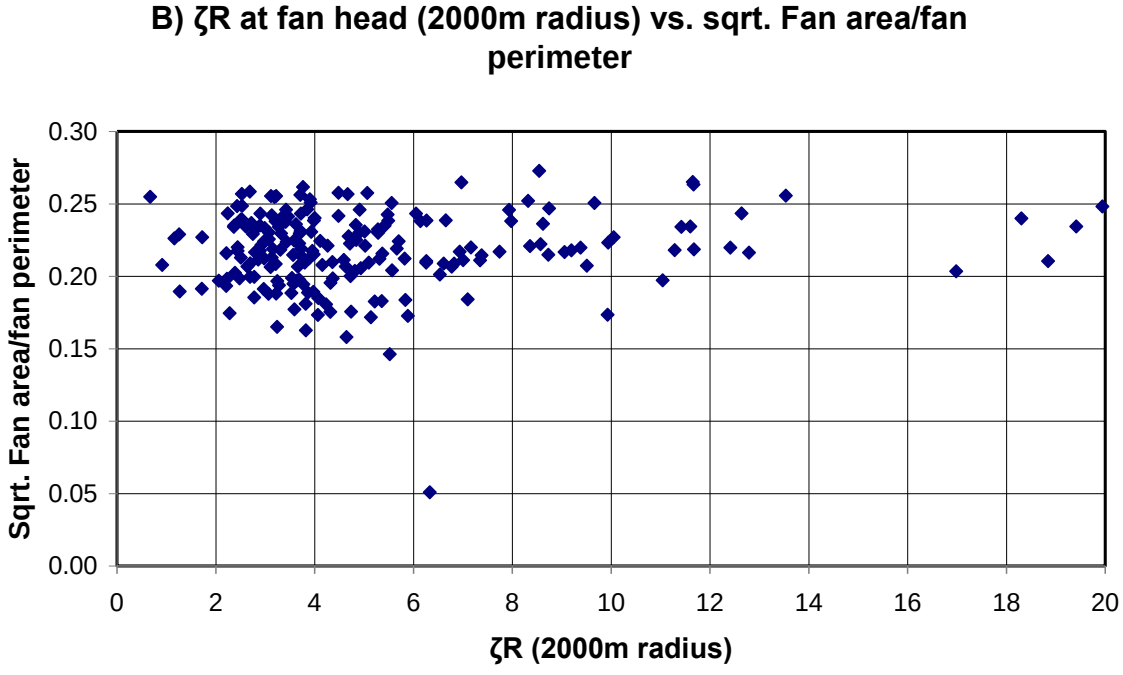

See over for caption

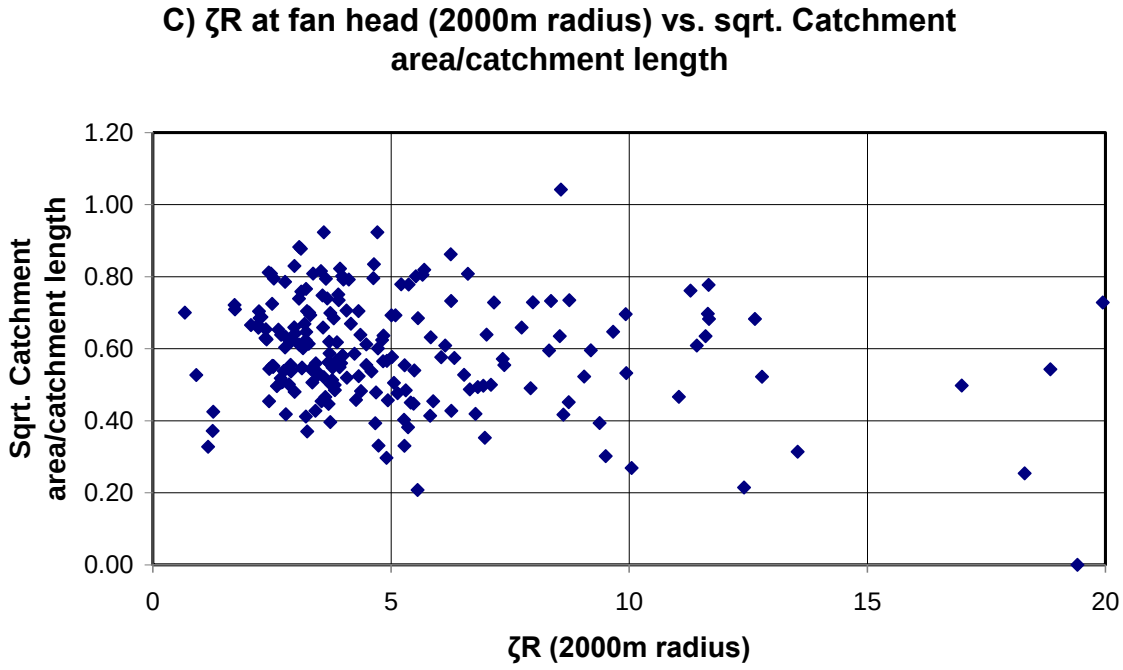

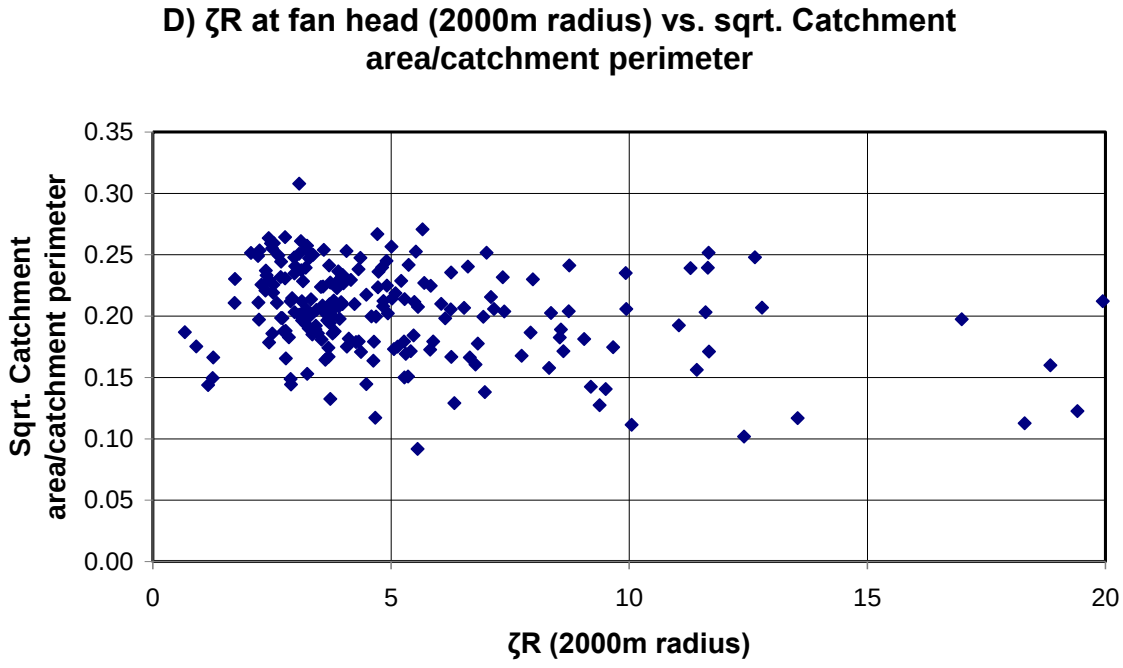

4.26 – Scale-independent fan parameters against ζR values: *A) ζR versus square root of fan area divided by fan progradation length. B) ζR versus square root of fan area divided by fan perimeter. C) ζR versus square root of catchment area divided by catchment length. D) ζR versus square root of catchment area divided by catchment perimeter. All the graphs show there is no relationship between ζR and the scale-independent measures of fan planform geometry.*

4.6.5.1 Climate as part of ζR's control on fan morphology

Rainfall is closely linked to the ζR variable. The pattern of annual rainfall is very similar to the distribution of ζR across the study area, except inverted (see figures 4.11 and 4.14). This is due to the orographic control on rainfall, where rainfall is limited within the plateau interior due to the orographic rain shadow effect of the plateau (Frankel and Dolan, 2007; Roe, 2005; Roe et al., 2008). ζR is highest in the plateau interior (as that is what the parameter is designed to measure) and lowest in the high relief, plateau margin mountains, with intermediate values in the low elevation, low relief surrounding lowlands. In comparison, rainfall is lowest in the plateau interior where there is little slope to lift and dehydrate the atmospheric column, which is carrying little moisture at elevation. Rainfall is heaviest within the plateau margins, where the increased surface gradient drives condensation of water out of the atmosphere. As a result climate's control on alluvial fans is contained within the variation of fan parameters with ζR. This means that the variation in fan parameters with annual rainfall shows the same patterns (although inverted) as the variation in fan parameters with ζR.

The variation of scale dependent fan parameters with average annual rainfall shows this pattern well, with the fan parameter values reducing with increasing rainfall values.

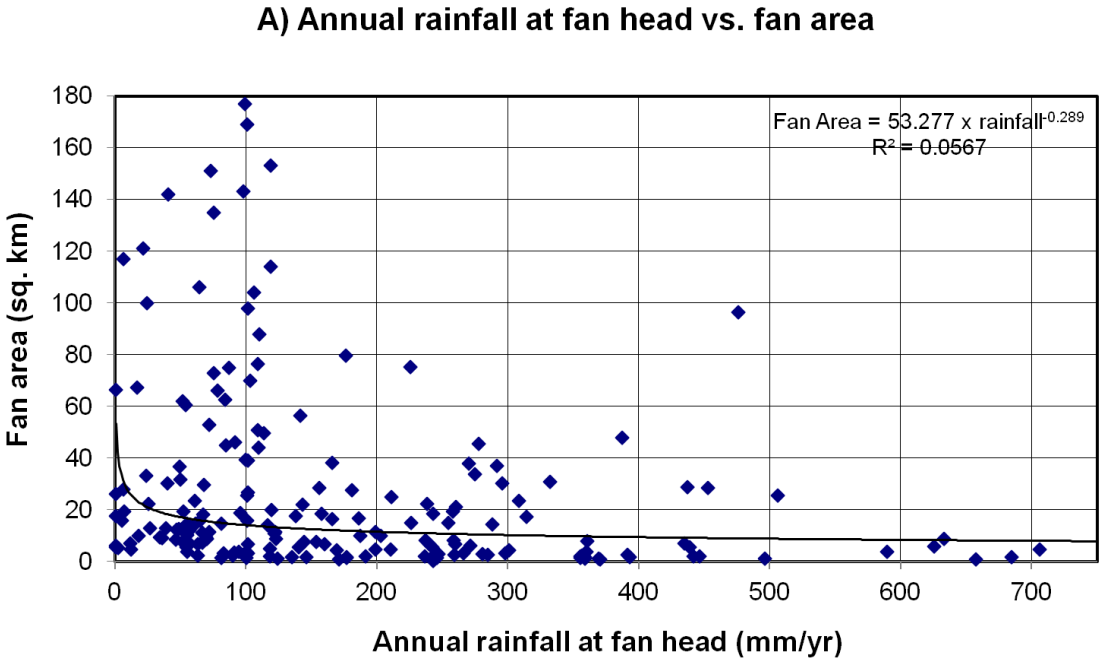

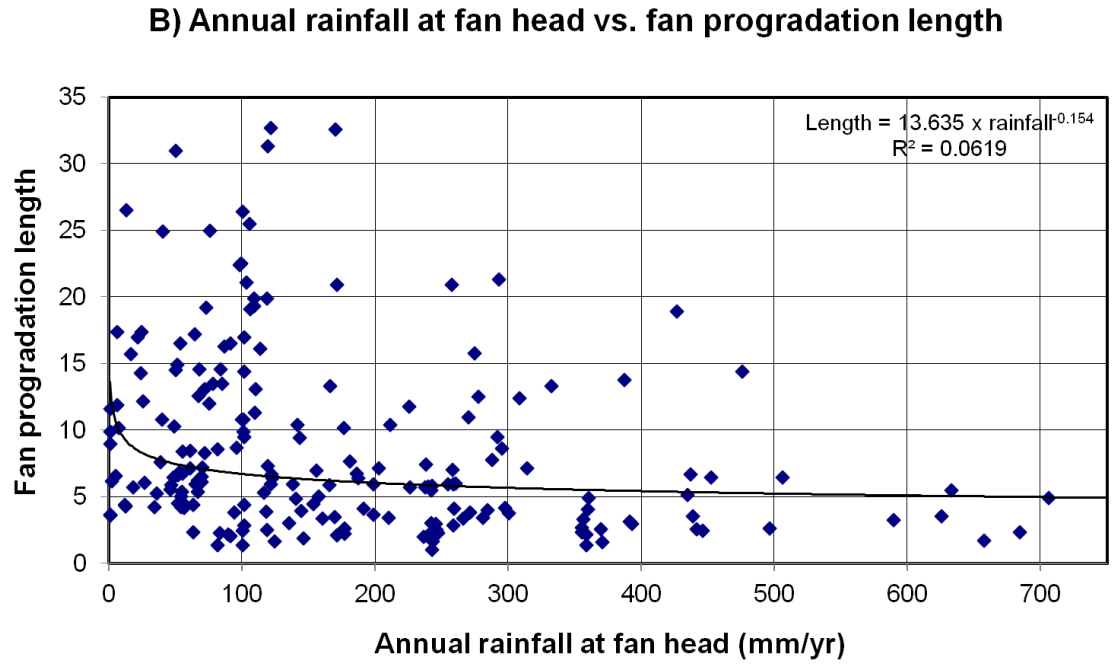

4.27 – Scale dependent fan parameters against average annual rainfall values: *A) Annual rainfall, versus fan area B) Annual rainfall versus fan progradation length. Both graphs show a negative correlation, with smaller fans present with higher rainfall levels. Trendlines are shown along with their description as equations and R-squared values. Due to the large number of data points, both trendlines are significant at the $p<0.1$ level, although the low R-squared values show that the influence of rainfall on these fan morphology properties is low, with other factors needing to be invoked to explain the distribution of data points seen.*

This pattern seems initially counter intuitive, as increased climatic input would be expected to drive increased erosion and sediment transport, allowing for the development of larger alluvial fans. However, the link between annual rainfall and ζR gives a possible explanation, as the topographic constraints on fan size within the higher rainfall, topographically rougher exterior areas have more of a control on fan size than the rainfall itself.

4.7 Discussion

The morphology of fans in the Turkish-Iranian plateau is a result of the balance between sediment accumulation and erosion throughout the late Pleistocene and Holocene (Armitage et al., 2011; Walker and Fattahi, 2011) acting as a record of the tectonic and climatic conditions they have experienced during their evolution. Fan populations distinguished by their tectonic and climatic setting are observed, those in the plateau interior and those at the thrusting plateau margin.

Previous studies of fan morphology have measured numerous morphological parameters of alluvial fans, including fan areas, progradation lengths, catchment areas, gradients at the fan apex and longitudinal profiles of fan surfaces for modern and ancient examples of alluvial fans (Al-Farraj and Harvey, 2000; Allen and Hovius, 1998; Volker et al., 2007). This research has taken similar measurable parameters and combined them with additional morphological data gained through the examination of Landsat Images and SRTM data (fan area, progradation length, fan perimeter, fan volume, catchment area, catchment perimeter, catchment length, surface gradient and Landsat band 7 reflectivity intensity).

The population of fans in the plateau interior have larger values of parameters that measure fan system size (fan area, progradation length, fan perimeter, fan volume, catchment area, catchment perimeter, catchment length), while the population of fans close to the plateau margin thrusting have the smallest values of the parameters that

measure fan system size (table 4.28). Larger fan area compared to the parent catchment area also distinguishes the fans in the plateau interior population, showing the fans in the plateau interior to not just be bigger compared to the ones at the plateau margins, but also to be proportionally larger compared to the catchments they are derived from. Another distinguishing characteristic between the population of fans in the plateau interior and those at the margins is fan surface gradient. This is higher for the fans at the margins and lower for those in the interior.

Variable	Fans nearest the seismogenic thrusting zone	Fans in the plateau interior
Median annual rainfall	**296 mm/yr**	**75 mm/yr**
Range of ζR values (25th - 75th percentile)	**2.75 - 4.59**	**6.33 – 11.42**
Range of fan area values (25th – 75th percentile)	**2.2 – 19.3 km^2**	**8.8 – 88.0 km^2**
Progradation length range (25th – 75th percentile)	**3.0 – 6.8 km**	**4.4 – 17.0 km**
Fan perimeter value range (25th – 75th Percentile)	**7.48 – 19.0 km**	**13.8 – 42.3 km**
Range of fan volume values (25th – 75th percentile)	**0.16 – 2.08 km^3**	**0.30 – 7.36 km^3**
Range of catchment area values (25th – 75th percentile)	**2.9 – 21.0 km^2**	**4.9 – 44.7 km^2**
Range of catchment length values (25th – 75th percentile)	**3.0 – 8.1 km**	**3.3 – 14 km**
Catchment perimeter value range (25th – 75th percentile)	**7.9 – 22.3 km**	**11.2 – 41.8**
Fan area/Catchment area range (25th – 75th percentile)	**0.39 – 1.26**	**0.90 – 3.41**
Fan surface gradient range (25th – 75th percentile)	**0.0129 – 0.0264**	**0.0046 – 0.0097**
√fan area/fan progradation length (25th – 75th percentile)	**0.480 – 0.640**	**0.508 – 0.678**
√fan area/fan perimeter range (25th – 75th percentile)	**0.200 – 0.231**	**0.211 – 0.249**
√catchment area/catchment length (25th – 75th percentile)	**0.518 – 0.693**	**0.454 – 0.685**
√catchment area/catchment perim. (25th–75th percentile)	**0.187 – 0.230**	**0.166 – 0.210**

4.28 – Table comparing relative fan parameters for fans near seismogenic thrusting and those in the plateau interior

Plotted relationships between fan area and catchment area and fan area and fan gradient are distinct for the three fan sub-populations. These distinctions are consistent with the variations in a single parameter, showing fans in the plateau interior to be larger in absolute terms, larger compared to their catchment areas and flatter than those in the plateau margin regions.

Ranges of the fan area/catchment area parameter are consistent with the ranges seen in the review of fans from the different tectonic settings seen in Allen and Hovius (1998). The fans studied there were from subsiding graben settings, providing the accommodation space needed for fan formation. In those settings fan area/catchment area ranged from 0.02 to 2.84, which is comparable to the values obtained for fans in and around the Turkish-Iranian plateau. While the two ranges are similar there is a large (two orders of magnitude) variation within the ranges, suggesting the parameter is not the best to constrain the setting of an individual fan. The values observed in the Turkish-Iranian case are slightly larger, two likely reasons for this are:

(1) Increased sediment mobilisation efficiency in the Turkish-Iranian case providing more material to fans for a given catchment area.

(2) Lower subsidence rates in the Turkish-Iranian setting, meaning a set amount of material spreads over a larger area.

As both this study and the work of Allen and Hovius (1998) look at fans in arid to semi-arid settings, (2) is a more likely explanation for the difference. This is consistent with Allen and Hovius' assertation that subsidence rate is the primary control on fan area.

Allen and Hovius also split their fans into two groups, comparing debris-flow to stream-flow fans. In this case they were distinguished by fan area/catchment area values being higher for the stream-flow fans, where subsidence is lower. These groups compare to the tectonically influenced versus plateau interior divisions made in this study. For the Turkish-Iranian case the higher fan area/catchment area values are for the fan population in the plateau interior. As neither the plateau interior, nor the uplifting margins are regions

of subsidence, the observed variations in the fan area/catchment area parameter are suggested to be controlled by lateral constrictions on the fan. In the lower relief plateau interior the less rough topography (compared to the margins) allows the same amount of material to spread further laterally. Accommodation space is a first order control on fan size, for a given catchment size, however this needs to be thought of as a whole, equating accommodation space with subsidence rate ignores the important lateral controls on fan deposition.

Beyond the simple ratio of fan area to catchment area, the power law relationships between fan area and catchment area for the Turkish-Iranian fans are consistent with those derived in previous studies (Bull, 1977; Dade and Verdeyen, 2007; Denny, 1965; Hooke, 1968; Lecce, 1990). Empirically derived coefficients and exponents for power laws that work for different fan populations show little consistency, so can't be used to make definitive conclusions about the fan populations described in this study. However, in common with the majority of power laws used to describe the relationship between fan areas and catchment areas for alluvial fan populations, the exponents for the relationships describing the Turkish-Iranian fan populations are less than 1, showing that the catchment area/fan area ratio, increases with size of these values. Doubling the size of a catchment, doesn't double the size of a fan, providing another argument for the fan area to be primarily controlled by the constraints in the deposition region, rather than the processes in the catchment. The similarity in the pattern of the data with previous studies on fan morphometrics, despite the unusual tectonic and climatic setting for the fan population in this study, suggests a conceptual model for fan formation based more around self-forming structures that assume the lowest energy state configuration, rather than active forcing of sediment into a fan configuration by tectonic and climatic processes.

Finding the largest fans in the relatively tectonically quiescent plateau interiors, not the uplifting plateau margins, demonstrates how conclusions from studies concentrating on range front fan deposition cannot be applied to the setting of an orogenic plateau (Allen

and Hovius, 1998; Densmore et al., 2007; Quigley et al., 2007). The results of this study run counter to that relationship, although it suggests that an orogenic plateau provides the accommodation space for larger fans due to the lack of lateral confinement, rather than due to tectonic subsidence. In the case of the orogenic plateau the more seismically active regions are also those where the topography is rougher, preventing the formation of laterally extensive fans.

The Iranian fan populations used in this study cover a large spatial area (1.3 million km^2). This is an unusually large geographic spread of data for a single study. By treating them as one dataset the effect of the different conditions across the plateau can be better seen and the effect of arbitrary divisions is minimised. Previous studies looking at a similar scale have concentrated on larger fans, rather than using the increased scope to look at how large populations of fans vary (Weissman et al., 2010; Hartley et al., 2010).

The populations of fans associated with each tectonic and climatic setting show a large amount of internal variation. This serves to highlight that using one or a small number of fans to draw conclusions about the forces driving its formation would be prone to errors. The large variation in fan morphology means that regional tectonics and climate need numerous fans to extrapolate a relationship. Investigating only a single fan or a sample of fans limited to one mountain front or fault block is only useful for getting information about local forcing factors such as individual faults (Dart et al., 1994; Talling et al, 1997;Gawthorpe and Leeder, 2000;).

While this study shows that fan characteristics can be used to distinguish between populations of fans in plateau interior and plateau margin settings, the variation in fan characteristics between the two is not so large that they are completely separate. For each parameter measured there is overlap in the range between these two populations, frequently enough overlap that the 25^{th} percentile value of the higher range is lower than the 75^{th} percentile range in the lower value. The conclusion drawn from this is that fan characteristics for a population of fans can distinguish between a seismogenic plateau

margin setting and an arid to semi-arid plateau interior setting, however a single fan cannot be definitively identified as belonging to one of these settings.

The values for the fan parameters of the intermediate sub-population are in between those for the plateau interior and plateau margin settings, although with a substantial overlap between the intermediate population and the other two sub-populations. Fan parameter values for the intermediate population not aligning with the other population values may mean that the setting for the intermediate population also has an intermediate tectonic and climatic setting. This would mean that there is not a sharp boundary between plateau interior and plateau margins and that the tectonic and climatic setting changes gradually between the two. In this case the intermediate fan parameter values suggest that the values of the fan parameters for a population of fans are sensitive to not just whether they are in a tectonically active or arid setting, but also the magnitude of those setting variables. Alternatively, the intermediate value fan parameters of the intermediate fan population may represent a combining of fan parameters from the plateau interior and sesimogenic thrusting zone fan sub-populations. This would be the case if there is a distinct change in fan parameters between these two settings and not a gradual change in setting from the plateau margin to interior. If this is the case, the intermediate fan sub-population would not actually be a sub-population of intermediate fans but a combination of plateau margin and plateau interior fans, excluded from those sub populations by the arbitrary condition that a third of the total fan population qualified for each sub-population. To get around this the fan sub-populations cut-off should be defined by only values of tectonic, topographic or climatic variables, but as no previous work study on comparing these fan variables to the tectonic, topographic and climatic settings of orogenic plateaux was done, the cut-offs chosen would have been just as arbitrary.

Parameters that measure planform geometry of alluvial fans (Square root of fan area/fan progradation length, square root of fan area/fan perimeter length, square root of catchment area/catchment length and square root of catchment area/catchment perimeter

length)show little variation with variables that measure the setting of the fans are in. While alluvial fan size seems to vary with the large scale change from plateau margin to plateau interior, the shape of the fans seems to be unaffected by this. This is not to say that alluvial fan shapes are near uniform, large changes in morphology between individual fans can be easily seen in satellite image of fans. Instead, the results show that these morphological changes are unrelated to the fans' larger scale tectonic, climatic and topographic setting and are more likely to represent individual local controls on the fans.

Larger fans within the plateau interior, compared to the fans at the plateau margin, shows that there is not a direct control on fan size by tectonics and climate. Increases in both would be expected to drive fan development, tectonics provides the gradient and accommodation space needed for fan development, while rainfall drives erosion and provides the discharge needed for material transport from catchment area to fan area (Dade and Verdeyen, 2007; Waters et al., 2010). That the results do not show these trends refutes this reasoning. Instead, topographic control could be the most important control on fan size. The increased topographic roughness within the plateau margin area constrains the extent of fans and the size of catchment that can supply a fan. In the plateau interior regions, the lower relief topography allows for alluvial fans to extend further and increases their area and progradation length characteristics. While this topography is obviously shaped by the tectonics and climate of an area, they are not working as first order controls on fan morphology. This idea of topographic control is further backed up by the variation in fan gradient between the different alluvial fan sub-populations, with lower gradients in the plateau interior sub-population. Having higher gradients near the seismic thrusting zone could be attributed to contemporary tectonic creation of higher slopes or due to a topographic constraint of the fans' areal extent by the rougher topography towards the plateau margins, recognising that rougher topography is formed by the area's tectonics. This parameter is particularly good for distinguishing between the two sub-populations as there is no overlap between the middle 50 percent of both distributions. The variation

within the fan area to catchment area ratio is also consistent with the hypothesis that larger fans are present in the plateau interior than the plateau margin due to a lack of topographic constraints. This ratio being larger suggests that the increase in fan size seen in the plateau interior is not solely down to an increase in sediment supply due to a larger catchment, instead there must be some effect within the depositional basin controlling the fans' areal extent.

This study found that the Landsat 7 ETM+ band 7 intensity proxy for fan lithology did nothing to distinguish between the different populations of fans. While lithology may have a control on the characteristics of individual fans, it does not affect patterns of fan morphology across the Turkish-Iranian orogenic plateau. This is consistent with a number of previous studies that have found source lithology to have little effect of fan morphology and the relationship between fan area and catchment area (Allen and Hovius, 1998; Ferrill et al., 1996; Whipple and Trayler, 1996).

One controlling parameter that cannot be measured using the remotely sensed data of this study is grain size. The grain size of the deposits an alluvial fan is made from is likely to have a direct effect on it size and morphology. It achieves this by effecting how much energy is needed to transport the fan material and also by the cohesiveness of the fan deposits (Harvey et al., 1995). Grain size is an important example of the controlling parameters that this study could not investigate, but are likely to be responsible for the relatively large amount of scatter seen in the observed trends between controlling variables and fan parameters. As there are controlling factors that cannot be parameterised by remotely sensed data, this highlights why it is important to look at a large number of fans to look for trends that are being controlled by the variables investigated. This work cannot provide a full description of an individual fan, but by looking at how a population as a whole varies with a particular parameter, general trends in the alluvial fans studied can be discerned.

Being able to distinguish between the tectonic, climatic and topographic settings of a plateau margin and the plateau interior based on the morphologies of alluvial fan populations in those settings has multiple implications. Firstly, in situations where these setting variables are unknown, alluvial fan morphology may allow them to be derived. This would be especially applicable to preserved ancient fans, where their shape may be derived, but the settings the fan was laid down in have changed. While this study has only been able to pick out relative and large scale variations between populations, smaller scale studies on individual fans, where the tectonics and climate are better defined for that locality, may allow a more defined linkage between an alluvial fan's morphology and the conditions of its deposition. Secondly, the intermediate characteristics of the fans in the sub-population that was neither topographically representative of a plateau nor near the seismogenic thrusting zone suggest that the cut-off between thrusting plateau margins and the non-thrusting, relatively tectonically quiescent plateau interior may not be as sharp as the pattern of seismic thrusts suggests (see chapter 1). These in-between values suggest that the there may be some sub-seismic tectonics present in this region and that as thrusting moves outwards (England and Molnar, 1997) there is a noticeable lag in the time for the topography to adjust from a orogenic mountain belt form to that of a plateau interior. The intermediate fans are a record of the landscape adjusting from an actively deforming type to that of the plateau interior. This study helps to characterise the difference between these intermediate fans and the fans that properly represent the plateau interior. If the intermediate type fans could be dated, it might be possible to get an estimate for the lag time between seismogenic thrusting moving outwards from an area and the topography of that area coming to represent that of an orogenic plateau.

4.8 Concluding comments

- The population of alluvial fans in the plateau interior is made of spatially larger fans than that at the plateau margins.

- Larger fans are not associated with more intense tectonics and rainfall. Instead they are located where the topographic constraints are smaller.
- With the exception of scale, the morphology of fan populations is independent of tectonic and climatic setting.

5. Overview and synthesis

The chapters presented in this thesis, although forming stand-alone contributions to our research understanding of orogenic plateaux and the rivers draining them, provide novel methods for analysing river dynamics and geomorphology of an orogenic plateau. They also highlight ways that the climatic and tectonic settings within and around an orogenic plateau interact with the geomorphology in those regions. While geomorphology is a representation of the tectonic and climatic history of an area, it can also affect future geomorphic changes, either directly, as shown by the topographic constrains on alluvial fan size in the Turkish-Iranian plateau, or through feedbacks that effect the tectonics and climate, as seen by the topographically maintained rain shadow that contributes to plateau aridity and therefore the formation of low incision, low gradient headwaters for plateau-draining rivers.

5.1 Novel methods of analysing geomorphology

Three novel approaches to analysing geomorphology were used in this thesis. They are:

1) Using the density of high or low $\delta \ln S / \delta \ln D$ values along a river to highlight reaches that are divergent from an equilibrium longitudinal form.

2) Smoothing longitudinal river profiles that are obtained using DEMs derived from SRTM data, concentrating on removing positive spikes imposed upon the real path of the longitudinal profiles.

3) Quantitative analysis of the geomorphology of alluvial fans and catchments feeding the fans with water and sediment. This is novel as it takes full advantage of remotely sensed data to quantify the shapes of current alluvial fans as fully as

possible. This goes beyond previous work on alluvial fan morphometrics (Allen and Hovius, 1998; Harvey et al., 2005), which have focused on fan size and progradation length.

Looking at the concentration of high or low δlnS/δlnD values along river profiles provides a way to obtain systematic information about disequilibrium along a river. It is shown to extract information in situations where merely plotting up lnS versus lnD for a river profile does not show a clear pattern (see figures 2.10 and 2.13). It works as a development of the more common approach to plot river profiles in a ln/ln space (Goldrick and Bishop, 2007; Knighton, 1998), expanding it to rivers where there is no obvious trend of slope against distance. Using the high and low δlnS/δlnD value density method also allows for the consideration of apparently chaotic river profiles as a whole. This avoids the subjective approach of dividing a ln slope versus ln downstream distance graph into distinct sections, with each section representing either a particular equilibrium to the conditions in that reach or a reach determined as being out of equilibrium (Bishop and Goldrick, 2000; Goldrick and Bishop, 2007; Talling and Sowter, 1998).

Longitudinal profiles extracted by tracing rivers across SRTM data, show unusual challenges for smoothing. They do not have randomly distributed noise around the actual profiles of the rivers, instead they are positive spikes superimposed upon the river profile. To remove those spikes, typical smoothing methods based on using a running average are inappropriate. These methods lift the elevation artificially and produce sections where the river appears to be running uphill. This latter problem is a real problem for any type of ln/ln analysis of the river form as it involves the impossible task of getting ln values for a negative value to represent ln slope. Producing a smoothing method that avoids both of these problems gives a method that allows manually (and more accurately) obtained river profiles to have the same ability to be manipulated as longitudinal profiles obtained from running the D8 algorithm over a DEM of an area.

Quantifying the shape of alluvial fans is done by delimiting the plan view extent of alluvial fans using STRM data and Landsat 7ETM+ images. Using such digital datasets allows for fan populations as a whole to be parameterised much more quickly than relying on field measurements. Having parameters for a large population of fans allows for more valid general statements to be made about their morphology than can be made from a smaller number of fans. Landsat images prove to be the most effective for locating alluvial fans, while highlighting topographic inflection points using the SRTM data allow for the fan perimeters to be accurately located. Accurately locating fan perimeters allows for their shapes to be parameterised and their plan-view shapes to compared separately to their sizes. In addition to extracting the plan view shape of alluvial fans, the use of the SRTM data allows for some categorisation of the 3-D shape of the fans. The fans' top surfaces can be measured allowing for the average gradients from the fan heads to the fan toes to be measured. With some assumptions about the nature of the fans' lower surfaces the volume of the fans can be estimated. Parameterising an alluvial fan's size in terms of volume rather than area or progradation length can be a more useful measurement of the fan's size. This is particularly the case when doing work based around the redistribution of sediment in a fluvial system, where volume provides a better estimate for how much material has been moved from one place to another.

5.2 Plateau fluvial geomorphology in response to plateau tectonic and climatic settings

The forms of plateau-draining rivers and alluvial fans within orogenic plateaux have been examined and categorised. Both of these systems are important parts of the geomorphology of orogenic plateaux, both in making up the landscape and in controlling the development of the plateaux as they grow.

Plateau draining rivers are the main route of transporting material from the plateaux interiors, through the plateau margins to the surrounding lowlands. By providing

a connection between these settings they are a direct control on the growth of orogenic plateaux. The rate of material removed from the plateau, relative to the rate of material tectonically advected into the region, directly determines whether (and how fast) the plateau expands or is retarded.

In contrast, alluvial fans are a large part of the material redistribution system acting within the plateaux interiors. As gravity driven systems, alluvial fans move material from the higher to lower elevation parts of the plateau interior. As they are not part of the plateau-draining river systems, they are the end points for material retained within the plateau interior. By redistributing material within the plateau they help turn the rough topography of an active orogen into the low relief terrain of an orogenic plateau. The importance of fans in forming plateau topography can be seen in their widespread distribution across the Turkish-Iranian plateau where they were studied (see figure 4.10 – which is not a complete catalogue of every fan seen at the plateau surface). Larger, flatter fans seen in the plateau interior are evidence of the sediment mobilisation taking place in the plateau interior, helping to build the observed plateau topography.

Plateau-draining rivers and alluvial fans are both important systems in the making of an orogenic plateau. The plateau draining rivers mediate the amount of material being moved into the orogen, directly controlling the rate of orogen building. The alluvial fans develop a low relief landscape helping turn a growing orogen in a topographic plateau.

Non-dissected plateau growth is only possible due to the form of plateau-draining rivers. These rivers have a sigmoidal form with low curvature at the river headwaters and high gradients and high curvatures seen below the elevations that mark the cut-off of seismogenic thrusting around the orogen. Profile form within the plateau interior is that associated with relatively low incision. Low incision in the plateau interior is a necessary condition for plateau formation to allow for the accumulation of material within the plateau interior. At its most extreme, rivers can be dissected in the vicinity of the plateau margin, removing rivers' connection to the material in the plateau interior (Sobel et al.,

2003). The connection between river form and low incision is further highlighted by rivers' sigmoidal form being similar to the shape of a topographical swath taken parallel to a plateau margin. The lack of incision stops rivers from making their own path, so they follow the topography of the plateau with little modification. Following plateau topography in river headwaters reduces relief generation between the river and adjacent interfluves, consistent with plateau topography. The pattern in form of rivers draining the two studied orogenic plateaux is identified by patterns in the value of $\delta \ln S / \delta \ln D$ along river lengths. This identifies reaches that appear to be out of topographic equilibrium along river lengths. This suggests that while the pattern of rivers draining from plateau interiors to the surrounding lowlands is consistent, this is not evidence that the rivers are in a stable configuration. Instead, as the orogens grow the rivers are changing in step. While the plan view of plateau-draining rivers may stay roughly the same (although evidence points to that not being the case (Walker et al., 2011) the long profiles change so that high curvature, high gradient reaches are located within the tectonically active thrust zones that surround plateau interiors. As the plateau grows outwards these reaches must also be moving outwards, otherwise they'd be located within the plateau interior instead. Plateau rivers cannot be thought of as contributing to the formation of orogenic plateaux (particularly as they are a primarily destructive surface process within plateaux interiors and the fringing mountain ranges), instead they 'allow' plateaux to be built by showing low gradients within plateau interiors. Even when the drainage area for these reaches is quite large, as can particularly be seen in some of the rivers draining the south of the Tibetan plateau, the relatively low gradients limit the amount of incision within the plateau interior and the amount of material that is removed from the plateau.

Modelling of the development of these plateau-draining rivers shows that rivers with sigmoidal longitudinal profiles would be expected in typical orogenic plateau growth situations throughout geological time. While the uplift pattern specified by a laterally expanding orogenic plateau is a necessary requirement in the formation of the sigmoidal

profile plateau-draining rivers, the system is most sensitive to changes in precipitation on stream ability to incise. This supports the idea that the plateau draining rivers follow the topography resulting from plateau formation as long as the climate conditions allow it and the sensitivity to the precipitation is not so high that incision overwhelms the uplift of the growing plateau. Although it is possible to identify that the shape of plateau-draining rivers is primarily controlled by climatic sensitivity that is not as simple as saying that climate is the primary control on plateau drainage. The climate and tectonics of a plateau region are linked. The precipitation pattern imposed on a plateau-draining river is only a result of the orogenic rain shadow that is itself a response to the tectonically constructed topography of a plateau.

The features of alluvial fans within orogenic plateaux and their margins show enough sensitivity to the setting that distinct populations can be recognised. However these controls are not strong enough that an individual fan could be used as guide to the regional climate and tectonics as there is too much variability within these populations. The fans from the plateau interior are larger (both area and volume) than those in the plateau margins and have a lower surface gradient, although the plan view shape of the fan populations is unaffected by setting. Having larger fans in the plateau interiors suggests that fan size is not correlated to sediment supply as might be expected. The factors which would be expected to increase sediment supply (tectonic activity, precipitation, and topographic steepness) are all higher in the plateau margins, where the fans are smaller. Instead fan size is more likely to be topographically controlled with the extra lateral accommodation space available in the plateau interior allowing for the growth of larger fans. This is consistent with previous studies that have found accommodation space being the greatest control on fan size (Allen and Hovius, 1998).

5.3 Outstanding challenges

Following on from the work done in this thesis there are a number of further avenues for research that build on the research outcomes outlined in the previous chapters:

- The second aim of the thesis could be better addressed. This thesis has described the tectonic and fluvial geomorphology arising from the tectonic and climatic setting in of a growing orogenic plateau. The next step is to take these descriptive relationships and see if they can be used to describe the setting in other study areas. In particular, expanding the catalogue of alluvial fans to other areas could be used to investigate areas that are not orogenic plateaux, to see if alluvial fans are also suitable tectonic and climatic indicators in other regions. Possible study areas with a suitably high density of alluvial fans would be Death Valley and the East African rift.

- Similarly to expanding the collation of fan parameter data to other areas, the $\delta lnD/\delta lnS$ method of identifying reaches of rivers in disequilibrium could be extended to other river systems. This would be particularly interesting in rivers that are not similar to those draining orogenic plateaux, to see if the $\delta lnD/\delta lnS$ method extracts useful patterns in the drainage outside of orogenic plateau settings. Rivers draining the Central Range of Taiwan would be a suitable set for an initial expansion of the study. The tectonic and climatic setting is relatively well known along the Central Range and the ability to use along strike distance as a proxy for age, would allow for an investigation into how the $\delta lnD/\delta lnS$ values change along river lengths as they evolve. This would contrast with the work done on orgoenic plateaux which has effectively taken a snapshot of an evolving system and suggested that the morphology of a plateau requires river disequilibria reaches to

move outwards in step with a laterally growing plateau, but is unable to show this happening.

- The remotely sensed data used for the analyses in this thesis should be backed up with ground truthing. Obtaining temporal data of alluvial fans would allow for an investigation as to whether the larger fans seen in the plateau interior are more mature, partially explaining their greater size. In the case of plateau-draining rivers obtaining discharge values along the river lengths would help to confirm the primary sensitivity to discharge's effect on river incision that modelling of the rivers presents. Identification of reaches in disequilibria can be enhanced by field work to look at any river terraces that may be preserved, thereby allowing for an analysis of river evolution through time. This can then be compared to the disequilibria patterns obtained from the $\delta \ln D / \delta \ln S$ method for both the Tibetan and Turkish Iranian plateaux.

- The hypothesis that fan size is controlled by lateral availability of accommodation space should be fully tested. This would require choosing a test area with a reasonable sized population of alluvial fans, where climatic and tectonic variables show little difference across the region, but topographic roughness is variable.

6. Research findings

The main research findings are (These are grouped according to which of the research questions from chapter one they address):

- Rivers that connect the interior of the Turkish-Iranian and Tibetan orogenic plateaux and the surrounding lowlands, passing through the plateau margins show sigmoidal longitudinal profiles, instead of the concave-up profiles associated with a river in topographic equilibrium (question1).

- The locations of disequilibria of orogenic plateau-draining rivers from the Turkish-Iranian and Tibetan plateaux correlate with the cut-off between the actively thrusting and thickening plateau margins and the plateau interior (question 1).

- Sigmoidal longitudinal river profiles are a topographic response of rivers to orogenic plateau growth and not specific tectonic and climatic variables (question 2).

- The form of plateau draining-rivers is most sensitive to changes in the effect of precipitation and drainage area in the river's incision (question 2).

- The populations of alluvial fans in plateau interiors and the populations of alluvial fans in plateau margins have distinct morphological properties (question 3).

- Alluvial fans in the interior of orogenic plateaux are larger and less steep than those in the rugged plateau margins, suggesting that tectonic or climatically driven

sediment supply is not the primary control on alluvial fan size in orogenic plateaux (question 3).

- Alluvial fan populations across the variety of settings found in orogenic plateaux show the same plan-view shapes (question 3).

Appendix A: GIS techniques to produce fluvial networks from underlying DEMs

The flow of surface water that forms fluvial networks is determined entirely by the interaction of topography, gravity and infiltration of water into the groundwater system. This allows knowledge of the topography of a region to determine the patterns of surface water flow across a landscape, based on the simple principle that water will flow along the steepest local gradient.

To determine the location of fluvial networks using this principle the D8 algorithm is used with a DEM produced from SRTM data (Tarboton et al., 1991). The D8 algorithm has the following steps:

1) The elevation of the each cell is compared to the 8 cells surrounding it (less in the case that the cell is at the border of the DEM). The cell with the lowest elevation is flagged up.

    1a) If the central cell has the lowest elevation it is designated as a sink, representing a termination point for the fluvial network.

2) The direction of the cell with the lowest elevation relative to the central cell is assigned to the central cell. This is the flow direction of water from the cell. If the algorithm is being carried out by a computer this is done by assigning a number coded to one of the 8 possible flow directions to the cell.

3) Each cell is then given a number representing the cumulative total of cells whose flow directions point to it. This is the flow accumulation value and its derivation is shown in diagram B.1.

A)

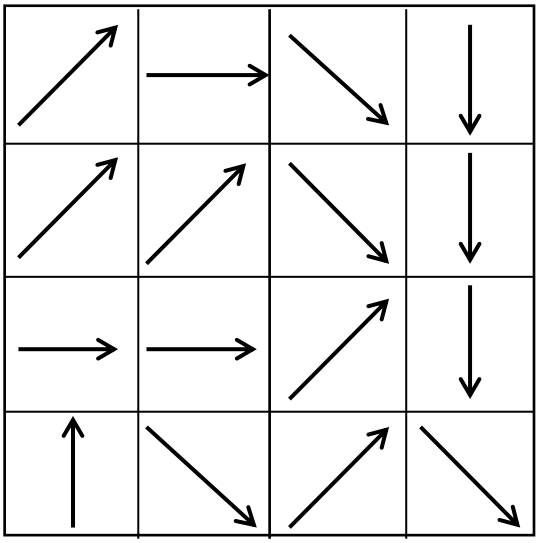

B)

0	1	3	0
0	0	0	9
1	2	3	12
0	0	0	13

A.1 - Diagram showing the determination of flow accumulation values in a grid where flow directions are known: *A) Shows the flow directions associated with each cell in this grid. B) is based on the flow directions of A). In this grid the numbers in each cell are the cumulative number of cells whose flow direction points at the cell. In essence the number is the amount of cells that drain in to that cell.*

4) An arbitrary flow accumulation value is used as a cut-off. Every cell with a value higher than that is designated as part of the fluvial network.

Using this method to designate the location of a fluvial network depends on a number of assumptions:

1) That precipitation across the area is uniform. This can be countered by weighting the value each cell contributed to the flow accumulation values by the relative precipitation it receives.

2) All the water in one cell will flow to an adjacent cell. Using just remotely sensed data it is impossible to quantify the amount of groundwater sapping or pooling within a cell. It is possible for water to be stored within a cell (the likelihood of this increasing with cell size), but to allow the fluvial network to be derived from remotely sensed data, this and groundwater infiltration are ignored.

3) Water can only flow from a cell in one of eight directions. This limitation is imposed by having a square grid, where each cell is surrounded by eight others. This limitation means that the resulting fluvial networks are going to be imprecise on the scale of single to tens of cells. Over larger scales, an amalgamation of cells where water can only flow in one of eight directions approximates a situation where the water drains in any direction.

4) Water can only flow from a cell to one of the surrounding cells. This can be averted by dividing up the flow accumulation value of a cell among all the cells surrounding it that have a lower elevation. However, doing this can result in fluvial networks that bifurcate more than in reality. Furthermore, deciding how to

portion up the flow accumulation values among the surrounding cells is a non-trivial problem, as any bifurcation of a river is likely to depend on more than just elevation values.

The accuracy and precision of the fluvial networks generated by the D8 algorithm depend on the size of the cells of the base DEM and the accuracy of its elevation values. Larger cells exacerbate the problem of water only flowing in one of eight directions, meaning the resulting networks are only realistic on larger scales, as the water has to flow further before the aggregate flow directions approximate a river flowing in any direction, instead of just one of eight directions from cell to cell. Precision and accuracy of elevation values is particularly important in topography where adjacent cells have elevation values close to each other. In this case a small difference in elevation can change the cell that water is modelled as draining into, thereby routing the flow accumulation away from the location of the real fluvial networks.

The arbitrary number chosen as a cut-off to distinguish between the fluvial network and the surrounding terrain represents a particular drainage area/water discharge needed to form a river. As there are no measurements of the flow accumulation needed to form a river (and the value would vary depending on the underlying material, steepness of the region and the climate) an empirically determined value is used. Values are chosen to produce fluvial networks that resemble the patterns of rivers that can be seen on maps of the investigated region. The comparison between a fluvial network generated by the D8 algorithm and the locations of rivers seen on a map should be cursory, focusing on only the main features. A more in depth comparison, involving detailed mapping of river locations in the investigated area would render running the D8 algorithm across an area unnecessary, as the location of rivers would be manually (and more time-consumingly) determined as part of the process. If the cut-off value is too high the resulting fluvial

network will not include reaches present in real rivers, while a value that is too low will add extra branches to the river network that are not observable in reality.

Appendix B: Method for smoothing noisy longitudinal river profiles

River profiles extracted by using SRTM data are inherently noisy. This noise comes from two main sources. Firstly, it is due to noise in the elevation values used to produce the river profiles. Secondly, there are digitisation errors in picking out the route of river across the landscape that can result in extracting elevation values from the adjacent river banks, rather than from the river surface itself.

In the first case random errors are of the order of ±1 metre in magnitude (Jarvis et al., 2004; Rodriguez et al., 2005). These are compounded by systematic errors due to regions where the radar returns are from material above the earth surface (tree canopies, buildings, etc.). Other systematic errors are where rivers' width is less than the cell size (90 m in the case of SRTM data). In this case, while the elevation value is an average of the elevation of the topography within the cell, it is an overestimate of the river's elevation, which will be lower than the average cell elevation, due to rivers being located in gorges and water following the lowest topography as it flows. Both these systematic errors cause an over estimate of the elevation of rivers longitudinal profiles.

The digitisation errors in extracting river longitudinal profiles also cause over estimates in the elevation of river profiles. When such errors are made they sample cells slightly off the real course of the river. This can be due to operator error or slight mismatches between the satellite imagery used to trace a river's location and the SRTM data used to extract elevation values to make up the long profile. These mismatches are to be expected in fluvial systems that avulse and move laterally on timescales comparable to the gaps between when imagery is obtained. By sampling cells that are off the course of the river, cells that correspond to the banks of the river are sampled, these have a higher elevation than the river course itself.

As the majority of sources of error increase the elevation of the river profiles extracted from SRTM data a particular pattern of noise in the profiles is formed. Instead of a completely random pattern of noise which would vary positively and negatively around the real trace of the river, the noise manifests as spikes which rise above the actual long profile of the river (see figure C.1).

A)

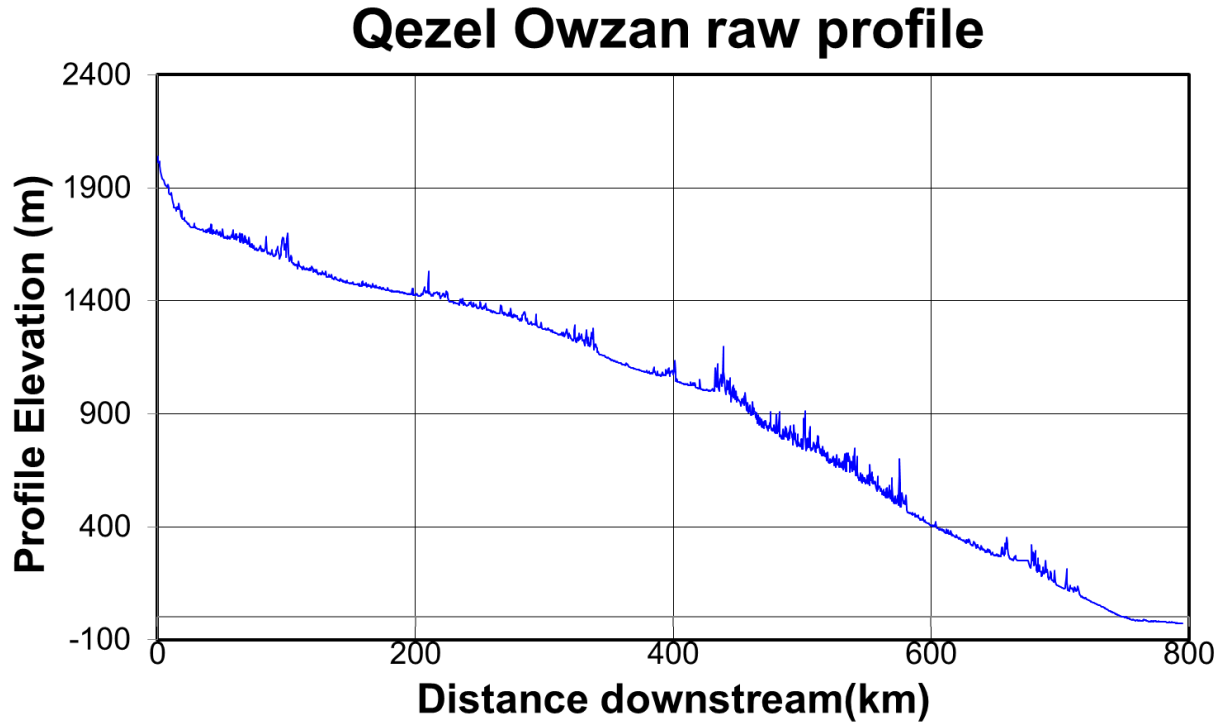

B)

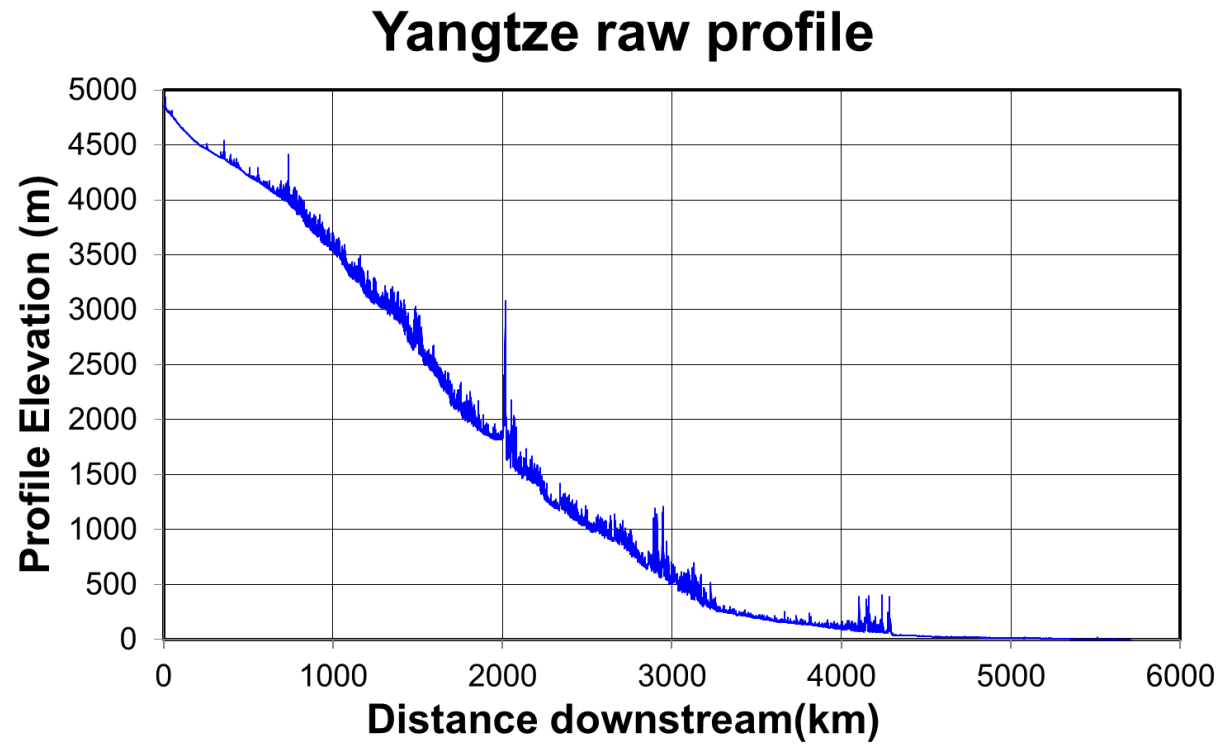

B.1 - Examples of unsmoothed river profiles: *A) Qezel Owzan draining the Turkish-Iraninan plateau. B) Yangtze draining the Tibetan plateau. These profiles are representative of all unsmoothed longitudinal profiles obtained using SRTM data. Positive spikes are superimposed upon the actual shape of the long profiles.*

The unusual pattern of noise makes standard smoothing approaches unsuitable for removing the noise. The standard approach of taking a moving average of the values along the river length, or using a smoothing approach similar to that, such as exponential smoothing, is inappropriate for two reasons.

Firstly, when using a moving average approach to smoothing, the resulting profile is an average of the spikes and the underlying 'real' profile. This gives a smoothed profile that has a higher elevation than the underlying profile, being 'pulled up' by the positive spikes imposed upon the profile. Secondly, the high contrast between values at the peak of the spikes and those that represent the baseline longitudinal profile means the smoothed profiles can end up with reaches where water drains uphill, representing a positive gradient, in contrast to the negative gradient that defines most of a longitudinal profile. This reverse gradient is not only physically impossible in reality, but makes any analysis of the river gradient in a ln/ln context fail as there is no value for the ln of a negative number.

Due to the inappropriateness of traditional smoothing methods, a different approach is taken to remove the positive spikes imposed upon the base profiles. The steps taken to remove spikes are detailed below:

1) Points where the elevation value is equal to, or higher than both the points either side of them are identified. This property is the definition of the tip of a spike. This can be done in Excel by using the IF function to compare a point's elevation values to the points above and below it in a column of elevation values.

2) These identified points are deleted as they represent spurious data, not the actual longitudinal profile of a river.

3) Return to step (1) to identify the new tips of the spikes, after the previous tips have been deleted. After deleting the tips of spikes, some spikes may have ‘flat’ instead of ‘spiky’ tips. This makes it important to identify points whose elevation values are equal to the points either side, as well as those whose elevation is higher than those either side.

4) Repeat steps (1) and (2) until no further points are identified in step (1).

This smoothing method removes all the spurious data leaving only elevation values that correspond to the longitudinal profiles of the rivers being studied. By using an approach that removes data, rather than one that modifies the values of the data, it affects the sample spacing of the profile elevation values. The sample spacing is increased as points are removed and what may have previously been regular sample spacing becomes inconsistently distributed. Where there are more spikes, and therefore more data points that are removed through the smoothing, the spacing between the resulting data points increases, relative to regions with few spikes superimposed upon the profile.

Appendix C: Statistical comparisons between 3-D surfaces

To evaluate the similarity between two 3-D surfaces so that it can be compared to other pairings of surfaces, the root mean square normalised deviation between surfaces is used. This produces a single value to show the difference between the shapes of two 3-D surfaces, where a value of 0 shows the two surfaces have exactly the same shape, and a value of 1 shows the surfaces to be as divergent as possible. This method works at comparing two rasters in a GIS environment with a one to one correlation between cells in the rasters. If the cells are different sizes one raster should be resampled to have a pixel size the same as the other. If the extent of the two rasters is different, one should be clipped to the extent of the other. As such, this method allows for the comparison of two properties across the same region. The steps to obtain the root mean square normalised deviation value are outlined below and an example from the Tibetan plateau is shown underneath that:

1) Both surfaces are normalised by dividing every value by the largest value in the raster. Normalising the rasters allows for a comparison of 2 3-D surfaces even if the Z-direction of the surfaces represents different quantities. It also allows for a comparison of the shapes, rather than just whether the average magnitudes of the surfaces' Z- values are similar.

    1a) If the values of the rasters appear to be far from normally distributed it may be more appropriate to normalise the values to the median instead. In this case, 1 would not be the maximum value for the root mean square normalised deviation, but would represent two surfaces with widely divergent median Z-values.

2) Take one raster away from the other. This is done on a cell by cell basis to produce a new deviation raster where each cell contains a value with the difference between the corresponding cells in the original pair of rasters.

3) Square the values in each cell of the deviation raster. This removes any negative values, so that positive and negative deviations don't cancel out.

4) Calculate the mean of all the squared values from the cells in the raster.

5) Take the square root of the mean value to compensate for squaring the values earlier. This final value is the root mean square normalised deviation between the original two surfaces.

A)

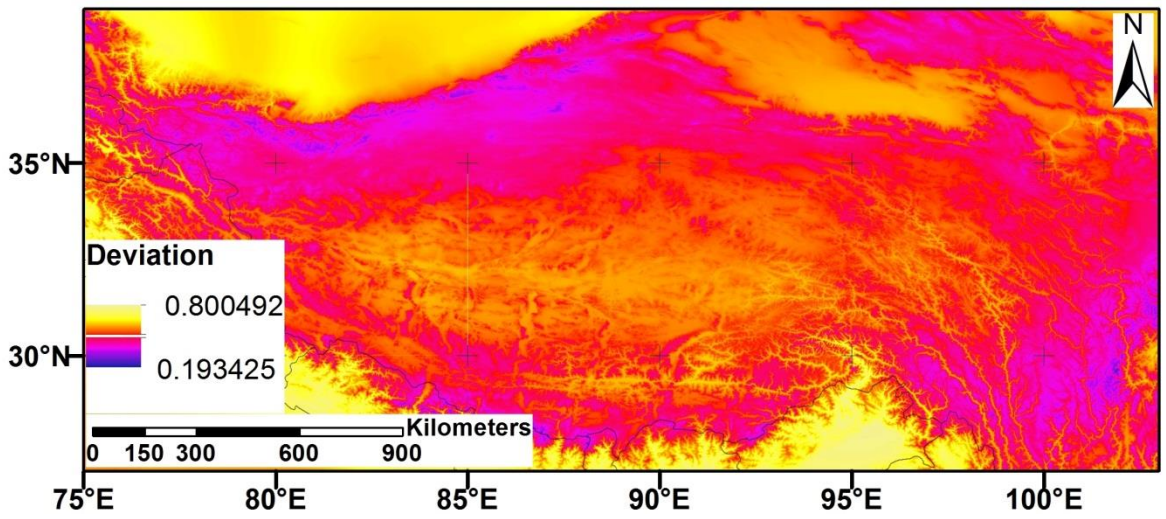

See over for caption

B)

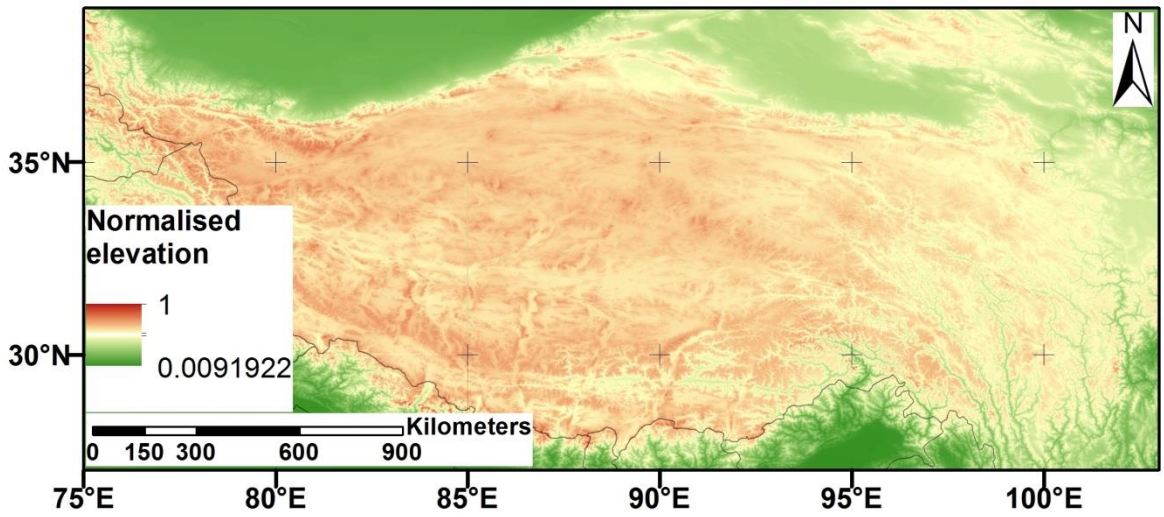

C)

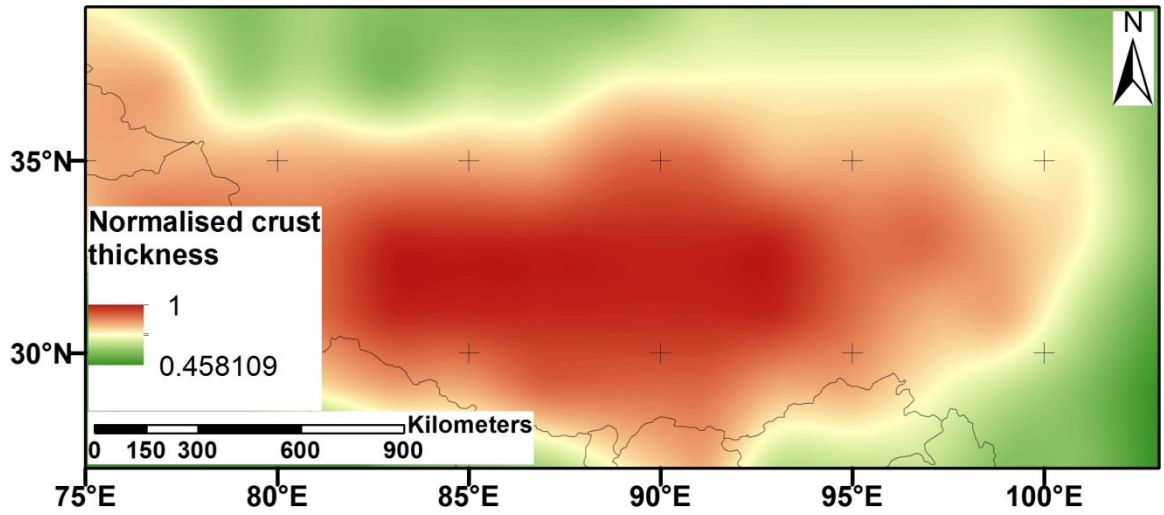

C.1 - Comparison of elevation and crustal thickness rasters for Tibet. *A) The deviation between normalised elevation values (B) and normalised crust thickness (C). The elevation values have been smoothed with a 1 km diameter circular moving average. Crustal thicknesses are taken from the Crust 2.0 project (Bassin et al., 2000; Mooney et al., 1998). Deviation is high along river gorges as these relatively small scale changes in elevation are not isostatically compensated by crustal thickening. As such the correspondence between crustal thickness and elevation smoothed by a larger sized window would be higher. Deviation is also high in the lowlands surrounding the plateau as elevation can have a value of zero, but crustal thickness cannot. A better deviation map could be made by taking the minimum crustal thickness value away from every pixel of the elevation raster before normalising the raster. The RMS normalised deviation between elevation smoothed by a 1km window and crustal thickness for Tibet is 0.15, showing high correlation between these two rasters.*

Appendix D: Catalogued river profiles

This is a collection of river profiles extracted as part of the research done for chapter 2. These profiles represent a more complete catalogue of rivers draining the Turkish-Iranian plateaux. Many of these rivers were not included as part of the analysis as they do not straddle the border between plateau interior and plateau margin, but were extracted as part of the initial data gathering, where all the larger rivers draining the region were catalogued and their profiles extracted. These rivers are those shown in figure 2.2b. A labelled map showing their locations is below:

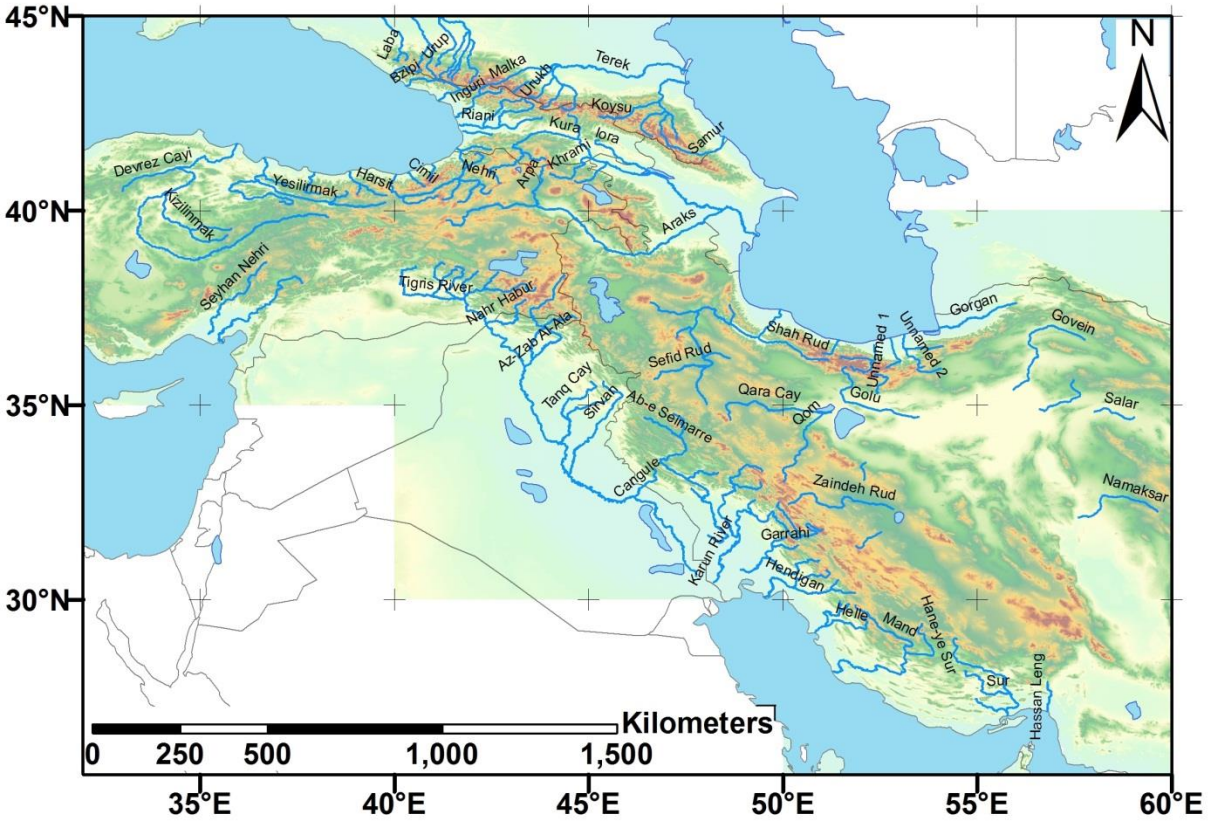

Ab-e Bid longitudinal profile

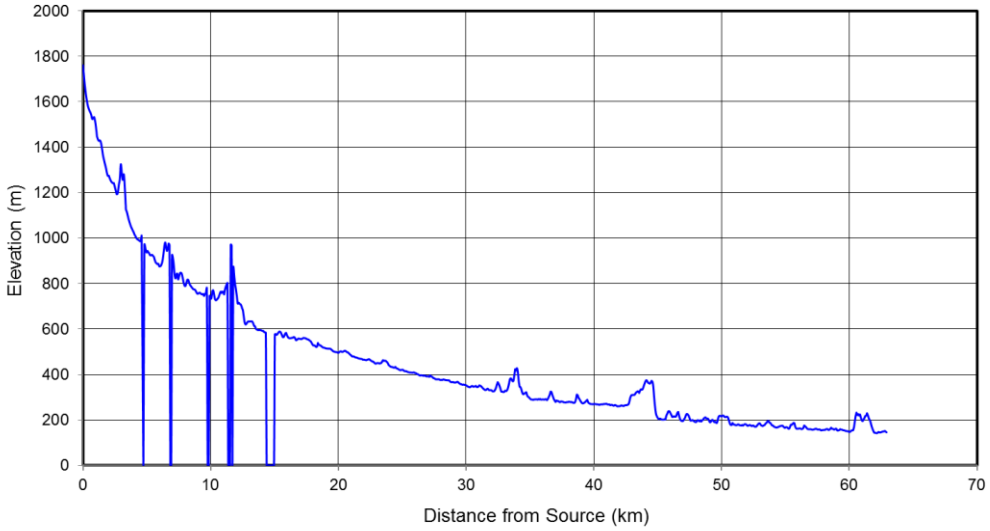

Ab-e Horramabad longitudinal profile

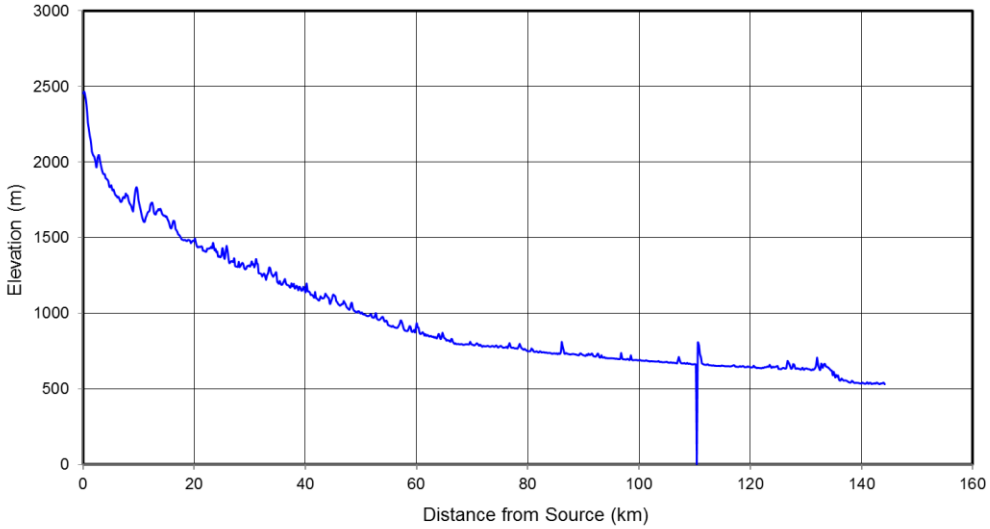

Ab-e Rahmat longitudinal profile

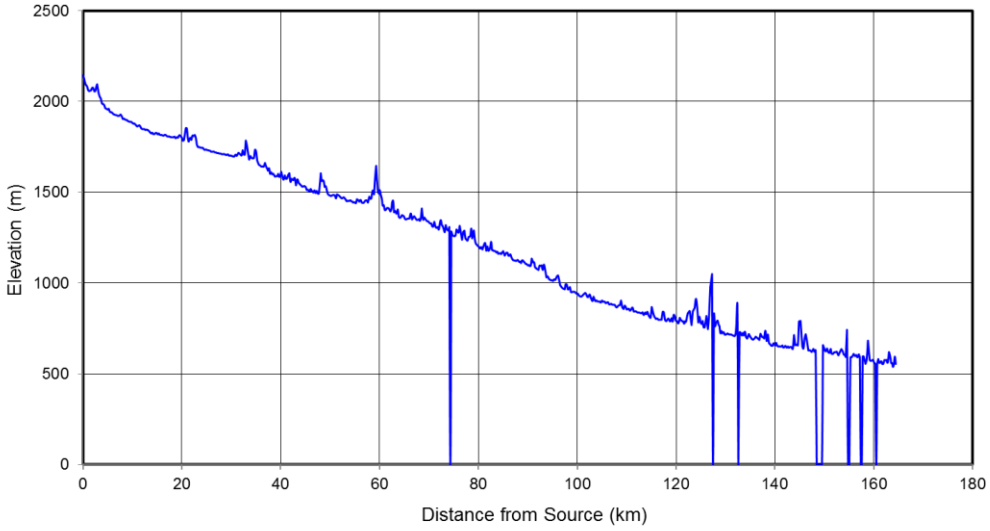

Ab-e Seimarre longitudinal profile

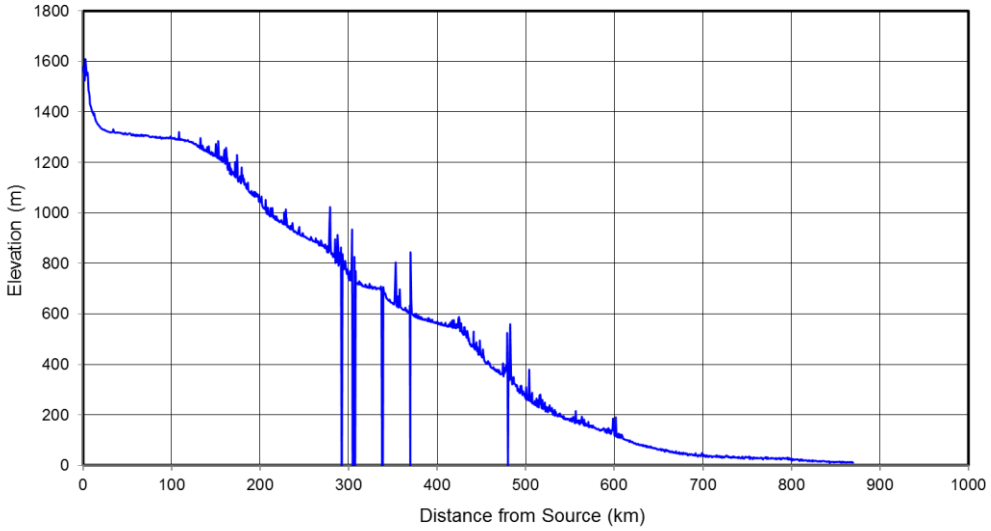

Ab-e Seimarre tributary A longitudinal profile

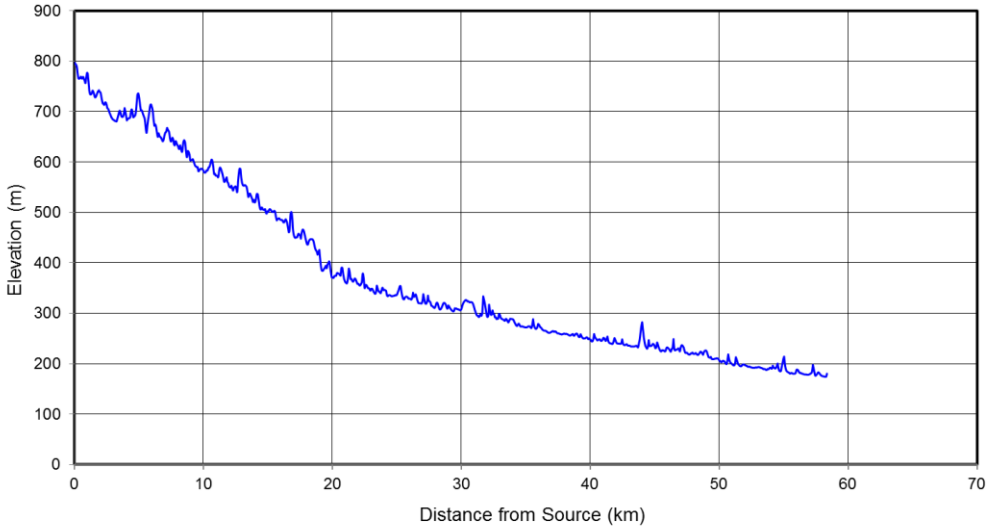

Araks longitudinal profile

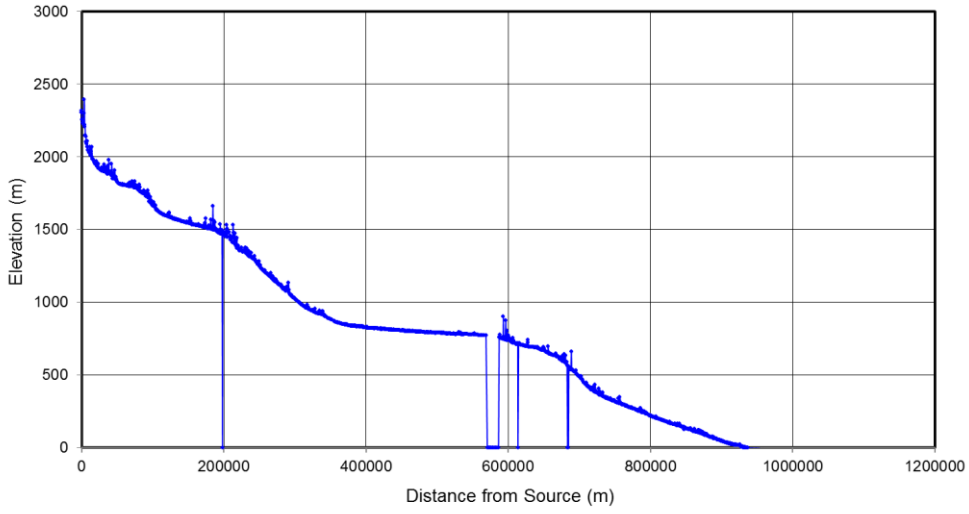

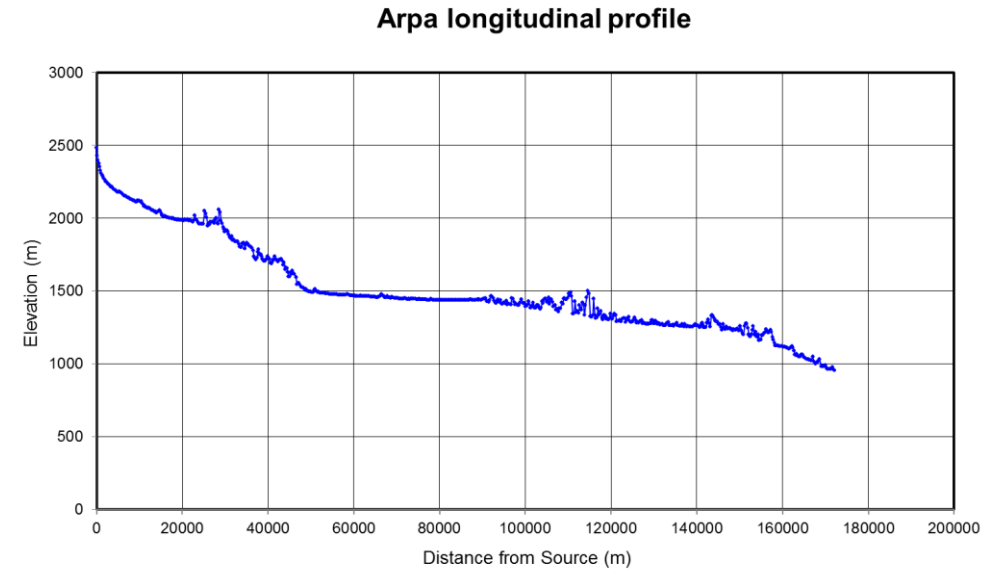
Arpa longitudinal profile
Elevation (m)
3000
2500
2000
1500
1000
500
0
0
20000
40000
60000
80000
100000
120000
140000
160000
180000
200000
Distance from Source (m)

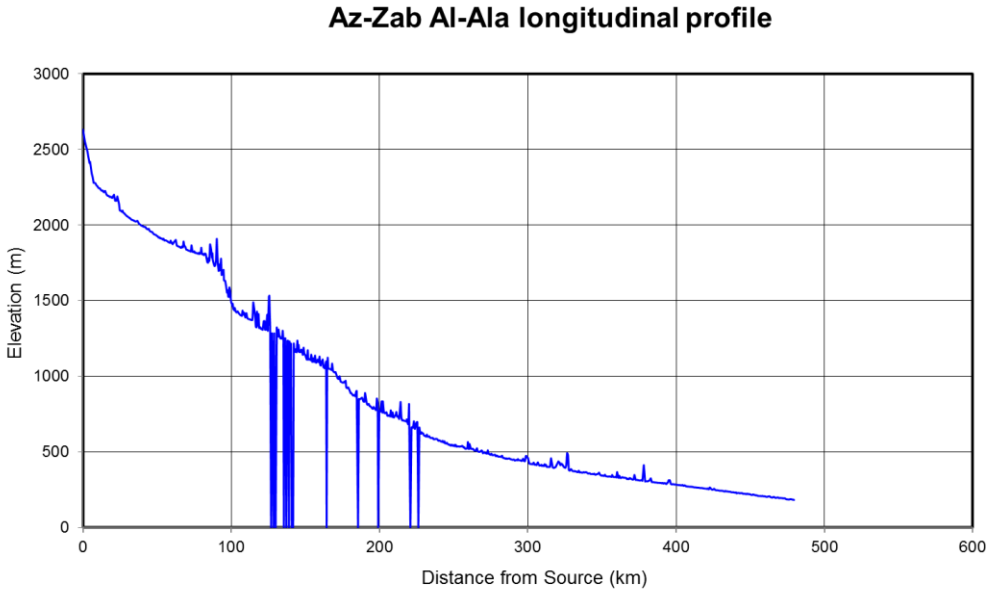
Az-Zab Al-Ala longitudinal profile
Elevation (m)
3000
2500
2000
1500
1000
500
0
0
100
200
300
400
500
600
Distance from Source (km)

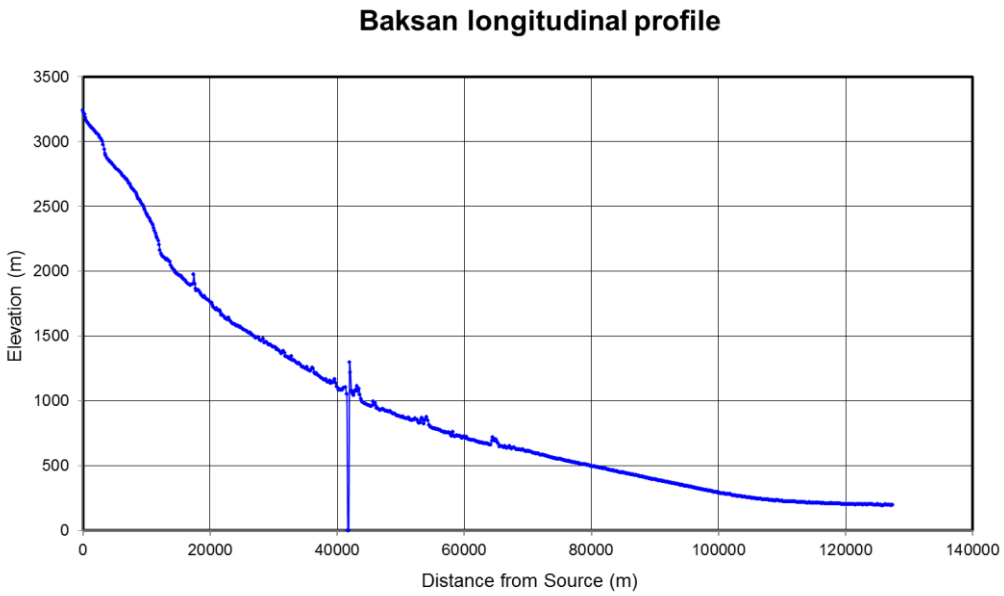
Baksan longitudinal profile
Elevation (m)
3500
3000
2500
2000
1500
1000
500
0
0
20000
40000
60000
80000
100000
120000
140000
Distance from Source (m)

Basur Cayi longitudinal profile

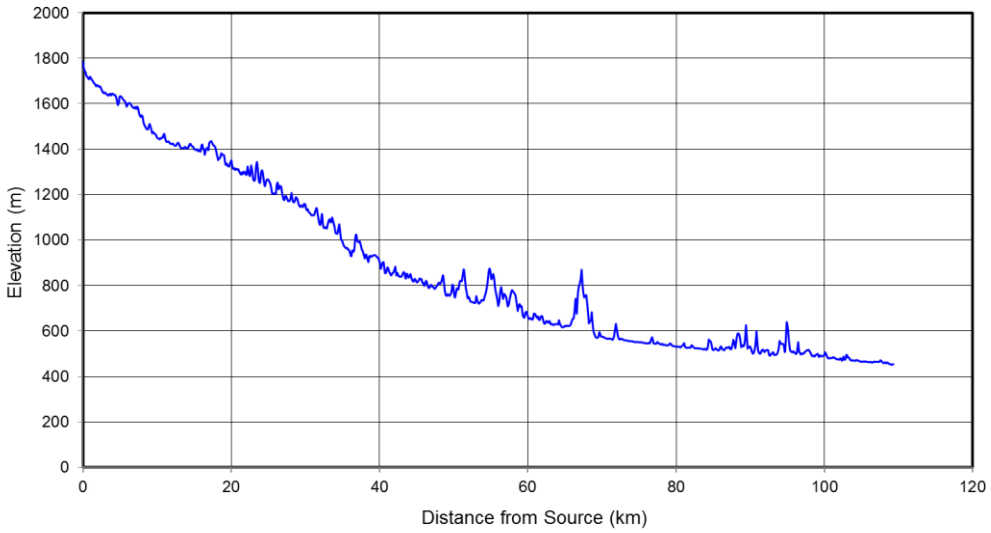

Batman Cayi longitudinal profile

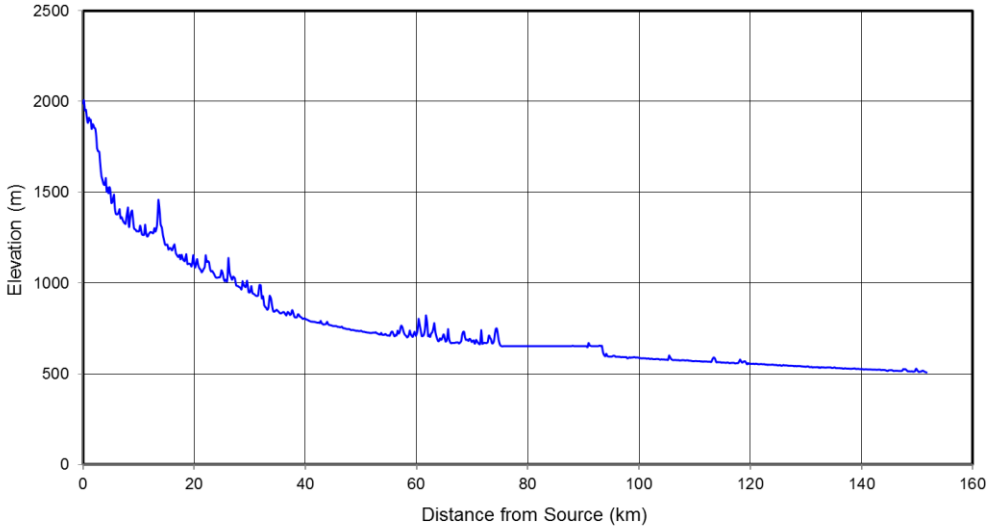

Batman Cayi tributary A longitudinal profile

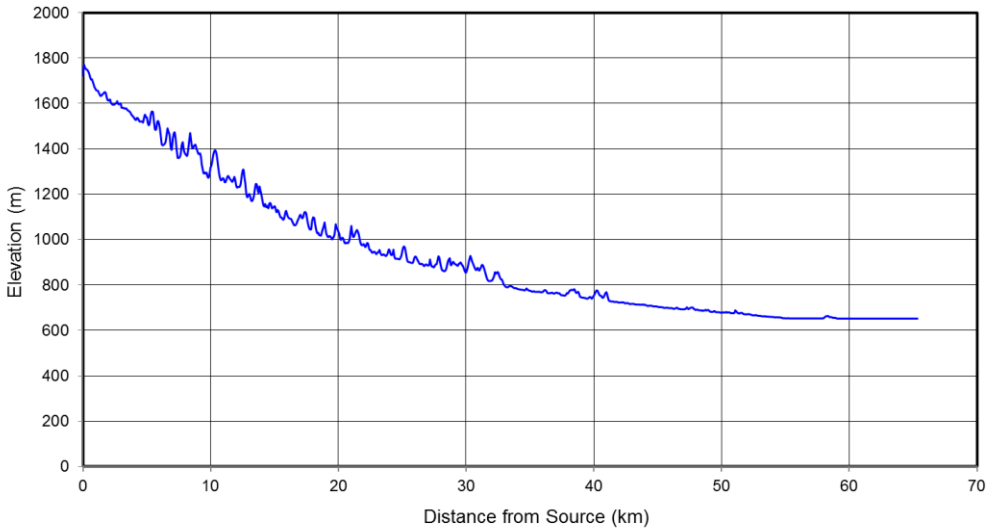

Bertasuyu longitudinal profile

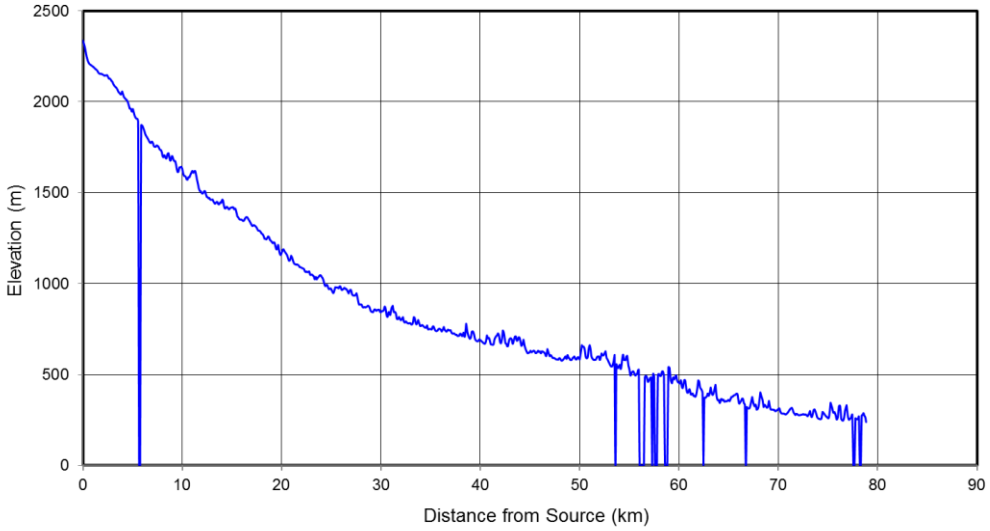

Botan Cayi longitudinal profile

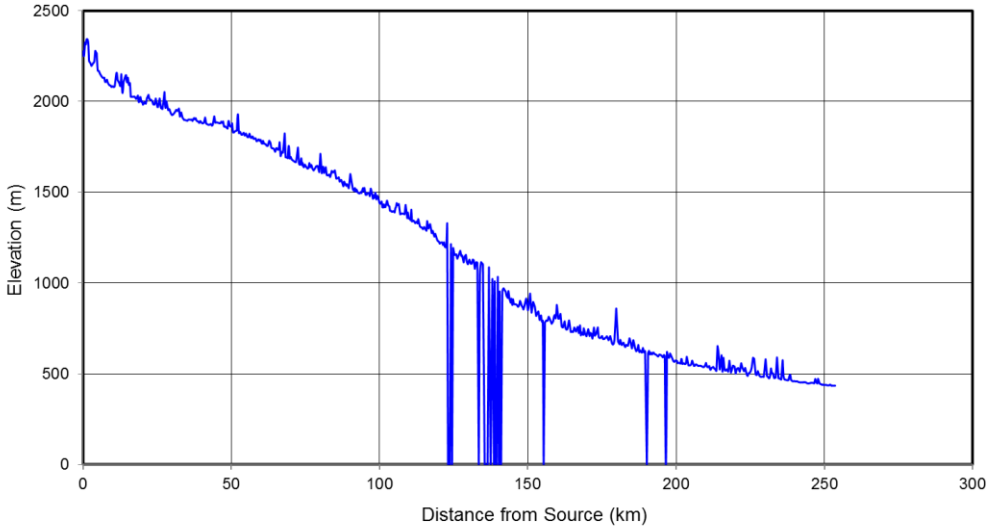

Botan Cayi tributary A longitudinal profile

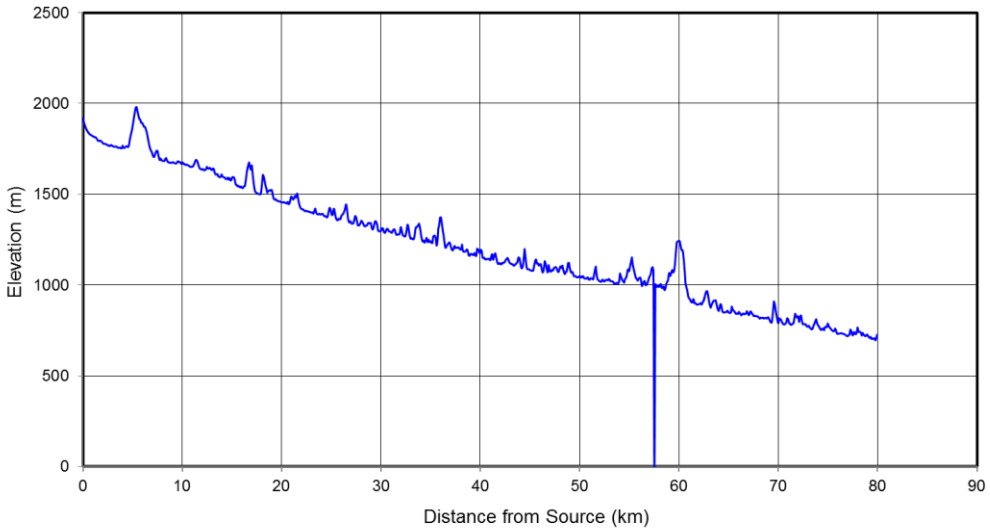

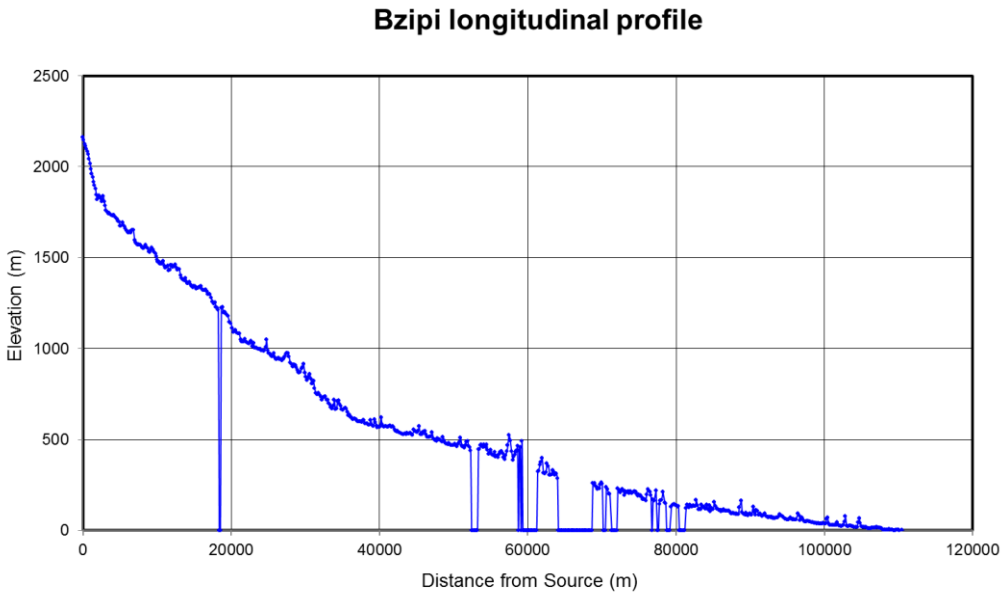
Bzipi longitudinal profile
Elevation (m)
2500
2000
1500
1000
500
0
0
20000
40000
60000
80000
100000
120000
Distance from Source (m)

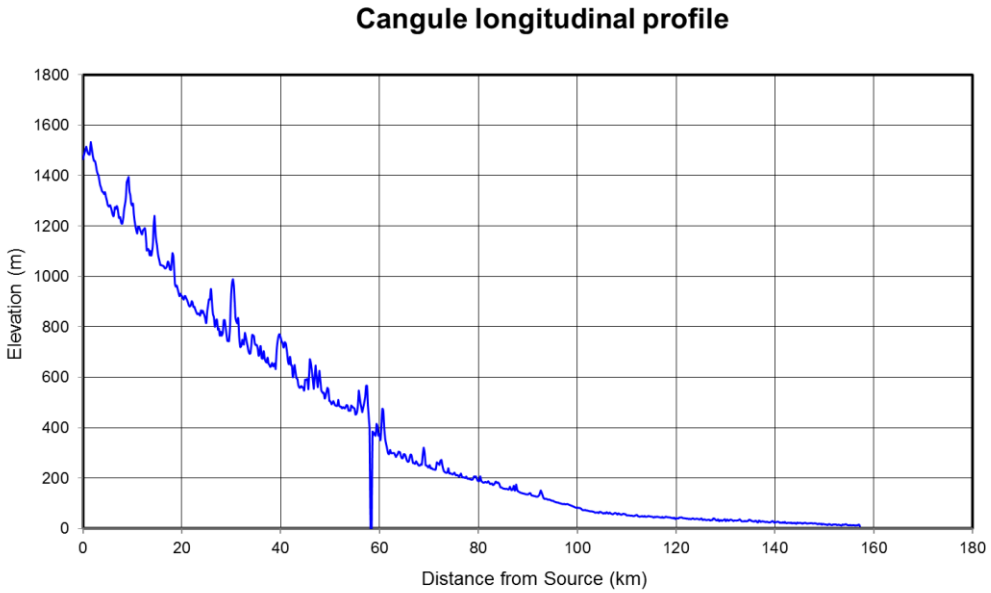
Cangule longitudinal profile
Elevation (m)
1800
1600
1400
1200
1000
800
600
400
200
0
0
20
40
60
80
100
120
140
160
180
Distance from Source (km)

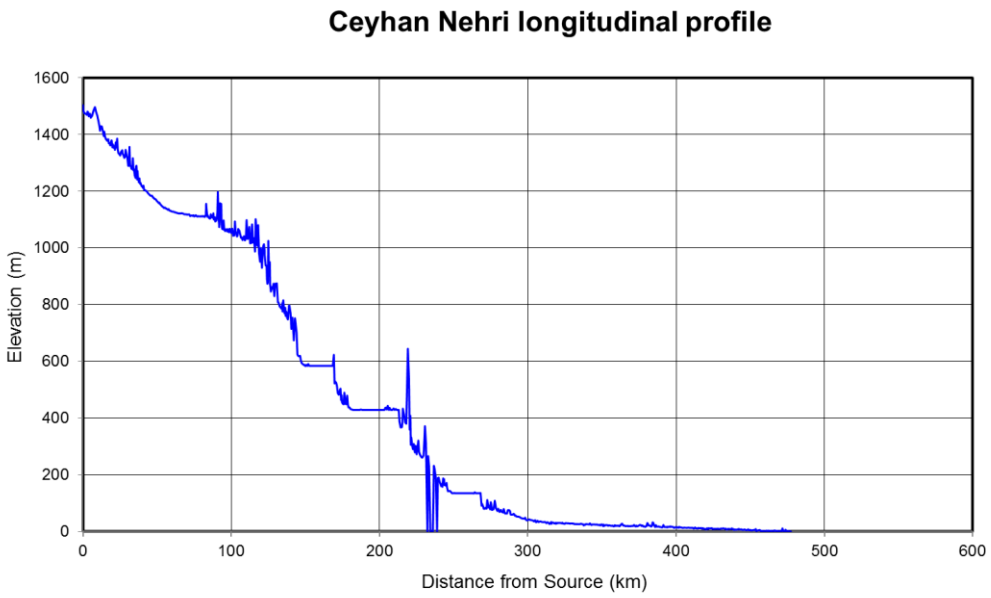
Ceyhan Nehri longitudinal profile
Elevation (m)
1600
1400
1200
1000
800
600
400
200
0
0
100
200
300
400
500
600
Distance from Source (km)

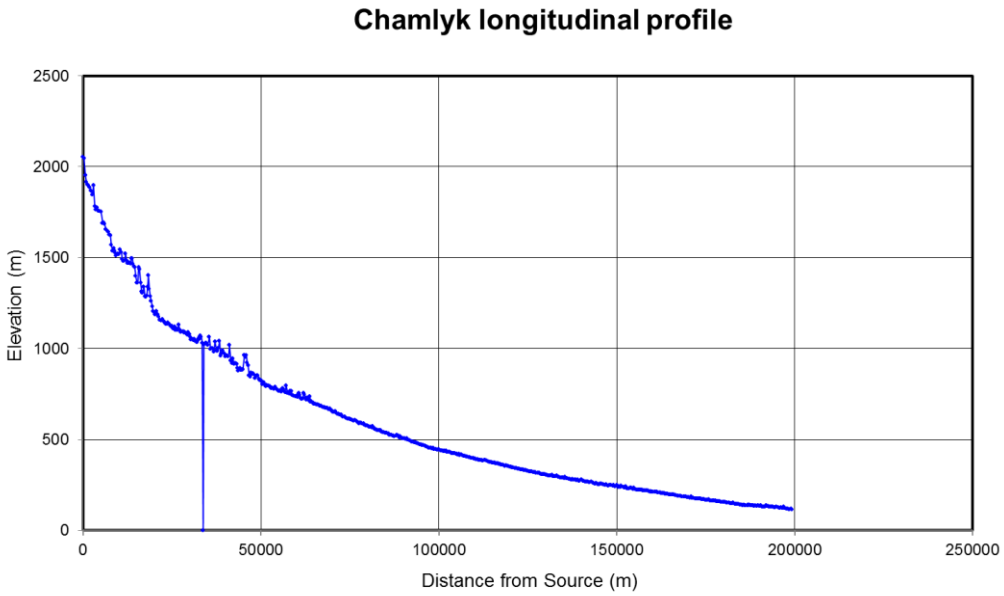
Chamlyk longitudinal profile
Elevation (m)
2500
2000
1500
1000
500
0
0
50000
100000
150000
200000
250000
Distance from Source (m)

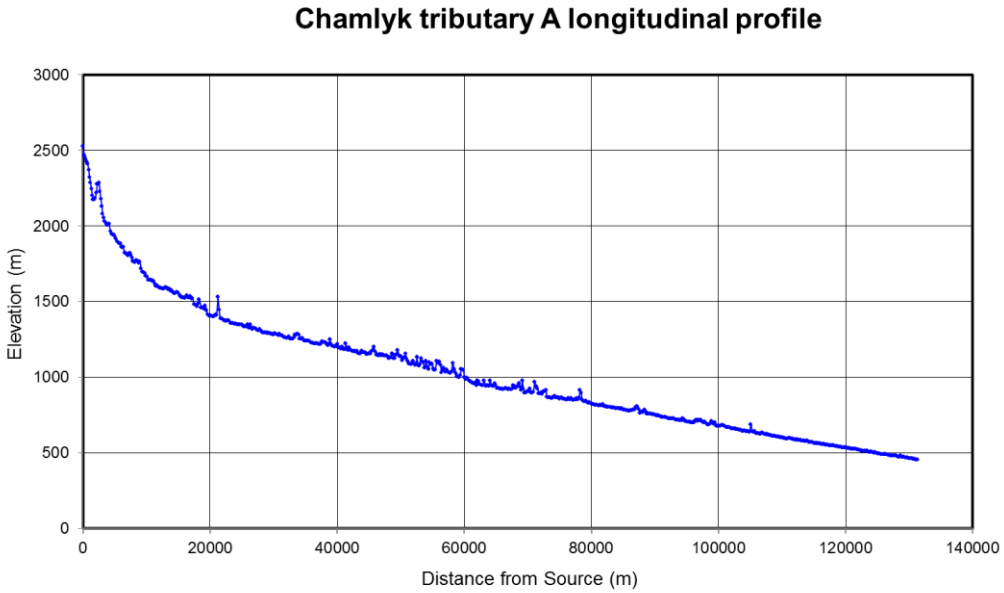
Chamlyk tributary A longitudinal profile
Elevation (m)
3000
2500
2000
1500
1000
500
0
0
20000
40000
60000
80000
100000
120000
140000
Distance from Source (m)

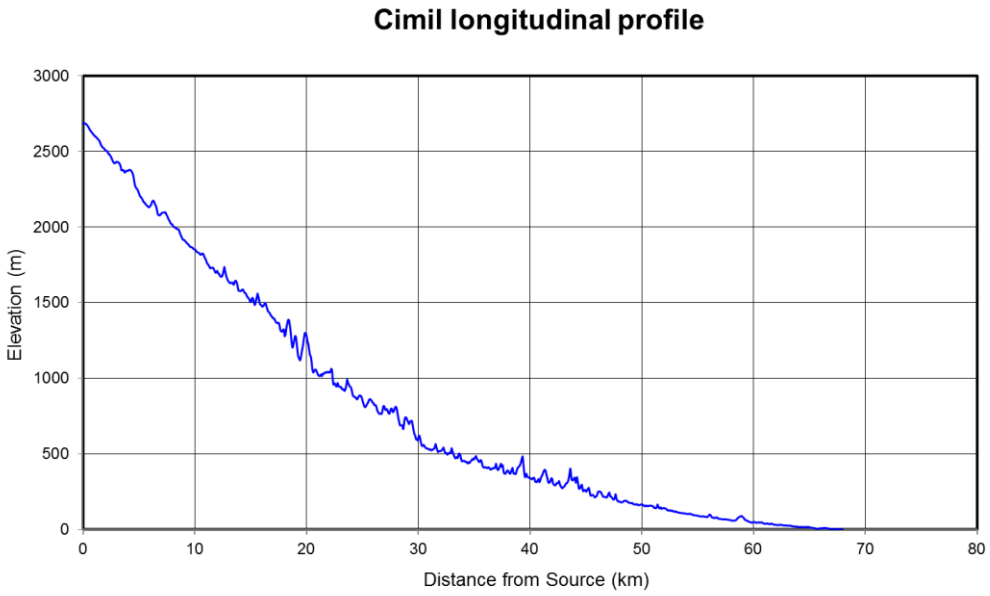
Cimil longitudinal profile
Elevation (m)
3000
2500
2000
1500
1000
500
0
0
10
20
30
40
50
60
70
80
Distance from Source (km)

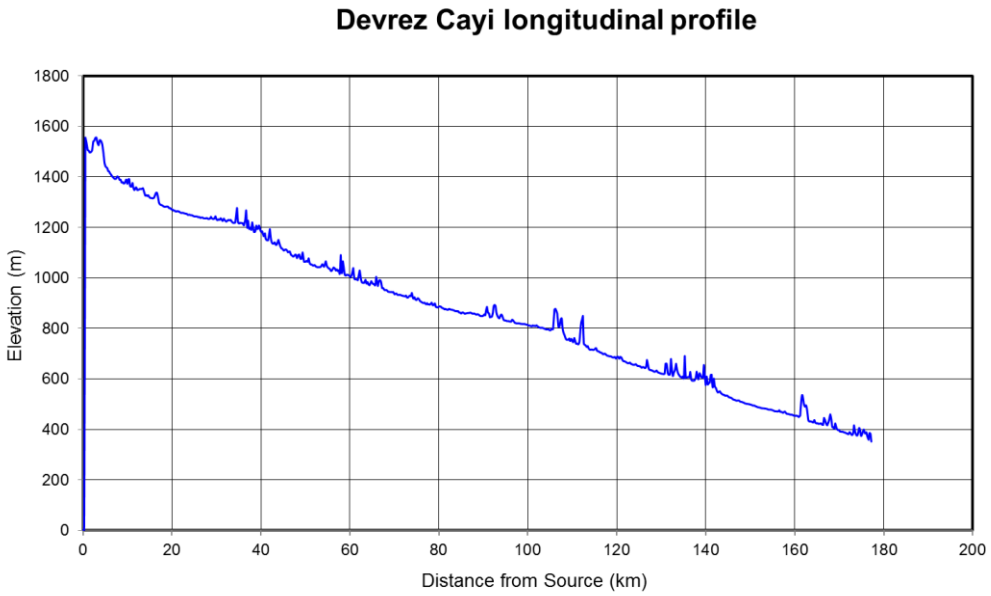
Devrez Cayi longitudinal profile
Elevation (m)
1800
1600
1400
1200
1000
800
600
400
200
0
0
20
40
60
80
100
120
140
160
180
200
Distance from Source (km)

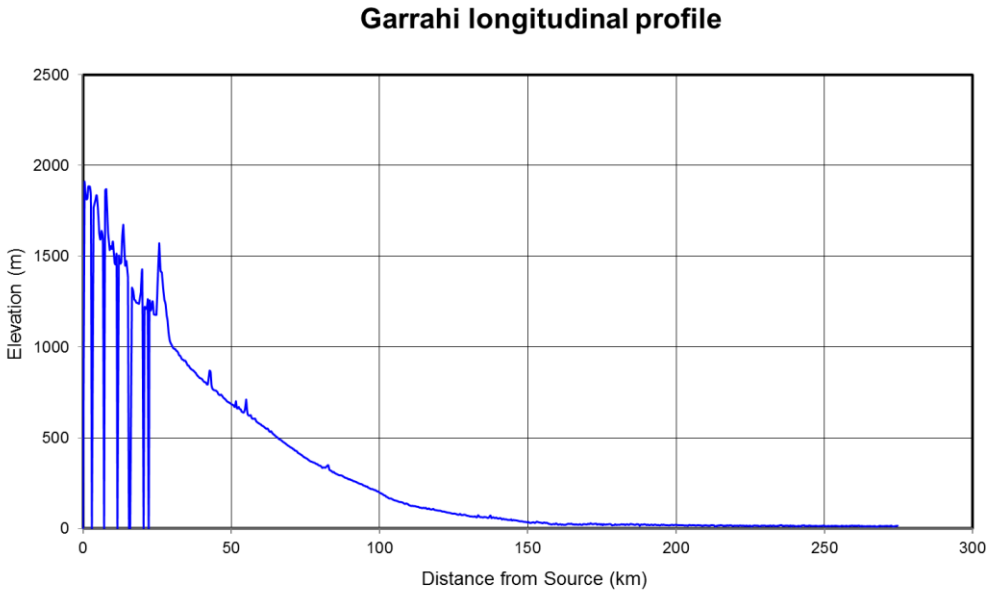
Garrahi longitudinal profile
Elevation (m)
2500
2000
1500
1000
500
0
0
50
100
150
200
250
300
Distance from Source (km)

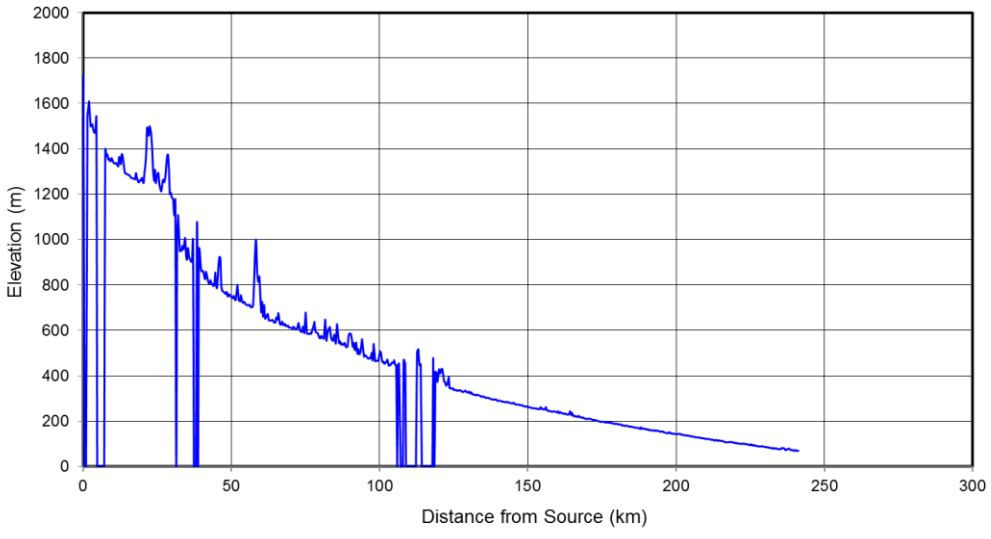
Garrahi tributary A longitudinal profile
Elevation (m)
2000
1800
1600
1400
1200
1000
800
600
400
200
0
0
50
100
150
200
250
300
Distance from Source (km)

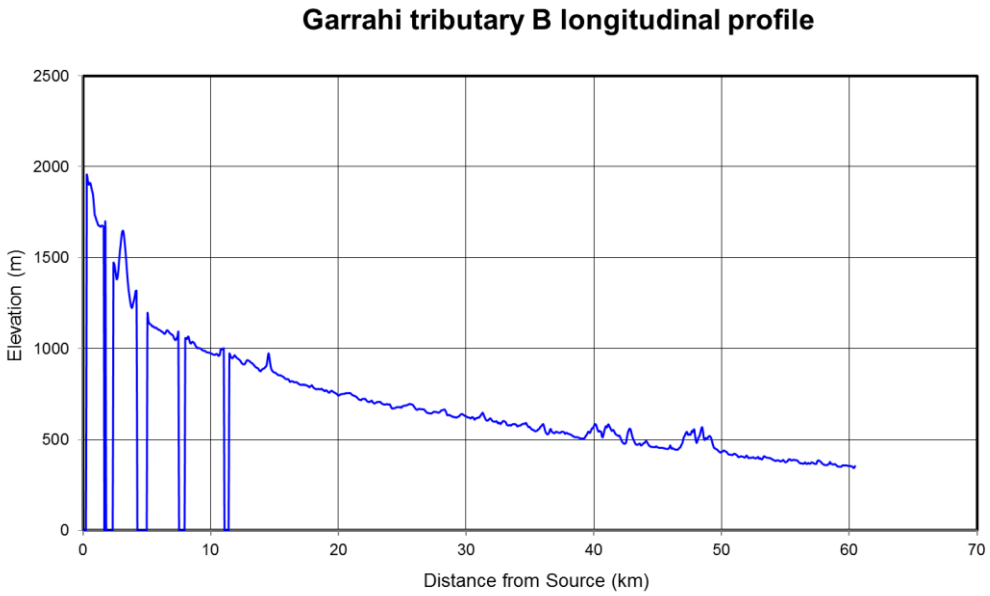
Garrahi tributary B longitudinal profile
Elevation (m)
2500
2000
1500
1000
500
0
0
10
20
30
40
50
60
70
Distance from Source (km)

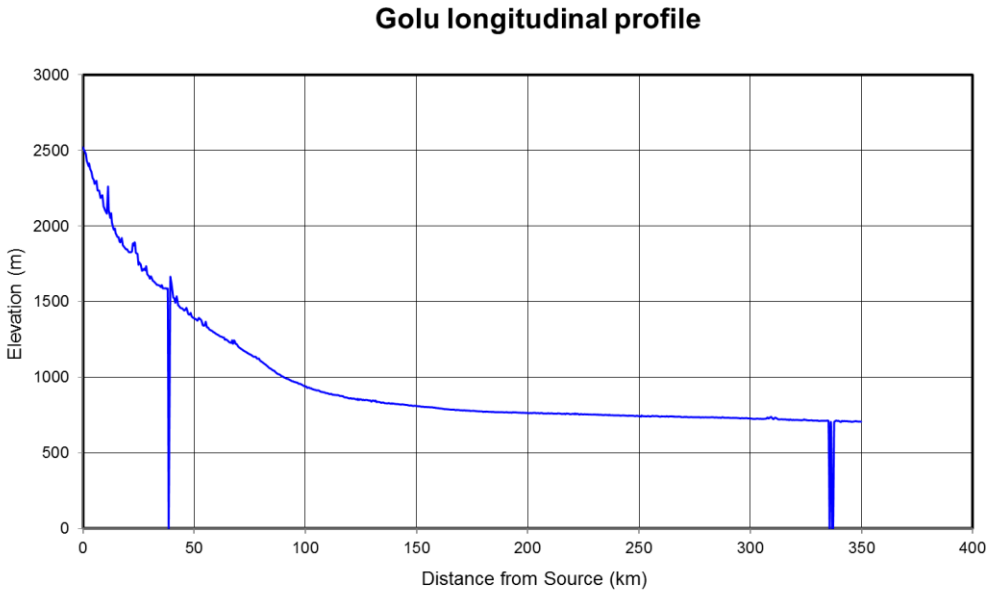
Golu longitudinal profile
Elevation (m)
3000
2500
2000
1500
1000
500
0
0
50
100
150
200
250
300
350
400
Distance from Source (km)

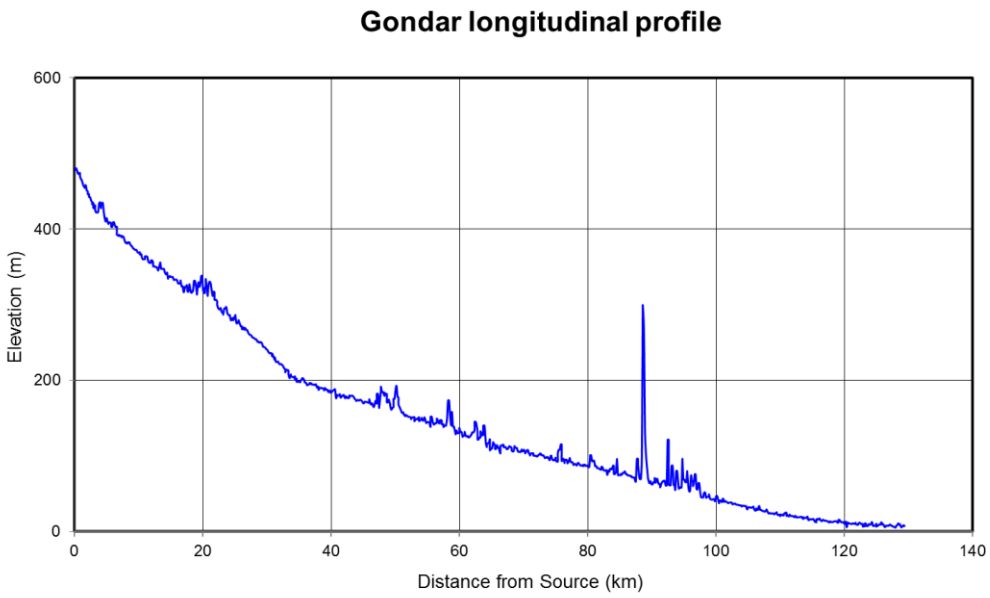
Gondar longitudinal profile
Elevation (m)
600
400
200
0
0
20
40
60
80
100
120
140
Distance from Source (km)

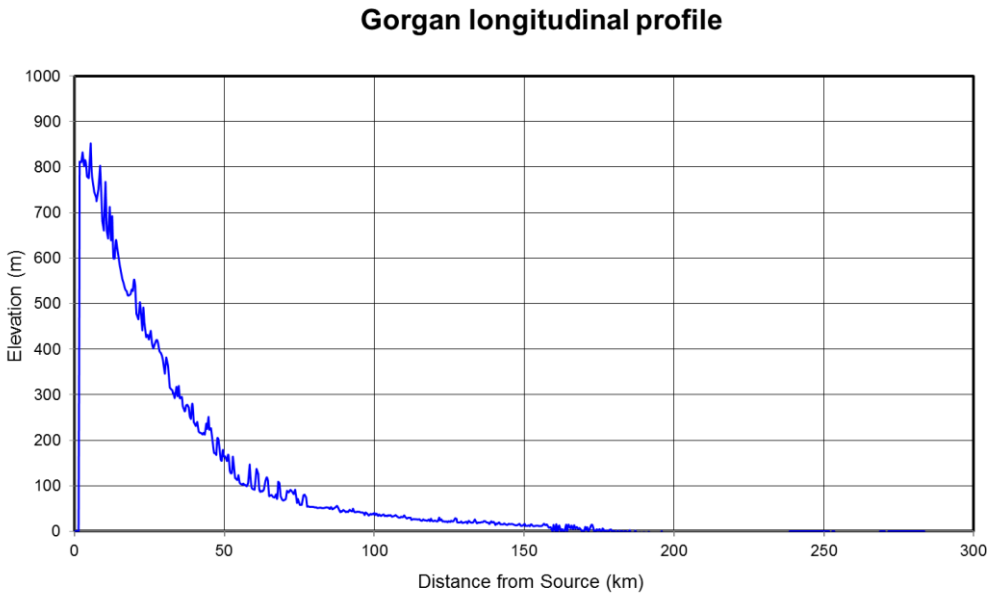
Gorgan longitudinal profile
Elevation (m)
1000
900
800
700
600
500
400
300
200
100
0
0
50
100
150
200
250
300
Distance from Source (km)

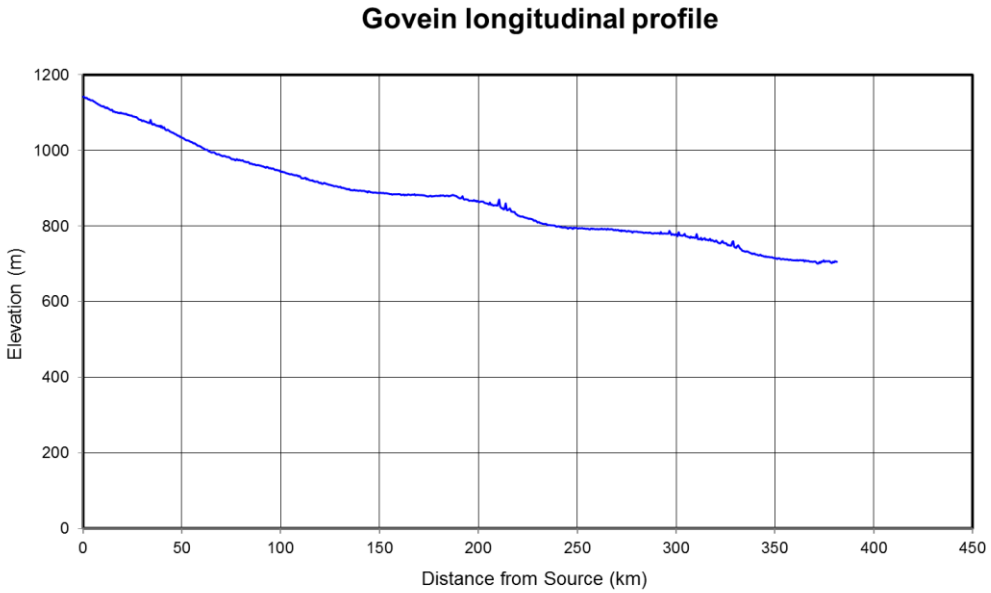
Govein longitudinal profile
Elevation (m)
1200
1000
800
600
400
200
0
0
50
100
150
200
250
300
350
400
450
Distance from Source (km)

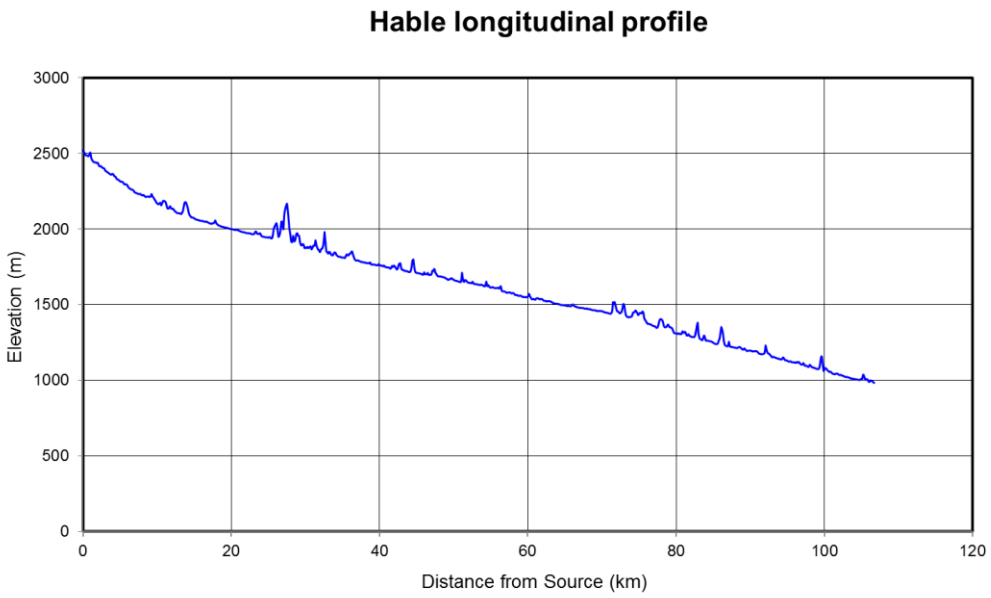
Hable longitudinal profile
Elevation (m)
3000
2500
2000
1500
1000
500
0
0
20
40
60
80
100
120
Distance from Source (km)

Han-ye Sur longitudinal profile

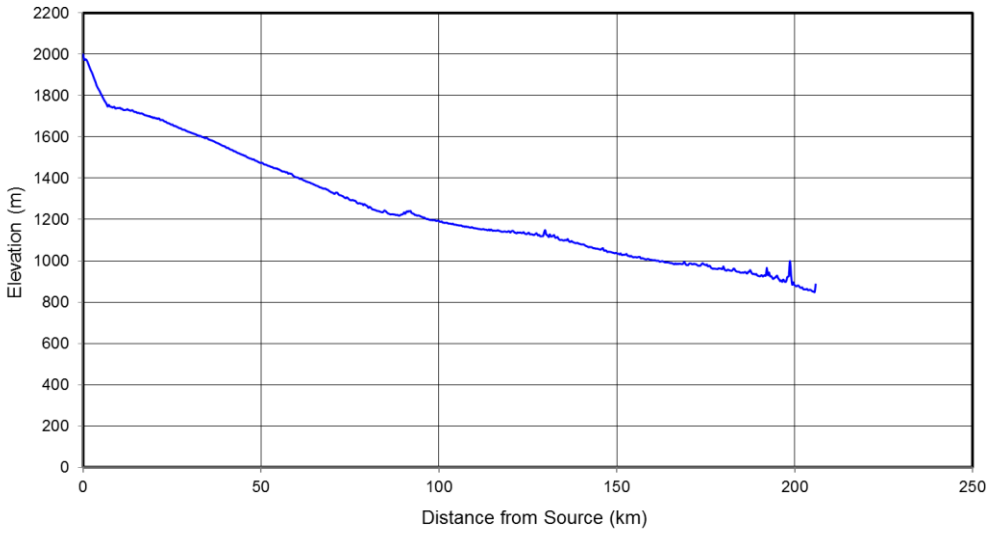

Harsit longitudinal profile

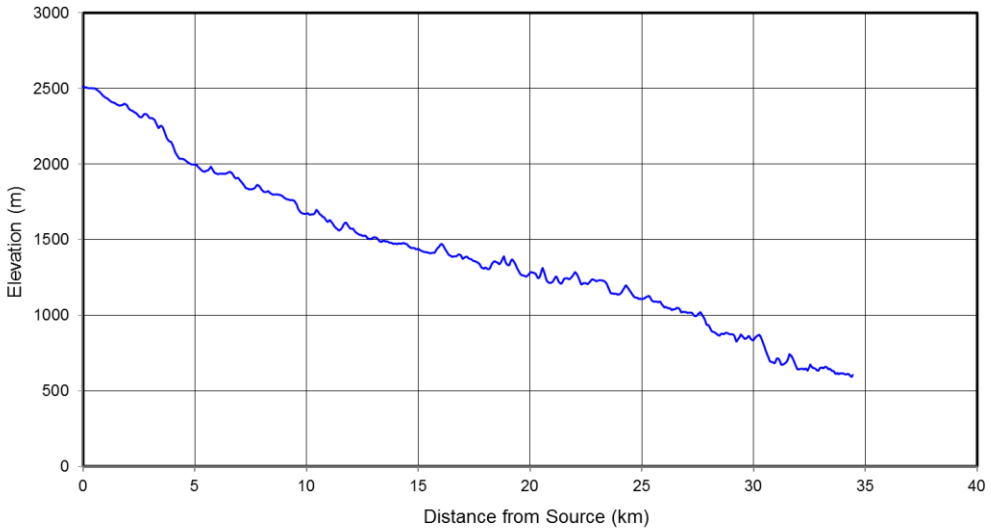

Harsit tributary A longitudinal profile

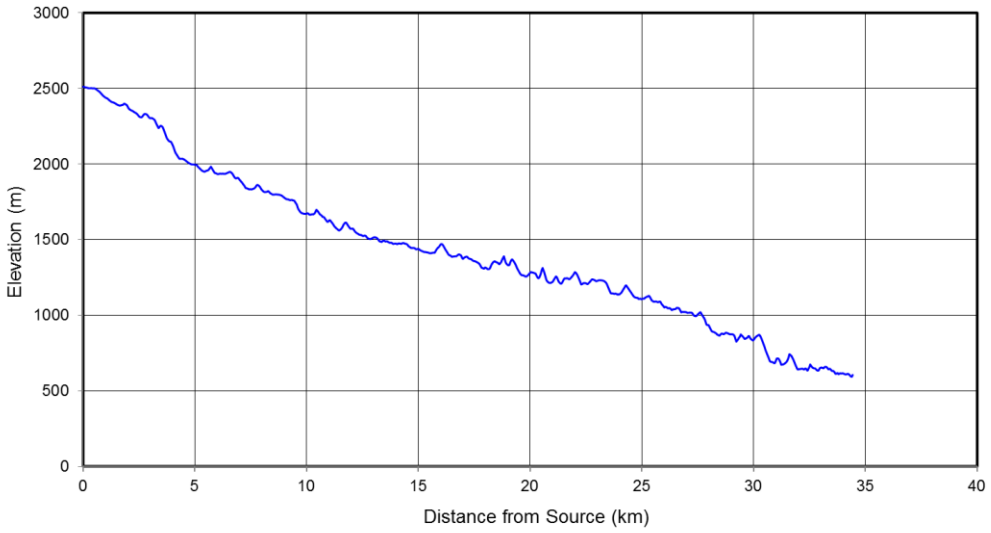

Hassan Lang longitudinal profile

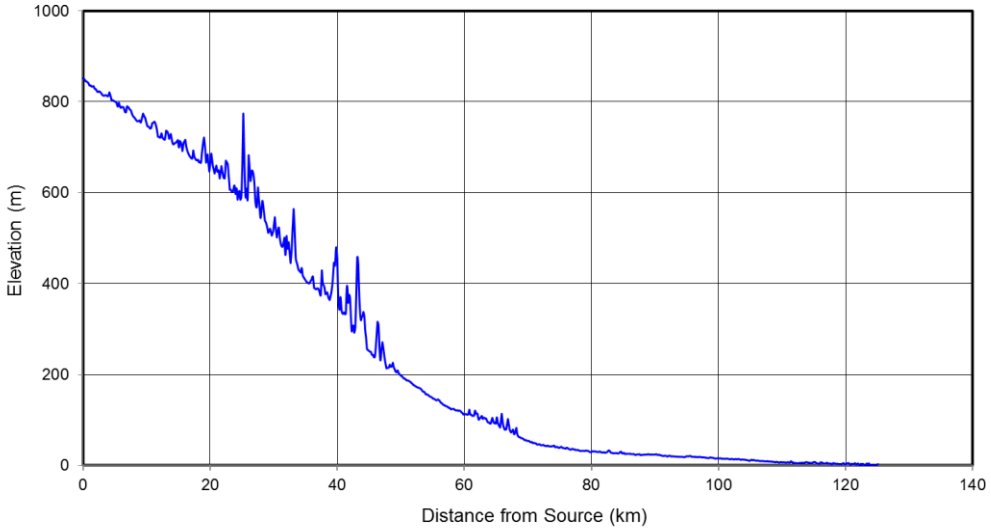

Heirabad longitudinal profile

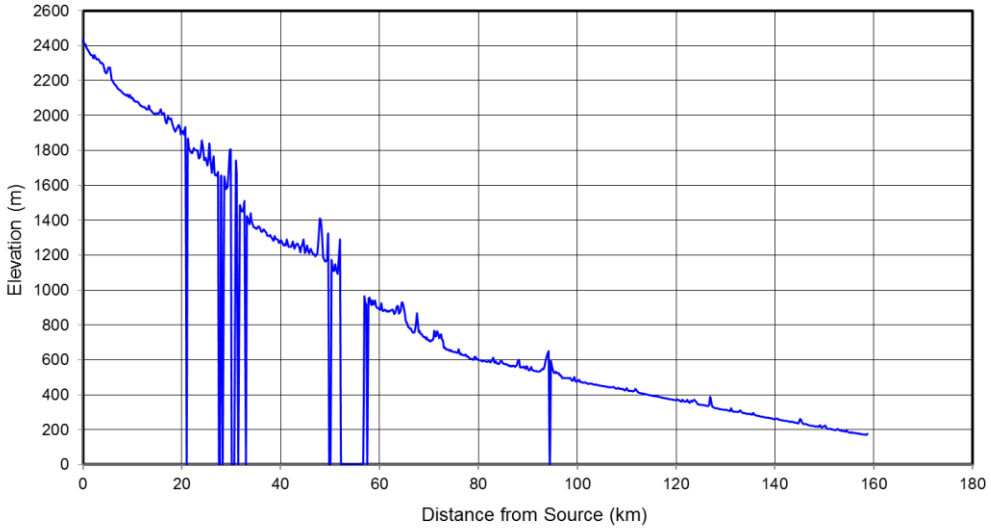

Helle longitudinal profile

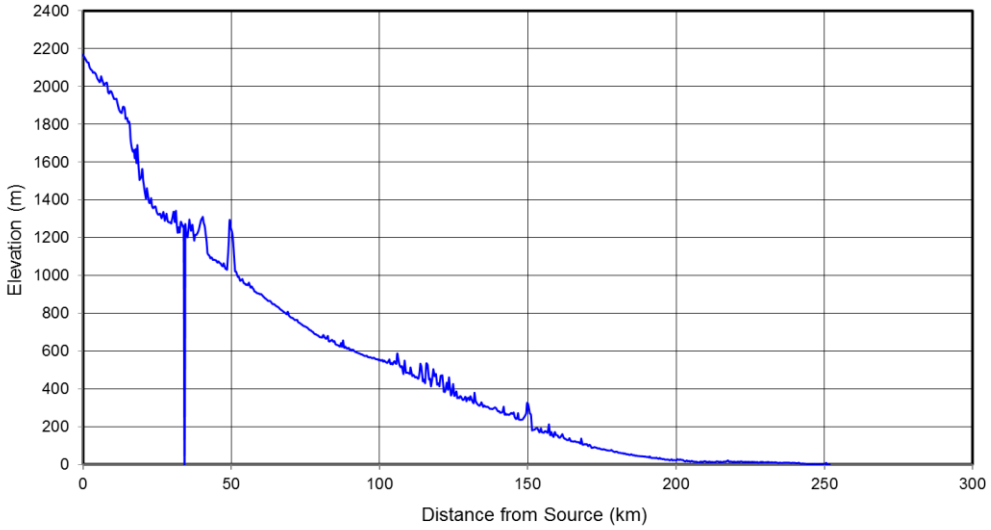

Hendigan longitudinal profile

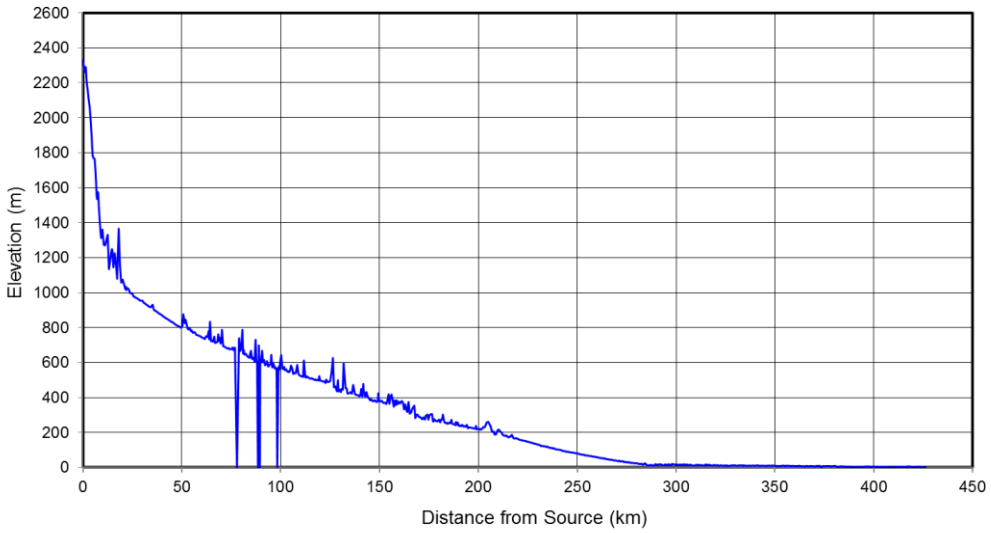

Hendigan tributary A longitudinal profile

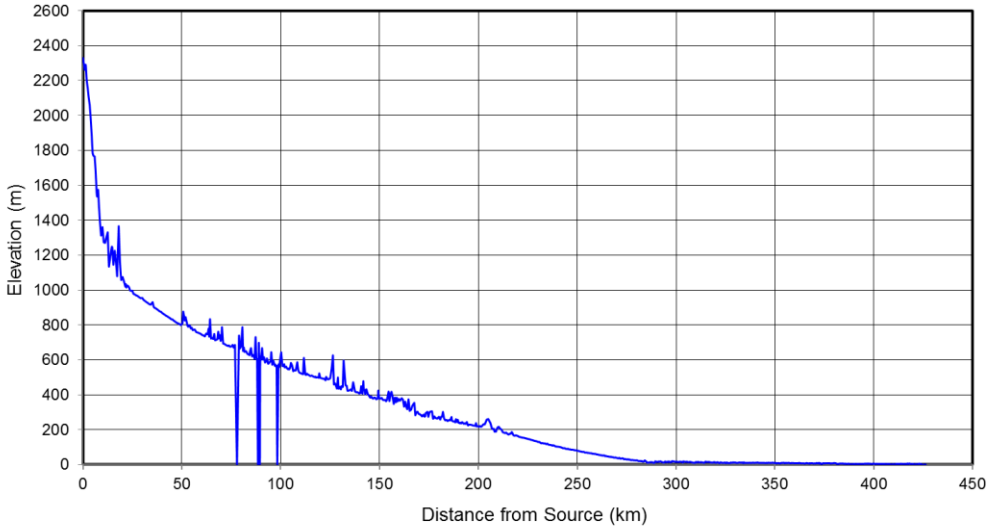

Inguri longitudinal profile

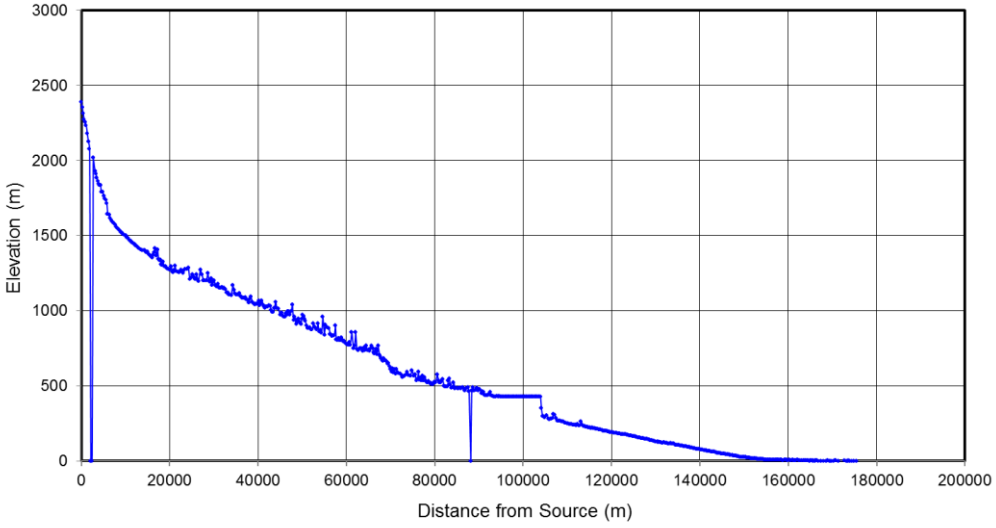

Inguri tributary A longitudinal profile

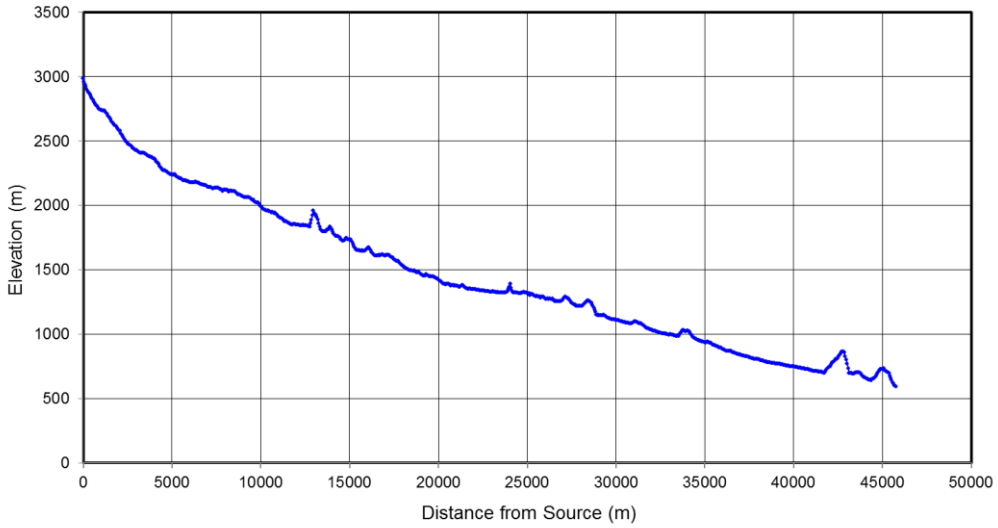

Iora longitudinal profile

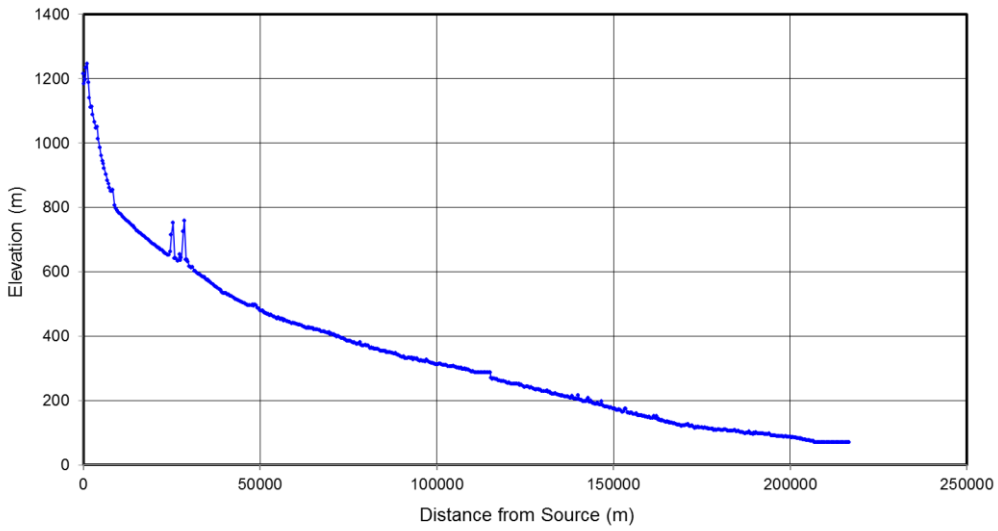

Kal-e Gabrestan longitudinal profile

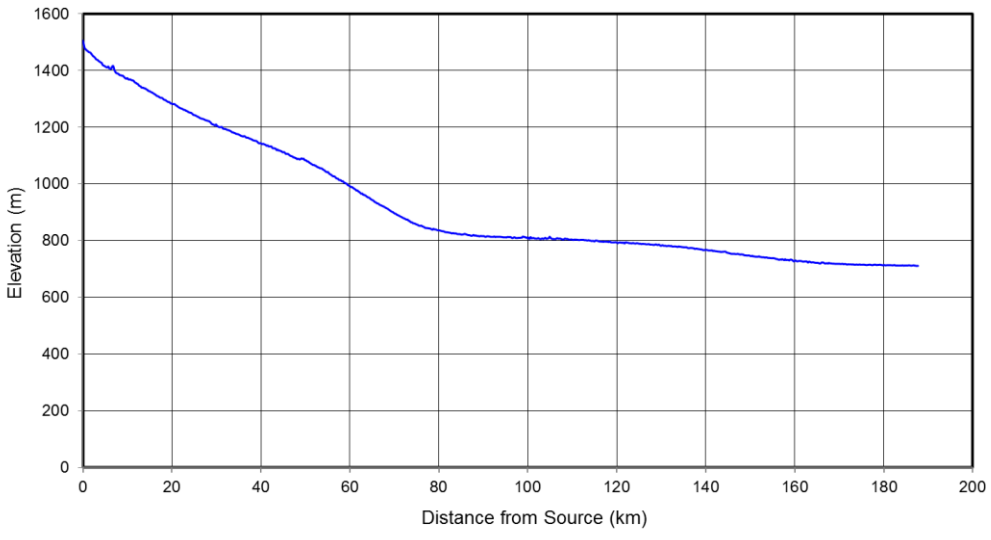

Kara Dere longitudinal profile

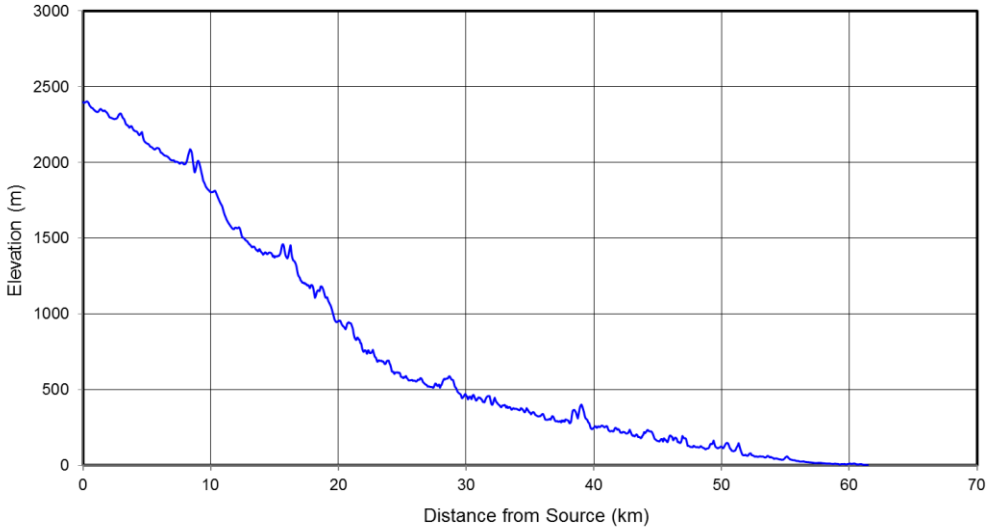

Kara Koysu longitudinal profile

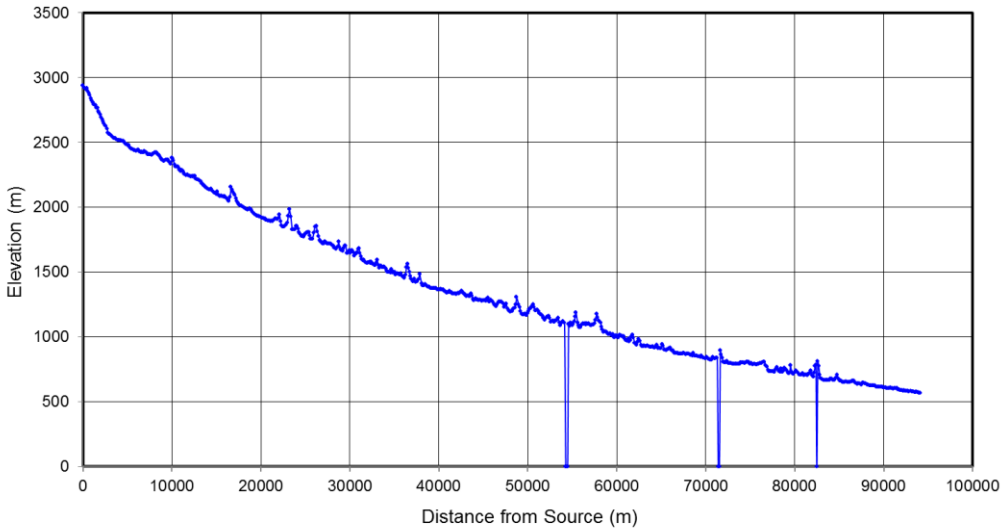

Kara Koysu tributary A longitudinal profile

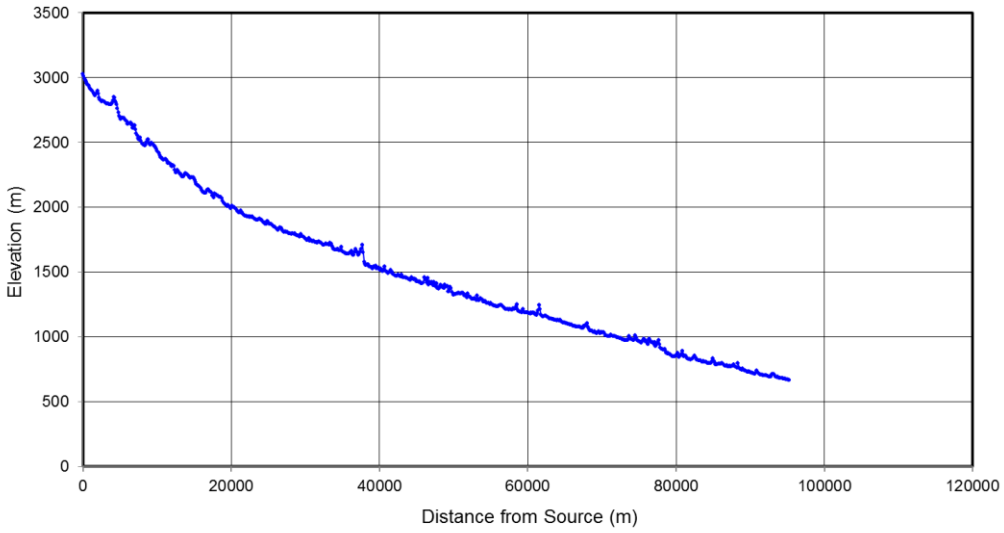

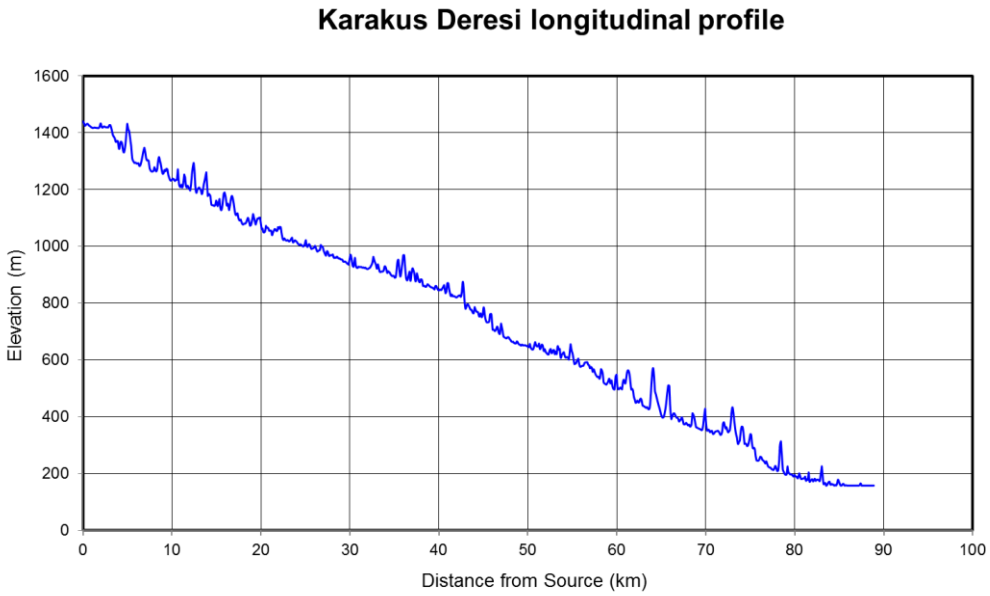
Karakus Deresi longitudinal profile
Elevation (m)
1600
1400
1200
1000
800
600
400
200
0
0
10
20
30
40
50
60
70
80
90
100
Distance from Source (km)

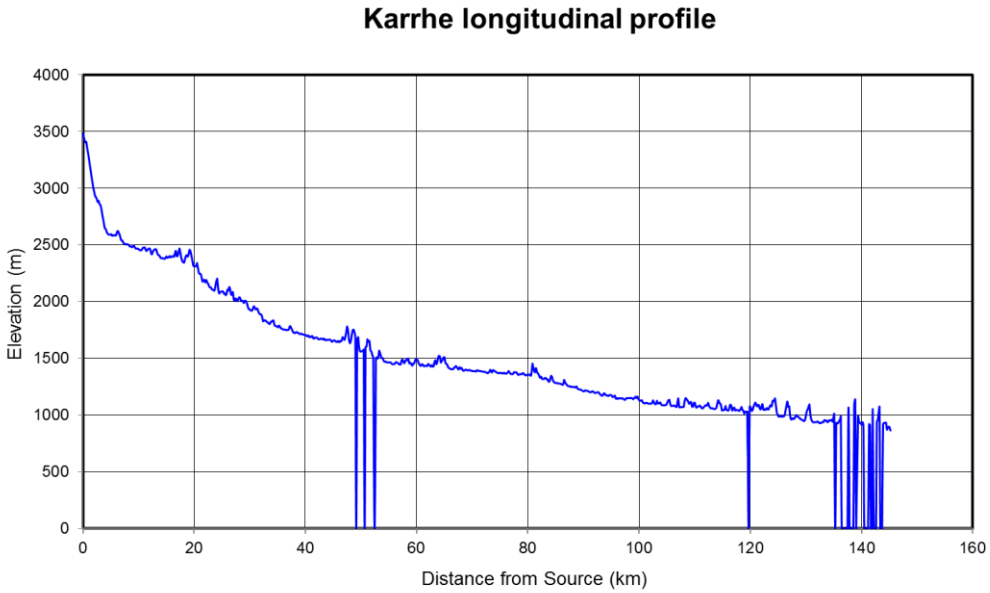
Karrhe longitudinal profile
Elevation (m)
4000
3500
3000
2500
2000
1500
1000
500
0
0
20
40
60
80
100
120
140
160
Distance from Source (km)

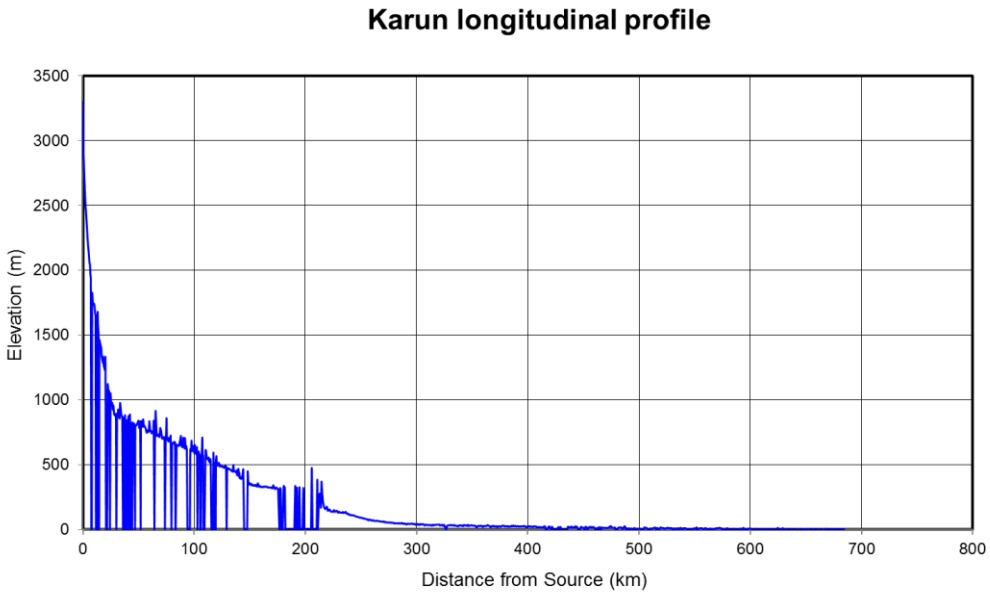
Karun longitudinal profile
Elevation (m)
3500
3000
2500
2000
1500
1000
500
0
0
100
200
300
400
500
600
700
800
Distance from Source (km)

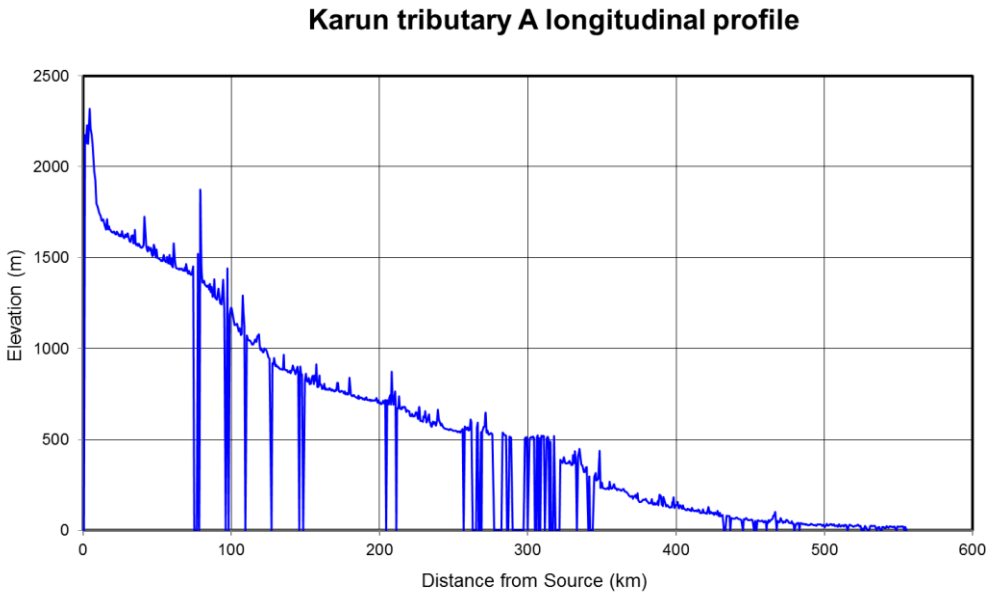
Karun tributary A longitudinal profile
Elevation (m)
2500
2000
1500
1000
500
0
0
100
200
300
400
500
600
Distance from Source (km)

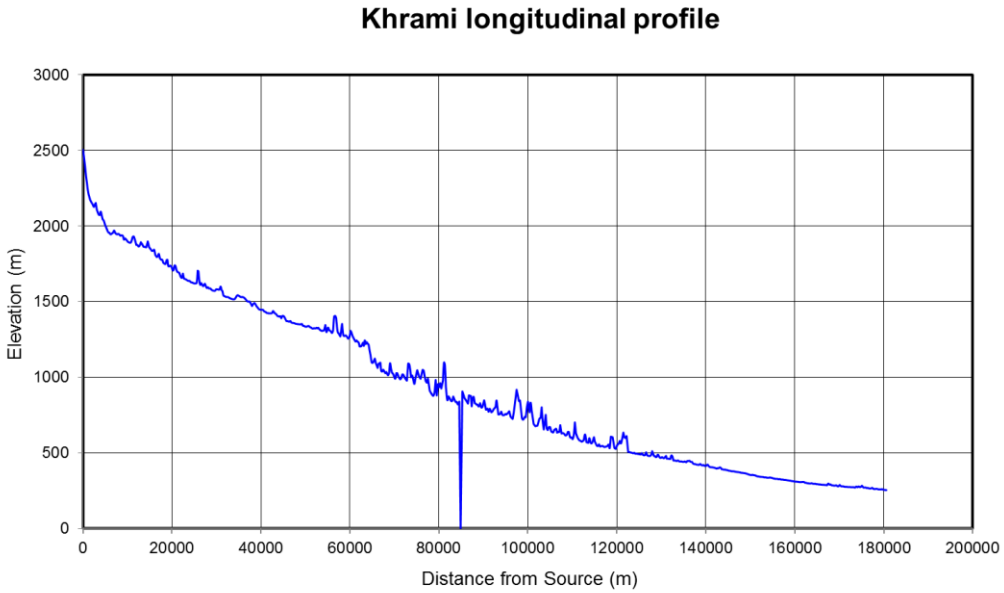
Khrami longitudinal profile
Elevation (m)
3000
2500
2000
1500
1000
500
0
0
20000
40000
60000
80000
100000
120000
140000
160000
180000
200000
Distance from Source (m)

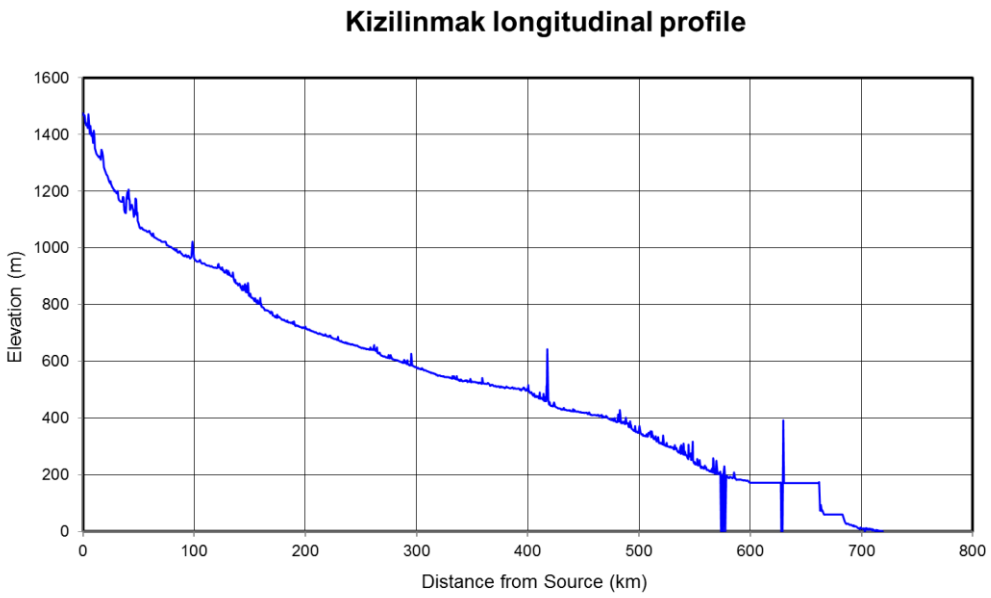
Kizilinmak longitudinal profile
Elevation (m)
1600
1400
1200
1000
800
600
400
200
0
0
100
200
300
400
500
600
700
800
Distance from Source (km)

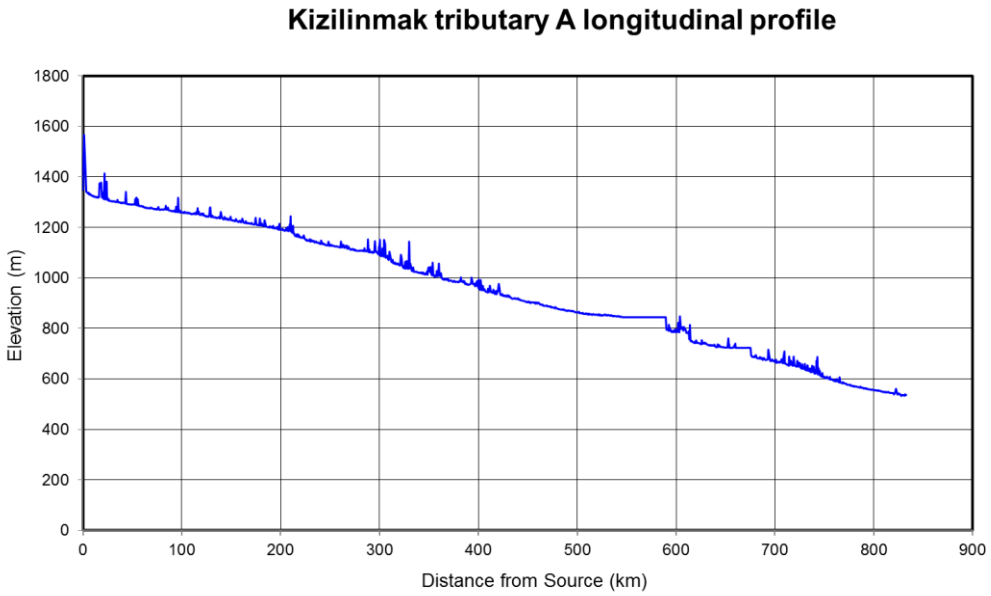
Kizilinmak tributary A longitudinal profile
Elevation (m)
1800
1600
1400
1200
1000
800
600
400
200
0
0
100
200
300
400
500
600
700
800
900
Distance from Source (km)

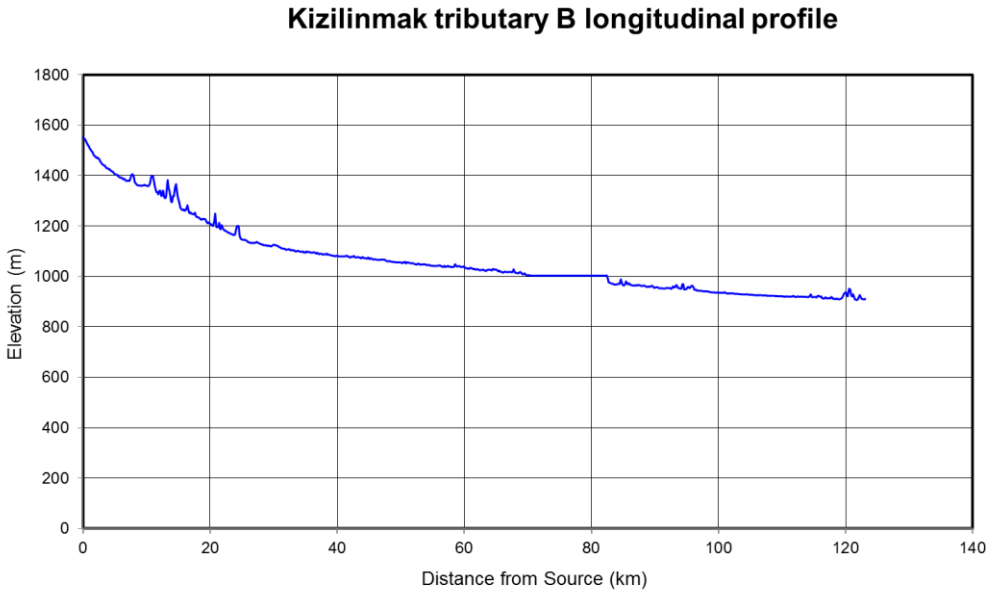
Kizilinmak tributary B longitudinal profile
Elevation (m)
1800
1600
1400
1200
1000
800
600
400
200
0
0
20
40
60
80
100
120
140
Distance from Source (km)

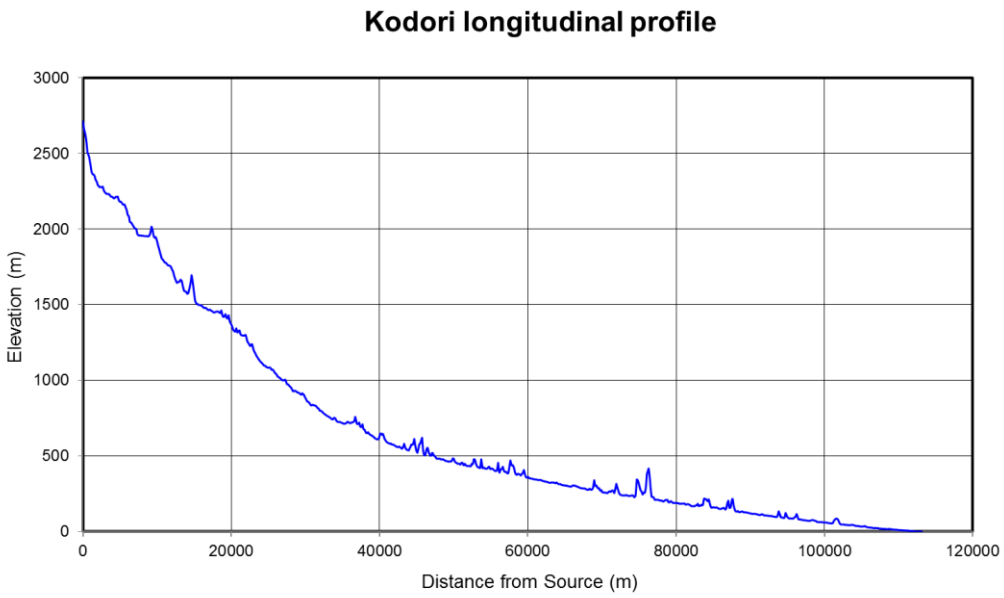
Kodori longitudinal profile
Elevation (m)
3000
2500
2000
1500
1000
500
0
0
20000
40000
60000
80000
100000
120000
Distance from Source (m)

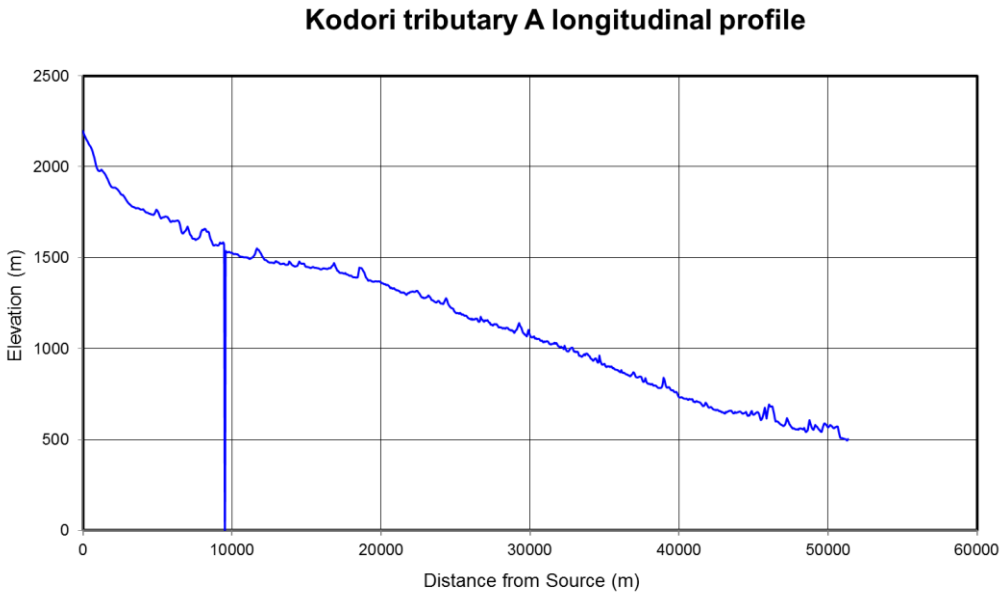
Kodori tributary A longitudinal profile
Elevation (m)
2500
2000
1500
1000
500
0
0
10000
20000
30000
40000
50000
60000
Distance from Source (m)

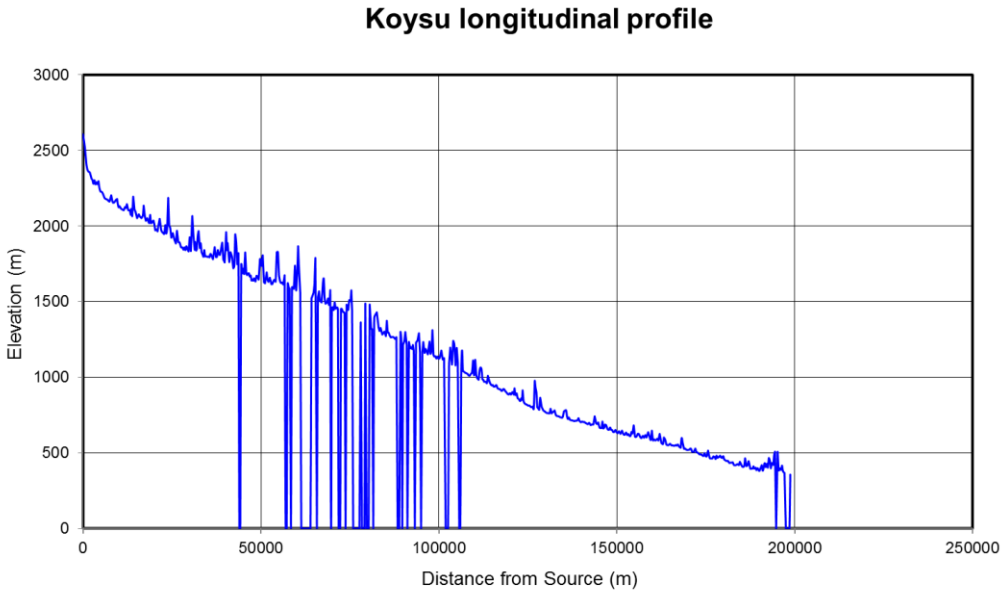
Koysu longitudinal profile
Elevation (m)
3000
2500
2000
1500
1000
500
0
0
50000
100000
150000
200000
250000
Distance from Source (m)

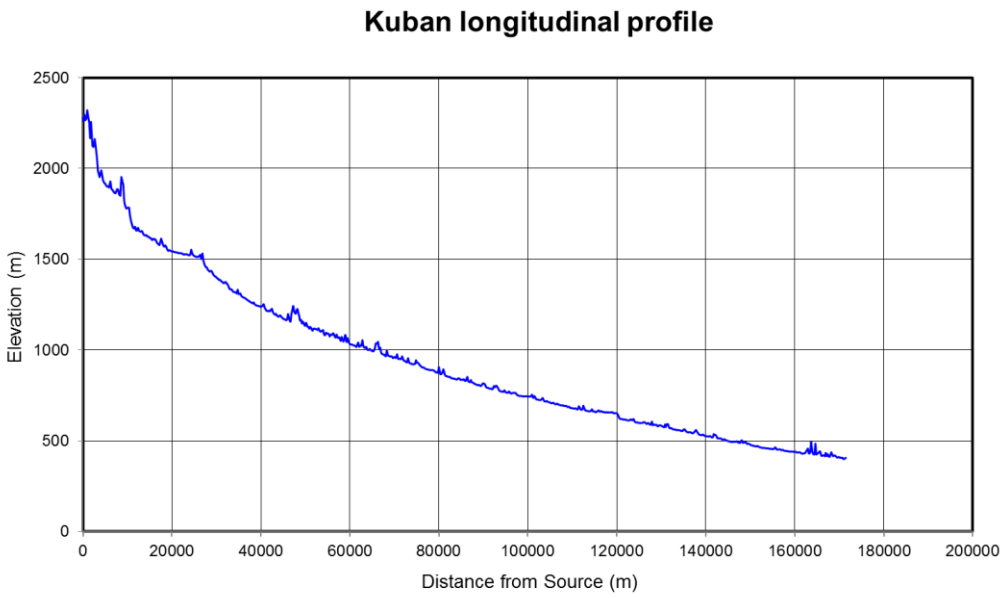
Kuban longitudinal profile
Elevation (m)
2500
2000
1500
1000
500
0
0
20000
40000
60000
80000
100000
120000
140000
160000
180000
200000
Distance from Source (m)

Kura longitudinal profile

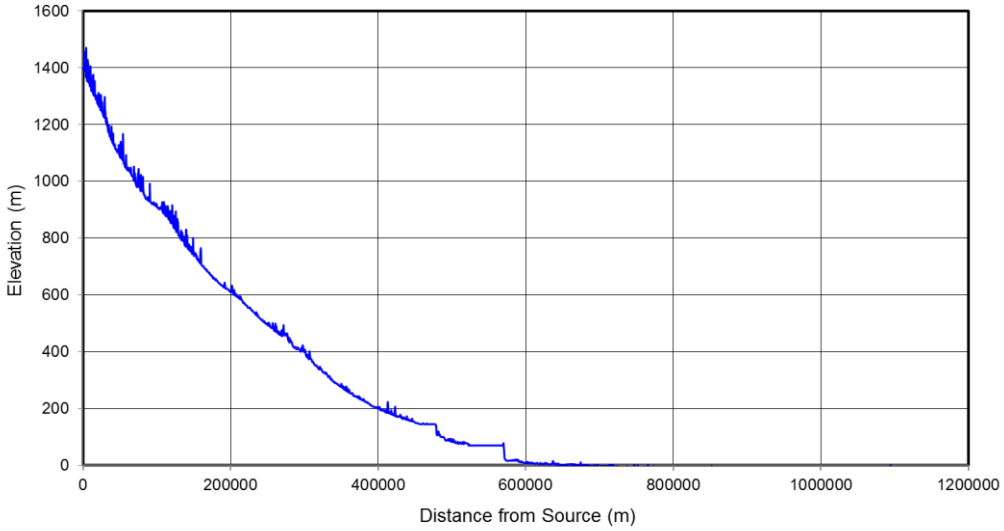

Kura tributary A longitudinal profile

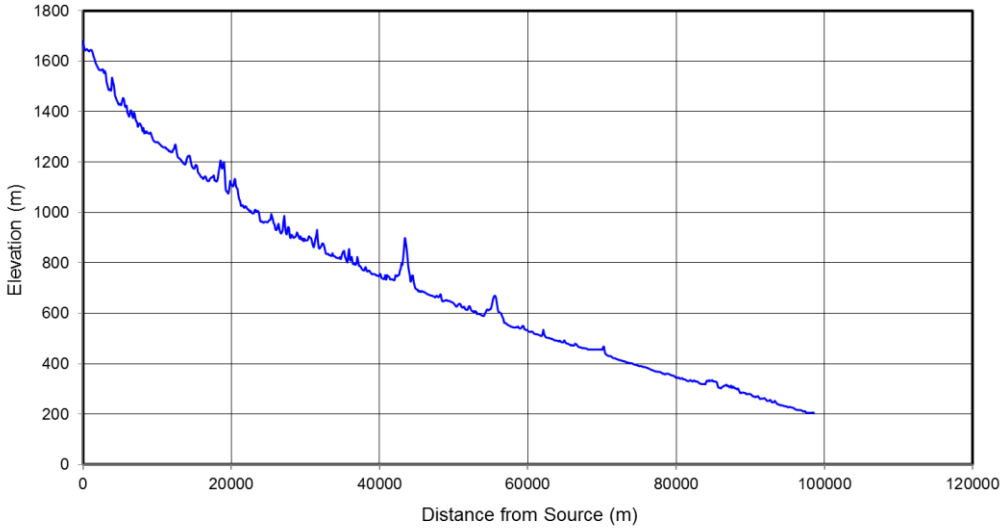

Kura tributary B longitudinal profile

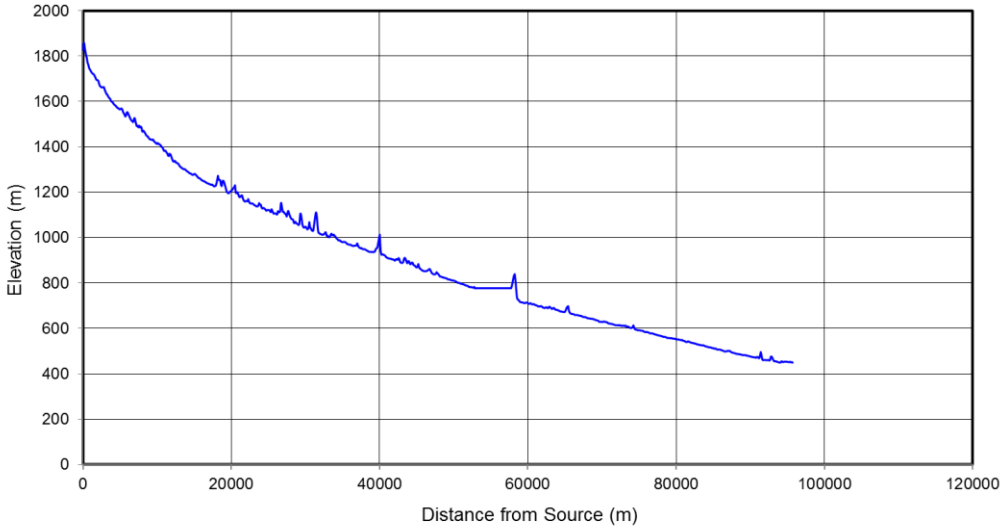

Kura tributary C longitudinal profile

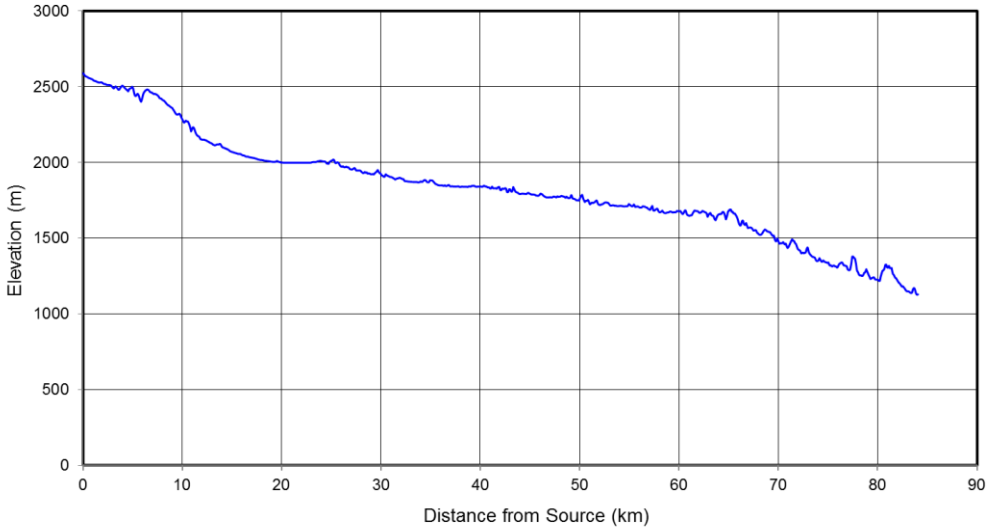

Laba longitudinal profile

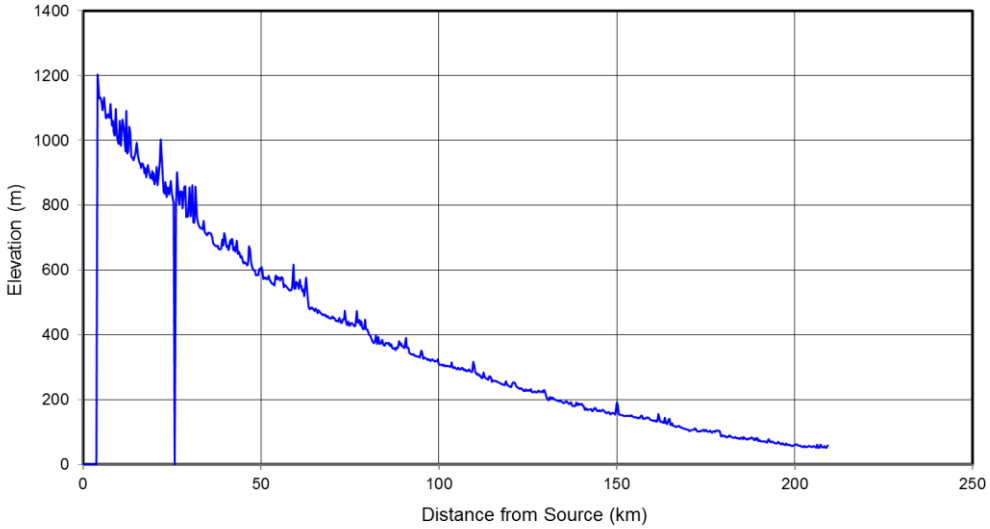

Laba tributary A longitudinal profile

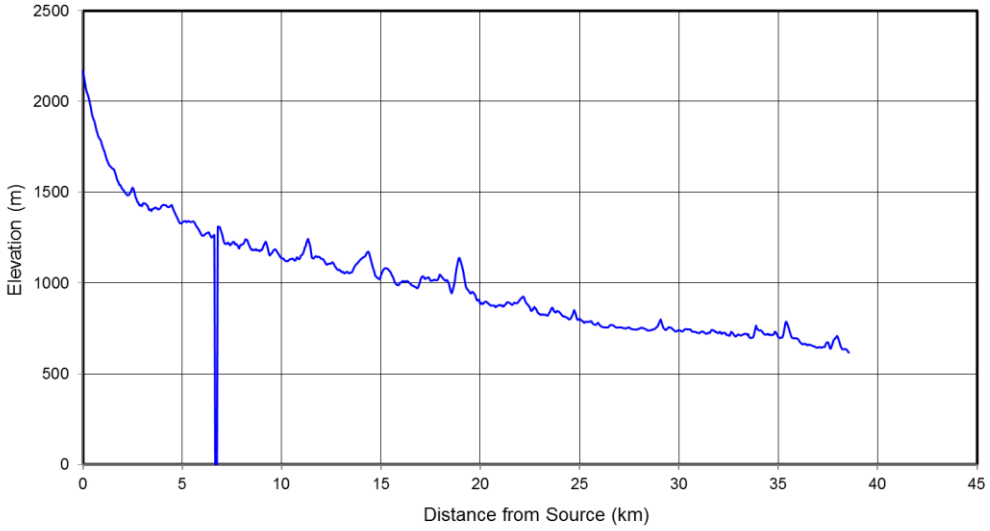

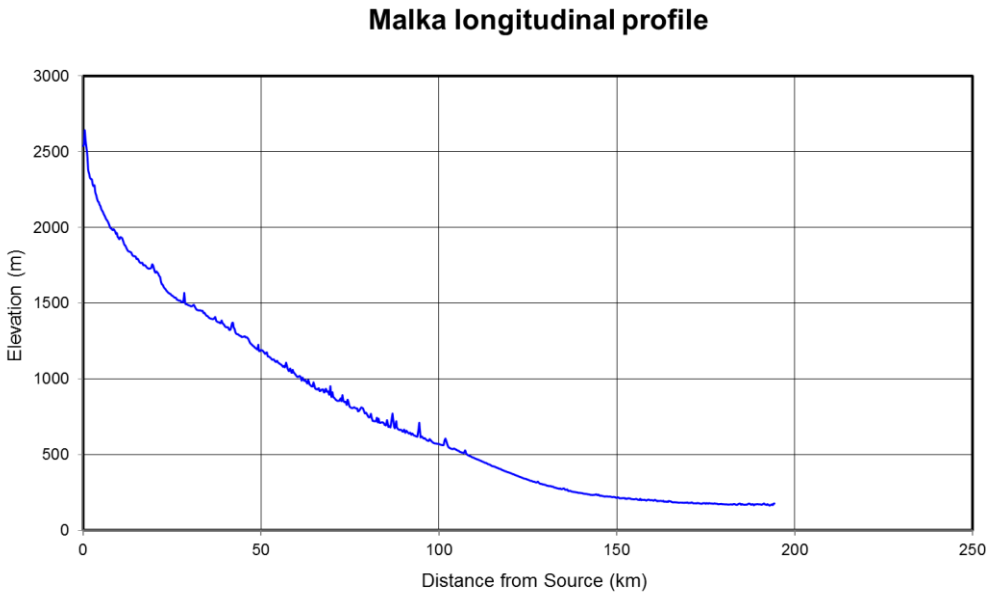
Malka longitudinal profile
Elevation (m)
3000
2500
2000
1500
1000
500
0
0
50
100
150
200
250
Distance from Source (km)

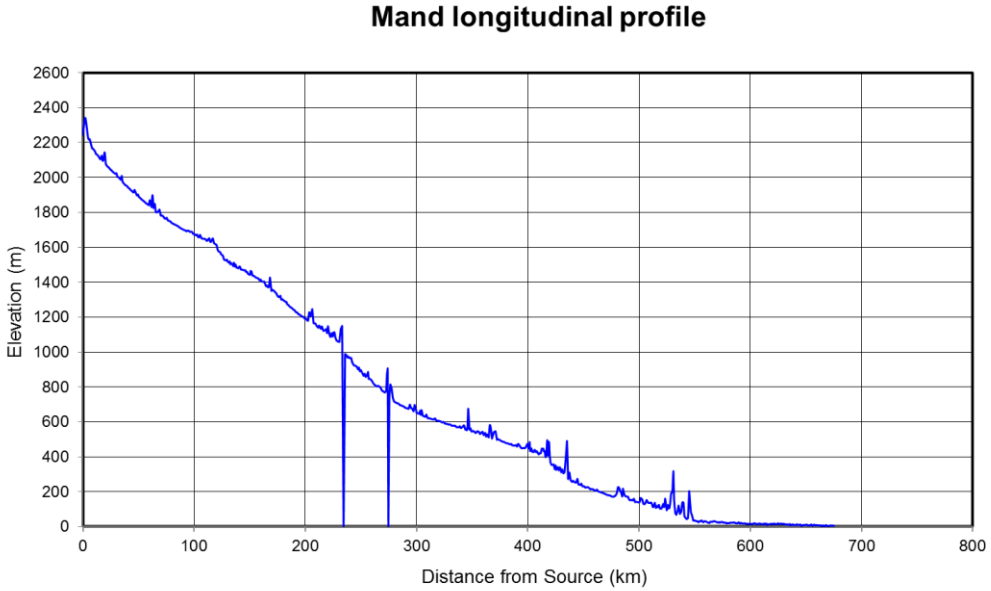
Mand longitudinal profile
Elevation (m)
2600
2400
2200
2000
1800
1600
1400
1200
1000
800
600
400
200
0
0
100
200
300
400
500
600
700
800
Distance from Source (km)

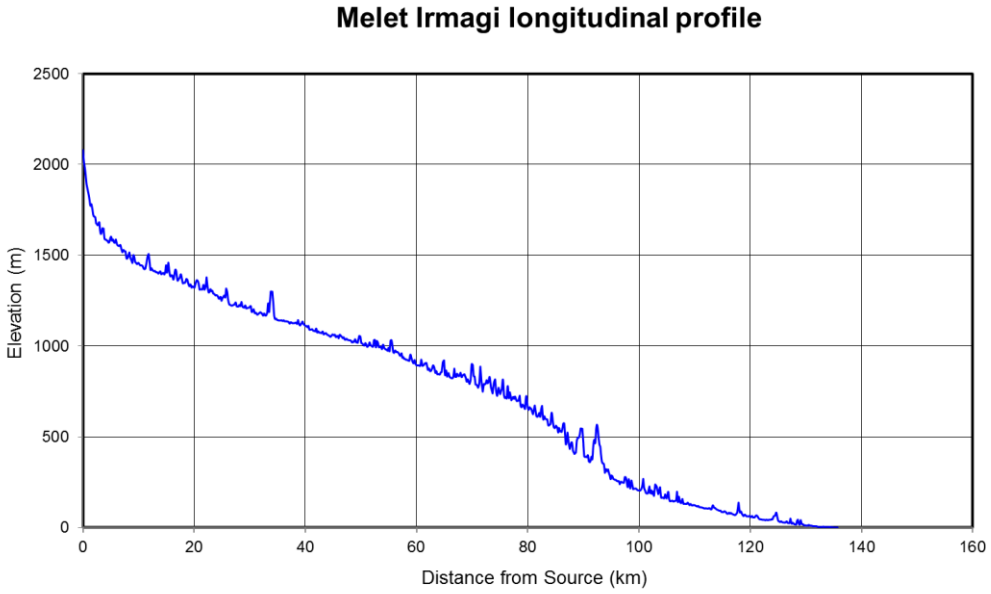
Melet Irmagi longitudinal profile
Elevation (m)
2500
2000
1500
1000
500
0
0
20
40
60
80
100
120
140
160
Distance from Source (km)

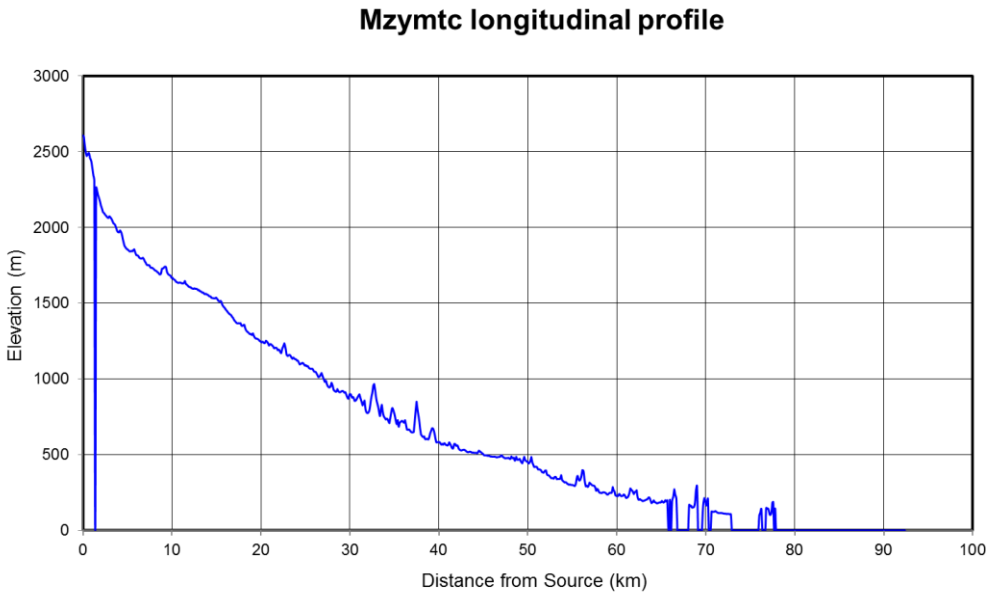
Mzymtc longitudinal profile
Elevation (m)
3000
2500
2000
1500
1000
500
0
0
10
20
30
40
50
60
70
80
90
100
Distance from Source (km)

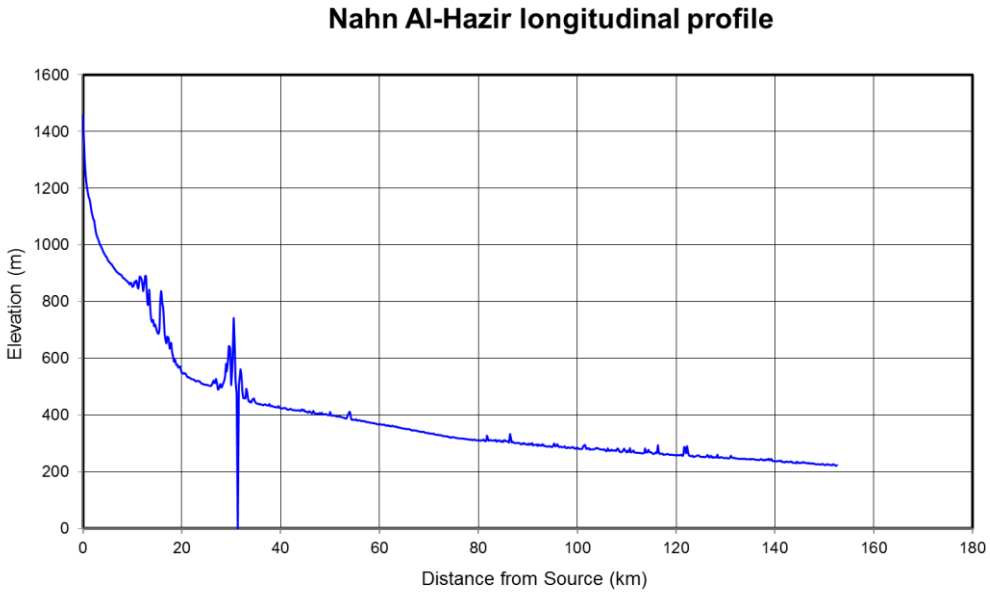
Nahn Al-Hazir longitudinal profile
Elevation (m)
1600
1400
1200
1000
800
600
400
200
0
0
20
40
60
80
100
120
140
160
180
Distance from Source (km)

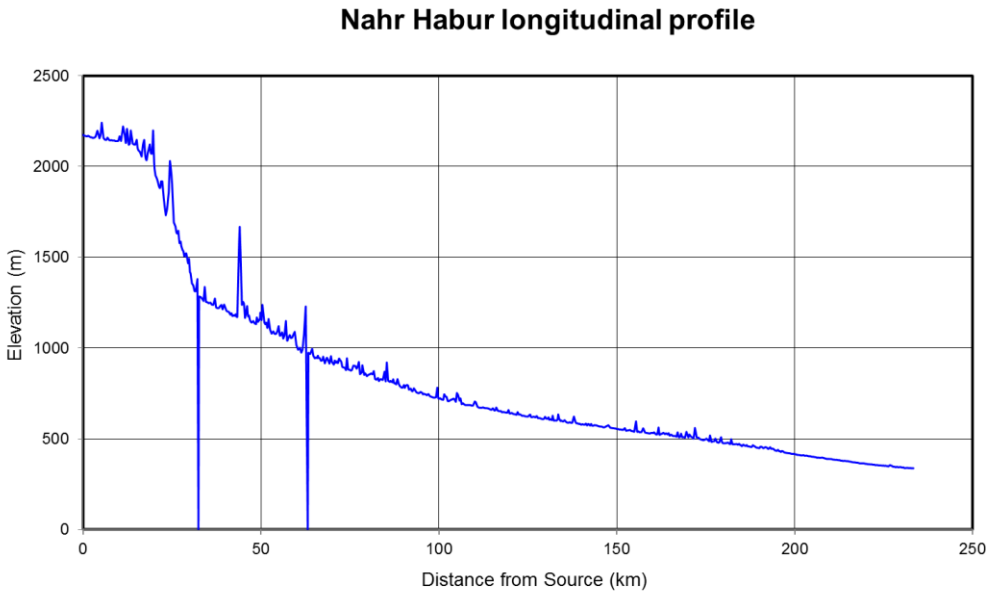
Nahr Habur longitudinal profile
Elevation (m)
2500
2000
1500
1000
500
0
0
50
100
150
200
250
Distance from Source (km)

Namaksar longitudinal profile

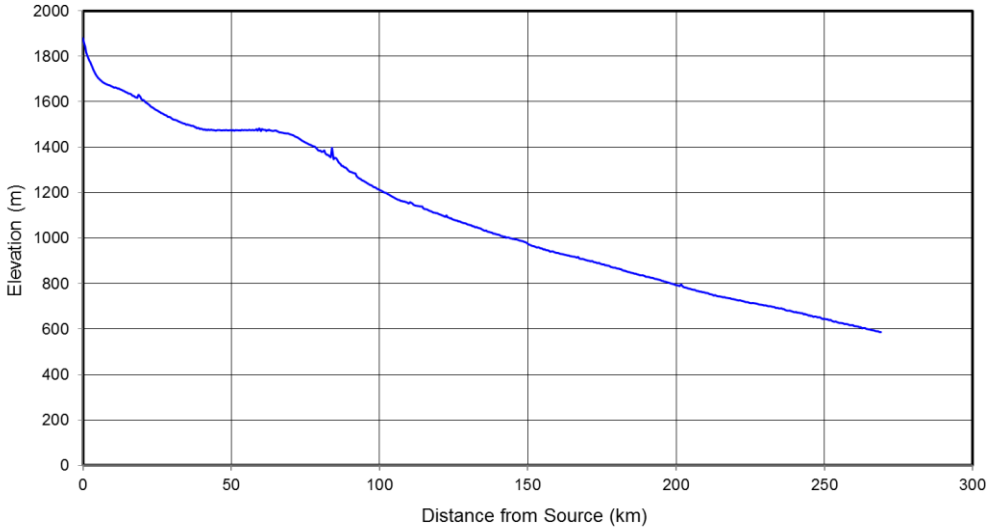

Nehri longitudinal profile

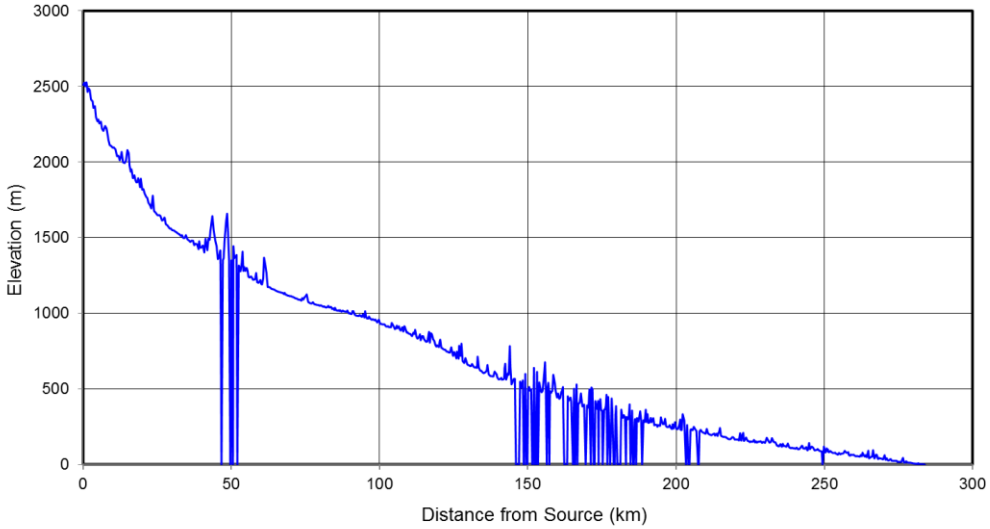

Nehri tributary A longitudinal profile

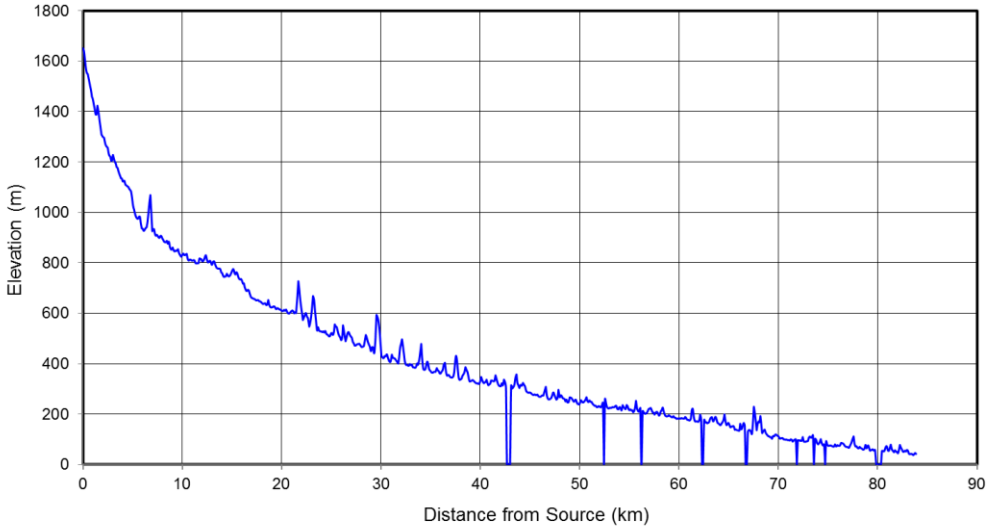

Nehri tributary B longitudinal profile

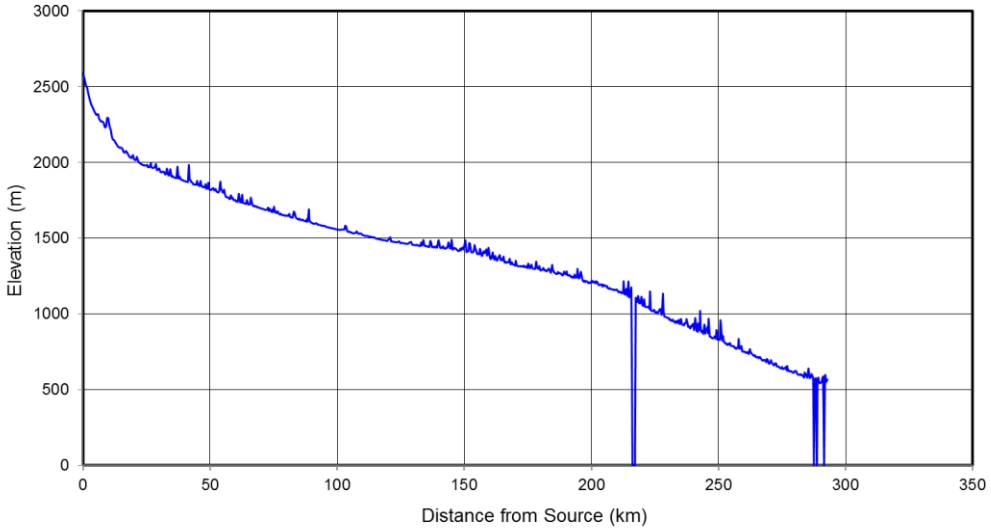

Oltu Cayi longitudinal profile

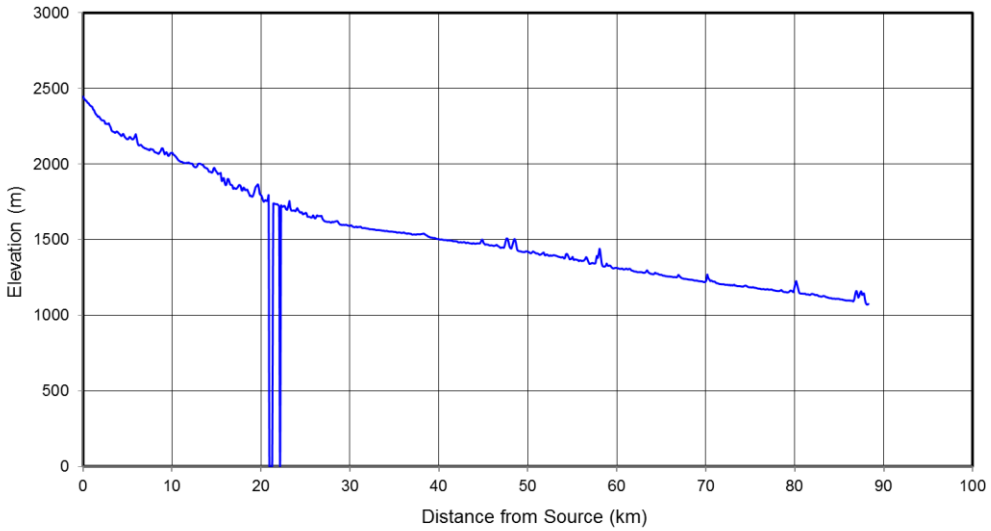

Qara Cay longitudinal profile

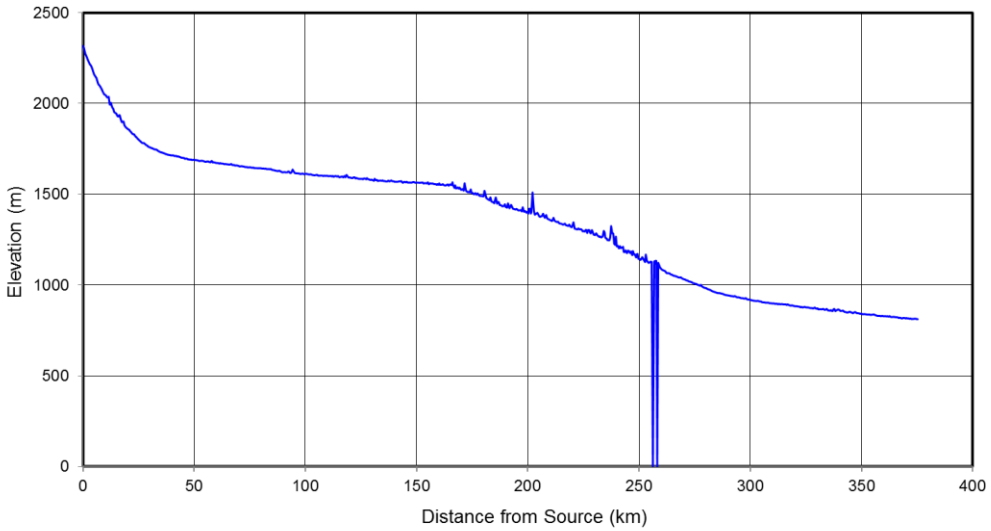

Qolleh-Ye Damavand longitudinal profile

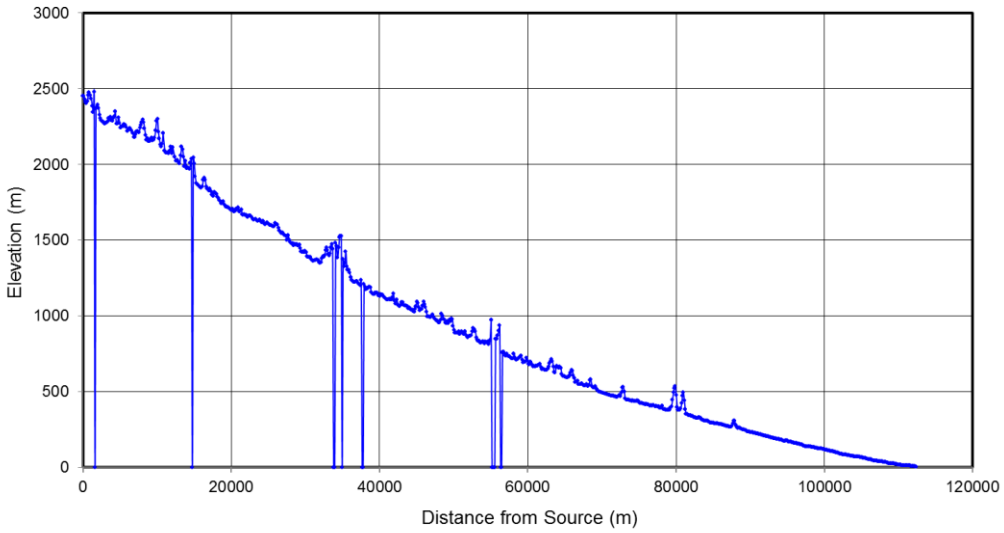

Qolleh-Ye Damavand tributary A longitudinal profile

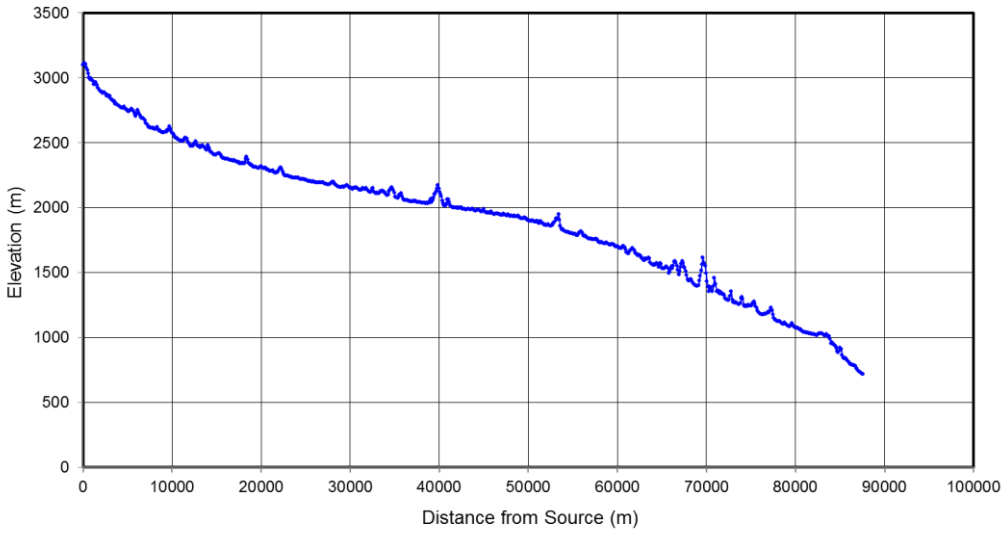

Qom longitudinal profile

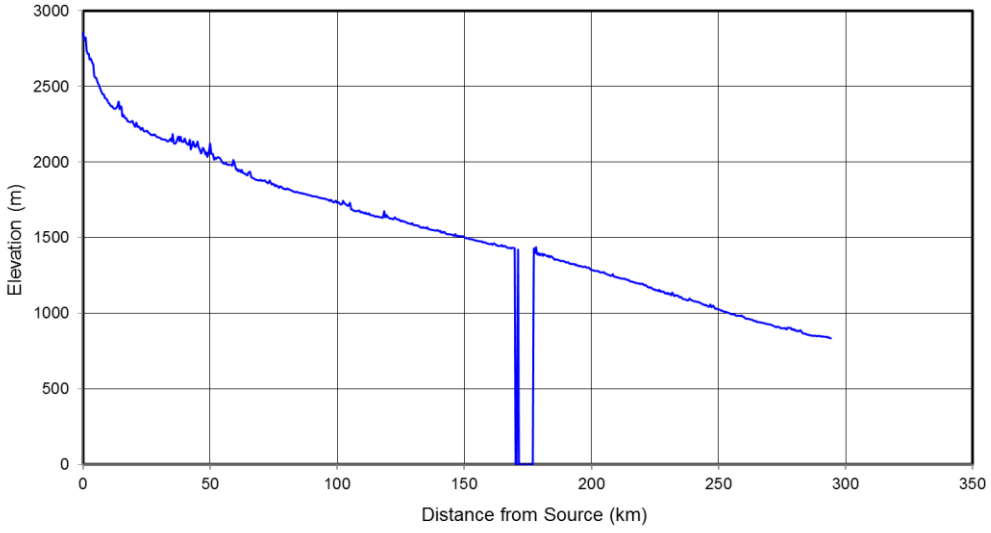

Riani longitudinal profile

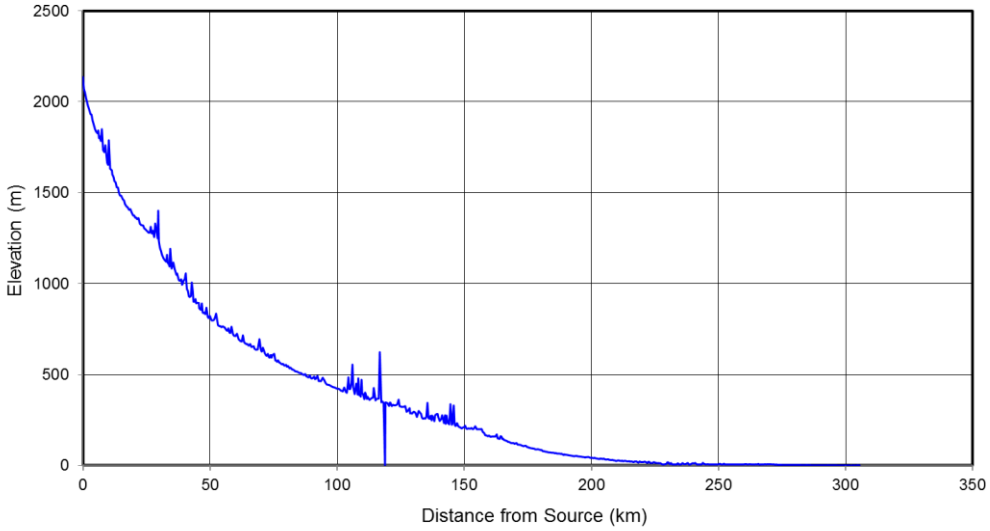

Riani tributary A longitudinal profile

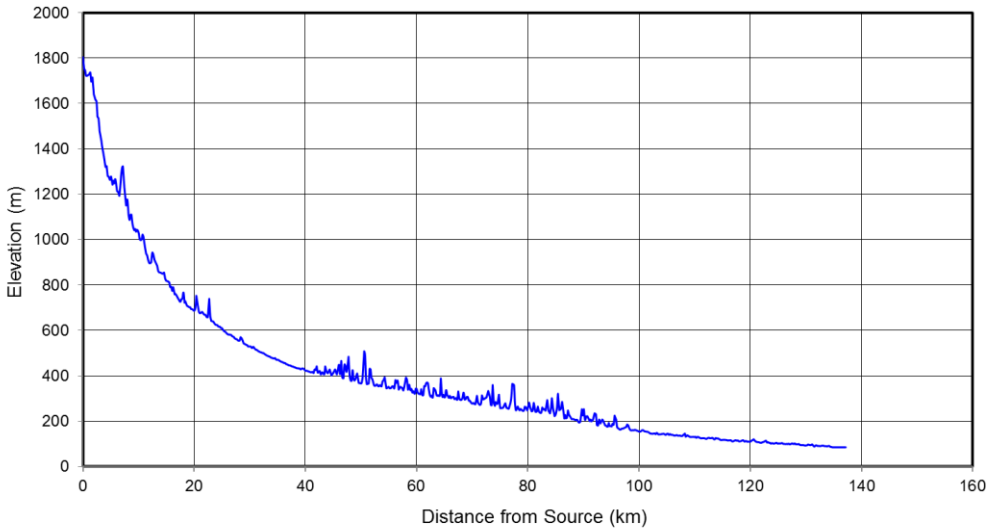

Rubar Haggi-Beg longitudinal profile

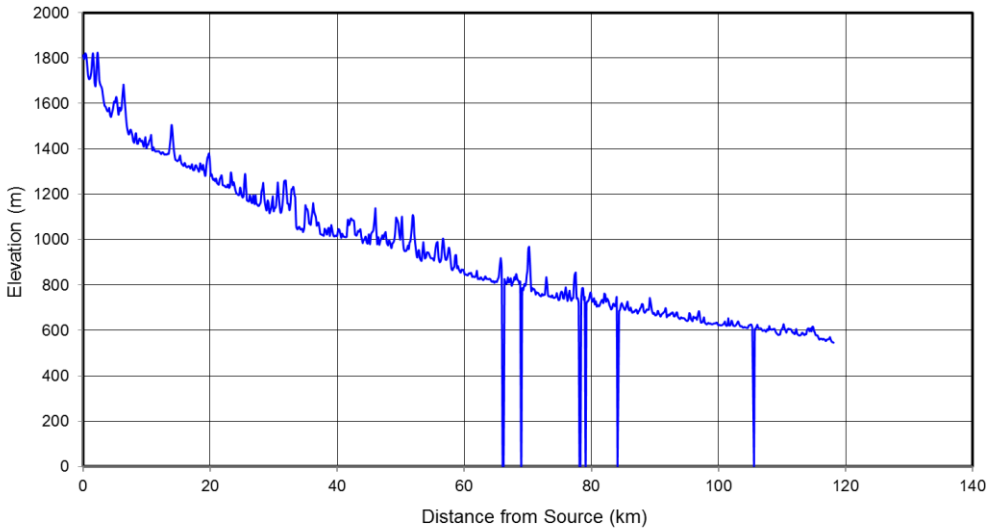

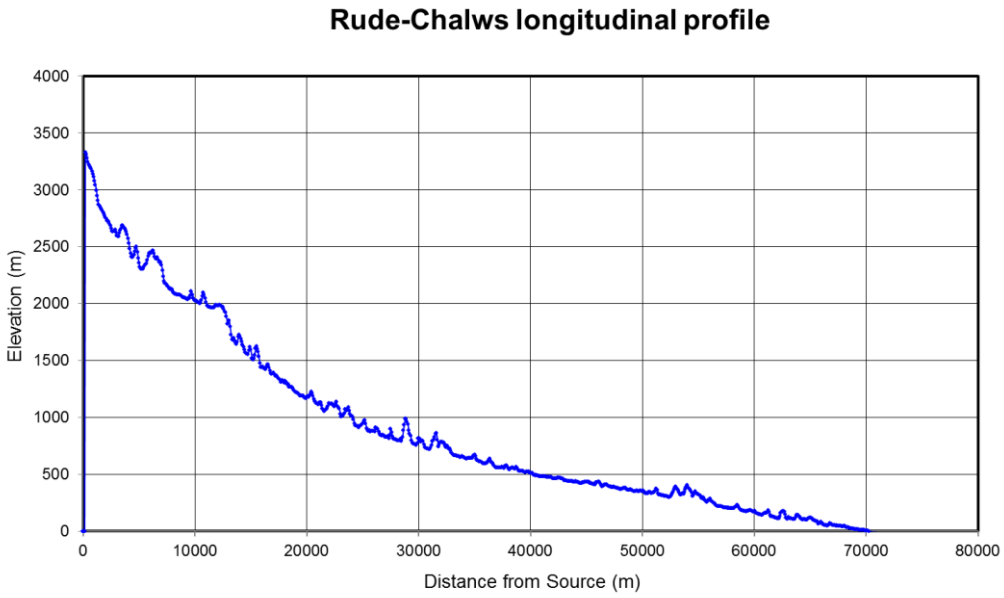
Rude-Chalws longitudinal profile
Elevation (m)
4000
3500
3000
2500
2000
1500
1000
500
0
0
10000
20000
30000
40000
50000
60000
70000
80000
Distance from Source (m)

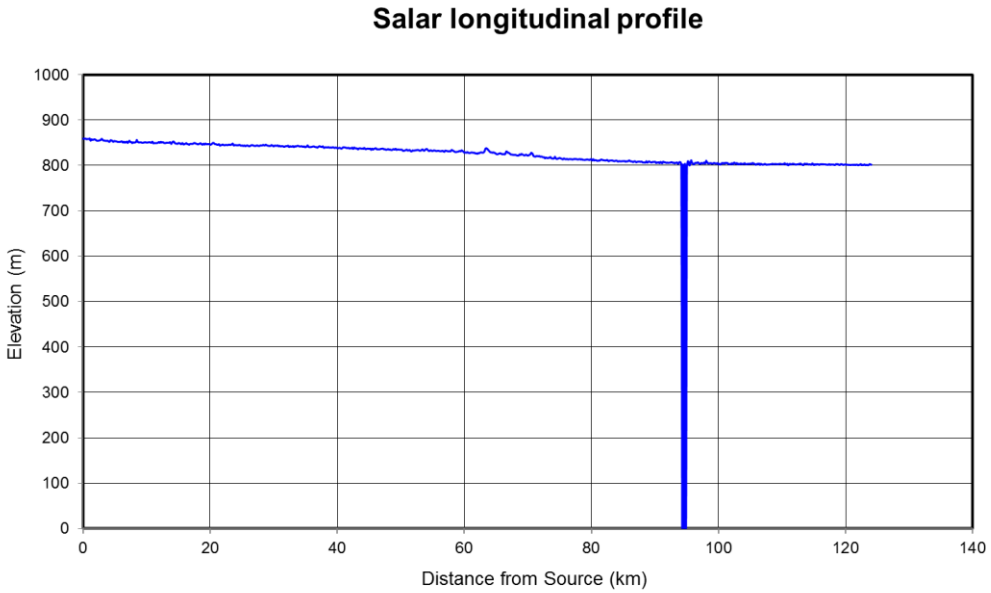
Salar longitudinal profile
Elevation (m)
1000
900
800
700
600
500
400
300
200
100
0
0
20
40
60
80
100
120
140
Distance from Source (km)

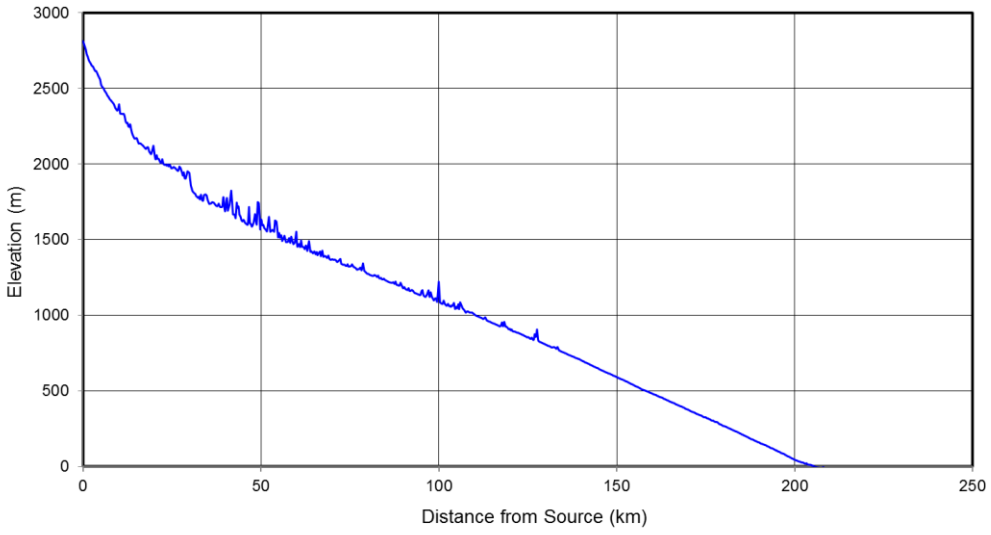
Samur longitudinal profile
Elevation (m)
3000
2500
2000
1500
1000
500
0
0
50
100
150
200
250
Distance from Source (km)

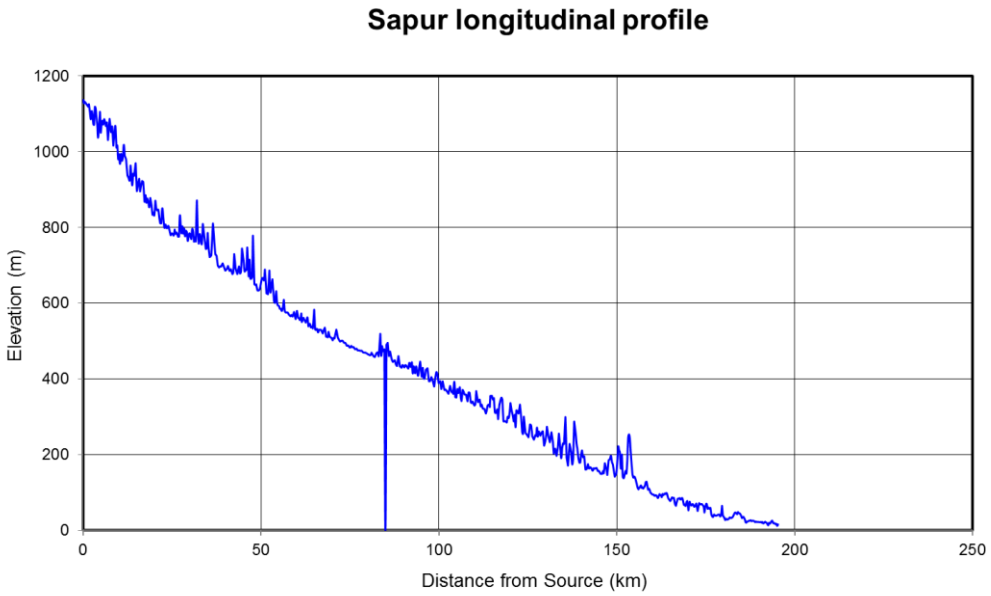
Sapur longitudinal profile
Elevation (m)
1200
1000
800
600
400
200
0
0
50
100
150
200
250
Distance from Source (km)

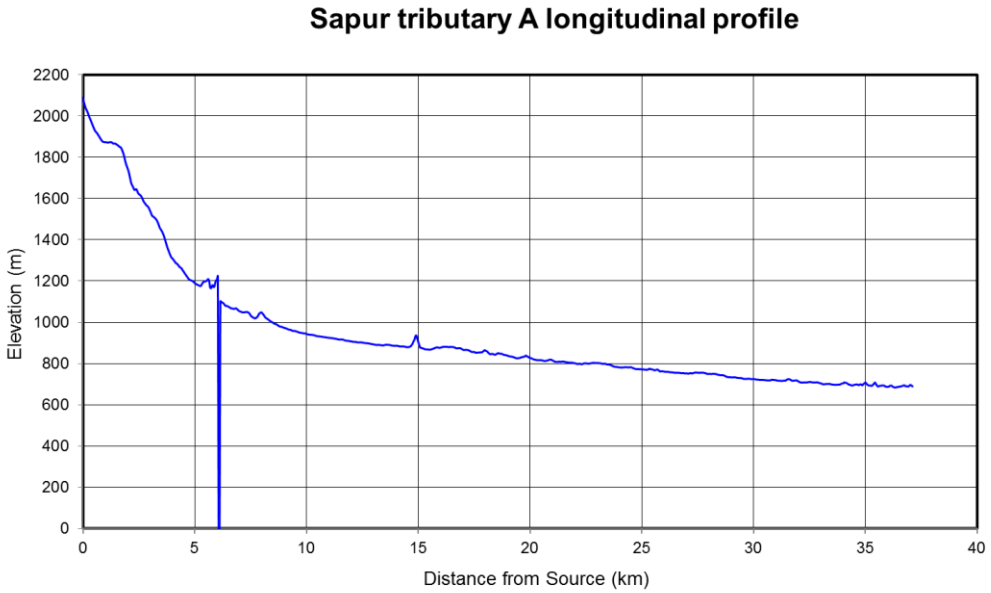
Sapur tributary A longitudinal profile
Elevation (m)
2200
2000
1800
1600
1400
1200
1000
800
600
400
200
0
0
5
10
15
20
25
30
35
40
Distance from Source (km)

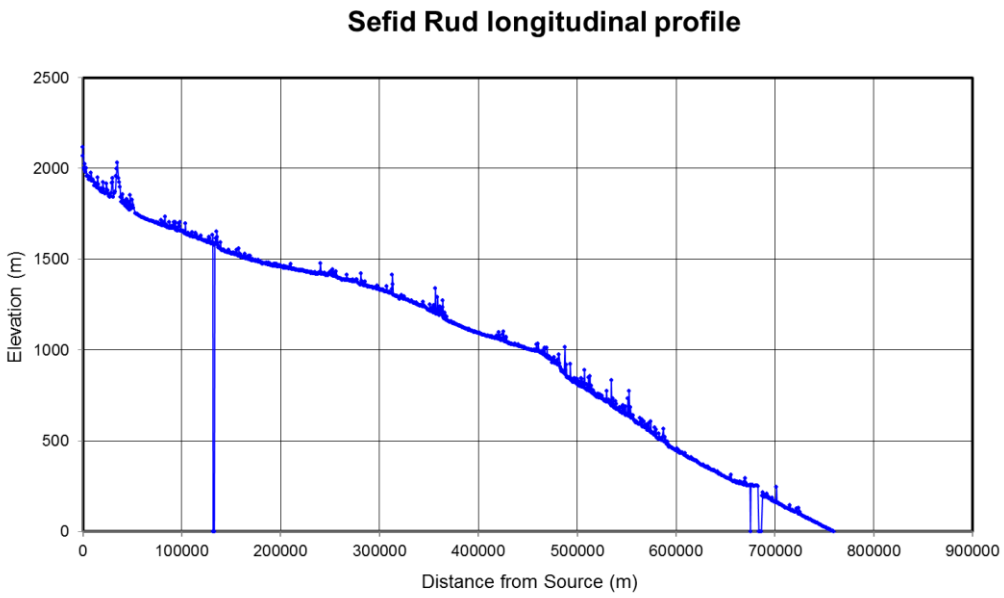
Sefid Rud longitudinal profile
Elevation (m)
2500
2000
1500
1000
500
0
0
100000
200000
300000
400000
500000
600000
700000
800000
900000
Distance from Source (m)

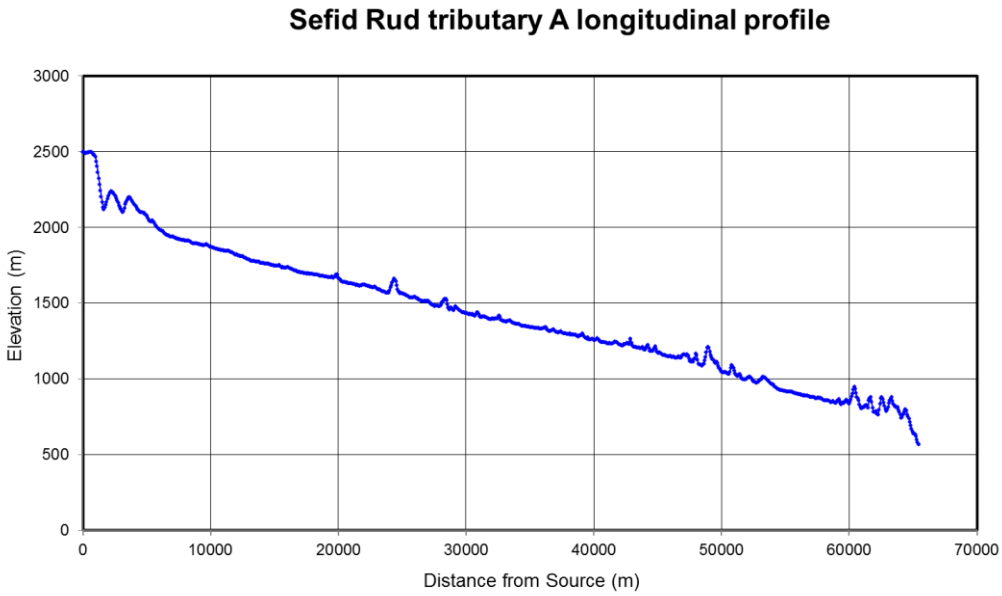
Sefid Rud tributary A longitudinal profile
Elevation (m)
3000
2500
2000
1500
1000
500
0
0
10000
20000
30000
40000
50000
60000
70000
Distance from Source (m)

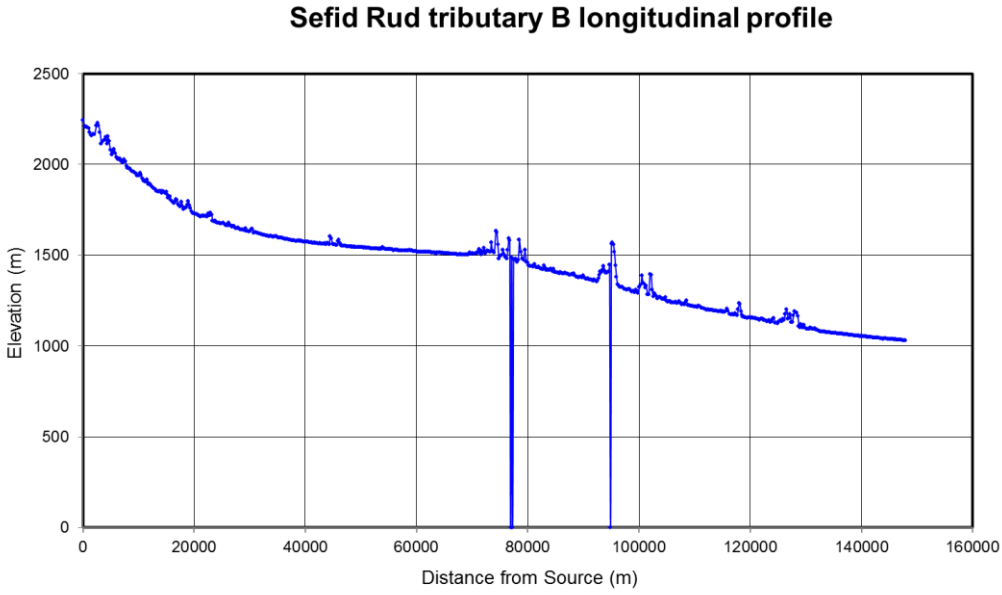
Sefid Rud tributary B longitudinal profile
Elevation (m)
2500
2000
1500
1000
500
0
0
20000
40000
60000
80000
100000
120000
140000
160000
Distance from Source (m)

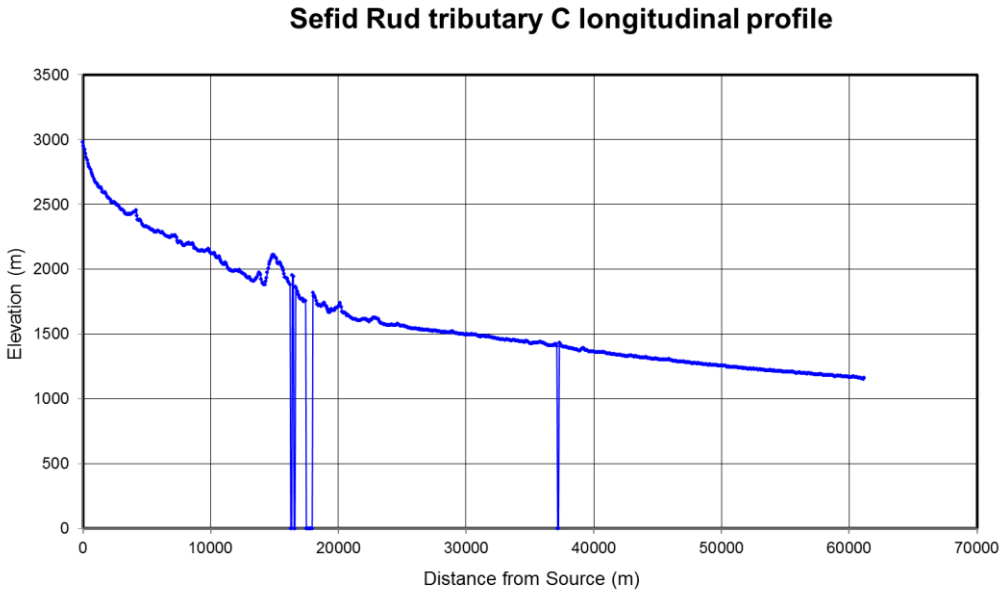
Sefid Rud tributary C longitudinal profile
Elevation (m)
3500
3000
2500
2000
1500
1000
500
0
0
10000
20000
30000
40000
50000
60000
70000
Distance from Source (m)

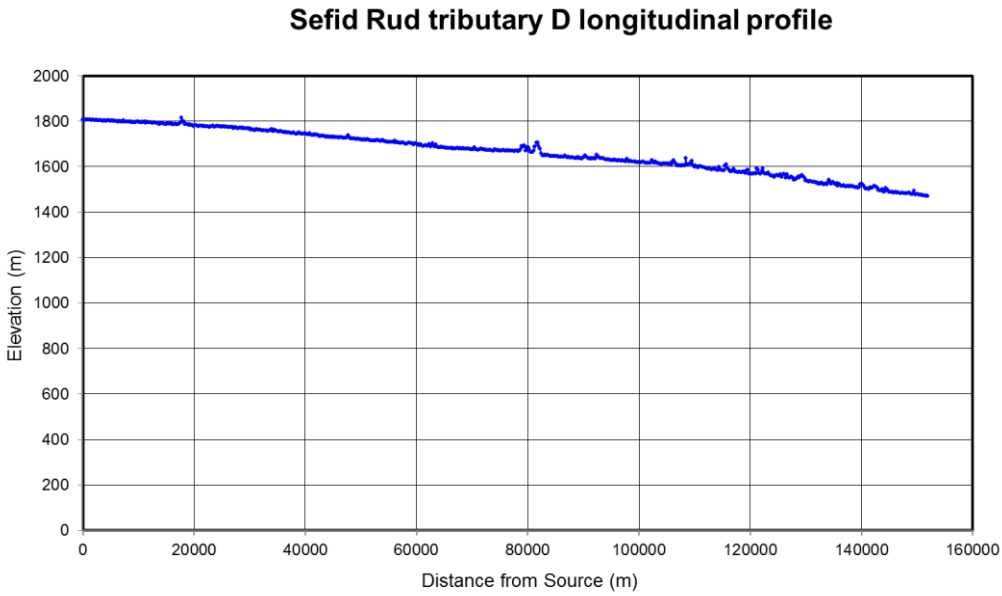
Sefid Rud tributary D longitudinal profile
Elevation (m)
2000
1800
1600
1400
1200
1000
800
600
400
200
0
0
20000
40000
60000
80000
100000
120000
140000
160000
Distance from Source (m)

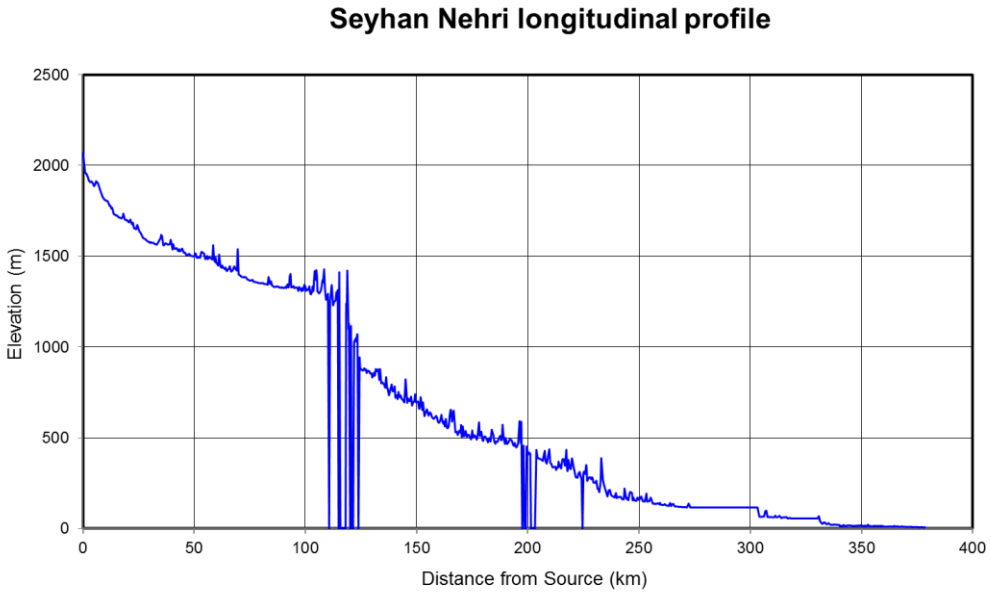
Seyhan Nehri longitudinal profile
Elevation (m)
2500
2000
1500
1000
500
0
0
50
100
150
200
250
300
350
400
Distance from Source (km)

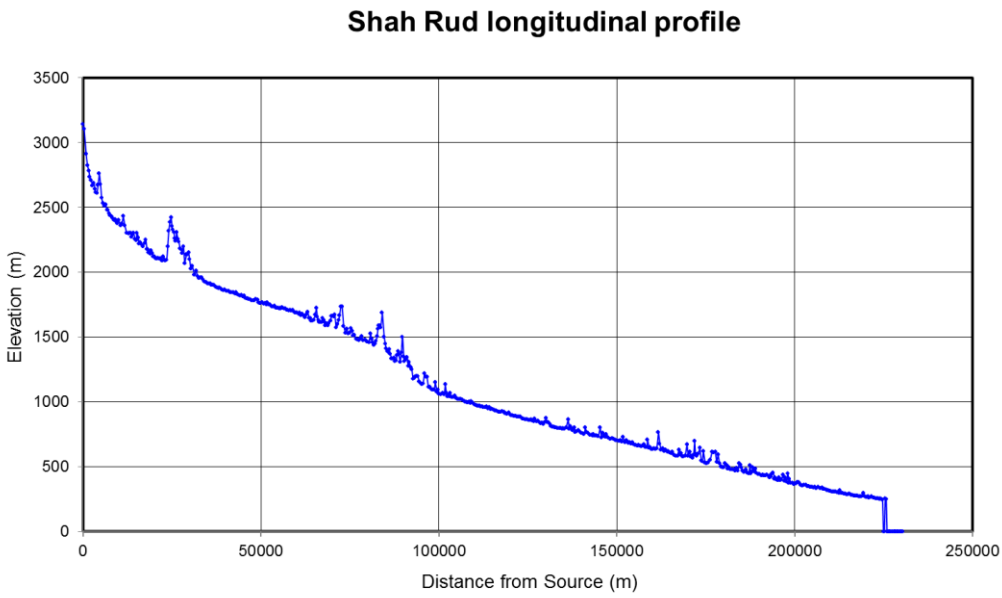
Shah Rud longitudinal profile
Elevation (m)
3500
3000
2500
2000
1500
1000
500
0
0
50000
100000
150000
200000
250000
Distance from Source (m)

Sirvan longitudinal profile

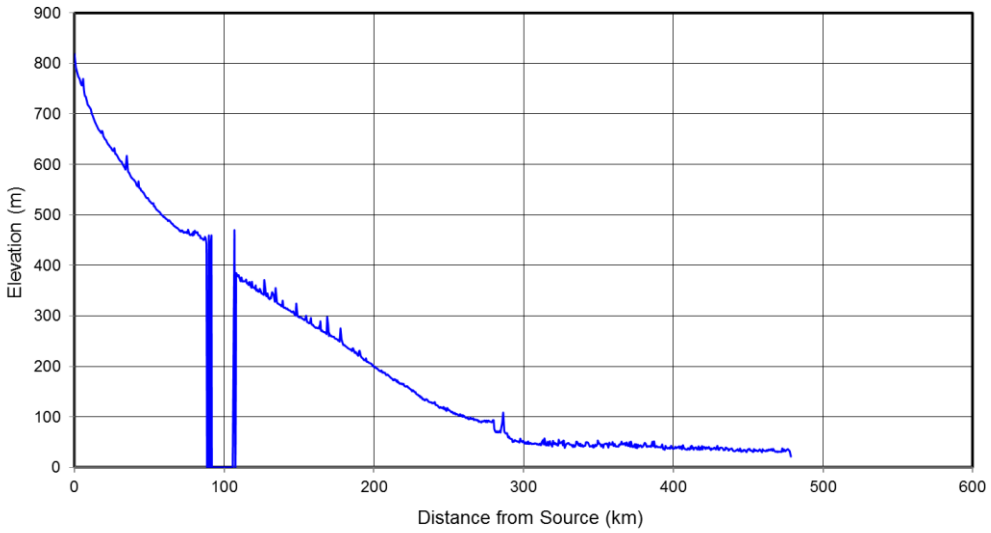

Sulak Andiyskoy longitudinal profile

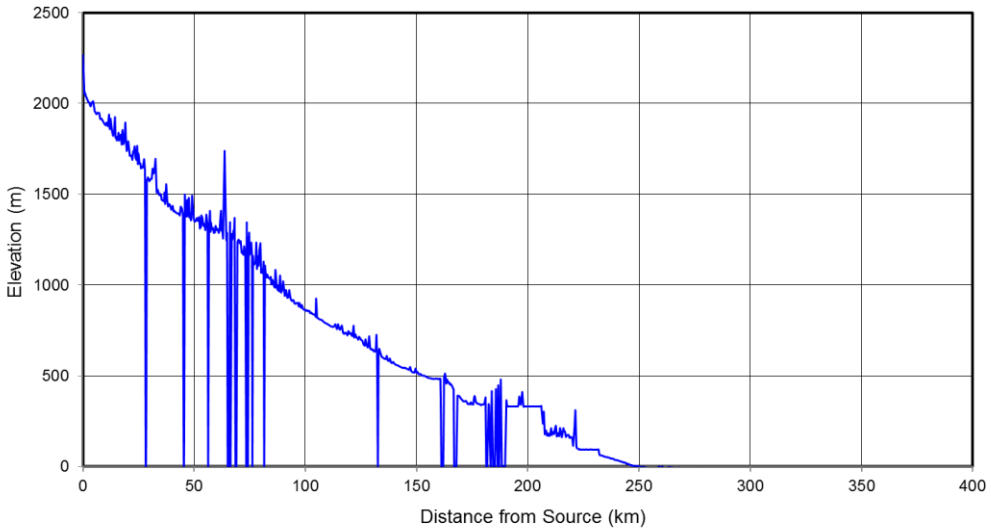

Supsa longitudinal profile

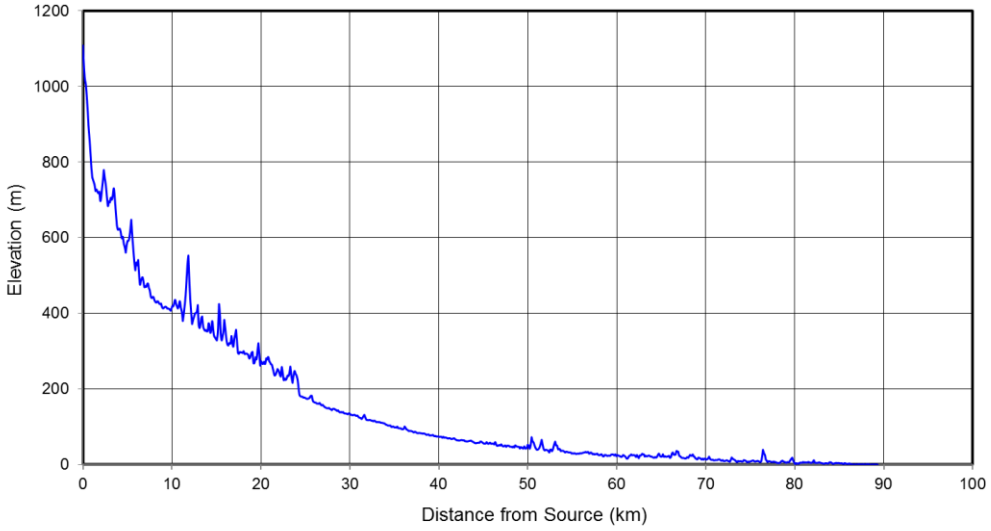

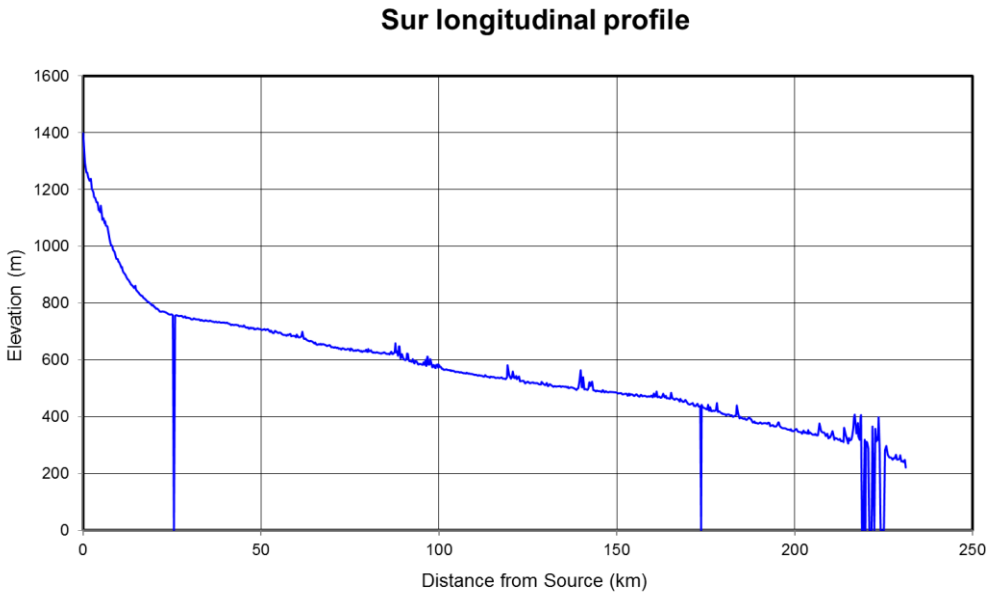
Sur longitudinal profile
Elevation (m)
1600
1400
1200
1000
800
600
400
200
0
0
50
100
150
200
250
Distance from Source (km)

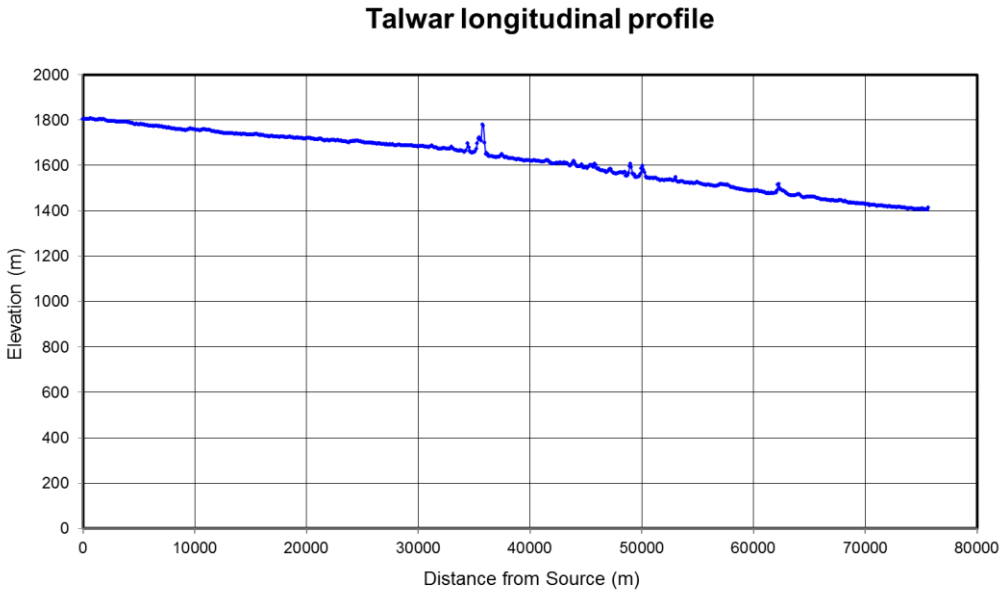
Talwar longitudinal profile
Elevation (m)
2000
1800
1600
1400
1200
1000
800
600
400
200
0
0
10000
20000
30000
40000
50000
60000
70000
80000
Distance from Source (m)

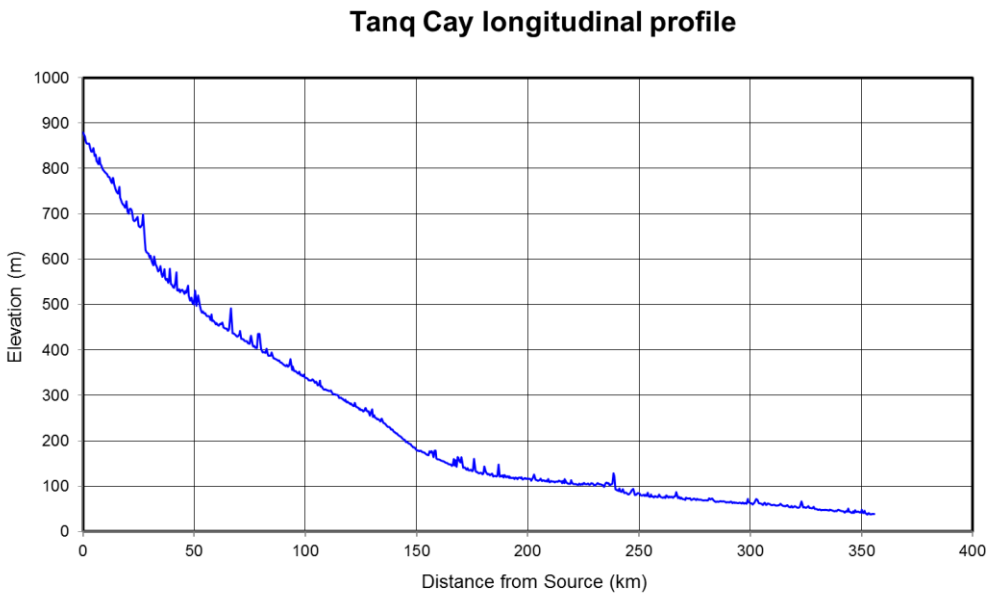
Tanq Cay longitudinal profile
Elevation (m)
1000
900
800
700
600
500
400
300
200
100
0
0
50
100
150
200
250
300
350
400
Distance from Source (km)

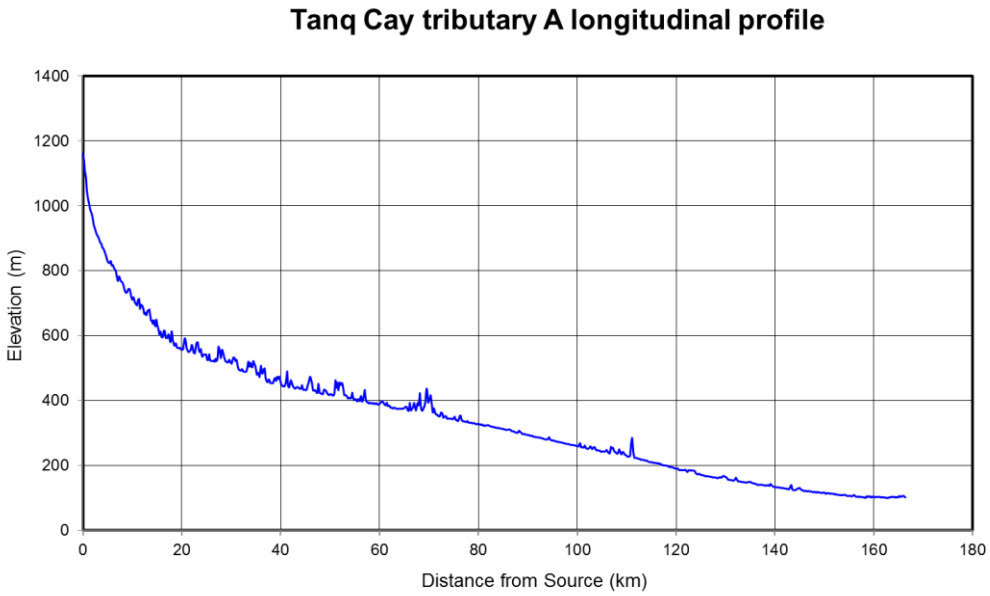
Tanq Cay tributary A longitudinal profile
Elevation (m)
1400
1200
1000
800
600
400
200
0
0
20
40
60
80
100
120
140
160
180
Distance from Source (km)

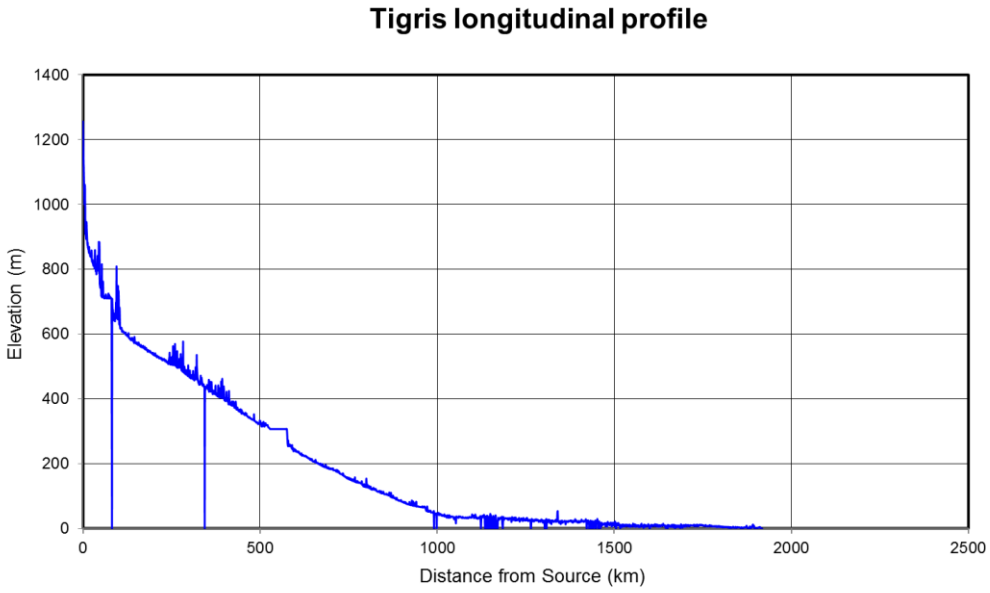
Tigris longitudinal profile
Elevation (m)
1400
1200
1000
800
600
400
200
0
0
500
1000
1500
2000
2500
Distance from Source (km)

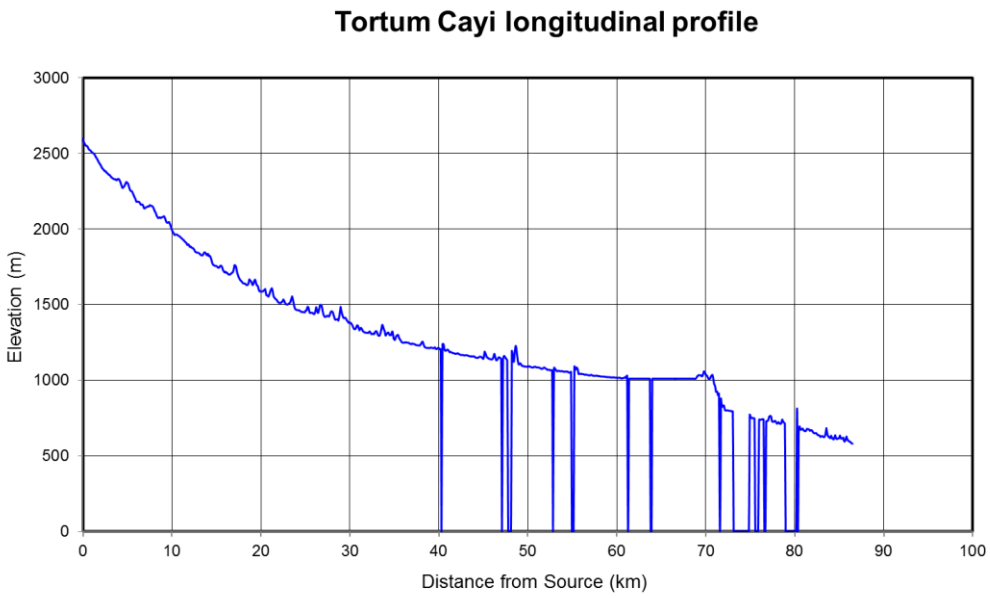
Tortum Cayi longitudinal profile
Elevation (m)
3000
2500
2000
1500
1000
500
0
0
10
20
30
40
50
60
70
80
90
100
Distance from Source (km)

Tozanli Irmagi longitudinal profile

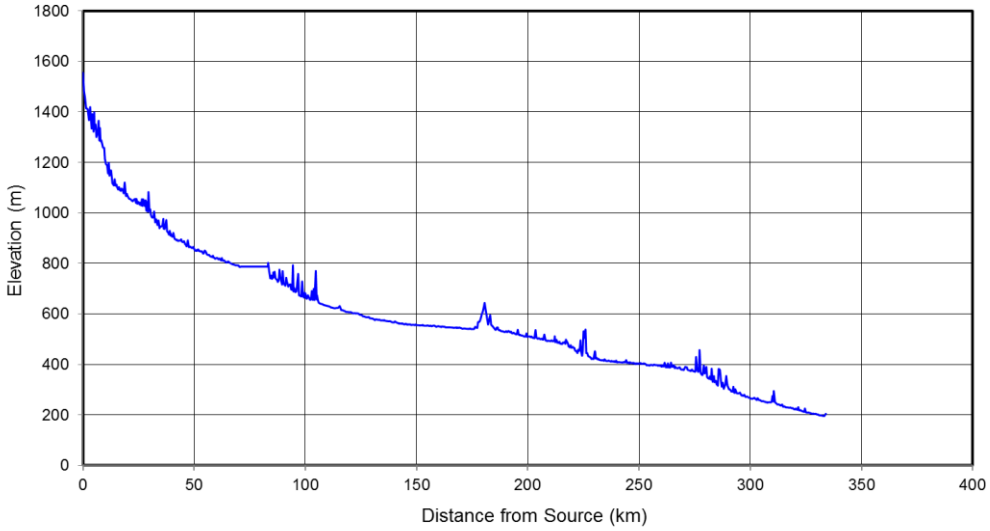

Tskhenis longitudinal profile

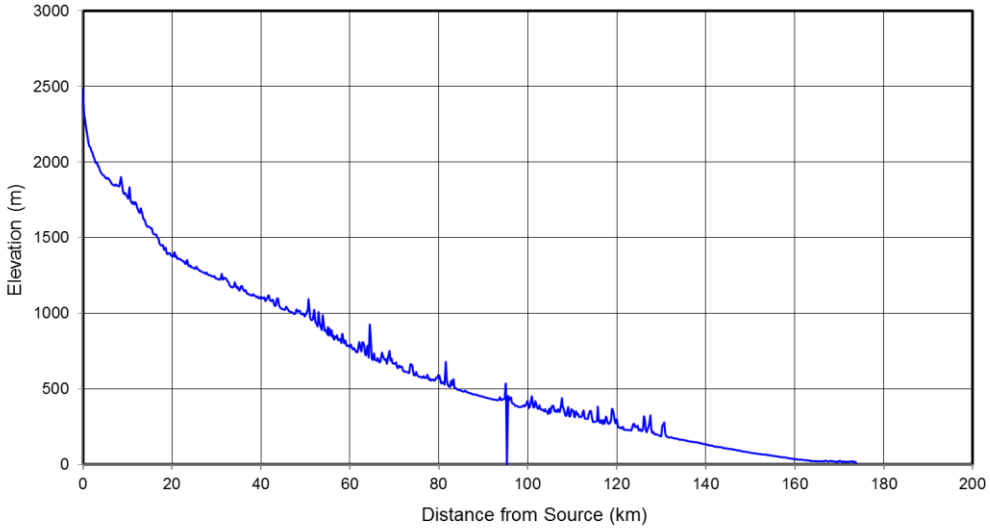

Urukh longitudinal profile

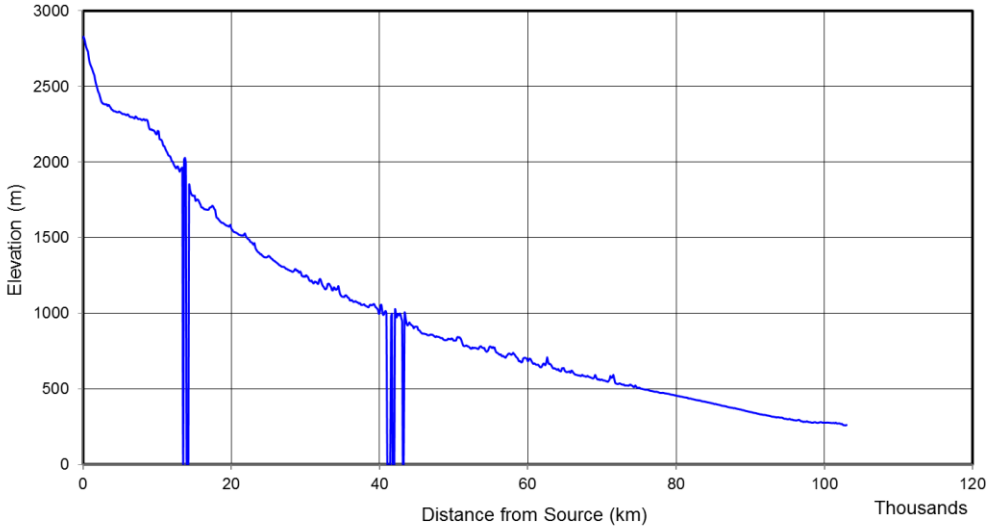

Urup longitudinal profile

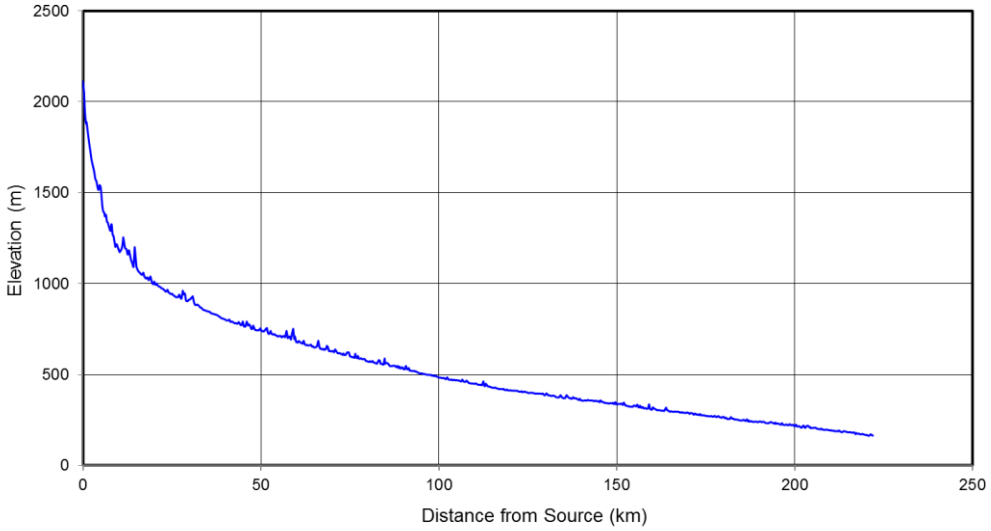

Yanarsu Cayi longitudinal profile

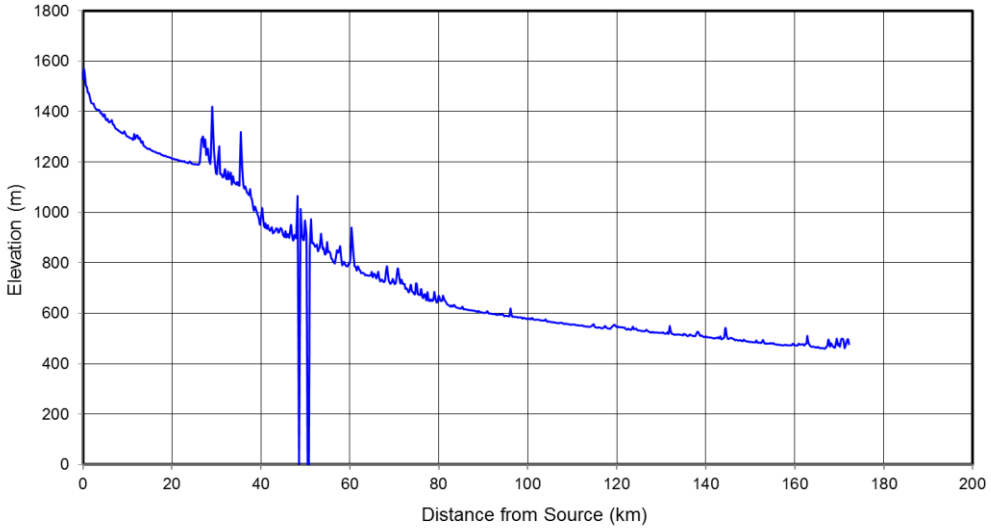

Yesilirmak longitudinal profile

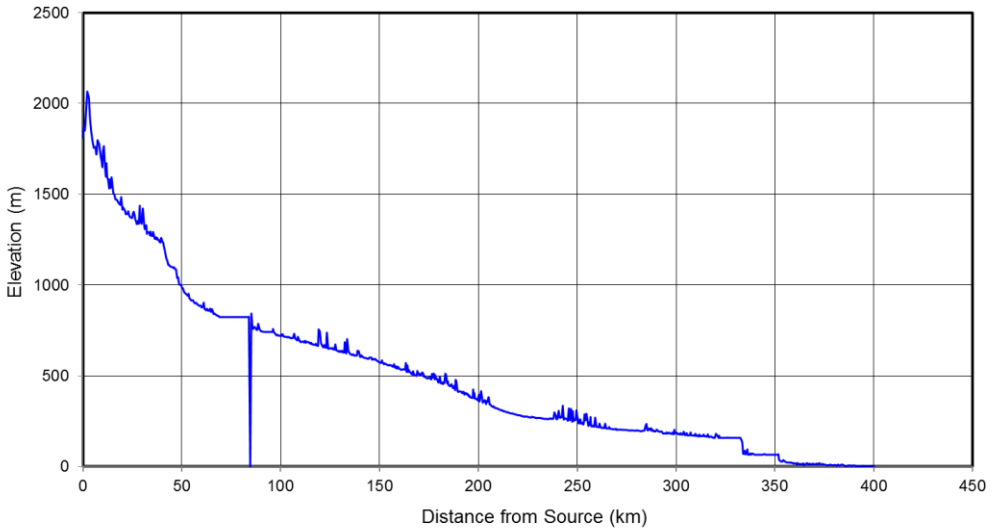

Yesilirmak tributary A Irmagi longitudinal profile

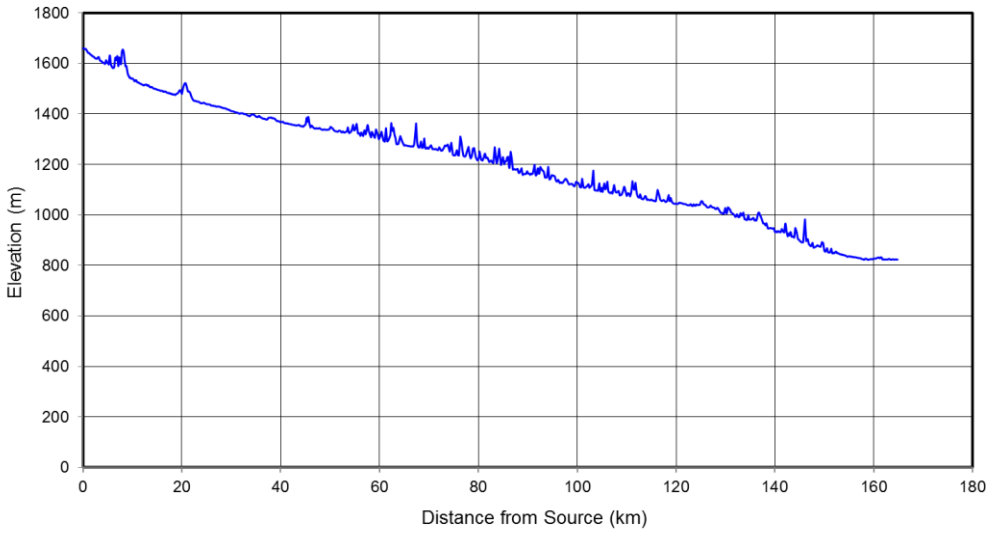

Zaindeh Rud longitudinal profile

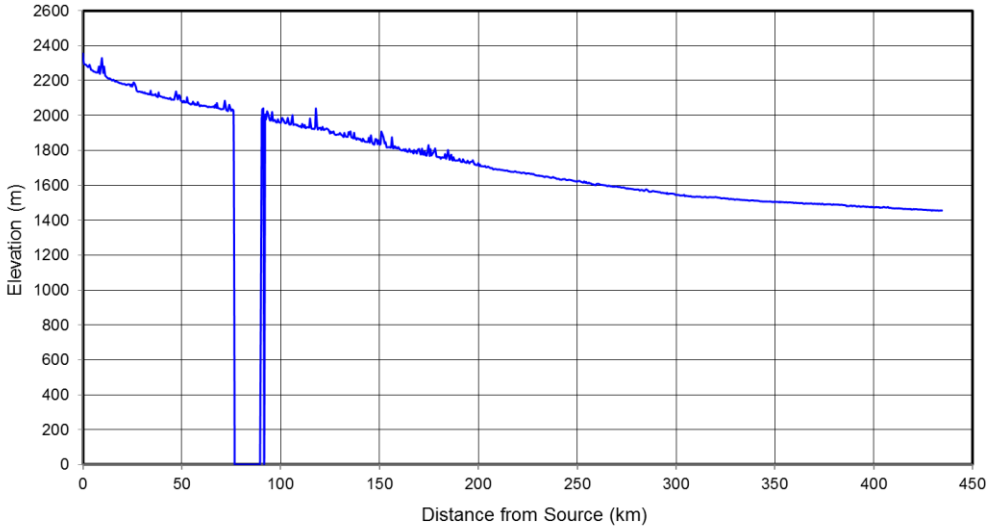

Zamani longitudinal profile

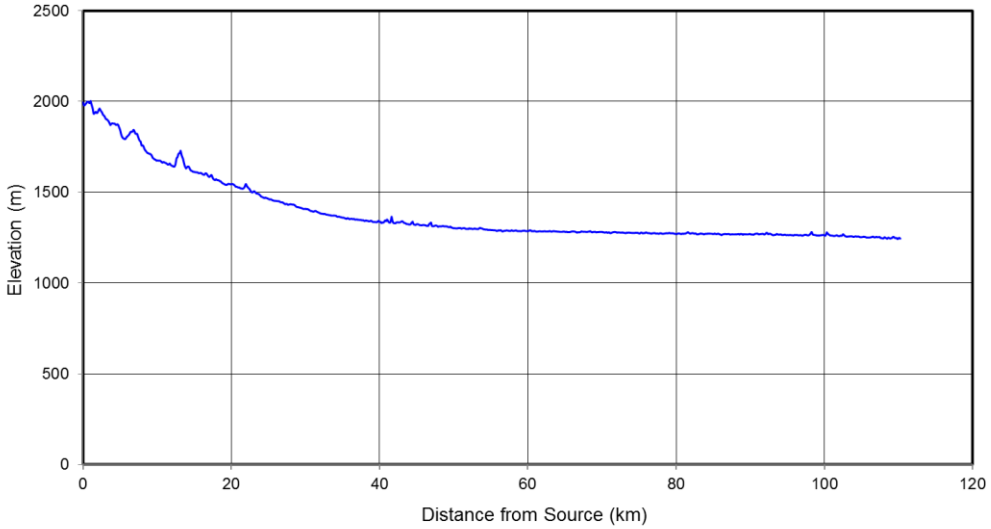

Zelenchuk longitudinal profile

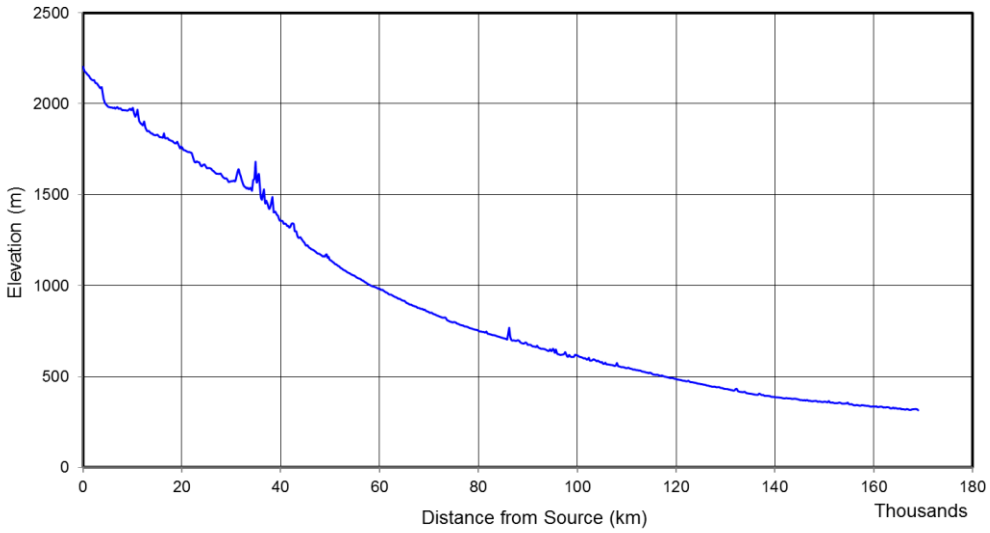

Zelenchuk tributary A longitudinal profile

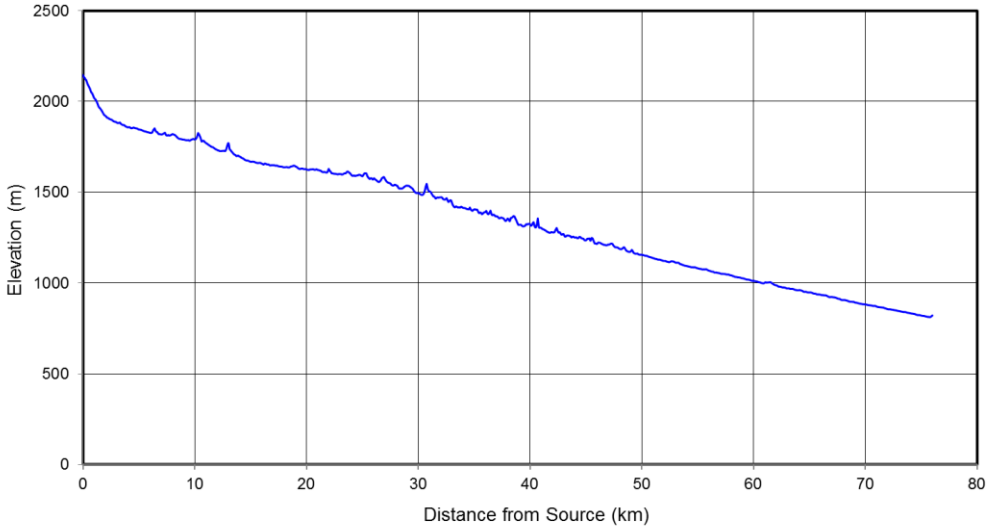

Bibliography

Ahmadhadi, F., Lacombe, O., and Daniel, J. M., 2007, Early reactivation of basement faults in Central Zagros (SW Iran): evidence from pre-folding fracture populations in Asmari Formation and lower Tertiary paleogeography: Thrust Belts and Foreland Basins, p. 205-228.

Ahnert, F., 1998, Introduction to geomorphology, London, Arnold, 352p. p.:

Aitchison, J. C., Ali, J. R., and Davis, A. M., 2007, When and where did India and Asia collide?: Journal of Geophysical Research, v. 112, no. B5.

Akansu, A. N., and Haddad, P. R., 2000, Multiresolution signal decomposition: transforms, subbands, and wavelets, Academic Press.

Al-Farraj, A., and Harvey, A. M., 2000, Desert pavement characteristics on wadi terrace and alluvial fan surfaces: Wadi Al-Bih, UAE and Oman: Geomorphology, v. 35, no. 3, p. 279-297.

Allen, M., Jackson, J., and Walker, R., 2004, Late Cenozoic reorganization of the Arabia-Eurasia collision and the comparison of short-term and long-term deformation rates: Tectonics, v. 23, no. 2, p. -.

Allen, M. B., and Davies, C. E., 2007, Unstable Asia: active deformation of Siberia revealed by drainage shifts: Basin Research, v. 19, no. 3, p. 379-392.

Allen, M. B., Ghassemi, M. R., Shahrabi, M., and Qorashi, M., 2003, Accommodation of late Cenozoic oblique shortening in the Alborz range, northern Iran: Journal of Structural Geology, v. 25, no. 5, p. 659-672.

Allen, M. B., Kheirkhah, M., Emami, M. H., and Jones, S. J., 2011a, Right-lateral shear across Iran and kinematic change in the Arabia-Eurasia collision zone: Geophysical Journal International, v. 184, no. 2, p. 555-574.

Allen, M. B., Mark, D. F., Kheirkhah, M., Barfod, D., Emami, M. H., and Saville, C., 2011b, 40Ar/39Ar dating of Quaternary lavas in northwest Iran: constraints on the landscape evolution and incision rates of the Turkish-Iranian plateau: Geophysical Journal International, v. 185, no. 3, p. 1175-1188.

Allen, P. A., 2008, From landscapes into geological history: Nature, v. 451, no. 7176, p. 274-276.

Allen, P. A., and Allen, J. R., 2005, Basin analysis : principles and applications, Malden, MA, Blackwell Pub, ix, 549 p.:

Allen, P. A., and Densmore, A. L., 2000, Sediment flux from an uplifting fault block: Basin Research, v. 12, no. 3-4, p. 367-380.

Allen, P. A., and Hovius, N., 1998, Sediment supply from landslide-dominated catchments: implications for basin-margin fans: Basin Research, v. 10, no. 1, p. 19-35.

Amos, C. B., and Burbank, D. W., 2007, Channel width response to differential uplift: Journal of Geophysical Research, v. 112, no. F2.

Andronicos, C. L., Velasco, A. A., and Hurtado, J. M., 2007, Large-scale deformation in the India-Asia collision constrained by earthquakes and topography: Terra Nova, v. 19, no. 2, p. 105-119.

Armijo, R., Tapponnier, P., Mercier, J., and Tong-Lin, H., 1986, Quaternary extension in southern Tibet: Field observations and tectonic implications: Journal of Geophysical Research, v. 91, no. B14, p. 13803-13813.

Armitage, J. J., Duller, R. A., Whittaker, A. C., and Allen, P. A., 2011, Transformation of tectonic and climatic signals from source to sedimentary archive: Nature Geoscience, v. 4, no. 4, p. 231-235.

Axen, G. J., Lam, P. S., Grove, M., Stockli, D. F., and Hassanzadeh, J., 2001, Exhumation of the west-central Alborz Mountains, Iran, Caspian subsidence, and collision-related tectonics: Geology, v. 29, no. 6, p. 559-562.

Bahrami, S., 2012, Tectonic controls on the morphometry of alluvial fans around Danehkhoshk anticline, Zagros, Iran: Geomorphology, v. 180-181, p. 217-230.
Bassin, C., Laske, G., and Masters, G., 2000, AGU, 81 (2000), : F897.
Begin, Z. B., Meyer, D. F., and Schumm, S. A., 1981, Development of Longitudinal Profiles of Alluvial Channels in Response to Base-Level Lowering: Earth Surface Processes and Landforms, v. 6, no. 1, p. 49-68.
Bhang, K. J., Assessment and reduction of the vertical error in SRTM DEMs using Icesat, *in* Proceedings 2005 Salt Lake City Annual Meeting2005.
Bishop, P., 2007, Long-term landscape evolution: linking tectonics and surface processes: Earth Surface Processes and Landforms, v. 32, no. 3, p. 329-365.
Bishop, P., and Goldrick, G., 2000, Geomorphological evolution of the East Australian continental margin.
Bishop, P., Hoey, T. B., Jansen, J. D., and Artza, I. L., 2005, Knickpoint recession rate and catchment area: the case of uplifted rivers in Eastern Scotland: Earth Surface Processes and Landforms, v. 30, no. 6, p. 767-778.
Blum, M. D., and Tornqvist, T. E., 2000, Fluvial responses to climate and sea-level change: a review and look forward: Sedimentology, v. 47, p. 2-48.
Bollinger, L., Henry, P., and Avouac, J. P., 2006, Mountain building in the Nepal Himalaya: Thermal and kinematic model: Earth and Planetary Science Letters, v. 244, no. 1-2, p. 58-71.
Bolton, D., 1980, The computation of equivalent potential temperature: Monthly Weather Review, v. 108, no. 7, p. 1046-1053.
Bookhagen, B., and Burbank, D. W., 2006, Topography, relief, and TRMM-derived rainfall variations along the Himalaya: Geophysical Research Letters, v. 33, no. 8.
Bouwer, H., 1978, Groundwater hydrology, McGraw-Hill New York.
Brookfield, M. E., 1998, The evolution of the great river systems of southern Asia during the Cenozoic India-Asia collision: rivers draining southwards: Geomorphology, v. 22, no. 3-4, p. 285-312.
Bull, W. B., 1977, The alluvial-fan environment: Progress in Physical Geography, v. 1, no. 2, p. 222-270.
Burbank, D. W., Leland, J., Fielding, E., Anderson, R. S., Brozovic, N., Reid, M. R., and Duncan, C., 1996, Bedrock incision, rock uplift and threshold hillslopes in the northwestern Himalayas: Nature, v. 379, no. 6565, p. 505-510.
Carretier, S., and Lucazeau, F., 2005, How does alluvial sedimentation at range fronts modify the erosional dynamics of mountain catchments?: Basin Research, v. 17, no. 3, p. 361-381.
Carson, M. A., and Kirby, M., 1972, Hillslope Form and Process, The University Press.
Chang, H. H., 1979, Minimum stream power and river channel patterns: Journal of Hydrology, v. 41, no. 3, p. 303-327.
Clarke, L., Quine, T. A., and Nicholas, A., 2010, An experimental investigation of autogenic behaviour during alluvial fan evolution: Geomorphology, v. 115, no. 3-4, p. 278-285.
Clift, P. D., Giosan, L., BIusztajn, J., Campbell, I. H., Allen, C., Pringle, M., Tabrez, A. R., Danish, M., Rabbani, M. M., Alizai, A., Carter, A., and Lueckge, A., 2008, Holocene erosion of the Lesser Himalaya triggered by intensified summer monsoon: Geology, v. 36, no. 1, p. 79-82.
Codilean, A. T., Bishop, P., and Hoey, T. B., 2006, Surface process models and the links between tectonics and topography: Progress in Physical Geography, v. 30, no. 3, p. 307-333.
Cohen, S., Willgoose, G., and Hancock, G., 2008, A methodology for calculating the spatial distribution of the area-slope equation and the hypsometric integral within a catchment: Journal of Geophysical Research-Earth Surface, v. 113, no. F3.

Cook, K. L., and Royden, L. H., 2008, The role of crustal strength variations in shaping orogenic plateaus, with application to Tibet: Journal of Geophysical Research-Solid Earth, v. 113, no. B8.
Copley, A., Avouac, J. P., and Wernicke, B. P., 2011, Evidence for mechanical coupling and strong Indian lower crust beneath southern Tibet: Nature, v. 472, no. 7341, p. 79-81.
Craddock, W. H., Kirby, E., Harkins, N. W., Zhang, H., Shi, X., and Liu, J., 2010, Rapid fluvial incision along the Yellow River during headward basin integration: Nature Geoscience, v. 3, no. 3, p. 209-213.
Dade, W. B., and Verdeyen, M. E., 2007, Tectonic and climatic controls of alluvial-fan size and source-catchment relief: Journal of the Geological Society, v. 164, p. 353-358.
Dadson, S. J., Hovius, N., Chen, H., Dade, W. B., Lin, J. C., Hsu, M. L., Lin, C. W., Horng, M. J., Chen, T. C., Milliman, J., and Stark, C. P., 2004, Earthquake-triggered increase in sediment delivery from an active mountain belt: Geology, v. 32, no. 8, p. 733-736.
Dadson, S. J., Hovius, N., Chen, H. G., Dade, W. B., Hsieh, M. L., Willett, S. D., Hu, J. C., Horng, M. J., Chen, M. C., Stark, C. P., Lague, D., and Lin, J. C., 2003, Links between erosion, runoff variability and seismicity in the Taiwan orogen: Nature, v. 426, no. 6967, p. 648-651.
Denny, C. S., 1965, Alluvial fans in the Death Valley region, California and Nevada, US Government Printing Office.
Densmore, A. L., Allen, P. A., and Simpson, G., 2007, Development and response of a coupled catchment fan system under changing tectonic and climatic forcing: Journal of Geophysical Research-Earth Surface, v. 112, no. F1.
Devi, R. K. M., Bhakuni, S. S., and Bora, P. K., 2011, Neotectonic study along mountain front of northeast Himalaya, Arunachal Pradesh, India: Environmental Earth Sciences, v. 63, no. 4, p. 751-762.
Dewey, J. F., Shackleton, R. M., Chang, C. F., and Sun, Y. Y., 1988, The tectonic evolution of the Tibetan plateau: Philosophical Transactions of the Royal Society a-Mathematical Physical and Engineering Sciences, v. 327, no. 1594, p. 379-413.
Dorn, R. I., 2009, The role of climatic change in alluvial fan development: Geomorphology of Desert Environments, p. 723-742.
Duval, A., Kirby, E., and Burbank, D., 2004, Tectonic and lithologic controls on bedrock channel profiles and processes in coastal California: Journal of Geophysical Research-Earth Surface, v. 109, no. F3.
Egger, J., Bajrachaya, S., Egger, U., Heinrich, R., Reuder, J., Shayka, P., Wendt, H., and Wirth, V., 2000, Diurnal winds in the Himalayan Kali Gandaki Valley. Part I: Observations: Monthly Weather Review, v. 128, no. 4, p. 1106-1122.
Emanuel, K. A., 1994, Atmospheric convection, Oxford University Press, USA.
England, P., and Houseman, G., 1985, Role of Lithospheric Strength Heterogeneities in the Tectonics of Tibet and Neighboring Regions: Nature, v. 315, no. 6017, p. 297-301.
England, P., and McKenzie, D., 1982, A thin viscous sheet model for continental deformation: Geophysical Journal of the Royal Astronomical Society, v. 70, no. 2, p. 295-321.
-, 1983, Correction to - A thin viscous sheet model for continental deformation: Geophysical Journal of the Royal Astronomical Society, v. 73, no. 2, p. 523-532.
England, P., and Molnar, P., 1991, Inferences of deviatoric stress in actively deforming belts from simple physical models: Philosophical Transactions of the Royal Society of London. Series A: Physical and Engineering Sciences, v. 337, no. 1645, p. 151-164.

-, 1997, Active deformation of Asia: From kinematics to dynamics: Science, v. 278, no. 5338, p. 647-650.
England, P. C., and Houseman, G. A., 1988, The Mechanics of the Tibetan Plateau: Philosophical Transactions of the Royal Society of London Series a-Mathematical Physical and Engineering Sciences, v. 326, no. 1589, p. 301-320.
ESRI, 2010, National Geographic world map: ESRI, ESRI basemap with data provided by National Geographic.
Essenhigh, R. H., 2006, Prediction of the Standard Atmosphere profiles of temperature, pressure, and density with height for the lower atmosphere by solution of the (SS) integral Equations of Transfer and evaluation of the potential for profile perturbation by combustion emissions: Energy & fuels, v. 20, no. 3, p. 1057-1067.
Ferrill, D. A., Stamatakos, J. A., Jones, S. M., Rahe, B., McKague, H. L., Martin, R. H., and Morris, A. P., 1996, Quaternary slip history of the Bare Mountain fault (Nevada) from the morphology and distribution of alluvial fan deposits: Geology, v. 24, no. 6, p. 559-562.
Finnegan, N. J., Hallet, B., Montgomery, D. R., Zeitler, P. K., Stone, J. O., Anders, A. M., and Yuping, L., 2008, Coupling of rock uplift and river incision in the Namche Barwa-Gyala Peri massif, Tibet: Geological Society of America Bulletin, v. 120, no. 1-2, p. 142-155.
Formento-Trigilio, M. L., and Pazzaglia, F. J., 1998, Tectonic geomorphology of the Sierra Nacimiento: Traditional and new techniques in assessing long-term landscape evolution in the Southern Rocky Mountains: Journal of Geology, v. 106, no. 4, p. 433-453.
Frankel, K. L., and Dolan, J. F., 2007, Characterizing arid region alluvial fan surface roughness with airborne laser swath mapping digital topographic data: Journal of Geophysical Research, v. 112, no. F2, p. F02025.
Fraser, S., and DeCelles, P. G., 1992, Geomorphic control on sediment accumulation at margins of foreland basins: Basin Research, v. 4, p. 233 - 252.
Frostick, L. E., and Jones, S. J., 2002, Impact of periodicity on sediment flux in alluvial systems: grain to basin scale, *in* Jones, S. J., and Frostick, L. E., eds., Sediment Flux to Basins: Causes, Control and Consequences, Volume 191: Bath, Geological Soc Publishing House, p. 81-95.
Gan, W. J., Zhang, P. Z., Shen, Z. K., Niu, Z. J., Wang, M., Wan, Y. G., Zhou, D. M., and Cheng, J., 2007, Present-day crustal motion within the Tibetan Plateau inferred from GPS measurements: Journal of Geophysical Research-Solid Earth, v. 112, no. B8.
Garcia-Castellanos, D., 2007, The role of climate during high plateau formation. Insights from numerical experiments: Earth and Planetary Science Letters, v. 257, no. 3-4, p. 372-390.
Gardner, T. W., 1983, Experimental-Study of Knickpoint and Longitudinal Profile Evolution in Cohesive, Homogeneous Material: Geological Society of America Bulletin, v. 94, no. 5, p. 664-672.
Gilotti, J. A., and McClelland, W. C., 2007, Characteristics of, and a tectonic model for, Ultrahigh-Pressure metamorphism in the overriding plate of the Caledonian orogen: International Geology Review, v. 49, no. 9, p. 777-797.
Goldrick, G., and Bishop, P., 2007, Regional analysis of bedrock stream long profiles: evaluation of Hack's SL form, and formulation and assessment of an alternative (the DS form): Earth Surface Processes and Landforms, v. 32, no. 5, p. 649-671.
Guest, B., Axen, G. J., Lam, P. S., and Hassanzadeh, J., 2006, Late Cenozoic shortening in the west-central Alborz Mountains, northern Iran, by combined conjugate strike-slip and thin-skinned deformation: Geosphere, v. 2, no. 1, p. 35-U29.

Hack, J. T., 1973, Drainage adjustment in the Appalachians: Fluvial geomorphology. Publications in Geomorphology. State University of New York, Binghamton, New York, p. 51-69.
Hack, J. T., and Young, R. S., 1961, Shorter Contributions to General Geology: US Geological Survey professional paper, no. 354-355, p. 1.
Hanmar, O. P., and Clifford, N. J., 2007, Geomorphological explanation of the long profile of the Lower Mississippi River: Geomorphology, v. 84, no. 3-4, p. 222-240.
Harkins, N., Kirby, E., Heimsath, A., Robinson, R., and Reiser, U., 2007, Transient fluvial incision in the headwaters of the Yellow River, northeastern Tibet, China: Journal of Geophysical Research-Earth Surface, v. 112, no. F3.
Harrison, T. M., Copeland, P., Kidd, W. S. F., and Yin, A., 1992, Raising Tibet: Science, v. 255, no. 5052, p. 1663-1670.
Hartley, A. J., Mather, A. E., Jolley, E., and Turner, P., 2005, Climatic controls on alluvial-fan activity, Coastal Cordillera, northern Chile, *in* Harvey, A. M., Mather, A. E., and Stokes, M., eds., Alluvial Fans: Geomorphology, Sedimentology, Dynamics, Volume 251: Bath, Geological Soc Publishing House, p. 95-116.
Hartley, A. J., Weissmann, G. S., Nichols, G. J., and Warwick, G. L., 2010, Large distributive fluvial systems: characteristics, distribution, and controls on development: Journal of Sedimentary Research, v. 80, no. 2, p. 167-183.
Harvey, A., 2012, Processes of Sediment Supply to Alluvial Fans and Debris Cones: Dating Torrential Processes on Fans and Cones, p. 15-32.
Harvey, A. M., Mather, A. E., and Stokes, M., 2005, Alluvial fans: geomorphology, sedimentology, dynamics - introduction. A review of alluvial-fan research, *in* Harvey, A. M., Mather, A. E., and Stokes, M., eds., Alluvial Fans: Geomorphology, Sedimentology, Dynamics, Volume 251: Bath, Geological Soc Publishing House, p. 1-7.
Harvey, A. M., Silva, P. G., Mather, A. E., Goy, J. L., Stokes, M., and Zazo, C., 1999, The impact of Quaternary sea-level and climatic change on coastal alluvial fans in the Cabo de Gata ranges, southeast Spain: Geomorphology, v. 28, no. 1, p. 1-22.
Hatzfeld, D., and Molnar, P., 2010, Comparisons of the kinematics and deep structures of the Zagros and Himalaya of the Iranian and Tibetan plateaus and geodynamic implications: Reviews of Geophysics, v. 48.
Hessami, K., Nilforoushan, F., and Talbot, C. J., 2006, Active deformation within the Zagros Mountains deduced from GPS measurements: Journal of the Geological Society, v. 163, p. 143-148.
Higgins, C. G., 1984, Piping and sapping: Development of landforms by groundwater outflow: Groundwater as a geomorphic agent, p. 18-58.
Hjelstuen, B. O., Elverhoi, A., and Faleide, J. I., 1996, Cenozoic erosion and sediment yield in the drainage area of the Storfjorden Fan: Global and Planetary Change, v. 12, no. 1-4, p. 95-117.
Hobley, D. E. J., Sinclair, H. D., and Cowie, P. A., 2010, Processes, rates, and time scales of fluvial response in an ancient postglacial landscape of the northwest Indian Himalaya: Geological Society of America Bulletin, v. 122, no. 9-10, p. 1569-1584.
Hobley, D. E. J., Sinclair, H. D., Mudd, S. M., and Cowie, P. A., 2011, Field calibration of sediment flux dependent river incision: Journal of Geophysical Research-Earth Surface, v. 116.
Hooke, R. L., 1968, Steady-state relationships on arid region alluvial fans in closed basins: American Journal of Science, v. 266, no. 8.
Houseman, G., and England, P., 1986, Finite strain calculations of contintnetal deformation 1. Method and general results for convergent zones: Journal of Geophysical Research-Solid Earth and Planets, v. 91, no. B3, p. 3651-3663.
Hovius, N., Stark, C. P., and Allen, P. A., 1997, Sediment flux from a mountain belt derived by landslide mapping: Geology, v. 25, no. 3, p. 231-234.

Howard, A. D., Dietrich, W. E., and Seidl, M. A., 1994, Modeling Fluvial Erosion on Regional to Continental Scales: Journal of Geophysical Research-Solid Earth, v. 99, no. B7, p. 13971-13986.
Howard, A. D., and Kerby, G., 1983, Channel changes in badlands: Geological Society of America Bulletin, v. 94, no. 6, p. 739-752.
Hu, X. M., Sinclair, H. D., Wang, J. G., Jiang, H. H., and Wu, F. Y., 2012, Late Cretaceous-Palaeogene stratigraphic and basin evolution in the Zhepure Mountain of southern Tibet: implications for the timing of India-Asia initial collision: Basin Research, v. 24, no. 5, p. 520-543.
Huang, X. J., and Niemann, J. D., 2006, Modelling the potential impacts of groundwater hydrology on long-term drainage basin evolution: Earth Surface Processes and Landforms, v. 31, no. 14, p. 1802-1823.
Humphrey, N. F., and Heller, P. L., 1995, Natural Oscillations in Coupled Geomorphic Systems - an Alternative Origin for Cyclic Sedimentation: Geology, v. 23, no. 6, p. 499-502.
Ijjasz-Vasquez, E. J., and Bras, R. L., 1995, Scaling regimes of local slope versus contributing area in digital elevation models: Geomorphology, v. 12, no. 4, p. 299-311.
IMO, 1997, Iranian climate data for the period 1951 - 1995, Iranian Meterological Organisation.
Jackson, J., 2001, Living with earthquakes: Know your faults: Journal of earthquake engineering, v. 5, p. 5-123.
Jackson, J. A., Austrheim, H., McKenzie, D., and Priestley, K., 2004, Metastability, mechanical strength, and the support of mountain belts: Geology, v. 32, no. 7, p. 625-628.
Jade, S., Bhatt, B. C., Yang, Z., Bendick, R., Gaur, V. K., Molnar, P., Anand, M. B., and Kumar, D., 2004, GPS measurements from the Ladakh Himalaya, India: Preliminary tests of plate-like or continuous deformation in Tibet: Geological Society of America Bulletin, v. 116, no. 11-12, p. 1385-1391.
Jarvis, A., Reuter, H. I., Nelson, A., and Guevara, E., 2008, Hole-filled seamless SRTM data, *in* Agriculture, C. f. T., ed.
Jarvis, A., Rubiano, J., Nelson, A., Farrow, A., and Mulligan, M., 2004, Practical use of SRTM data in the tropics: comparisons with digital elevation models generated from cartographic data: Working document, v. 198, p. 32.
Jiang, Y., Luo, Y., Zhao, Z. C., and Tao, S. W., 2010, Changes in wind speed over China during 1956-2004: Theoretical and Applied Climatology, v. 99, no. 3-4, p. 421-430.
Jones, S. J., 2004, Tectonic controls on drainage evolution and development of terminal alluvial fans, southern Pyrenees, Spain: Terra Nova, v. 16, no. 3, p. 121-127.
Jones, S. J., Frostick, L. E., and Astin, T. R., 1999, Climatic and tectonic controls on fluvial incision and aggradation in the Spanish Pyrenees: Journal of the Geological Society, v. 156, p. 761-769.
Karlstrom, K. E., Coblentz, D., Dueker, K., Ouimet, W., Kirby, E., Van Wijk, J., Schmandt, B., Kelley, S., Lazear, G., Crossey, L. J., Crow, R., Aslan, A., Darling, A., Aster, R., MacCarthy, J., Hansen, S. M., Stachnik, J., Stockli, D. F., Garcia, R. V., Hoffman, M., McKeon, R., Feldman, J., Heizler, M., Donahue, M. S., and Grp, C. W., 2012, Mantle-driven dynamic uplift of the Rocky Mountains and Colorado Plateau and its surface response: Toward a unified hypothesis: Lithosphere, v. 4, no. 1, p. 3-22.
Kirby, E., and Whipple, K., 2001, Quantifying differential rock-uplift rates via stream profile analysis: Geology, v. 29, no. 5, p. 415-418.
Knighton, D., 1998, Fluvial forms and processes : a new perspective, London, Arnold.

Kobor, J. S., and Roering, J. J., 2004, Systematic variation of bedrock channel gradients in the central Oregon Coast Range: implications for rock uplift and shallow landsliding: Geomorphology, v. 62, no. 3, p. 239-256.
Kooi, H., and Beaumont, C., 1996, Large-scale geomorphology: classical concepts reconciled and integrated with contemporary ideas via a surface processes model: Journal of Geophysical Research, v. 101, no. B2, p. 3361-3386.
Korup, O., 2006, Rock-slope failure and the river long profile: Geology, v. 34, no. 1, p. 45-48.
Lague, D., and Davy, P., 2003, Constraints on the long-term colluvial erosion law by analyzing slope-area relationships at various tectonic uplift rates in the Siwaliks Hills (Nepal): Journal of Geophysical Research, v. 108, no. B2, p. 2129.
Lague, D., Hovius, N., and Davy, P., 2005, Discharge, discharge variability, and the bedrock channel profile: Journal of Geophysical Research-Earth Surface, v. 110, no. F4.
Larsen, I. J., Montgomery, D. R., and Korup, O., 2010, Landslide erosion controlled by hillslope material: Nature Geoscience, v. 3, no. 4, p. 247-251.
Larue, J. P., 2011, Longitudinal profiles and knickzones: the example of the rivers of the Cher basin in the northern French Massif Central: Proceedings of the Geologists Association, v. 122, no. 1, p. 125-142.
Le Dortz, K., Meyer, B., Sébrier, M., Braucher, R., Nazari, H., Benedetti, L., Fattahi, M., Bourles, D., Foroutan, M., and Siame, L., 2011, Dating inset terraces and offset fans along the Dehshir Fault (Iran) combining cosmogenic and OSL methods: Geophysical Journal International, v. 185, no. 3, p. 1147-1174.
Lecce, S. A., 1990, The alluvial fan problem: Alluvial Fans: A Field Approach. Wiley, Chichester, p. 3-24.
Leeder, M., and Gawthorpe, R., 1987, Sedimentary models for extensional tilt-block/half-graben basins: Geological Society, London, Special Publications, v. 28, no. 1, p. 139-152.
Leopold, L. B., and Langbein, W. B., 1962, The concept of entropy in landscape evolution, US Government Printing Office Washington, DC.
Li, S., Mooney, W. D., and Fan, J., 2006, Crustal structure of mainland China from deep seismic sounding data: Tectonophysics, v. 420, no. 1, p. 239-252.
Liu-Zeng, J., Tapponnier, P., Gaudemer, Y., and Ding, L., 2008, Quantifying landscape differences across the Tibetan plateau: Implications for topographic relief evolution: Journal of Geophysical Research-Earth Surface, v. 113, no. F4.
Maddy, D., Demir, T., Bridgland, D. R., Veldkamp, A., Stemerdink, C., van der Schriek, T., and Westaway, R., 2005, An obliquity-controlled Early Pleistocene river terrace record from Western Turkey?: Quaternary Research, v. 63, no. 3, p. 339-346.
Maggi, A., Jackson, J. A., McKenzie, D., and Priestley, K., 2000, Earthquake focal depths, effective elastic thickness, and the strength of the continental lithosphere: Geology, v. 28, no. 6, p. 495-498.
Maggi, A., and Priestley, K., 2005, Surface waveform tomography of the Turkish-Iranian plateau: Geophysical Journal International, v. 160, no. 3, p. 1068-1080.
Maritan, A., Rinaldo, A., Rigon, R., Giacometti, A., and Rodríguez-Iturbe, I., 1996, Scaling laws for river networks: Physical review E, v. 53, no. 2, p. 1510.
Masek, J. G., Isacks, B. L., Gubbels, T. L., and Fielding, E. J., 1994, Erosion and tectonics at the margins of continental plateaus: Journal of Geophysical Research-Solid Earth, v. 99, no. B7, p. 13941-13956.
Masek, J. G., Vermote, E. F., Saleous, N. E., Wolfe, R., Hall, F. G., Huemmrich, K. F., Gao, F., Kutler, J., and Lim, T. K., 2006, A Landsat surface reflectance dataset for North America, 1990-2000: Geoscience and Remote Sensing Letters, IEEE, v. 3, no. 1, p. 68-72.

Mather, A. E., and Hartley, A., 2005, Flow events on a hyper-arid alluvial fan: Quebrada Tambores, Salar de Atacama, northern Chile, *in* Harvey, A. M., Harvey, A. M., Mather, A. E., and Stokes, M., eds., Alluvial Fans: Geomorphology, Sedimentology, Dynamics, Volume 251, p. 9-24.

McClay, K. R., 1992, Thrust tectonics, London, Chapman & Hall, 447 p.:

Metivier, F., Gaudemer, Y., Tapponnier, P., and Meyer, B., 1998, Northeastward growth of the Tibet plateau deduced from balanced reconstruction of two depositional areas: The Qaidam and Hexi Corridor basins, China: Tectonics, v. 17, no. 6, p. 823-842.

Meyer, B., Mouthereau, F., Lacombe, O., and Agard, P., 2005, Evidence of Quaternary activity along the Deshir Fault: implication for the Tertiary tectonics of Central Iran: Geophysical Journal International, v. 164, no. 1, p. 192-201.

Miller, J. R., 1991, The Influence of Bedrock Geology on Knickpoint Development and Channel-Bed Degradation Along Downcutting Streams in South-Central Indiana: Journal of Geology, v. 99, no. 4, p. 591-605.

Moglen, G. E., and Bras, R. L., 1995, The importance of spatially heterogeneous erosivity and the cumulative area distribution within a basin evolution model: Geomorphology, v. 12, no. 3, p. 173-185.

Molnar, P., 2003, Geomorphology - Nature, nurture and landscape: Nature, v. 426, no. 6967, p. 612-614.

Molnar, P., and England, P., 1990, Late Cenozoic uplift of mountain ranges and global climate change: chicken or egg?: Nature, v. 346, no. 6279, p. 29-34.

Molnar, P., England, P., and Martinod, J., 1993, Mantle Dynamics, Uplift of the Tibetan Plateau, and the Indian Monsoon: Reviews of Geophysics, v. 31, no. 4, p. 357-396.

Molnar, P., Houseman, G. A., and England, P. C., 2006, Earth science - Palaeo-altimetry of Tibet: Nature, v. 444, no. 7117.

Molnar, P., and Lyoncaen, H., 1989, Fault Plane Solutions of Earthquakes and Active Tectonics of the Tibetan Plateau and Its Margins: Geophysical Journal International, v. 99, no. 1, p. 123-153.

Molnar, P., and Stock, J. M., 2009, Slowing of India's convergence with Eurasia since 20 Ma and its implications for Tibetan mantle dynamics: Tectonics, v. 28, no. 3.

Montgomery, D. R., and Dietrich, W. E., 1992, Channel initiation and the problem of landscape scale: Science, v. 255, no. 5046, p. 826-830.

Mooney, W. D., Laske, G., and Masters, T. G., 1998, CRUST 5.1: A global crustal model at 5× 5: Journal of Geophysical Research, v. 103, no. B1, p. 727-747.

Morris, P. H., and Williams, D. J., 1997, Exponential longitudinal profiles of streams: Earth Surface Processes and Landforms, v. 22, no. 2, p. 143-163.

Nandi, A., 2000, Evaluation of the cycloid as a function for describing longitudinal river profiles: The University of Akron.

Nixon, M., and Aguado, A. S., 2012, Feature Extraction & Image Processing for Computer Vision, Academic Press.

Owens, P. N., and Slaymaker, O., 2004, Mountain geomorphology, Arnold, Hodder Headline Group.

Palmer, T. N., and Ralsanen, J., 2002, Quantifying the risk of extreme seasonal precipitation events in a changing climate: Nature, v. 415, no. 6871, p. 512-514.

Patranabis-Deb, S., and Chaudhuri, A. K., 2007, A retreating fan-delta system in Neoproterozoic Chattisgarh rift basin, central India: Major controls on its evolution: Aapg Bulletin, v. 91, no. 6, p. 785-808.

Patriat, P., and Achache, J., 1984, India Eurasia collision chronology has implication for crustal shortening and driving mechanism of plates: Nature, v. 311, no. 5987, p. 615-621.

Peakall, J., Leeder, M., Best, J., and Ashworth, P., 2000, River response to lateral ground tilting: a synthesis and some implications for the modelling of alluvial architecture in extensional basins: Basin Research, v. 12, no. 3-4, p. 413-424.
Peixoto, J. P., and Oort, A. H., 1992, Physics of climate.
Pollastro, R. M., Persits, F. M., and Steinhower, D. W., 1999, Map showing geology, oil and gas fields and geologic provinces of Iran: USGS.
Pratt-Sitaula, B., Burbank, D. W., Heimsath, A., and Qjha, T., 2004, Landscape disequilibrium on 1000-10,000 year scales Marsyandi River, Nepal, central Himalaya: Geomorphology, v. 58, no. 1-4, p. 223-241.
Purvis, M., and Robertson, A., 2004, A pulsed extension model for the Neogene-Recent E-W-trending Alasehir Graben and the NE-SW-trending Selendi and Gordes Basins, western Turkey: Tectonophysics, v. 391, no. 1-4, p. 171-201.
Quigley, M. C., Sandiford, M., and Cupper, M. L., 2007, Distinguishing tectonic from climatic controls on range-front sedimentation: Basin Research, v. 19, no. 4, p. 491-505.
Radjaee, A., Rham, D., Mokhtari, M., Tatar, M., Priestley, K., and Hatzfeld, D., 2010, Variation of Moho depth in the central part of the Alborz Mountains, northern Iran: Geophysical Journal International, v. 181, no. 1, p. 173-184.
Ramsey, L., A, 2006, Topographic evolution of emerging mountain belts [PhD: Univeristy of Cambridge, 240 p.
Ramsey, L. A., Walker, R. T., and Jackson, J., 2008, Fold evolution and drainage development in the Zagros mountains of Fars province, SE Iran: Basin Research, v. 20, no. 1, p. 23-48.
Raymo, M. E., and Ruddiman, W. F., 1992, Tectonic forcing of late Cenozoic climate: Nature, v. 359, no. 6391, p. 117-122.
Reuter, H., Nelson, A., and Jarvis, A., 2007, An evaluation of void-filling interpolation methods for SRTM data: International Journal of Geographical Information Science, v. 21, no. 9, p. 983-1008.
Rey, P., Vanderhaeghe, O., and Teyssier, C., 2001, Gravitational collapse of the continental crust: definition, regimes and modes: Tectonophysics, v. 342, no. 3-4, p. 435-449.
Ritter, J. B., Miller, J. R., Enzel, Y., and Wells, S. G., 1995, Reconciling the Roles of Tectonism and Climate in Quaternary Alluvial-Fan Evolution: Geology, v. 23, no. 3, p. 245-248.
Roberts, G. G., White, N. J., Martin-Brandis, G. L., and Crosby, A. G., 2012, An uplift history of the Colorado Plateau and its surroundings from inverse modeling of longitudinal river profiles: Tectonics, v. 31.
Rodriguez-Iturbe, I., Ijjasz-Vasquez, E., Bras, R., and Tarboton, D., 1992, Power law distributions of discharge mass and energy in river basins: Water Resources Research, v. 28, no. 4, p. 1089-1093.
Rodriguez, E., Morris, C., Belz, J., Chapin, E., Martin, J., Daffer, W., and Hensley, S., 2005, An assessment of the SRTM topographic products: Jet Propulsion Laboratory, Pasadena.
Rodriguez, E., Morris, C. S., and Belz, J. E., 2006, A global assessment of the SRTM performance: Photogrammetric Engineering and Remote Sensing, v. 72, no. 3, p. 249-260.
Roe, G. H., 2005, Orographic precipitation: Annual Review of Earth and Planetary Sciences, v. 33, p. 645-671.
Roe, G. H., Montgomery, D. R., and Hallet, B., 2002, Effects of orographic precipitation variations on the concavity of steady-state river profiles: Geology, v. 30, no. 2, p. 143-146.
-, 2003, Orographic precipitation and the relief of mountain ranges: Journal of Geophysical Research-Solid Earth, v. 108, no. B6.

Roe, G. H., Whipple, K. X., and Fletcher, J. K., 2008, Feedbacks among climate, erosion, and tectonics in a critical wedge orogen: American Journal of Science, v. 308, no. 7, p. 815-842.
Rorabaugh, M., 1964, Estimating changes in bank storage and groundwater contribution to streamflow: International Association of Scientific Hydrology, v. 63, p. 432-441.
Schuerch, P., Densmore, A. L., McArdell, B. W., and Molnar, P., 2006, The influence of landsliding on sediment supply and channel change in a steep mountain catchment: Geomorphology, v. 78, no. 3-4, p. 222-235.
Schumm, S. A., Dumont, J. F., and Holbrook, J. M., 2000, Active tectonics and alluvial rivers, Cambridge, Cambridge University Press, 276 p.:
Searle, M. P., Elliott, J. R., Phillips, R. J., and Chung, S. L., 2011, Crustal-lithospheric structure and continental extrusion of Tibet: Journal of the Geological Society, v. 168, no. 3, p. 633-672.
Searle, M. P., Windley, B. F., Coward, M. P., Cooper, D. J. W., Rex, A. J., Rex, D., Li, T. D., Xiao, X. C., Jan, M. Q., Thakur, V. C., and Kumar, S., 1987, The closiing of tethys and the tectonics of the Himalaya: Geological Society of America Bulletin, v. 98, no. 6, p. 678-701.
Seeber, L., and Gornitz, V., 1983, River Profiles Along the Himalayan Arc as Indicators of Active Tectonics: Tectonophysics, v. 92, no. 4, p. 335-367.
Seidl, M., and Dietrich, W., 1993, The problem of channel erosion into bedrock: Catena supplement, v. 23, p. 101-101.
Seidl, M. A., Dietrich, W. E., and Kirchner, J. W., 1994, Longitudinal Profile Development into Bedrock - an Analysis of Hawaiian Channels: Journal of Geology, v. 102, no. 4, p. 457-474.
Sella, G. F., Dixon, T. H., and Mao, A. L., 2002, REVEL: A model for Recent plate velocities from space geodesy: Journal of Geophysical Research-Solid Earth, v. 107, no. B4.
Sinclair, M. R., 1994, A diagnostic model for estimating orographic precipitation: Journal of applied meteorology, v. 33, no. 10, p. 1163-1175.
Snow, R. S., and Slingerland, R. L., 1987, Mathermatical-modeling of graded river profiles: Journal of Geology, v. 95, no. 1, p. 15-33.
Snyder, N. P., Whipple, K. X., Tucker, G. E., and Merritts, D. J., 2000, Landscape response to tectonic forcing: Digital elevation model analysis of stream profiles in the Mendocino triple junction region, northern California: Geological Society of America Bulletin, v. 112, no. 8, p. 1250-1263.
Sobel, E. R., Hilley, G. E., and Strecker, M. R., 2003, Formation of internally drained contractional basins by aridity-limited bedrock incision: Journal of Geophysical Research-Solid Earth, v. 108, no. B7, p. -.
Stepisnik, U., 2010, Relict alluvial fans of Matarsko Podolje and Vrhpoljska Brda, Slovenia: Zeitschrift Fur Geomorphologie, v. 54, no. 1, p. 17-29.
Stock, J. D., and Montgomery, D. R., 1999, Geologic constraints on bedrock river incision using the stream power law: Journal of Geophysical Research-Solid Earth, v. 104, no. B3, p. 4983-4993.
Szulc, A. G., Najman, Y., Sinclair, H. D., Pringle, M., Bickle, M., Chapman, H., Garzanti, E., Ando, S., Huyghe, P., Mugnier, J. L., Ojha, T., and DeCelles, P., 2006, Tectonic evolution of the Himalaya constrained by detrital Ar-40-Ar-39, Sm-Nd and petrographic data from the Siwalik foreland basin succession, SW Nepal: Basin Research, v. 18, no. 4, p. 375-391.
Talling, P. J., and Sowter, M. J., 1998, Erosion, deposition and basin-wide variations in stream power and bed shear stress: Basin Research, v. 10, no. 1, p. 87-108.
Tapponnier, P., Peltzer, G., and Armijo, R., 1986, On the mechanics of the collision between India and Asia: Geological Society, London, Special Publications, v. 19, no. 1, p. 113-157.

Tarboton, D. G., Bras, R. L., and Rodriguez-Iturbe, I., 2006, On the extraction of channel networks from digital elevation data: Hydrological Processes, v. 5, no. 1, p. 81-100.
Tarboton, D. G., Bras, R. L., and Rodrigueziturbe, I., 1991, On the Extraction of Channel Networks from Digital Elevation Data: Hydrological Processes, v. 5, no. 1, p. 81-100.
Tealdi, S., Camporeale, C., and Ridolfi, L., 2011, Long-term morphological river response to hydrological changes: Advances in Water Resources, v. 34, no. 12, p. 1643-1655.
Tucker, G. E., and Bras, R. L., 1998, Hillslope processes, drainage density, and landscape morphology: Water Resources Research, v. 34, no. 10, p. 2751-2764.
Turowski, J. M., Hovius, N., Meng-Long, H., Lague, D., and Men-Chiang, C., 2008, Distribution of erosion across bedrock channels: Earth Surface Processes and Landforms, v. 33, no. 3, p. 353-363.
USGS, 2008, Global visualisation viewer http://glovis.usgs.gov/, v. 2008.
-, 2010, National earthquake information centre and Global centroid moment tensor catalogues, USGS.
Velbel, M. A., 1993, Temperature dependence of silicate weathering in nature: How strong a negative feedback on long-term accumulation of atmospheric CO2 and global greenhouse warming?: Geology, v. 21, no. 12, p. 1059-1062.
Vernant, P., Nilforoushan, F., Chery, J., Bayer, R., Djamour, Y., Masson, F., Nankali, H., Ritz, J. F., Sedighi, M., and Tavakoli, F., 2004a, Deciphering oblique shortening of central Alborz in Iran using geodetic data: Earth and Planetary Science Letters, v. 223, no. 1-2, p. 177-185.
Vernant, P., Nilforoushan, F., Hatzfeld, D., Abbassi, M. R., Vigny, C., Masson, F., Nankali, H., Martinod, J., Ashtiani, A., Bayer, R., Tavakoli, F., and Chery, J., 2004b, Present-day crustal deformation and plate kinematics in the Middle East constrained by GPS measurements in Iran and northern Oman: Geophysical Journal International, v. 157, no. 1, p. 381-398.
Viseras, C., Calvache, M. L., Soria, J. M., and Fernandez, J., 2003, Differential features of alluvial fans controlled by tectonic or eustatic accommodation space. Examples from the Betic Cordillera, Spain: Geomorphology, v. 50, no. 1-3, p. 181-202.
Vita-Finzi, C., 1968, Late Quaternary alluvial chronology of Iran: Geologische Rundschau, v. 58, no. 2, p. 951-973.
Volker, H., Wasklewicz, T., and Ellis, M., 2007, A topographic fingerprint to distinguish alluvial fan formative processes: Geomorphology, v. 88, no. 1, p. 34-45.
Walker, R. T., and Fattahi, M., 2011, A framework of Holocene and Late Pleistocene environmental change in eastern Iran inferred from the dating of periods of alluvial fan abandonment, river terracing, and lake deposition: Quaternary Science Reviews, v. 30, no. 9-10, p. 1256-1271.
Walker, R. T., Ramsey, L. A., and Jackson, J., 2011, Geomorphic evidence for ancestral drainage patterns in the Zagros Simple Folded Zone and growth of the Iranian plateau: Geological Magazine, v. 148, no. 5-6, p. 901-910.
Walvoord, M. A., and Striegl, R. G., 2007, Increased groundwater to stream discharge from permafrost thawing in the Yukon River basin: Potential impacts on lateral export of carbon and nitrogen: Geophysical Research Letters, v. 34, no. 12, p. L12402.
Wang, H., Harvey, A. M., Xie, S. Y., Kuang, M. S., and Chen, Z. Y., 2008, Tributary-junction fans of China's Yangtze Three-Gorges valley: Morphological implications: Geomorphology, v. 100, no. 1-2, p. 131-139.
Waters, J. V., Jones, S. J., and Armstrong, H. A., 2010, Climatic controls on late Pleistocene alluvial fans, Cyprus: Geomorphology, v. 115, no. 3-4, p. 228-251.

Whipple, K. X., 2001, Fluvial landscape response time: How plausible is steady-state denudation?: American Journal of Science, v. 301, no. 4-5, p. 313-325.
Whipple, K. X., and Trayler, C. R., 1996, Tectonic control of fan size: The importance of spatially variable subsidence rates: Basin Research, v. 8, no. 3, p. 351-366.
Whipple, K. X., and Tucker, G. E., 1999, Dynamics of the stream-power river incision model: Implications for height limits of mountain ranges, landscape response timescales, and research needs: Journal of Geophysical Research-Solid Earth, v. 104, no. B8, p. 17661-17674.
Whitehead, J. A., and Clift, P. D., 2009, Continent elevation, mountains, and erosion: Freeboard implications: Journal of Geophysical Research, v. 114, no. B5, p. B05410.
Whittaker, A. C., 2012, How do landscapes record tectonics and climate?: Lithosphere, v. 4, no. 2, p. 160-164.
Whittaker, A. C., Cowie, P. A., Attal, M., Tucker, G. E., and Roberts, G. P., 2007, Bedrock channel adjustment to tectonic forcing: Implications for predicting river incision rates: Geology, v. 35, no. 2, p. 103-106.
Willett, S. D., 1999, Orogeny and orography: The effects of erosion on the structure of mountain belts: Journal of Geophysical Research-Solid Earth, v. 104, no. B12, p. 28957-28981.
Wobus, C., Pringle, M., Whipple, K., and Hodges, K., 2008, A Late Miocene acceleration of exhumation in the Himalayan crystalline core: Earth and Planetary Science Letters, v. 269, no. 1-2, p. 1-10.
Wobus, C. W., Tucker, G. E., and Anderson, R. S., 2006, Self-formed bedrock channels: Geophysical Research Letters, v. 33, no. 18.
Wohl, E. E., 1993, Bedrock Channel Incision Along Piccaninny Creek, Australia: Journal of Geology, v. 101, no. 6, p. 749-761.
Wohl, E. E., 2000, Mountain rivers, Washington, D.C., American Geophysical Union, Water resources monograph ; 14., 320 p.:
Wohl, E. E., Greenbaum, N., Schick, A. P., and Baker, V. R., 1994, Controls on bedrock channel incision along Nahal Paran, Israel: Earth Surface Processes and Landforms, v. 19, no. 1, p. 1-13.
Wright, S. A., Topping, D. J., Rubin, D. M., and Melis, T. S., 2010, An approach for modeling sediment budgets in supply-limited rivers: Water Resources Research, v. 46.
Wu, B. S., Zheng, S., and Thorne, C. R., 2012, A general framework for using the rate law to simulate morphological response to disturbance in the fluvial system: Progress in Physical Geography, v. 36, no. 5, p. 575-597.
Xu, J. X., 2002, Complex behaviour of natural sediment-carrying streamflows and the geomorphological implications: Earth Surface Processes and Landforms, v. 27, no. 7, p. 749-758.
Yin, A., and Harrison, T. M., 2000, Geologic evolution of the Himalayan-Tibetan orogen: Annual Review of Earth and Planetary Sciences, v. 28, p. 211-280.
Zhang, H. P., Zhang, P. Z., Kirby, E., Yin, J. H., Liu, C. R., and Yu, G. H., 2011, Along-strike topographic variation of the Longmen Shan and its significance for landscape evolution along the eastern Tibetan Plateau: Journal of Asian Earth Sciences, v. 40, no. 4, p. 855-864.
Zhang, P. Z., Shen, Z., Wang, M., Gan, W., Bürgmann, R., Molnar, P., Wang, Q., Niu, Z., Sun, J., and Wu, J., 2004, Continuous deformation of the Tibetan Plateau from global positioning system data: Geology, v. 32, no. 9, p. 809-812.